THE INTERACTION OF THE OXIDES OF CARBON, HYDROGEN AND WATER WITH UNSUPPORTED COPPER CATALYSTS

By

RAYMOND ANTHONY HADDEN

A THESIS SUBMITTED FOR THE DEGREE OF DOCTOR OF PHILOSOPHY OF THE UNIVERSITY OF GLASGOW

DEPARTMENT OF CHEMISTRY, SEPTEMBER, 1987.

ProQuest LLC.
789 East Eisenhower Parkway
P.O. Box 1346
Ann Arbor, MI 48106 – 1346

TO MY MOTHER AND FATHER

ACKNOWLEDGEMENTS

I should like to express my gratitude to my supervisor, Dr. G. Webb, for his generous encouragement and advice throughout the course of this study. It has also been a pleasure to work with Dr. K.C. Waugh, whose interest and concern are most deeply appreciated.

My sincere thanks are also due to Tom Boyle for technical advice and repartee, to Danny Vandervell and to many others, including glassblowers, who eased the pain of technical mishaps.

I acknowledge the award of a maintenance grant from the S.E.R.C. and the help of I.C.I. plc. in allowing access to experimental apparatus.

I remain indebted to friends and colleagues whose kindness, and assistance in all manner of ways, was overwhelming. Many thanks to one and all.

Lastly, to Alpa, without whom I would never have made it.

TABLE OF CONTENTS

Table of Contents Contd.

Table of Contents Contd.

Table of Contents Contd.

Table of Contents Contd.

Table of Contents Contd. Page

Table of Contents Contd.

SUMMARY

An investigation of the adsorption and reaction of carbon monoxide, carbon dioxide, water and hydrogen on polycrystalline copper is presented. These studies were carried out by (i) the use of [14-C]radiotracers in a static adsorption system and (ii) mass spectrometric analysis of adsorption and reaction in a flow microreactor.

Carbon monoxide was found to interact with the copper surface in two distinct forms. The bulk of the adsorbate was relatively weakly adsorbed (ΔH_{ads} = ca. 43 KJ mol^{-1}), while 7% of the carbon monoxide monolayer had an activation energy of desorption of ca. 100 KJ mol^{-1}.

Carbon dioxide readily chemisorbed on polycrystalline copper. This process involved a limited oxidation of the copper surface by carbon dioxide decomposition. The adsorbed oxygen generated by this dissociative chemisorption allowed further, extensive, molecular carbon dioxide adsorption. The carbon monoxide species formed by carbon dioxide dissociation had an activation energy of desorption of ca. 100 KJ mol^{-1}. The presence of preadsorbed oxygen on the copper surface allowed carbon dioxide to adsorb in a partially dissociated form and, by this means, promoted direct interconversion of carbon monoxide and carbon dioxide.

The interaction of water with copper readily produced 8% of a monolayer of oxygen, together with molecularly adsorbed water (ΔH_{ads} = 46 KJ mol^{-1}) and a more strongly held hydroxyl species.

Hydrogen was found to exist on the copper surface in a variety of adsorbed states. The most strongly held species were not removed from the surface until temperatures in excess of 100°C were reached in T.P.D. experiments.

The presence of a monolayer of carbon monoxide, on copper, did not prevent carbon dioxide adsorption, which proceeded by a displacement mechanism. Carbon monoxide was found to adsorb, without displacement, on a carbon dioxide pretreated surface.

The coadsorption of hydrogen with carbon monoxide caused a 20% reduction in the extent of carbon monoxide adsorption. However, no interaction of hydrogen and carbon monoxide was evident. In contrast, hydrogen completely modified carbon dioxide adsorption, at ambient temperature, by an interaction which generated a surface formate species.

Despite an extensive surface coverage of formate species during the progress of the water gas shift reaction, the mechanism of the reaction is proposed to involve a sequential oxidation and reduction of a small number of highly active sites on the unsupported copper catalyst. The rates of both the forward and reverse shift reactions are considered to be desorption limited.

CHAPTER 1

INTRODUCTION

INTRODUCTION

1.1 General Introduction

Catalysis by metals has been recognised for nearly a century as being of great industrial significance, yet it is only in the past two decades that any large scale heterogeneous catalytic process has invoked the use of copper as the primary reactive surface. For example, methanol is produced, at a rate of up to one metric tonne per minute, by the hydrogenation of a mixture of carbon monoxide and carbon dioxide, at moderate temperatures and pressures, over a copper-zinc oxide-alumina catalyst. A similar catalyst, containing a smaller percentage of copper, is also used to increase the rate of attainment of equilibrium in the water gas shift reaction.

The viability of copper surfaces as components of heterogeneous catalytic hydrogenation systems prompted this study, which has considered the interaction of a variety of gaseous materials with a polycrystalline copper surface.

The object of this chapter is to discuss the potential of copper as an adsorbent, and consequently as a good catalytic surface, in relation to two well known theories of chemisorption and catalysis. The adsorbed layers formed on the copper surface by the adsorption of carbon monoxide, hydrogen, carbon dioxide, water and oxygen will then be detailed. Finally, the possible mechanisms of the methanol synthesis and water gas shift reactions will be considered in the light of this and other published data.

1.2 Copper as Adsorbent

1.2.1 Theories of Chemisorption and Catalysis

Since it was first recognised that metals could act as catalysts in a variety of heterogeneous systems, a clear, precise and unifying theory of adsorption and catalysis has been the ultimate goal of many theoretical and experimental studies. No such theory has yet proved to be infallible, although two closely related postulates have gained wide usage and, consequently, general acceptance. Beeck et al.[1] thought it reasonable to assume that a relationship must exist between the physical size of reacting gaseous molecules and the spacings of metal particles on the catalytic surface. Furthermore, using the hydrogenation of ethylene as a test reaction, a smooth increase in hydrogenation activity was observed with increasing lattice spacing in the different metals. The activity subsequently decreased as the spacing moved beyond the optimum, that is the most active, separation. It was noted, however, that this geometric theory could only partially explain the presence, or absence, of catalytic activity in any particular system. However, in the case of differences in activity between the crystal planes of a particular metal, a geometric specificity is often enough to explain the observed behaviour[2].

In order to produce a catalytic effect, it is reasonable to assume that the metal surface must perturb, or modify to some degree, the electronic distribution within the reacting materials. This procedure is normally effected by chemisorption of the reactant and this therefore implies adsorbate-adsorbent chemical interactions

and electron exchange and/or sharing. The electronic properties of the metal may then hold the key to the activity within a catalytic system. This theory is worth considering in some detail, since it may provide some interesting information with regard to copper surfaces, which are of relevance to the study described in this thesis.

1.2.2 Metallic Bonding

Two theories have been proposed to account for the particular peculiarities of the electronic metallic state. In the electron band theory, the discrete electronic orbitals in separate atoms are visualised as being compelled, by the Pauli Exclusion Principle, to form continuous bands when the bulk metallic state is attained. In the metal lattice these bands are found to be non-continuous and are contained within Brillouin zones, which are determined by the periodicity of the lattice. It is also of relevance to note that, although the different valence orbitals form their own particular bands, among the transition elements it is not uncommon for these bands to overlap. As shown in Figure 1.1, the s-orbitals in bulk copper metal are strongly interacting and form a broad continuum, while the d-band is relatively narrow. This density of states diagram shows that the d-band in metallic copper is expected to be completely filled.

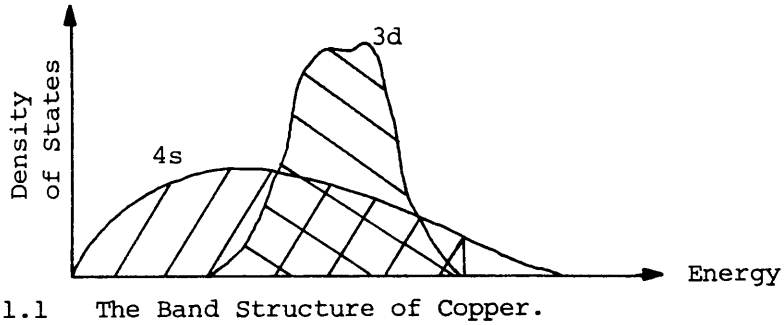

Fig. 1.1 The Band Structure of Copper.

The valence bond theory treats the metallic state somewhat differently (3). It considers the bonding in the bulk metal as being described by discrete covalent bonds between the metal atoms. These are produced by overlap between hybrid orbitals formed between the nine atomic s, p and d-orbitals. This could not account for many of the properties of a variety of metals; for example, no systematic increase in bond strength (as described by metallic radius) is observed along a transition metal series. Therefore, in an elegantly simple treatment, Pauling assumes that a fraction of the five d-orbitals are not involved in metallic bonding, but rather exist as atomic d-orbitals which are available for electron occupancy. It is again of relevance to this discussion to note that the atomic d-orbitals are calculated to be completely filled in metallic copper.

Although these two theories appear different they are, qualitatively, very similar. In both cases, a fraction of the valence electrons are considered to be involved in metallic bonding (filled d-bands or s, p, d hybrids), while, in many of the transition elements, the presence of either d-band vacancies or atomic d-orbitals allows a pleasing malleability which helps to account for many of the properties specific to metal substances.

1.2.3 d-band Chemisorption

The postulated lack of d-band vacancies (or atomic d-orbitals) at a copper metal surface has allowed a tidy classifaction of extent of chemisorption and hence catalytic activity to be generated. By collating those metals which showed a tendency to adsorb the same number and type of gases, Trapnell[4] classified the metals

in order of decreasing capacity for adsorption. The best adsorbents consisted of the transition metals, while copper, like a variety of metalloids and non-metals, was considered a poor material for adsorption studies. It seemed apparent that the availability of d-band vacancies, and/or atomic d-orbitals, was essential to the adsorption, modification and hence reaction of adsorbates on metal surfaces.

Dowden[5] generated the d-band theory of bonding and catalytic activity and since then the catalytic properties of various alloys have been used to fortify, or negate, this postulate. The use of alloys involving various compositions of a transition metal and a group Ib metal appears, initially, to be an ideal system in which to study the role of metallic electronic properties. Bragg[6] discovered that copper metal has a face-centred cubic packing arrangement and it is known that, on forming an alloy with, for example, nickel, this lattice structure is retained [7], although the percentage of copper within the alloy rises. More importantly, the electronic structure of the alloy undergoes dramatic changes as the copper concentration increases. Pure nickel has a number of d-band vacancies available for electron pairing, but as the concentration of copper in the alloy increases these 'holes' are filled by the copper valence electrons until, at 60% copper, the d-band is completely full. It may be expected therefore that a dramatic change in catalytic activity would be obtained between a 50-50 copper-nickel alloy and a 60-40 alloy. Dramatic changes in activity have been observed through these compositional ranges,

for example Reynolds[8] studied benzene hydrogenation over these catalysts and observed a curtailment of benzene conversion as the d-hole concentration in the alloys fell to zero.

1.2.4 The Copper Anomaly

It appears, both from Trapnell's original classification and from alloy studies, that, in relation to the other transition metals, copper may have little or no potential as a catalytic material. Some alloy studies have, however, shown little change in catalytic activity as d-bond filling occurs (9), and copper metal has indeed been used as a catalytic surface for many years. It is fascinating to note that the water gas shift reaction, which has only relatively recently been performed over copper containing catalysts, was somewhat fortuitously discovered by Sabatier in 1892[10]. When he passed carbon dioxide and hydrogen over heated copper he produced carbon monoxide rather than the expected methane reduction product. Another classic copper-catalysed system is that involving the dehydrogenation of ethanol[11]. The fact that both of these reactions are feasible on these catalysts leaves copper in a rather anomalous position. According to Trapnell [4], neither carbon dioxide nor hydrogen will adsorb on copper metal but, as noted above, a copper-catalysed carbon dioxide-hydrogen reaction does occur.

It appears that Trapnell's original classification cannot possibly hold for all reactions and under all conditions. Indeed Trapnell's adsorption studies were carried out at temperatures and pressures vastly different to those of the reaction conditions utilised by Sabatier, but this does not answer the question of why

the catalytic and chemisorptive ability of copper metal is not that predicted by either the valence bond or d-band models.

1.2.5 Hydrogen Chemisorption

In order to consider the catalytic activity of copper metal, it is necessary to briefly outline the adsorption characteristics of one of the components of both the methanol synthesis and water gas shift reactions, hydrogen, which is discussed in section 1.5 in rather more detail.

As noted above, Trapnell found no hydrogen adsorption on copper metal films at low temperatures. Ponec et al.[12] concurred finding no adsorption on copper films at 0°C. However, Sieverts[13] discovered that adsorption would occur at elevated temperatures (400°C) and that the quantity adsorbed significantly increased with temperature. Kwan[14] only observed chemisorption on carefully reduced copper powders at 300°C and found the activation energy for the adsorption process to be 86 KJ mol^{-1}. An elegant study of the hydrogen-deuterium equilibration reaction on high purity copper foils[15] gave further evidence for a high temperature hydrogen dissociative chemisorption. An activation energy of 97 KJ mol^{-1} was calculated for the reaction, which occurred at temperatures above 300°C. These facts suggested that, at elevated temperature, equilibration occurred by surface recombination of adsorbed atoms - the so called Bonhoeffer-Farkas mechanism. In summary therefore, these copper surfaces only showed a tendency to facilitate adsorption and catalysis at high reaction temperatures.

However, it has been found that metallic copper films will readily chemisorb atomic hydrogen[16,17,18]. This fact caused Dowden[19] and Boudart[15] to reassess the original concepts of catalytic bonding and adsorbate activation. The fact that atomic hydrogen and other adsorbates, for example sulphur[20], will readily adsorb on copper surfaces, made it apparent that s, p, d hybrid orbitals could, by themselves, effectively allow adsorption to occur. The proposed covalency between the atomic d-orbitals and adsorbates did not appear essential for this process. An elegant alternative theory was therefore proposed involving these unfilled d-orbitals. As hydrogen chemisorption on copper involved a large activation energy and necessitated relatively high temperatures, it was proposed that transition metal atomic d-orbitals allowed the formation of surface intermediates which were then converted to chemisorbed atomic hydrogen. In contrast copper, lacking these orbitals, did not allow the 'type-C' intermediates to form. The high temperature activity of copper surfaces could then be explained in terms of a thermal promotion of electrons from the filled copper d-band to the s-band[4,15].

A number of other studies have found that dissociative hydrogen chemisorption does occur, albeit rather slowly, at far lower temperatures. Beebe *et al.*[21] found chemisorption to occur at relatively low temperatures with an initial heat of adsorption of 46 KJ mol^{-1} on copper powder, while Pritchard[18] determined an isosteric heat of adsorption of 40 KJ mol^{-1} at a temperature of $-31^{\circ}C$ on copper films.

A number of hydrocarbon hydrogenation reactions have also been shown to occur fairly readily over copper catalysts at near ambient temperatures. Pease[22] hydrogenated ethylene over copper powder at a variety of temperatures between $0^{o}C$ and $200^{o}C$, while the same reaction has been carried out over copper-silica at $80^{o}C$[23]. Acetylene may also be hydrogenated over copper on pumice at $150^{o}C$[9]. The apparent activation energies of these reactions are available, but give little useful information since the kinetics of the various processes are not clear. However, it is noticeable that, in all the dihydrogen chemisorption, hydrogen-deuterium exchange and hydrocarbon hydrogenation reactions discussed, copper, although showing more activity than the 'type-C' theory suggests, is, compared to the transition elements, a rather poor and relatively inactive catalyst.

1.2.6 Generation of 'in-situ' Copper Activity

The 'residual' activity which this s, p metal shows has provoked much discussion concerning the copper anomaly. Most proposed solutions relatethe activity to changes in the level of the metal d-band, which could allow d-band vacancies to be generated more easily. It is obvious that a real copper surface will carry point and line defects and have a variety of faces exposed, which will destroy the calculated valence state of each surface atom. Impurities may lower (or raise) the d-band level and the presence of supports may lead to significant d-band variations. Indeed, it has been suggested that the number of electrons in the d-band of copper is actually 9.8 ± 0.2[24] and hence some low temperature activity may be expected.

These facts may explain the relative inactivity of copper in the dihydrogen and hydrocarbon reactions, but do not render any satisfactory explanation for the high activity of the copper catalysts used, for example,in formic acid decomposition, ethanol decomposition, water gas shift and methanol synthesis reactions. It is also important to note that the copper catalysts used in many of the industrial processes are also highly attractive because of their incredibly high selectivity for the desired reaction product. For example, the hydrogenation of carbon dioxide is 99% selective for methanol formation on copper-zinc oxide-alumina catalysts[25].

In these types of 'ternary' industrial catalysts the activity has been ascribed to a chemically unique component of the catalyst produced by the interaction of two or more of the individual materials. A fascinating example of this 'synergic' effect is that described by Kleir[26], concerning the possibility that a copper(I) cation, substitutionally dissolved in a zinc oxide matrix, may be a highly active centre for methanol production.

Another possible clue to the anomalous behaviour of copper may be gained by again referring to a hydrocarbon hydrogenation reaction. McCabe and Halsey[27] studied ethylene hydrogenation over reduced copper wire and observed an autocatalytic effect. It was found that preadsorption of hydrogen on the copper increased the activity of the catalyst, while this hydrogen species did not itself become involved in the hydrogenation reaction. In their summary the authors state that 'hydrogen functions as part of the catalyst'. It may be of relevance to note that, in most of the reactions catalysed

by copper surfaces, the reactants are oxygen containing species. The possibility that, in all of these systems, the active surface is not metallic copper, but copper modified by an oxygen species must therefore be considered. Indeed, evidence for a promoting effect of oxygen in an isopropanol-acetone hydrogenation, over copper catalysts, has been detailed[28].

In conclusion, it is apparent that the potential of many metals, particularly copper, as catalytic surfaces, cannot wholly be decided by either theoretical studies of the purely metallic bonding state, or by adsorption studies on clean or even 'dirty' metallic forms. The activity may lie within a modified metallic surface.

1.3 The Adsorption of Carbon Monoxide on Copper Surfaces

1.3.1 The Bonding of Carbon Monoxide to Copper

The details of the formation of a chemical bond between carbon monoxide and transition metal surfaces were originally formulated by Blyholder[29] using the principal of a synergic interaction, which had already found usage in studies of metal-carbonyl clusters[30]. This foresaw bonding occurring by a donor-acceptor mechanism between the adsorbate and adsorbent. Formation of a σ-bond was postulated by a dative interaction of the lone pair of electrons on the carbon atom (5σ orbital) with unoccupied surface metal orbitals which were considered to be d-orbitals. The effective negative charge thus generated on the metal atoms was proposed to be dispersed by back-donation of electrons, from occupied metal orbitals, to the relatively low energy $2\pi^*$ antibonding orbital on the carbon monoxide

molecule.

As previously discussed (section 1.2), the number of partially filled d-orbitals at a copper surface is considered to be, at most, very limited. It has therefore been proposed that the metal 4s orbitals play a partial role in binding with the carbon monoxide 5σ orbitals[31,32]. An alternative possibility[33] considers that d-orbitals are required to facilitate this chemisorption and, on copper surfaces, this will necessitate spin unpairing. The promotional energy required for this purpose is seen as the reason for the relatively low heats of adsorption determined for carbon monoxide-copper systems.

The role of d-orbitals in back-bonding to the carbon monoxide species has also been reassessed with regard to copper metal[34]. An almost wholly σ-bonded molecule is postulated, simply because the d-bands are considered to be too low lying to effect significant back-donation. A UPS study[35], which yields information regarding detailed changes in bonding orbitals, has questioned this postulate and notes that, at ambient temperature, rehybridisation of the metal d and s orbitals appears to occur. This produces transition metal-like characteristics and is considered to be similar to the proposal of d-s promotion. In this study, substantial backbonding was indeed noted at ambient temperature and the adsorbed species was designated as $CO^{\delta-}$ to exemplify this effect.

The movement of electrons in this donor-acceptor bonding allows a variety of other means of studying this particular system. For example, on adsorption, changes in the work function and surface potential of the metal should occur. Also, although the 5σ orbital

in the carbon monoxide molecule is non-bonding with respect to the carbon and oxygen atoms, backdonation of electrons into the anti-bonding 2π orbital should cause significant changes in the vibrational frequencies of the C-O bond.

1.3.2 Infra-red and Surface Potential Studies

Infra-red and surface potential studies have been carried out on evaporated copper films, supported copper catalysts and a variety of copper single crystals. In all of these systems similar trends can be recognised. Supported copper catalysts (for example copper on silica, alumina or magnesia) show considerable variations in the recorded vibrational frequencies (2081 - 2120 cm^{-1})[36]. This may be due to the differing preparative and reductive techniques employed and, consequently, to the degree of surface roughness and differing particle sizes inherent in each sample. A good example of this effect was determined by Boccuzzi *et al.*[37] who, studying carbon monoxide adsorption on small copper particles deposited on micro-crystalline zinc oxide, concluded that the two bands seen at 2098 cm^{-1} and 2078 cm^{-1} were due to adsorption on stepped close packed sites and open corner or edge sites respectively. It should also be noted that, in complete contrast to most of the reported studies using single crystal surfaces, an absorption band persisting above ambient temperature was observed following the adsorption of carbon monoxide on a copper-silica catalyst[38]. The tabulated values for evaporated copper films show a typical peak frequency at 2105 cm^{-1} [39], which is found to change only slightly with increasing coverage. In contrast, surface potential measurements

indicate two distinct adsorption regions[40]. At low surface coverages ($\theta<0.25$) the surface potential increased but, as the coverage reached $\theta = 0.5$, a significant decrease was observed.

Studies of copper single crystals show similar surface potential characteristics to that of evaporated copper films. Following carbon monoxide adsorption on Cu(111), Pritchard[41] found that the surface potential increased to 0.47v then decreased until, at saturation coverage, a value of 0.05v was noted. A Cu(100) surface showed a rise to 0.23v and a subsequent decrease to 0.07v, while a Cu(110) surface showed maxima and minima of 0.29v and 0.18v.

The infra-red spectra obtained following carbon monoxide adsorption on a variety of copper single crystals has provided much interesting data. Most surprising was the discovery that the band frequencies reported for Cu(111) and Cu(100) crystals, 2075 cm^{-1} and 2079 cm^{-1}[42,43], were found to be appreciably less than those of the polycrystalline film. The major low index faces do not, therefore, appear to be the main features of polycrystalline surfaces. Indeed, it has been shown that the frequencies associated with the Cu(110) face, 2088 cm^{-1}[44], and with a variety of other high index faces[36], are closer to that of the film. The fact that the absorption bands change little with increasing surface coverage is also remarkable. For example, as saturation coverage was attained on the Cu(100) surface the absorption band shifted by only 9 cm^{-1}[43].

This is remarkable when compared to the corresponding LEED analyses, since all the low index faces show abrupt changes in the overlayer structure at or near the coverage corresponding to maximum

surface potential. On all three major low index faces the original well-defined overlayers (C(2x2) on Cu(100), (2x1) on (110) and $(\sqrt{3}x\sqrt{3})R30^{o}$ on (111) [44,45,46]) are all modified to form what are described as 'compression structures'. This is expected to produce little change in the linear stretching frequency of the adsorbed species.

The possibility that infra-red inactive, horizontally bonded carbon monoxide species are produced at high coverages must also be considered[47]. Another alternative interpretation[41] is that the high coverages induce the formation of both linear and bridge-bonded species, and although little spectroscopic evidence previously existed for these dually bonded carbon monoxide species[48], recent FT-RAIRS studies have confirmed the presence of this type of adsorbate[49]. Rydberg claims that a model in which the carbon monoxide molecule changes from tilted to normal with respect to the surface is consistent with the experimental data[50], while both Woodruff and Anderson[51,31] invoke the possibility of a 'through space' interaction between the 2π orbitals of the adsorbed species, which would cause the frequency shift.

1.3.3 Heats of Adsorption

In his classic study Trapnell[4] determined the heat of adsorption of carbon monoxide on an evaporated copper film, at relatively low temperatures ($-78.5^{o}C$ and $-63.5^{o}C$), as 39 KJ mol^{-1}. More recently, Pritchard[42] found an initial heat of 67 KJ mol^{-1} which fell to 50 KJ mol^{-1} at higher coverages. Single crystal studies concur, showing initial heats of adsorption of 50 KJ mol^{-1}

on Cu(111)[52], 59 KJ mol^{-1} on Cu(100)[42] and 58 KJ mol^{-1} on Cu(110)[53]. Joyner[35] and Kirstein[54] studied the adsorption and thermal desorption of carbon monoxide on Cu(100) and Cu(111) single crystals. Following adsorption at -193°C and -168°C, the adsorbate was not retained on the single crystal surfaces after heating to ambient temperature.

Heats of adsorption have also been determined from studies using copper powders as the adsorbent. A microcalorimetric investigation[55] found the heat of adsorption of carbon monoxide to vary between 66 and 43 KJ mol^{-1} on metallic copper. Using a frontal chromatographic technique, Waugh[56] determined the heat of adsorption of carbon monoxide as 50 KJ mol^{-1}, while in an earlier study Bell, Stone and Tilley[57] quote a value of 71 KJ mol^{-1}. Indeed, values at least as high as 85 KJ mol^{-1}, which fell to 56 KJ mol^{-1} at higher coverages, were determined by Beebe and Wildner in 1934[58]. Kleir[59], while not attempting to quantify his experiment, did find that 5% of the carbon monoxide adsorbed on a low area copper powder was resistant to evacuation at ambient temperature.

Further evidence for a relatively strongly adsorbed species has also been obtained from a study of a supported copper surface. Following adsorption at -196°C, Smith and Quets[38] found that carbon monoxide desorbed from a 10% copper-silica catalyst at temperatures corresponding to heats of adsorption of 42 and 84 KJ mol^{-1}. If carbon monoxide was allowed to adsorb at higher temperatures, a desorption peak was noted at temperatures corresponding to an activation energy of desorption of 125 KJ mol^{-1}.

In his study of Cu(100) surfaces, Joyner[35] noted that, following carbon monoxide adsorption at 22°C, the adsorbed species did not desorb until a temperature of 87°C was attained.

1.3.4 Adsorbate Interaction

That a strong interaction exists between adsorbed carbon monoxide species must be given full consideration. Indeed, changes in the expected carbon monoxide stretching frequency on adsorption of $^{12}CO/^{13}CO$ isotopic mixtures confirms such an interaction[44]. However, this 'strong interaction' was shown in a new light when Jackson[60], working at atmospheric pressure and at 20°C on a copper-alumina catalyst, found that mixtures of ^{13}CO and $C^{18}O$ underwent isotopic equilibration. This effect has also been observed by Kleir on a copper-zinc - alumina catalyst[61], although he pronounced the scrambling as due to the presence of residual hydroxyl species on the copper catalyst. However, Au and Roberts[62] could find no evidence of a carbon monoxide-hydroxyl interaction on a Cu(111) surface at 22°C. Scrambling may also occur following dissociation of the adsorbed species on the copper surface. This appears unlikely at the temperatures used in this study, although Bertholet[63] produced evidence for carbidic species following the reaction of carbon monoxide and copper at 55°C and a fascinating SIMS study[64] found evidence for the formation of carbidic species at temperatures of 120°C following carbon monoxide adsorption on polycrystalline copper at ambient temperature.

1.3.5 Adsorption on Copper Cation Sites

The adsorption of carbon monoxide on a copper cation site substitutionally dissolved within a host lattice has been ascribed an important role in the activity of methanol synthesis catalysts (section 1.9.2). The possible adsorption characteristics of these sites must therefore be discussed.

The essence of the activity of these sites is, first, the presence of neighbouring zinc and oxygen atoms (which are considered to activate a hydrogen molecule) and, second, a stronger carbon monoxide chemisorption than is possible on a metallic copper site. This is apparently effected by increased d-electron back-donation in to the carbon monoxide molecule, which is more easily accomplished in the absence of a screening 4s electron. Two heats of adsorption of carbon monoxide on these types of sites have been given as 75 KJ mol^{-1} and 110 KJ mol^{-1} [65,66].

1.4 The Adsorption of Water on Copper Surfaces

Despite the fact that the interaction of water with copper surfaces may be vitally important in both the water gas shift and methanol synthesis reactions, only relatively few adsorption studies have been performed on this particular system. Those studies which do exist describe water adsorption on copper single crystals and clearly show that this is a surface sensitive adsorption process.

The least reactive surface appears to be the (100) since a UPS and work function study [2] could only find molecular water adsorption

on this face. Total molecular water desorption occurred between $-133^{o}C$ and $-123^{o}C$ and there was no evidence of hydroxyl formation at these or higher temperatures.

The (111) surface also appears relatively inert with respect to water adsorption. An XPS study[67] concluded that 90% of the water adsorbed at $-193^{o}C$ (0.82×10^{15} species cm^{-2}) desorbed at temperatures between $-133^{o}C$ and $-113^{o}C$, corresponding to a heat of adsorption of 34 KJ mol^{-1}. However, even after warming to room temperature, a residual hydroxylconcentration (0.14×10^{15} species cm^{-2}) was noted on the (111) surface. Campbell[68] has also studied the adsorption characteristics of the (111) surface and reported that the heat of adsorption of molecularly adsorbed water is 42 KJ mol^{-1}. The dissociative sticking probability of a water molecule on this surface was found to be very small (10^{-6} at $377^{o}C$).

Conflicting results have been obtained from studies of the (110) surface. Bange *et al.*[69] found only molecular adsorption on this face, with desorption occurring in two stages at $-113^{o}C$ and $-98^{o}C$. Spitzer and Luth[70] also found molecular adsorption on the (110) plane at temperatures between $-183^{o}C$ and $-98^{o}C$. LEED analysis confirmed that a C(2x2) water overlayer was formed at these temperatures. However, at temperatures of $-93^{o}C$ or greater,a combination of UPS and work function studies produced conclusive evidence of hydroxylation of the copper surface. At higher temperatures ($>-23^{o}C$) a disproportionation reaction was proposed to account for the observed 8% oxygen coverage of the copper surface.

Following the adsorption of water on Cu(110), at $-93^{o}C$, Wachs and Madix[53] undertook a desorption analysis of the system.

Water was found to desorb from the surface at two distinct temperatures, i.e. $-38^{o}C$ and $12^{o}C$. If first order desorption kinetics and a pre-exponential factor of 10^{13} sec^{-1} are assumed, these values are equivalent to respective desorption activation energies of 59 and 72 KJ mol^{-1}.

Further evidence of the structure sensitivity of this reaction has been obtained from a study using vapour deposited copper films[71]. At $-196^{o}C$ dissociative water adsorption was found to occur, but, following an annealing process, no uptake of water could be determined.

1.5 The Adsorption of Hydrogen on Copper Surfaces

In section 1.2.5 it was noted that the chemisorption of hydrogen on copper metal was proposed to involve the bonding of atomic hydrogen species with d-orbitals on the metallic surface. However, this proposal must be reconsidered in view of a recent study[72] which considers that covalent bonding between atomic hydrogen and metallic 4s orbitals enables strong hydrogen chemisorption on copper surfaces.

1.5.1 The Effect of the Copper Reduction Regime

In 1949 Kwan published a now frequently cited study[14] which related the effect of differing reduction procedures to hydrogen adsorption on copper powder. He considered that the results from studies which had found hydrogen to adsorb on copper powder[21,73,74] may have been invalid due to incomplete reduction of the copper oxide precursors. In his study, following reduction under pure hydrogen at $400^{o}C$ for 1 week, he found an activated adsorption (E_A = 82 KJ mol^{-1}) at temperatures greater than $300^{o}C$. A heat of adsorption of 146 KJ mol^{-1} was calculated for this process.

A further study of the hydrogen— deuterium reaction on copper foil[15] produced very similar results. No isotopic exchange occurred below 310°C and an activation energy of 96 KJ mol^{-1} was determined, which appeared to vindicate Kwan's theories. However, a number of early papers show that the reduction procedures used in many cases were extremely severe. Pease[22] reduced copper oxide at 200°C in pure hydrogen for 30-40 hours and yet found a hydrogen adsorption at temperatures less than 300°C. More recently Sinfelt[75] has observed hydrogen adsorption on copper, prepared by the reduction of copper oxide under pure hydrogen for 2 hours, at 450°C. The adsorption was characterised as weak, since all the hydrogen could be removed by 10 min. evacuation at ambient temperature. A thermal desorption study[76] of hydrogen from copper-zinc oxide mixtures also shows a very slight and broad hydrogen desorption from pure copper at temperatures between 127°C and 400°C.

These polycrystalline powder surfaces may be considered 'dirty' with respect to other adsorbents. Indeed, it should be noted that the low temperature activity of copper powders has been attributed to the presence of segregated transition metal impurities[77].

1.5.2 Adsorption of Hydrogen on Copper Films and Single Crystals

A number of studies have considered the interaction of hydrogen with evaporated copper films and the results are generally in good agreement. At ambient temperature, or higher, Beeck *et al.*[1] could find no hydrogen adsorption on porous, large surface area copper films. Further studies by Trapnell[4], Ponec *et al.*[12] and Allen and Mitchell[78] also failed to detect any hydrogen

adsorption on a variety of copper films.

The inactivity of the hydrogen-copper system appears to be confirmed by studies which found that deuterium would not adsorb on a Cu(110) single crystal[53] and hydrogen did not interact with a Cu(100) surface[79].

1.5.3 Surface Potential Studies of Hydrogen Adsorption on Copper

In 1963 a surface potential study[40] gave good evidence for an activated hydrogen chemisorption on evaporated copper films at temperatures as low as $0^{o}C$. In a subsequent and far more detailed study[18], Pritchard found that a negative surface potential was generated on copper metal by this activated chemisorption. The activation energy of the process was found to be 40 KJ mol^{-1} and a heat of adsorption was calculated to be 30-40 KJ mol^{-1}. This compared favourably with previous studies which reported heats of adsorption of 40 KJ mol^{-1}[80] and 49-43 KJ mol^{-1}[21].

Pritchard[18] rationalized the conflicting results of Kwan[14] in a postulate which did not invoke the possibility of either under-reduced or transition metal contaminated surfaces. He found that, in complete contrast to hydrogen, atomic hydrogen often produced a positive surface potential following adsorption on a Cu(111) plane. No such effect was noted for hydrogen and it was therefore concluded that this plane did not chemisorb the hydrogen molecule. Pritchard suggested that the high temperature reduction procedure of Kwan would leave only the (111) plane of polycrystalline copper intact, while other planes would develop (111) faces. This explained the inactivity of the 'high temperature' copper compared to many other copper powders, for which significant activity following

reduction at lower temperatures had been reported.

In a subsequent study, Pritchard[81] produced evidence from surface potential data to show that low index copper faces ((100), (111) and (110)) did not chemisorb hydrogen while the higher index (211), (311) and (755) planes showed enhanced dissociative ability. The heat of adsorption of hydrogen on Cu(311) was calculated to be 40 KJ mol^{-1}.

In complete contrast, molecular beam studies have found no evidence for structure sensitivity in the adsorption of hydrogen on copper faces[82]. A similar activation energy of hydrogen adsorption (21 KJ mol^{-1}) on Cu(100) and (310) surfaces implied that ledges, boundaries and other fault sites were not the principal regions of dissociative hydrogen chemisorption.

In summary, the experimental evidence generally points to an activated dissociation of hydrogen on copper surfaces. However, the temperature range in which this effect is observed and the structure sensitivity of the process are not yet fully clarified. Some evidence also exists for a more weakly adsorbed species existing on the copper surfaces. Indeed, a recent theoretical study[83] of the copper — hydrogen system, using calculations involving excited copper atomic states, led the authors to the conclusion that two chemisorbed forms of hydrogen could exist on copper. These are described as (i) involving very weak H-H bonds and (ii) involving atomic hydrogen. The calculations gave an activation energy of 117 KJ mol^{-1} for the latter adsorption process, compared with an experimentally observed value of 40 KJ mol^{-1}[18].

1.6 The Adsorption of Carbon Dioxide on Copper Surfaces

The most surprising aspect of studies relating to the adsorption of carbon dioxide on copper metal is, in fact, their relative scarcity. Unlike the adsorption of carbon monoxide and hydrogen on copper, the information relating to this particular adsorption system can at best be described as limited.

1.6.1 The Bonding of Carbon Dioxide to Copper

In a molecular orbital study, Anderson[31] calculated that carbon dioxide molecules adsorbed on a Cu(100) surface rest in a μ-bridging position, which involves the carbon atom interacting directly with two copper atoms (Cu-C distance = 1.5Å). As a result of metal d-orbital mixing with the carbon dioxide π^* orbitals, a bent carbon dioxide geometry was postulated with a $O-C-O$ angle of approximately 120°. The binding energy of this surface species was calculated to be 46 KJ mol^{-1}. More recently, ab-initio valence bond calculations[84] have considered the possibility of three different molecular carbon dioxide co-ordination geometries: pure carbon, pure oxygen and mixed carbon and oxygen co-ordination. In contrast to Anderson, only the purely carbon bonding mode was considered unlikely. However, as in Anderson's calculations, a bent, negatively charged carbon dioxide moiety was considered to be the most likely form of adsorbed species for all the differing geometries. On the basis of the deduced carbon dioxide-metal bonding scheme the reactivity of co-ordinated carbon dioxide was investigated and, while dissociation of the molecules was considered likely on transition metal surfaces, the apparently low binding energy of the carbon dioxide decomposition

products on Group 1B surfaces rendered this path unlikely. It is interesting to note that a value of 58 KJ mol^{-1} was used as the heat of adsorption of carbon monoxide on copper while, as discussed in section 1.3, far higher initial heats have actually been determined.

1.6.2 The Heat of Adsorption of Carbon Dioxide on Copper

The relatively weak bonding of carbon dioxide on copper surfaces, calculated theoretically in the above studies, has been verified experimentally. In a UPS/XPS study of carbon dioxide adsorption on evaporated copper films, Norton and Tapping[33] found little shift in both the carbon and oxygen 1s binding energies of adsorbed carbon dioxide, with respect to gaseous carbon dioxide, and noted little attenuation of the copper valence bands. This led them to consider that carbon dioxide was 'almost certainly' physically adsorbed and the heat of adsorption was estimated as $\leq$38 KJ mol^{-1}. A heat of adsorption of 19 KJ mol^{-1} was generated by Waugh[56], from studies of carbon dioxide adsorption on copper powder, by a frontal chromatographic technique. Other, more qualitative, studies generally concur. Using a combination of AES, LEED and ellipsometry Habraken *et al.*[85] could find no interaction of carbon dioxide with a Cu(111) surface at a pressure of 10^{-3} torr and temperatures of 24°C and 364°C. Trapnell[86] could find no evidence for carbon dioxide adsorption, at -78°C, on sintered copper films, although the films did have very low surface areas and detection of small amounts of adsorption was considered difficult. Stone and Tilley[87] could find only 'slight' carbon dioxide adsorption on copper, but no indication of the copper surface area or adsorption temperature was given. In contrast,

Taylor and Burns[73] found a measurable uptake of carbon dioxide, at 25°C, on a 'spongy' copper adsorbent, prepared by hydrogen reduction (at 250°C) of a nitrate generated copper oxide.

1.6.3 Carbon Dioxide Decomposition

In all these theoretical and experimental studies the production of carbon monoxide during the adsorption is given little credence. It is therefore surprising to note that, in the 19th century, Pfaundler[88] produced evidence showing that carbon dioxide dissociation did occur on copper surfaces. A later [14-C]isotope study[89] found dioxide dissociation to occur at high temperatures with an activation energy of 253 KJ mol^{-1}.

In complete contrast, Wachs and Madix[53], who studied carbon dioxide adsorption on Cu(110) single crystals at -93°C, determined that over 99% of the adsorbed carbon dioxide dissociated to form carbon monoxide and a surface oxygen species. This reaction formed an adsorbed carbon monoxide species whose activation energy for desorption was calculated to be 58 KJ mol^{-1}.

Other, indirect, evidence exists for this carbon dioxide decomposition pathway. Kleir[90] found that copper-zinc oxide-alumina catalysts, which had been reduced by carbon monoxide, could be re-oxidised by the reaction of carbon dioxide at 250°C with the concomitant appearance of carbon monoxide. Another study of this ternary catalyst[91] found that the reduction of the catalyst (by hydrogen) was significantly delayed in the presence of carbon dioxide. However, doubt remains as to whether this is due to a surface reoxidation by the dioxide or to a blocking carbon dioxide adsorption on the oxidised copper surface.

It should be noted that none of the above experimental studies have considered the possibility that the adsorption process may be drastically altered by the presence of segregated alkali metal on the copper surface. A stunning example of this effect has been detailed by Solymosi[92] for carbon dioxide adsorption on palladium single crystals.

1.7 The Adsorption of Oxygen on Copper Surfaces

The deposition of oxygen on a copper surface may be effected by a number of adsorbates. As detailed in section 1.6.3, carbon dioxide may act as a source of surface oxygen via a dissociative chemisorption. However, no information regarding the surface overlayer formed by this process has been published. The facile reaction of dioxygen with copper metal has been extensively studied and will be briefly discussed in this section. Of more relevance to the present study is the controlled oxidation of copper surfaces which can be achieved by reaction with nitrous oxide at or near ambient temperatures. Oxygen can also be thought of as a copper 'activating' agent (section 1.2.6), in that a variety of reactions proceed on the oxidised surface, which would not readily occur on a fully reduced surface. The sometimes dramatic effect of surface (and sub-surface) oxygen on a variety of adsorbates will be discussed in section 1.8.

1.7.1 Dioxygen Chemisorption

The adsorption of dioxygen on copper single crystals was first studied by Rhodin in 1953 [93]. Although giving no quantitative

analysis, he determined that this process required little activation energy. More recently Habraken et al.[85,94,95,96] quote the activation energy for this dissociative chemisorption as 8-17 KJ mol^{-1} on Cu(111), 8 KJ mol^{-1} on Cu(110) and 5.4-14.6 KJ mol^{-1} on Cu(100). These controlled dosing experiments lead to a maximal coverage of one half monolayer of oxygen, but if more dioxygen and high temperatures are available further rapid oxidation can occur. Habraken[96] found that, on Cu(100), three stages of oxygen uptake could be observed, which correspond closely to results obtained from a study of the oxidation of copper powders at 20°C[57]. The first stage involves formation of a monolayer of oxygen with evolution of the heat of adsorption of 420 KJ mol^{-1}. Further rapid oxidation to a temperature dependent limiting thickness then occurs with a heat of 344 KJ mol^{-1} and finally an activated (E_A = 19 KJ mol^{-1}) adsorption of oxygen on the oxide layer completes the process. XPS and Auger studies[97,98] have found that the final oxide formed at the copper surface has an identical structure to that of bulk cuprous oxide. This suggests that some degree of surface reorganisation has occurred. In a fascinating NEXAFS study of a (2x1) oxygen overlayer on a Cu(110) single crystal[99], evidence has been produced which suggests that, even at these relatively low coverages, reconstruction of the surface is effected. In this case the original (110) surface was postulated to form a 'missing row' or 'saw-tooth' structure. An earlier study had also found that, following oxygen adsorption, when a (110) surface was heated from -196°C to ambient temperature, a surface rearrangement occurred which allowed further oxygen uptake[100].

1.7.2 Nitrous Oxide Decomposition

Unlike dioxygen, the reaction of nitrous oxide with metallic copper, at ambient temperatures, appears to occur to only a limited extent. Indeed, although the reactions of dioxygen and nitrous oxide with copper show a thermodynamic correspondence, their kinetics are completely different. For example, Dell, Stone and Tilley[57] found that, at 20°C, the heat of adsorption of oxygen was similar from both dioxygen and nitrous oxide. However, only a fraction of the polycrystalline copper surface was oxidised by nitrous oxide while full oxidation was possible by reaction with dioxygen.

Similarly, Osinga *et al.*[101], using a static reaction system, found no bulk oxidation of copper powder by nitrous oxide, at temperatures below 120°C and no effect of differing nitrous oxide pressures. When a flow or pulse-flow system has been utilised for this chemisorption, temperatures of less than 90°C[102] and 20-60°C[103] are considered to produce only monolayer oxygen coverage. This useful dissociative chemisorption is now routinely used for determination of copper metal surface areas in supported and unsupported copper catalysts[104], although some care must be taken when oxides of chromium, zinc and aluminium are integral components of the catalyst, since they have been found to promote bulk copper oxidation[105].

In contrast, Parris and Klein[59] obviously have little faith in this method for copper metal surface area determination. They consider that the use of static systems will lead to bulk copper oxidation, the effect of the supporting material (if any) is unclear, that the kinetics will depend on the copper crystallite size and that the

effect of reaction induced temperature transients is unknown. It is proposed that dioxygen chemisorption at -196^{o}C is a more viable method for surface area determination.

However, most of the available literature points to the fact that, at ambient temperature, following completion of the oxygen monolayer, nitrous oxide decomposition ceases. This has been confirmed by Narita et al.[106] who studied the decomposition reaction with a combination of a conventional volumetric adsorption apparatus and ultra-violet photoelectron spectroscopy. Between 70^{o}C and 100^{o}C a constant amount of nitrogen was evolved with the corresponding formation of a peak in the UPS spectrum attributable to the presence of a surface cuprous oxide. The kinetic features of this process on a number of single crystal surfaces and the form of the associated oxygen overlayers are of obvious interest and have been thoroughly investigated by Habraken et al.[85,94,95,96]. The salient features of these studies are summarised in Table 1.1. The overlayer structures determined by the LEED analyses were exactly repeated on dissociative chemisorption of dioxygen.

Single Crystal Surface	$\Theta_{sat.}$	S_o (at rm. temp)	$E_{Act.}$ (KJ mol^{-1})	Surface Overlayer
(111)	0.45	10^{-9}	44	$(\sqrt{2}x\sqrt{2})R45^{o}$
(110)	0.5	0.2	8.4	(2x1)
(100)	0.5	$5x10^{-5}$	13.4	Random

Table 1.1: Salient Features of Nitrous Oxide Decomposition on a variety of Copper Surfaces

1.8 The Modification of Adsorption on Copper Surfaces by Preadsorbed Oxygen

It has long been recognised that any material added to catalyse a specific reaction cannot, especially in heterogeneous gas-solid systems, be defined as the catalyst, but only as a catalytic precursor. An example of this effect is that of the carbonaceous material laid down on a variety of supported metal catalysts during a variety of hydrocarbon hydrogenation reactions. In a radiotracer study, Webb and Thomson[107] proved conclusively that these residues did not poison the hydrogenation reaction, but rather acted as vital hydrogen atom transfer agents within the catalytic system.

The previous sections have shown that it is entirely feasible for a copper surface to become partially or fully oxidised in the presence of methanol synthesis gas and the possible effects of this adsorbed oxygen on a variety of relevant adsorbates must therefore be considered.

1.8.1 Methanol

In 1964 Lawson and Thomson[108] determined that a variety of copper films, foils and wires could be activated for methanol dehydration by an oxidation process. Interestingly, sub-surface oxide layers were also found to promote the dehydration reaction and this led the authors to postulate that an n-type semi-conductor region, created at the metal oxide interface, was the effective catalyst in this system.

Wachs and Madix[53] and Russell[109] have also studied this reaction and find that, although methanol desorbs molecularly from a fully reduced copper surface at low temperatures, the presence of a

fraction of a monolayer of oxygen promotes methanol adsorption and allows decomposition to occur.

1.8.2 Carbon Monoxide

Stone and Tilley[87] have shown that carbon monoxide undergoes a slow reaction with an oxidised copper surface which, at slightly elevated temperatures, produces gaseous carbon dioxide. Habraken et al.[85,94,95,96] have shown that this reaction is essentially structure insensitive and proceeds with an initial reaction probability of 10^{-4} -10^{-5} and an apparent activation energy of 26-33 KJ mol^{-1}. In an earlier study Ertl[110] determined an activation energy of 125 KJ mol^{-1} for the surface process.

A number of other studies[47,111] have produced evidence to show that a variety of carbonato and, in the presence of hydrogen, formate species may also be produced by reaction of carbon monoxide with preadsorbed oxygen. In contrast, Wachs and Madix[53] found that oxygen simply blocked carbon monoxide adsorption on a Cu(110) surface and had no effect on the desorption activation energy of the adsorbed carbon monoxide species.

1.8.3 Hydrogen

Wachs and Madix[53] found no promoting effect of adsorbed oxygen in deuterium adsorption on a Cu(110) surface and Ponec et al.[112] could find no reaction of hydrogen with adsorbed oxygen, unless the hydrogen had been previously atomised. However, Roberts and Ryder[113] have produced evidence to show that hydroxyl species can be produced by the reaction of hydrogen with a partially oxidised copper

foil at 110°C and 1.3 KPa. A structure insensitive hydrogen reduction of an oxidised copper surface has also been characterised[114] and the activation energy determined to be 45 KJ mol^{-1}[115].

1.8.4 Water

Au, Breza and Roberts[67] have reported that the oxygen-hydrogen bond in a molecularly adsorbed water molecule may be activated by hydrogen bonding to an adsorbed oxygen species. Spitzer and Luth[70] also found that the presence of oxygen on a Cu(110) surface induced the formation of a hydroxyl species, at some 30°C lower than on a corresponding clean surface. However, in contrast to Au *et al.*[67], the latter workers concluded that the oxygen adsorbate did not participate directly in the hydroxylation.

Cu(100) surfaces may also be activated, for hydroxyl formation, by preadsorption of oxygen[2]. Bange *et al.*[69] reported that water desorption occurred at temperatures of -113°C and -175°C from a clean Cu(110) surface, but from three higher energy desorption states (-73°C, -43°C and 7°C) on an oxidised (110) surface.

1.8.5 Carbon Dioxide

An activated adsorption of carbon dioxide on oxidised copper, possibly involving formation of a carbonate, was reported by Stone and Tilley in 1950[87] with a heat of adsorption of 97 KJ mol^{-1}. Winter[116] found that bulk cuprous oxide facilitated an oxygen exchange reaction which occurred, again possibly via a carbonate species, with an activation energy of 17 KJ mol^{-1}. However, evidence has been reported to show that little carbonate formation prevails during this

adsorption process[111]. Temperature programmed desorption studies have also provided little evidence for carbonate formation[115], although dramatically increased carbon dioxide coverages were observed on oxidised copper surfaces. The preadsorbed oxygen was also found to induce a number of high energy adsorption states. Kinetic analysis of the desorption data gives desorption activation energies for these states of 67, 84, 109, 113 and 125 KJ mol^{-1}.

1.9 The Mechanism of Methanol Synthesis on Copper Based Catalysts

It is a strange fact, possibly unique to catalytic chemistry, that a detailed understanding of any particular catalytic system may only be obtained after it has proven commercially viable. The catalytic process developed by I.C.I. for the large scale production of methanol is a case in point. To facilitate the highly selective production of methanol, a mixture of carbon monoxide, carbon dioxide and hydrogen (10:10:80) is passed over a copper-zinc oxide-alumina catalyst (60:30:10) at 250^{o}C and 50 atm. pressure. Although this process was developed some twenty years ago it is only recently that any potential methanol precursors and their associated adsorption sites have been postulated.

In his 1955 review, Natta[20] stated that, although copper based catalysts were extremely active for methanol synthesis (with lower activation energies than the traditional zinc oxide-chromia combinations), they had only a very short durability since they were extremely sensitive to poisoning and ageing processes. At that time methanol synthesis was conducted with a carbon monoxide- hydrogen feed and at temperatures and pressures of 300^{o}C and 100 atm. Under

these conditions, Natta found pure copper to be 'practically inactive' for methanol production, but some copper-zinc oxide combinations (with 30-40% copper) did show good activity. Further addition of a third component, for example alumina, appeared to act by increasing the catalyst's resistance to ageing.

The copper-zinc oxide combinations utilised by Natta were studied in great detail by Kleir[90], who proposed that the methanol synthesis activity in these catalysts was due to a synergic interaction of copper and zinc oxide[26]. This postulate invoked the idea that the higher combined activity of the copper-zinc oxide couple, compared to that of the separate components, is due to the formation of a chemically unique and catalytically active species. Indeed, Kleir[90] produced good experimental evidence for the existence of a unique chemical entity within these catalysts. Elegant use of STEM, ESCA and infra-red spectroscopy found a surface species existing as a copper(I) cation, substitutionally dissolved in the zinc oxide matrix. Natta[20] had also proposed a copper(I) species (in copper chromite) which may have been responsible for the activity within many of his catalysts, but had no direct evidence for such a species.

Subsequent to Kleir's proposal of copper-zinc oxide synergy, many other studies have conclusively proved that a copper cation species does exist in a variety of copper catalysts. A series of papers by Apai[66,117] gives evidence for a copper cation species in copper-chromia catalysts and gives details of vacuum heating treatments which increase the concentration of this surface species and, consequently, the activity for methanol production. A recent EXAFS study of a copper-zinc oxide combination also postulates the existence of the copper(I) species[118]. In contrast, another EXAFS

study could find no evidence for this copper cation in a copper-zinc oxide-alumina combination[119].

Evidence for the copper cation species appears to be overwhelming and all that apparently remains is to deduce if and how this species becomes involved in the synthesis mechanism. Most authors agree with Kleir's original suggestion that the copper cation is the site which chemically activates a carbon monoxide molecule for further reaction[90]. As detailed in section 1.3.5, an increased heat of adsorption of carbon monoxide has been found on these sites.

Further details of the mechanism are not clear since, typically, a variety of studies have all found evidence for different intermediates on the surface of the catalyst. From a FTIR study, Edwards and Schrader[120] postulated that the activated monoxide species may react to form a formate species on the adjacent zinc oxide lattice, which is then further hydrogenated to methanol. Kleir[61,121] has also produced evidence for the formation of a formate intermediate by the interaction of a monoxide molecule and hydroxyl species, although, in a desorption study, Waugh *et al.*[115] could find no evidence of surface formate formation, from a carbon monoxide-hydrogen feed. Kleir has also used chemical trapping methods to obtain evidence for an aldehydic species on the catalytic surface which may exist as either an adsorbed formyl, formaldehyde or hydroxycarbene species[122]. Despite this confusion, Kleir has postulated a most convincing and credible mechanism for methanol synthesis from synthesis gas mixtures containing a large percentage of carbon monoxide and little carbon dioxide[90]. This consists of carbon monoxide

activation on a copper cation site, hydrogen activation on zinc oxide and a subsequent carbon monoxide-hydrogen interaction which leads to methanol formation.

The relevance of Kleir's mechanism to that which exists in the actual industrial synthesis is questionable. In the studies of Kleir et al.[90], methanol was produced from synthesis gas containing 98% carbon monoxide and only 2% carbon dioxide, compared to the equal mole fractions of carbon oxides used in industrial plants[25]. Kleir proposed that the role of carbon dioxide was that of a promoter in the system, that is acting to keep a proportion of the surface in an oxidised form. Too little dioxide would cause deactivation by over-reduction, while overloading the synthesis gas would again cause deactivation by carbon dioxide poisoning of the active copper sites.

Natta[20] also found a promoting effect of carbon dioxide, but attributed it, at least in part, to a temperature regulating effect which prevented sintering of the copper surface. This effect was caused by hydrogenation of carbon dioxide to methanol which was calculated to evolve less heat than the corresponding monoxide hydrogenation. The fact that carbon dioxide itself may form methanol is sadly overlooked by Kleir in his review[90]. This is most surprising since Russian research[123] had shown, several years previously, that in carbon monoxide-carbon dioxide reaction mixtures, it was the carbon dioxide component which was preferentially hydrogenated directly to methanol. In the same study, carbon monoxide-hydrogen mixtures were found to be inactive for methanol production over copper-zinc oxide-alumina catalysts. This work involved the use of

[14-C]radiotracers and has since been repeated, with similar findings, by Chinchen et al.[25].

Following this latter publication a flood of scientific data has appeared, all of which gives credence to these [14-C] studies. From a T.P.D. study, Waugh[56] found that the activity for methanol production, on copper-alumina, was at least an order of magnitude greater for carbon dioxide— hydrogen mixtures than the carbon monoxide-hydrogen combination. The activity and selectivity for methanol production has also been found to be higher for carbon dioxide-hydrogen mixtures, on copper-zinc oxide-alumina catalysts, by both Bardet[124] and Duprez[76] and a study of the kinetics of the synthesis has shown that carbon monoxide actually has an inhibiting effect on the rate of methanol production[125].

If the assumption is made that methanol is produced, under industrial conditions, by the hydrogenation of carbon dioxide, the role of the copper(I)-zinc oxide species which Kleir et al.[90] postulated as the active surface species must be re-examined. In fact a number of studies have obtained evidence which shows that the synergic interaction of the copper-zinc oxide couple may be of no catalytic significance.

Raney copper-zinc catalysts, containing 97% copper have been found[126] to possess an activity for methanol production and this led to the conclusion that the absolute inactivity of pure copper as determined by Kleir[90], was due to the small surface area of his sample. Further evidence for this was gained by revealing that a high area (45 $m^2 g^{-1}$) copper-silica catalyst had, initially, very high

activity for methanol synthesis. Waugh et al.[115] have also found the specific activity of unsupported copper to be comparable to that of a variety of supported catalysts. That the essence of methanol synthesis activity resides totally within the copper component of any catalyst has since been shown by Chinchen et al.[127] and Amenomiya et al.[128]. Their findings, that the activity of a copper based catalyst is dependent only on the total copper metal area and is completely independent of the presence of any particular oxidic support, give irrefutable evidence for this thesis.

Subsequent to these studies, a renewed search has begun for the active site for methanol production. This has been necessary since it is known that more than one type of copper-species may exist on the surface of a copper-zinc oxide-alumina catalyst. In an XPS analysis of a reduced copper-zinc oxide catalyst, Okamoto[129] concluded that copper metal particles and an easily oxidisable two dimensional copper monolayer co-exist on the catalytic surface, which is in good agreement with the findings of a more recent EXAFS study[118]. It may, however, be of more relevance to consider the state of the copper surface under industrial conditions and this has been achieved using an elegantly simple, in situ, nitrous oxide surface area determination[127]. This produced evidence that the copper surface is oxidised during methanol synthesis, to a degree vitally dependent on the carbon monoxide-carbon dioxide synthesis gas ratio. This has been confirmed by Gusi et al.[130], who also contrived to produce a number of interesting relationships between the total quantity of oxidised copper and copper in zinc oxide within the system and the

methanol synthesis activity.

The role of the oxidic components of a commercial copper based catalyst (which are zinc oxide and alumina) remains to be clarified. As previously noted, the oxidic materials, unlike copper, are not considered to be directly involved in the methanol synthesis mechanism. Yet Hoppener[131] found that, on addition of magnesium to the oxidic portion of a typical methanol synthesis catalyst, a significant suppression of catalytic activity was produced. This experiment proved that zinc oxide and alumina do have a significant role to play in generating catalytic activity. It is possible that the oxides act as structural promoters within the catalyst, for example by acting to prevent, or greatly hinder, copper crystallite sintering.

The mechanism by which carbon dioxide is transformed to methanol, on a copper surface,remains to be discussed. Early studies[132] have concluded that this process involved the formation and subsequent hydrogenation of carbon monoxide. However, the previously detailed radiotracer studies[25,123] conclusively proved that a direct hydrogenation of carbon dioxide had to occur independent of that of carbon monoxide. Waugh[56] has in fact found different kinetics for these hydrogenations on copper-alumina catalysts. The formation of methanol from carbon dioxide-hydrogen mixtures had an activation energy of 121 KJ mol^{-1} while that from carbon monoxide and hydrogen was far more temperature dependent, requiring an activation energy of 251 KJ mol^{-1}. In the carbon dioxide reaction, Waugh ascribed this activated process to hydrogenolysis of a formate intermediate, which had been successfully characterised by temperature programmed desorption. This formate species could be formed at 100^{o}C while

methanol production did not occur until 190°C. A high temperature and pressure infra-red study of the carbon dioxide- hydrogen reaction[133] produced evidence that bands, attributable to a formate species, appeared at 100°C and, thereafter, showed a decreasing intensity, coincident with the production of gas phase methanol.

It seems likely that, on copper-alumina catalysts, this is the definitive mechanism for methanol production. Unfortunately, the addition of zinc oxide may rather disrupt this model since Rameroson et al.[134] discovered, from chemical trapping, that both carbon monoxide-hydrogen and carbon dioxide-hydrogen mixtures formed formate species on copper-zinc oxide combinations. An [18-O]labelling study[135] has also added chaos to confusion, since the results obtained could only be explained by assuming that, under the conditions of the study (220°C, 17 atm, copper-zinc oxide catalyst in a batch reactor) methanol is formed by independent carbon monoxide and carbon dioxide hydrogenations. A direct carbon monoxide-carbon dioxide interconversion was also found to occur completely independent of the water-gas shift reaction.

1.10 The Mechanism of the Water Gas Shift Reaction on Copper Based Catalysts

The production of hydrogen from carbon monoxide and steam is a widely used process in the chemical industry. Iron based catalysts, operating at temperatures in excess of 300°C, are utilised to effect a fast hydrogen production, but since the reaction is exothermic (-40.6 KJ mol^{-1}) the conversion is thermodynamically limited at these

temperatures. Accordingly, a copper-zinc oxide-alumina catalyst has been developed which is active at lower temperatures ($\sim 200^{o}C$) and, therefore, allows conversion of a few per cent carbon monoxide to carbon dioxide.

The catalyst itself is similar to that used in methanol synthesis, although it has a smaller copper content (30%) than the traditional methanol catalyst (60% copper). The discussions surrounding the location of the catalytic activity within this catalyst are broadly similar to those previously detailed for the 60% copper catalyst. Kleir[61] considers that the synergic interactions of the copper and zinc oxide components of the catalyst, producing a chemically unique copper cation-zinc oxide site, hold the key to the activity of the system. Evidence is however accumulating which shows, categorically, that the activity of the catalyst is dependent only on the available copper metal surface area. As early as 1967 Uchida[136] produced a copper-alumina catalyst which he found to have similar activity to the copper-zinc oxide-alumina combinations. Kuijpers *et al.*[137] have also produced a variety of active copper catalysts, containing no zinc oxide, and recently Campbell[68] has determined that a Cu(111) surface has the same activation energy, reaction order and turnover number as a variety of supported catalysts.

The actual mechanism of the shift reaction has undergone less scrutiny than that of the methanol synthesis reaction, but debate relating to possible mechanisms of the process have been no less intense. An 'associative' mechanism has been considered, in which it is

assumed that the reacting gases adsorb, diffuse across the catalytic surface and thence together form a surface moiety which eventually decomposes to yield the reaction products. Kleir[61] considers that a formate species forms on the copper cation site within the ternary catalyst and this, in the absence of hydrogen, could act as an intermediate in the shift reaction. Grenoble[138] also proposed a formate species as intermediate although, on this copper-alumina catalyst, he considered it to be located on the alumina support. The high activity of this copper catalyst was ascribed to the 'ideal' heat of adsorption of carbon monoxide on copper, which allowed a reasonable coverage to acrue yet did not prevent diffusion on to the alumina component.

As detailed in section 1.9.5, it has become increasingly apparent that a formate species may also exist on the copper surface of these catalysts in the presence of the shift reaction gases[133,134]. Amenomiya[128] claims that this species is pivotal in both methanol synthesis and the shift reaction since, in a study of reaction transients, the formate species produced by the adsorption of carbon dioxide and hydrogen on copper catalysts, were found to decompose to carbon monoxide, or methanol in the presence of hydrogen. van Herwijnen and de Jong[139] also strongly favour an associative mechanism involving a formate intermediate. They found that formate species, produced on copper surfaces by the adsorption of formic acid, decomposed to form carbon dioxide and hydrogen with a selectivity of 98.5-99.5%. This apparently correlated well with the rates of the forward and reverse shift reactions. Further, and perhaps rather dangerously, the results of a kinetic study were explained in terms

of Langmuir-type rate equations, from which it was inferred that the active species on the surface was a formate moiety.

A drastically different 'regenerative' mechanism has also been considered as a possible reaction pathway. In this scheme sequential oxidation and reduction steps are proposed to occur on the copper surface.

$$CO_{2(g)} + (S) \rightleftharpoons CO(g) + O(ads)$$

$$H_{2(g)} + O(ads) \rightleftharpoons H_2O(g) + (S)$$

van Herwijnen[139] considered this thesis and subsequently rejected it because the thermodynamics of cuprous oxide formation were calculated to be improbable ($\Delta G = +80KJ\ mol^{-1}$). However, Waugh *et al.*[115] recalculated the thermodynamics, considering the formation of a surface oxygen species to be totally different to that found in bulk cuprous oxide, and produced figures proving that no equilibrium limitation existed to surface oxide formation. Indeed, this paper gave evidence for oxygen deposition on polycrystalline copper by water decomposition. The kinetics of methanol synthesis and the shift reaction were also found to be different and hence it was postulated that the formate intermediate, apparently pivotal in methanol synthesis, had no part to play in the shift reaction.

A further refinement of the regenerative mechanism is possible and of interest to this study.

In 1968 Uchida[140] proposed that the high specific activity of low temperature shift catalysts, containing a relatively low copper content, could be explained in terms of the redox mechanics. It was

suggested that the 'finer' copper particles, produced in the low percentage copper combinations, were more easily oxidised than those found in the methanol-type catalysts and this therefore allowed the redox mechanism to secure equilibrium yields more readily. Kuijpers et. al.[137] also found the reaction to be structure sensitive and although they could not rule out the associative mechanism on this basis, they acknowledged that this did allow consideration of the redox mechanism as a feasible alternative pathway.

A recent kinetic study of the shift reaction over a copper (111) single crystal found that the reaction was zero order in carbon monoxide and had distinctly positive order with respect to the water concentration[68]. This, and the relatively small dissociative sticking probability of water on the (111) surface, led the authors to propose that the regenerative mechanism could account for these findings. An apparent activation energy of 71 KJ mol^{-1} was calculated for the process which, if water adsorption is considered to be non-activated, infers an activation energy for the dissociation of a molecularly adsorbed water molecule of 113 KJ mol^{-1}.

C H A P T E R 2

OBJECTIVES OF THIS STUDY

OBJECTIVES OF THIS STUDY

The studies described in this thesis, that is the interaction of carbon monoxide, carbon dioxide, hydrogen and water with polycrystalline copper, were undertaken in an attempt to obtain:

(1) an understanding of the adsorption characteristics of carbon monoxide, carbon dioxide, hydrogen and water on polycrystalline copper,

(2) knowledge of the competition for adsorption sites between the different adsorbates,

(3) evidence for any catalytically significant interactions between the adsorbed species and

(4) kinetic data which would allow mechanistic pathways for both the methanol synthesis and water gas shift reactions to be proposed.

The detailed objectives of this thesis are to study:

(a) the separate and competitive adsorption of [14-C]radiolabelled carbon monoxide and carbon dioxide on polycrystalline copper at low pressures and ambient temperature,

(b) the influence, if any, of hydrogen on the adsorption of carbon monoxide and carbon dioxide on polycrystalline copper at ambient temperature,

(c) the adsorption of carbon monoxide and hydrogen on a preoxidised copper surface,

(d) the adsorption and reaction of carbon dioxide on polycrystalline copper at subambient and elevated temperatures,

(e) the adsorption and reaction of water with polycrystalline copper at a variety of temperatures,

(f) the desorption activation energies and surface coverages of the adsorbates produced by the separate adsorption of carbon dioxide, carbon monoxide, water and hydrogen on polycrystalline copper and

(g) the reaction of carbon monoxide and water and the reaction of carbon dioxide and hydrogen on polycrystalline copper.

CHAPTER 3

EXPERIMENTAL

EXPERIMENTAL

3.1 Introduction

The aim of this chapter is to set out the details of the experimental techniques applied in this study. This will involve a full description of the apparatus and materials used and a summary of the relevant experimental procedures. It is of interest to consider why these techniques have been applied in this project, and to gain a feel for the type of analysis that may be achieved using these experimental methods.

Although a large number of techniques may be applied to study the gas-surface interface, it is recognised that no technique, by itself, may allow total characterisation of a particular adsorption system. Even the techniques of surface science, which allow characterisation of the chemical form of adsorbates and description of the nature of individual adsorption sites, cannot possibly provide information regarding adsorptions at even moderately high gas pressures. Analysis of the adsorbate-adsorbent interaction may be effectively swamped at high gas pressures, simply because the amount of material interacting with the catalytic surface is only a small fraction of that within the whole system. However, the use of radiotracers does allow direct, non-destructive, in situ monitoring of adsorption processes, on catalytic surfaces, at relatively high ambient gas pressures. The details of this technique, which has evolved from the pioneering work of Thomson et al.[141,142] are described in section 3.2.2, but a brief discussion of the power (and inadequacies) of the technique are given in this section.

The fully reduced copper powder utilised in this study has a total surface area of $4m^2g^{-1}$ copper metal. When the amount of copper used in each experiment is considered (typically 0.18g) this provides an available area of $0.72m^2$ and, consequently, 7.2×10^{18} copper metal atoms for adsorption purposes. Monolayer coverage of this copper area can then be effected by only 1.2×10^{-5} moles of carbon monoxide (assuming a Cu:CO ratio of 1:1). However, if the carbon monoxide has been doped with a [14-C]radiolabel, and is known to have a specific activity of 1m Ci $mmole^{-1}$, this small quantity of adsorbed material will be undergoing 7400 d.p.m. It is obvious that a suitably positioned Geiger-Muller tube, whose efficiency may only be 5%, will detect the presence of the adsorbed radiolabel. In this example monolayer carbon monoxide coverage would provide a count rate of 370 c.p.m. compared to background levels of 40-50 c.p.m. Even small quantities of adsorbed species, corresponding to a few per cent of a monolayer, would then provide count rates outwith the standard deviation associated with the background reading.

This simple example outlines the potential power of the direct monitoring technique which has provided all of the data presented in Chapter 5. There are, of course, inherent problems with the technique, notably the fact that G.M. detectors are temperature sensitive, which therefore limits adsorption studies to ambient temperature. By far the most important limitation of the technique is the fact that, although the determination of a count rate emanating from a metal surface proves, irrefutably, that adsorption has occurred, the direct monitoring technique provides no information regarding the

chemical form of the adsorbed species. Temperature programmed desorption, coupled with a combined G.C.-proportional counter arrangement, provides a means whereby information regarding the chemical form of the adsorbed species present in these systems can be obtained. However, accurate and quantitative information regarding the thermodynamics and kinetics of the adsorption processes was only obtained by the use of on-line mass spectrometry. This experimental set-up, which is described in section 3.3, also allowed temperature programmed desorptions and temperature programmed reactions to be effected.

3.2 The Direct Monitoring Technique

3.2.1 The High Vacuum Apparatus

The apparatus consisted of a conventional glass high vacuum system as shown in Fig. 3.1. The pump section consisted of a mercury diffusion pump backed by a rotary oil pump, which allowed the pressure within the system to be maintained at $\leq 10^{-4}$ torr, as measured by a Pirani Gauge (Edwards G5C 2). Pressures of between 1 torr and 760 torr were measured by a mercury manometer.

Non-radiolabelled gases were stored in four 2 litre storage vessels, which were connected to the secondary manifold via 4mm taps. These bulbs could be filled by flowing gas, from a high pressure cylinder, through tap F, and into the evacuated storage vessel. The radiolabelled materials were stored in two adjacent 1 litre vessels, both of which had associated side arms for the attachment of ampoules of [14-C]carbon dioxide. All gases could be fed, in a

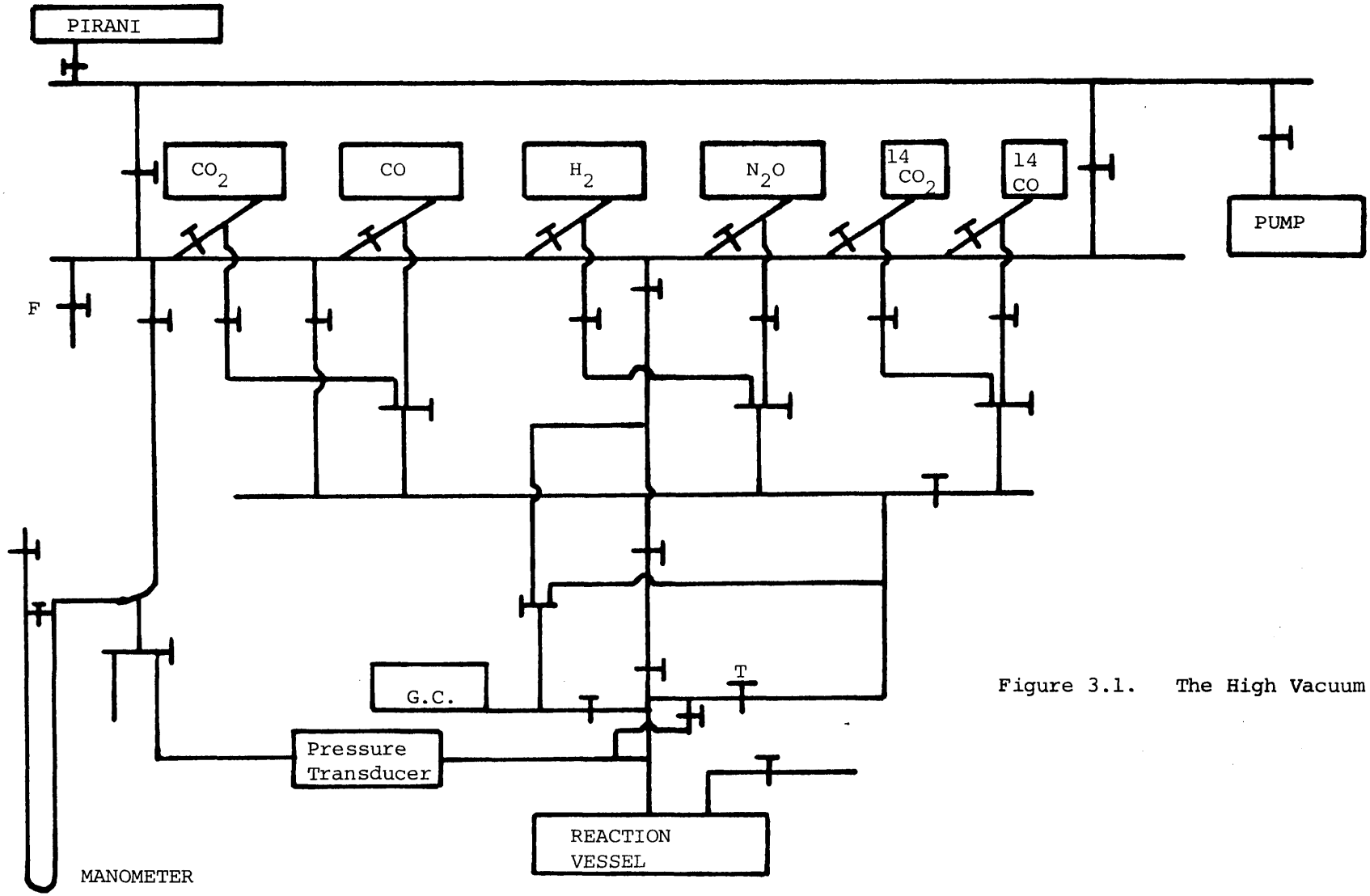

Figure 3.1. The High Vacuum Apparatus

controlled manner, through a series of pressure reducing volumes into the reaction vessel via tap T (2mm).

The reaction vessel, of volume 352 cm^3, was directly connected to the secondary manifold by a series of 4mm taps, thereby allowing fast and effective evacuation. Small pressure changes within the reaction vessel were monitored, to within ±0.0025 torr, by a differential pressure transducer (SE Labs (EMI) Ltd. SE 21/v) whose output was monitored graphically on a potentiometeric chart recorder (Servogor 420). The transducer was calibrated against the mercury manometer using a cathetometer to measure the height of the mercury columns.

3.2.2 The Reaction Vessel

Fig. 3.2. shows the reaction vessel and combined adsorption monitoring apparatus used in this study. The vessel has three B34 sockets, one of which is sealed with a B34 stopper and can easily be removed to allow access to the apparatus. Two intercalibrated G.M. tubes, sealed with Araldite into B34 cones, were positioned in the remaining sockets. When in this position the G.M. tubes were situated directly above a glass 'boat' whose surface was split into two equal portions by a glass dividing wall. The catalyst was spread evenly across one portion of the boat. This was effected by slurrying the catalyst and then heating the mixture, with constant agitation, to dryness in a stream of hot air.

The catalyst could be moved into the furnace region of the reaction vessel, for controlled oxidation or reduction, by the external

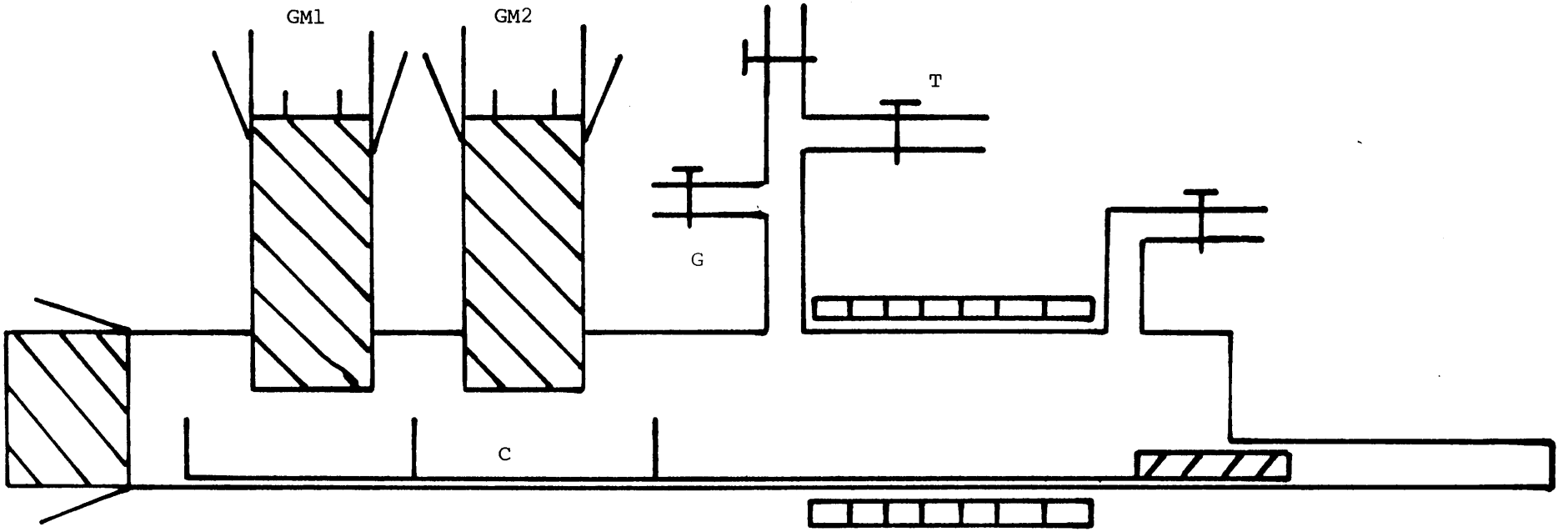

Figure 3.2. The Reaction Vessel

application of a magnet to a glass-sealed metal bar associated with the reaction boat. The temperature of the furnace could be raised by manually increasing the output from an associated Zenith variable transformer (V6 HM TF) or, for linear temperature programming, by coupling the furnace to a Stanton Redcroft Thyristor (LVP/CA40/R). On completion of the heating process the boat could be returned to its original position for adsorption studies.

On admission of a charge of radiolabelled gas into the reaction vessel, GM1 monitored the radioactivity present within the gas phase in a cone directly below its mica window, while GM2 monitored not only the ambient gas phase radioactivity, but also any of the radioactivity which had become associated with the catalytic surface. Simple subtraction of the GM1 count from that of GM2 allowed determination of the surface count rate. Experiments using a [14-C]polymethylmethacrylate source, in position C, proved that the dividing glass wall did not allow GM1 to monitor any of the surface radioactivity.

3.2.3 The Geiger-Muller Counting System

The G.M. tubes used in this work were of the Mullard ZP1481 end window type, filled with a mixture of neon, argon and halogen as quench gas. It is known that halogen-quenched counters usually have poorer plateau characteristics than many other types (i.e. a smaller region in which the count rate caused by a constant radiation source is independent of the applied voltage) but, as is shown in Fig.3.3., a reasonable plateau region was obtained. The working

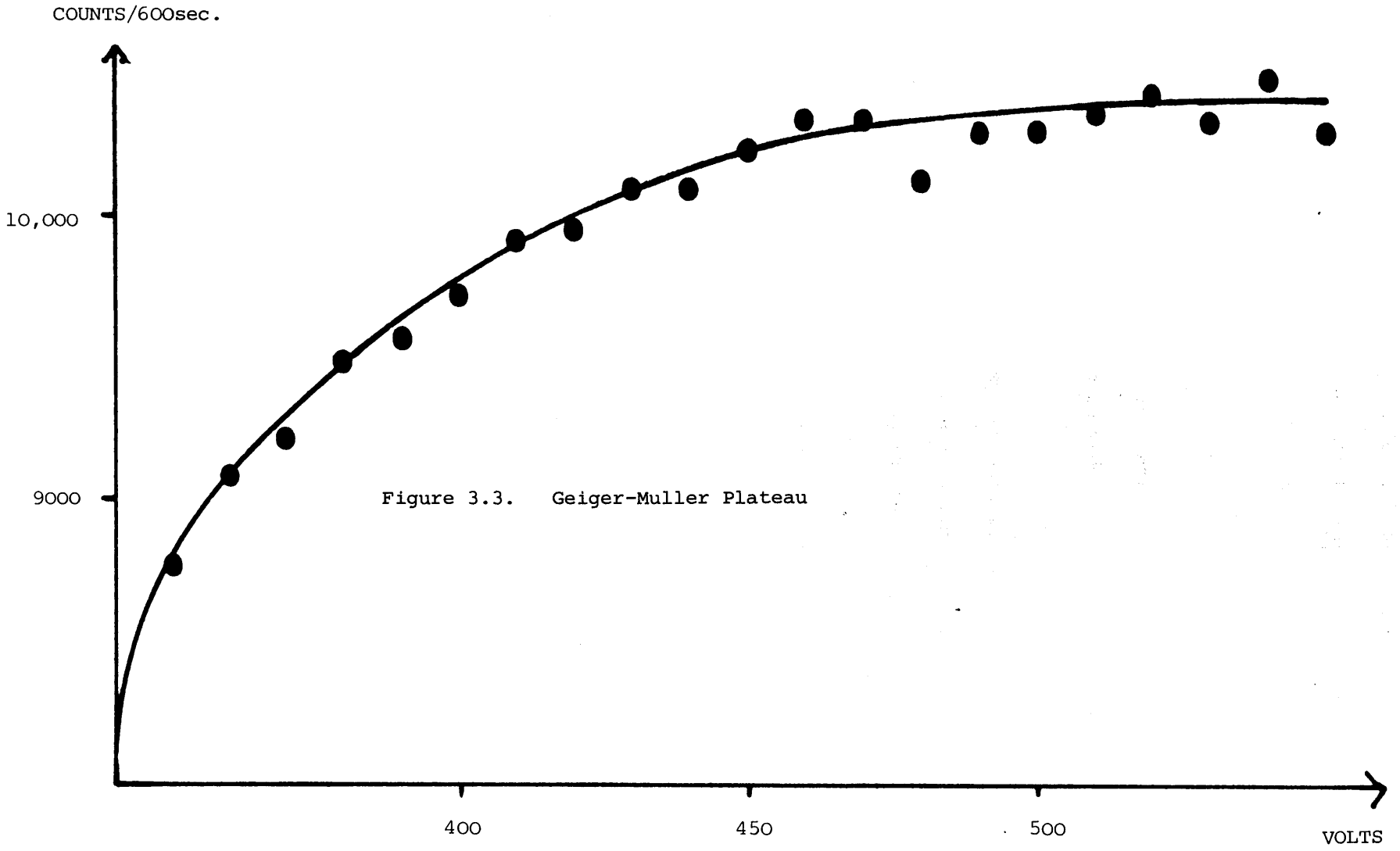

Figure 3.3. Geiger-Muller Plateau

voltage, for both counters, was taken as 500v. Under these conditions both counters were found to be stable and to give error values which lay within the calculated statistical deviation.

The associated electronics consisted of two Nuclear Enterprise Ltd. SR5 scaler ratemeters. The primary output from these scalers could not be used directly for adsorption analysis since a number of important corrections had first to be made.

1. Dead time corrections.

Unlike the proportional counter system described in section 3.2.5 the ionising event generated at the anode in a G.M. counter is of high intensity and is spread evenly along the entire length of the anode wire. This process prevents the counter functioning until the positive ions can migrate away from the anode to the cathode. This recovery, or dead time, of the counter becomes particularly important when large quantities of fast decaying radioisotopes are to be counted.

The true count rate, $N_t(sec^{-1})$, obtained from analysis of a decay process, is related to the actual count rate, No, by

$$N_t = \frac{N_o}{1-N_o T} \qquad (1)$$

where T = dead time of counter.

Rearranging, this provides

$$T = \frac{N_t - N_o}{N_t N_o} = \frac{\Delta}{N_t N_o} \qquad (2)$$

If a plot of count rate against the quantity of radiolabelled material present within the system is drawn (Fig. 3.4), it can be seen that, initially, a linear relationship exists between the amount of radioactivity present and the count rate generated. However, as the quantity of radioactivity increases, the effect of the dead time is clearly seen. By extrapolation, the difference, Δ, between the true and actual count rates can be determined, and the dead time calculated from equation (2). These counters were found to have a dead time of 484 μsecs., which is close to the manufacturers specification of 500 μsec.

All count rates generated were therefore corrected according to equation (1).

2. Background count rate.

These were determined before any adsorption analysis began and were simply subtracted from the scaler-ratemeter output.

3. The Intercalibration Factor.

The experimental procedure outlined in section 3.2.2 can only be followed if the amount of gas phase radioactivity monitored by GM1 and GM2 is exactly the same. Since the GM tubes were positioned at slightly different heights above the boat and may have differing counting efficiencies this is not necessarily the case. However, analysis of the count rates emanating from the two tubes in the presence of a constant amount of radiolabelled gas (with no catalyst present in the boat) allows determination of an intercalibration factor, Z, which can be applied to correct the above deficiencies.

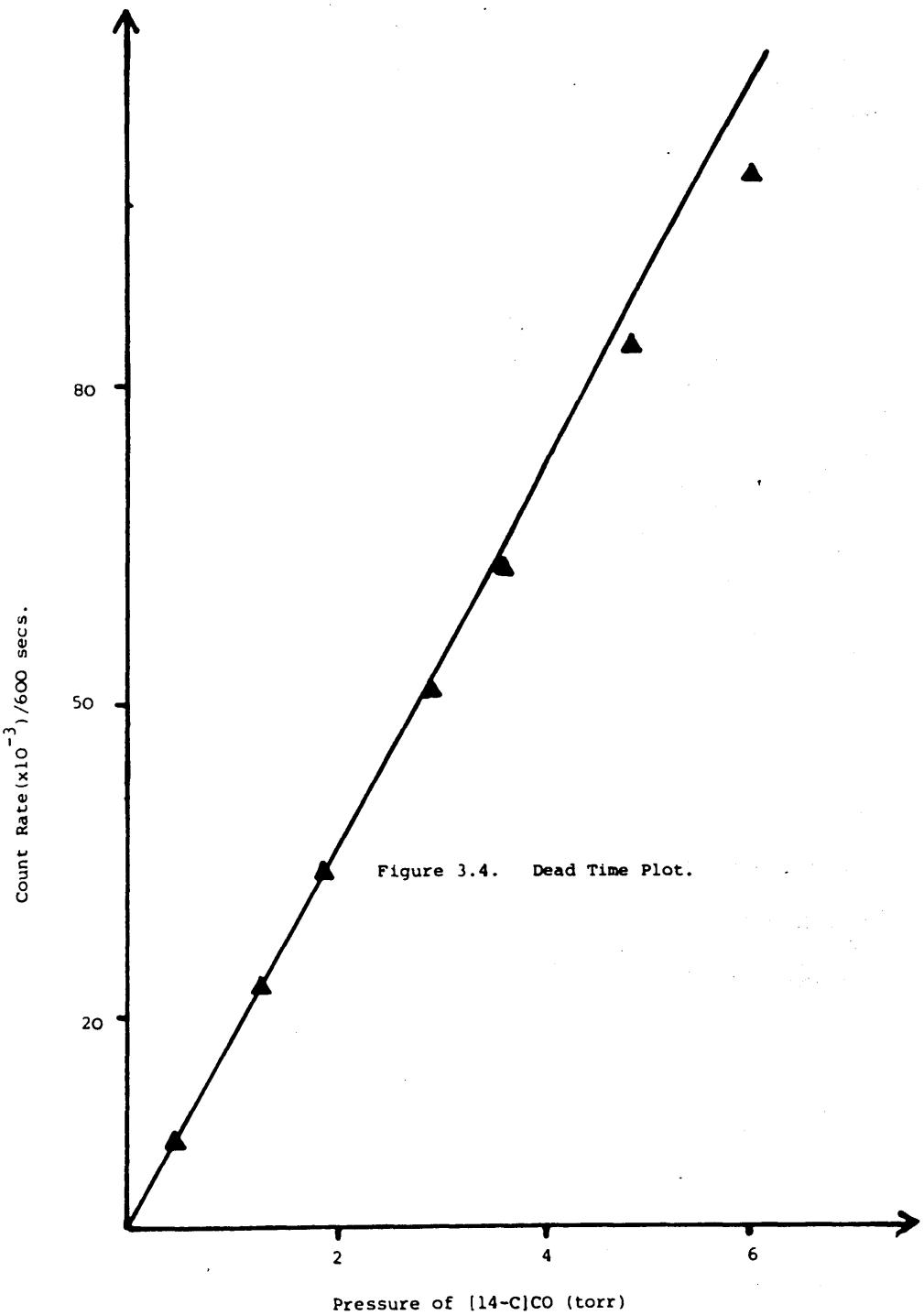

Figure 3.4. Dead Time Plot.

4. Absorption effects.

It is entirely possible that the energy of the decaying isotopes may be absorbed by the gas phase within the reaction vessel prior to Geiger-Muller analysis. Fig. 3.5 shows that up to pressures of 5 torr within the reaction system no gas phase self-absorption was evident. The possibility that the gas phase may absorb the energy produced by isotopic decay on the metal surface was also investigated. Once again no correction was required since the count rate associated with the surface, as monitored by the G.M. tubes, suffered no decrease until the gas pressure in the reaction vessel was at least 50 torr.

3.2.4 The Gas Chromatographic System

The reaction vessel was connected via tap G. (Fig. 3.2). to a gas sampling system of total volume 12.2 cm^3 (Fig. 3.6). This was constructed of 0.125 in. (o.d.) stainless steel tubing and Swagelok couplings. The directional flow of the various gas streams was controlled by the use of Whitey stainless steel three-way switching valves. The sampling system was connected directly to the main manifold via a glass-metal calibrated seal, which allowed ready evacuation of the 0.4 cm^3 sample loop.

Samples of the gas phase within the reaction vessel were expanded into the sample loop and, by manipulating taps 2 and 3 (Fig. 3.6), the material for analysis was purged to the chromatographic column. The pressure of gas within the sample loop was obtained by isolating the pressure transducer from the reaction vessel and, following

Figure 3.5. Determination of Gas Phase Self-Absorption

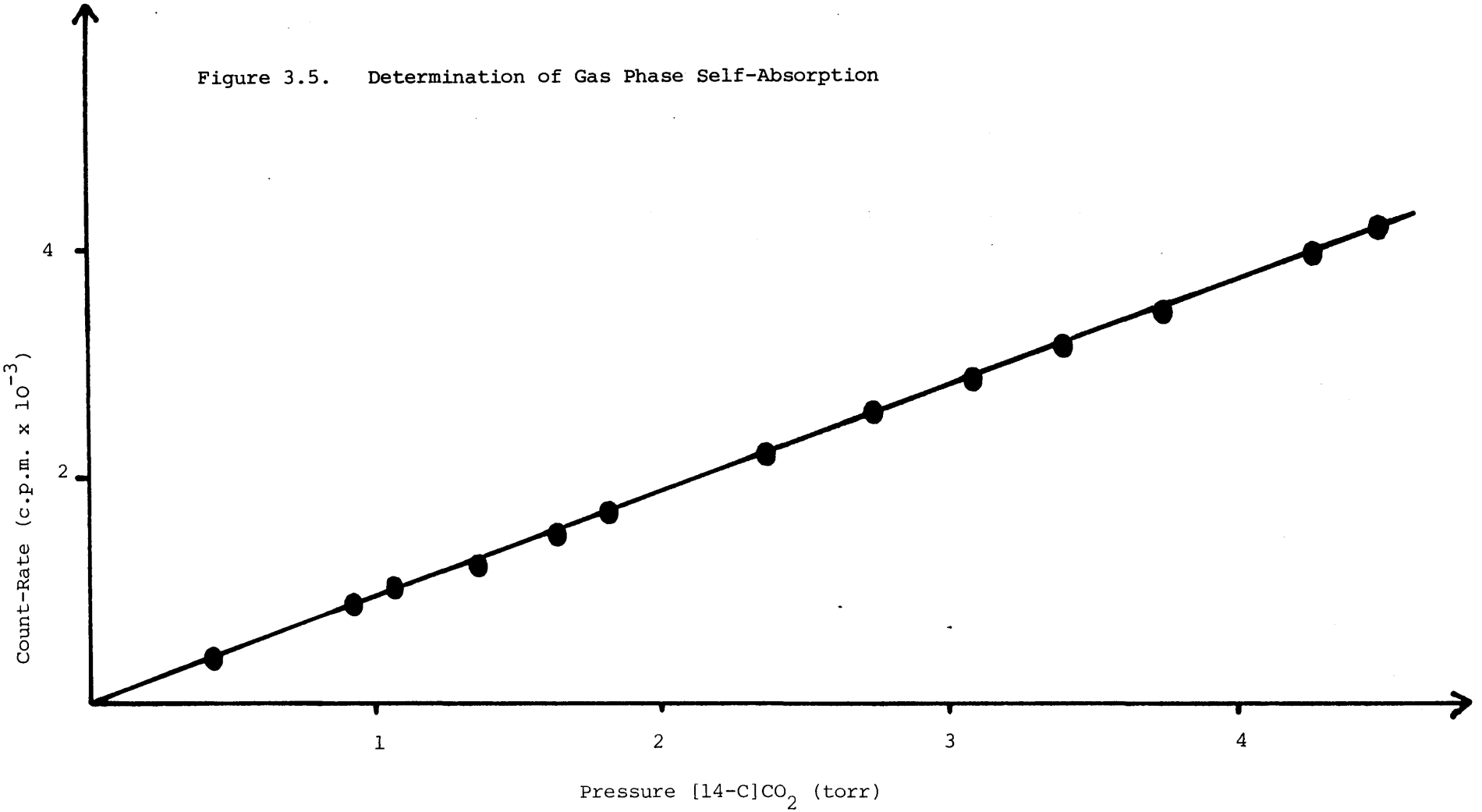

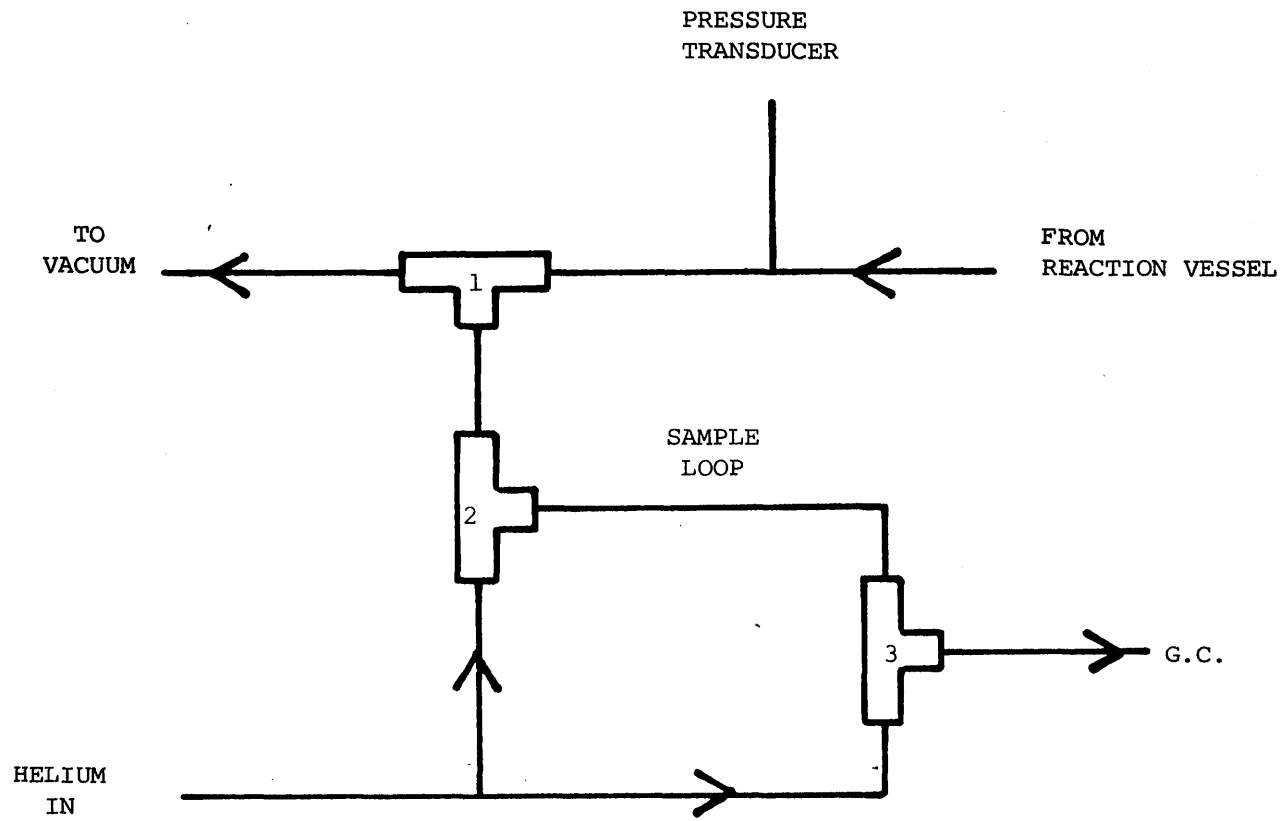

Figure 3.6. Gas Chromatograph Sampling System

evacuation, connecting it via a 2mm tap to the sampling system (Fig. 3.1).

Separation of the gaseous mixture was achieved by passing the sample through a 5ft (0.125 in. (o.d.)) stainless steel column packed with 1.9065g of Carboseive B (Mesh 80/100). The separated gases were then detected by a thermal conductivity detector (Gowmac, Model 1097), operating at a filament current of 200 mA, whose output was fed to a chart recorder (Servogor 420). The column was generally operated in conjunction with the proportional counter, which necessitated a helium flow rate of 30ml min^{-1} through the column. The working temperature of the column was 55°C, although it had previously been conditioned at a temperature of 180°C. The retention times of the various gases used in this study, under these conditions, are given in Table 3.1.

Gas	Retention Time
N_2	1 min 30 secs.
CO	1 min 50 secs.
CO_2	9 mins.
N_2O	17 mins.

Table 3.1. Retention times of gases on column

A quantitative gas-chromatographic analysis was essential to this study and hence sensitivity factors, relating the recorded peak area to the partial pressure of gas being sampled, were determined. The chart speed and recorder sensitivity were not varied for the different gases and the sensitivity factor was therefore determined as

$$S_f = \frac{\text{Peak area } (cm^2)}{\text{Partial pressure of gas (torr)}}$$

All peak areas were measured by triangulation. The sensitivity factors were found to vary by relatively large amounts from day to day and were, therefore, determined daily, before attempting any analysis.

3.2.5 The Proportional Counter

The proportional counter functions in a similar way to the previously described G.M. counter, although there are significant differences between the two pieces of apparatus. The voltages applied in the G.M. counters ensure that the ion current produced in the secondary ionisation process is large and totally independent of the original ionisation. However, at lower voltages the ion current remains proportional to the amount of energy lost by the primary ionising particle. The number of electrons generated by the initial ion pair in this region of proportionality may be controlled by varying the composition of the counting medium, which in this case was a helium-methane mixture. The lower ion currents produced at these voltages also necessitate the use of external amplifiers.

The counter used in these studies was similar to that constructed by Schmidt-Bleek and Rowland[143]. It is of robust design and consists of brass and teflon fittings with a very thin, (0.002in. diameter), stainless steel anode.

On elution from the chromatographic column, the helium flow (30 ml min^{-1}) was mixed with a methane stream before entering the counter (Fig. 3.7). It was found that a helium/methane ratio of

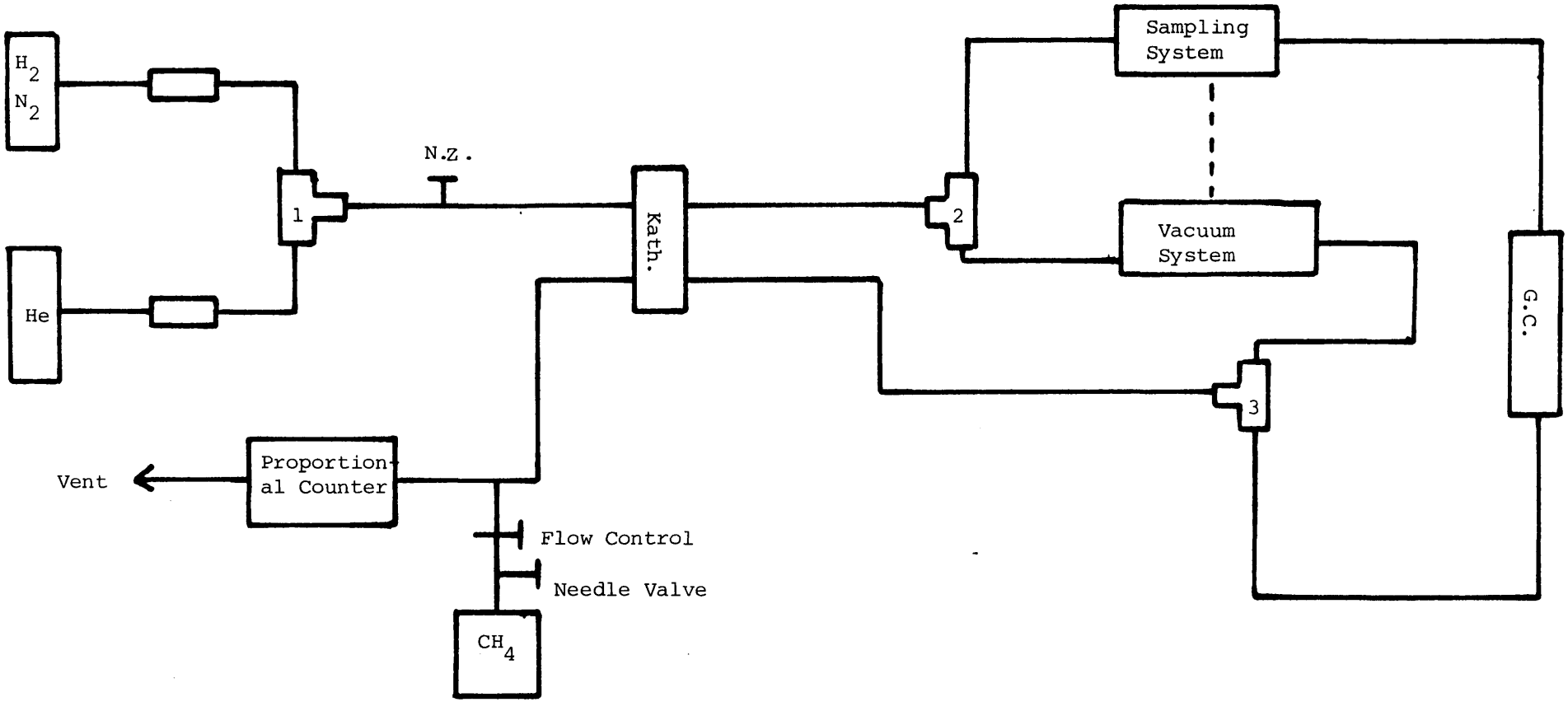

Figure 3.7. Schematic Diagram of Gas Flow System.

11:1 produced a counting medium, which enabled a plateau length of >100 volts and of negligible slope (<2%) to be attained (Fig. 3.8). The working voltage was taken as 1.96 keV. The statistical realibility of the system, under these conditions, was found to be excellent.

The helium-methane stream was obtained by adding a 2.7 ml min^{-1} methane flow to the 30 ml min^{-1} helium flow. A constant and invariant methane flow was achieved by the combination of a Nupro fine-control metering needle valve and a Brooks flow controller. A Negretti-Zambra flow control was found adequate to achieve a constant 30 ml min^{-1} helium stream.

The electronics consisted of an ESI Nuclear 5350 Scaler-ratemeter and an ESI Nuclear 425 pre-amplifier. The Function (A-∞), Gain (4) and T.C. (0.4) controls on the ratemeter were not utilised in this study, but by suitable variation of the range control, and the sensitivity of an associated chart recorder, a visual output of the data emanating from the scaler was provided.

Analysis

The presence of a [14-C]radiolabel in a particular component of the gas phase within the reaction vessel could be determined using the gas chromatograph, katherometer and proportional counting systems. Immediately before entering the proportional counter the gas phase species, previously separated by the chromatographic column, were detected by the katherometer (Fig. 3.7). At the very moment a deflection on the katherometer output indicated the presence of an eluting gaseous species, the scaler associated with the proportional counter was allowed to count for a period of 5 mins. In this time,

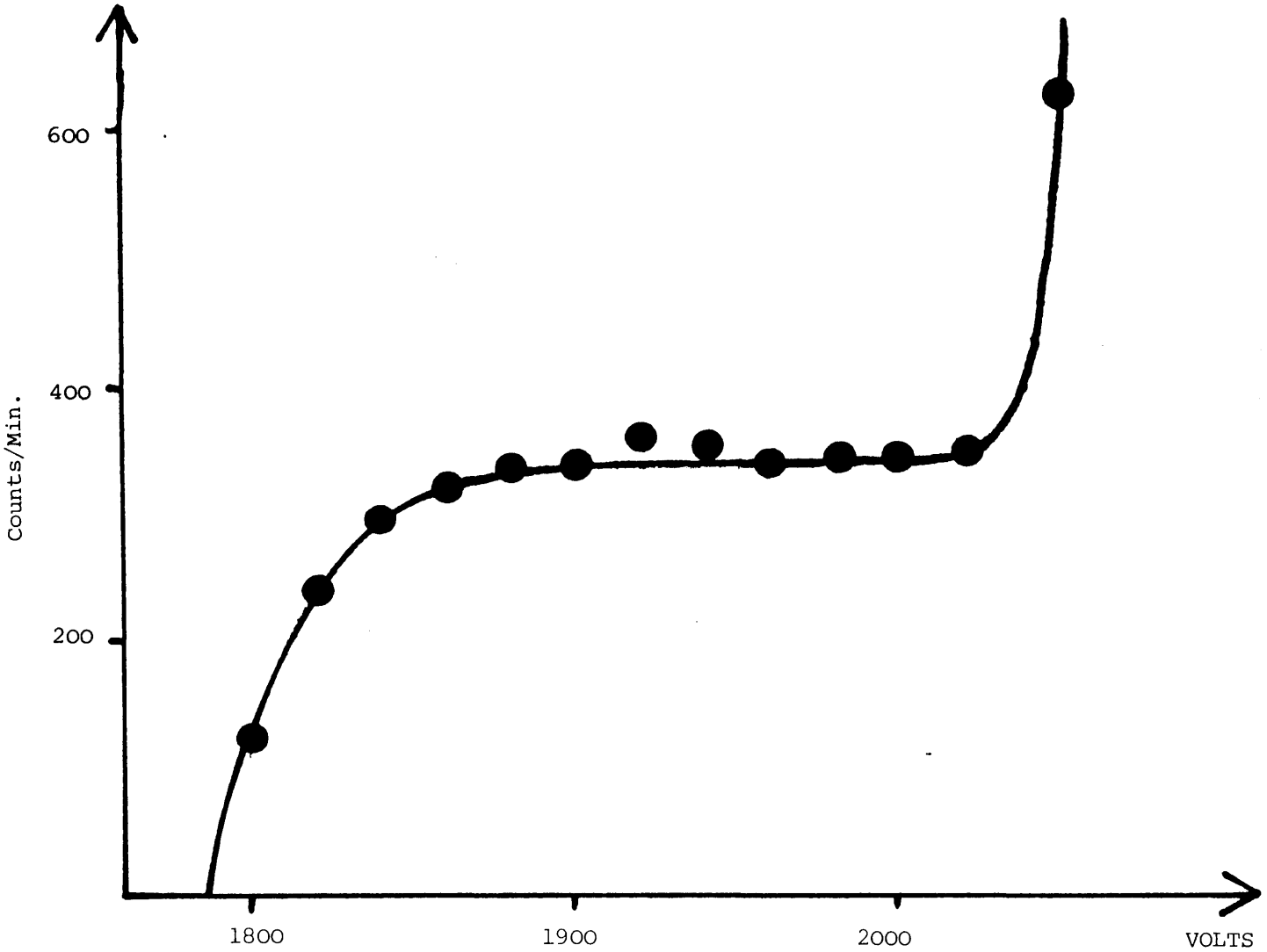

Figure 3.8. Proportional Counter Plateau

the plug of gas being carried in the helium stream would have left the katherometer and passed through the proportional counter. Any radioactive count, above previously determined background levels, would therefore indicate the presence of a [14-C]radiolabel. By comparison of the count rate produced by a sample of gas in the counter, with that obtained from a known quantity of radiolabelled carbon oxide (of pre-determined specific activity), the number of moles of radiolabelled gas being purged through the system could be calculated. Hence both the chemical form (from G.C.) and the total quantity of radiolabelled material being analysed was determined.

3.2.6 Catalysts

3.2.6.1 Copper(II) Oxide

The copper oxide used to prepare unsupported copper metal surfaces was B.D.H. analar cupric oxide whose maximum impurity level was stated as <2%. The major impurities are quoted as Iron (0.05%) and potassium, calcium and sodium (all 0.02%). It may be of relevance to note that if all these impurities were to segregate on the surface following reduction, 50% of a monolayer of these impurities could, conceivably, exist on the copper metal surface.

3.2.6.2 CuO/Al_2O_3

This catalyst, supplied by I.C.I. plc., was prepared by the co-precipitation, as carbonates, of copper and alumina from nitrate solutions. The copper carbonate formed was decomposed to the oxide by calcination for 16 hours at 300°C, which, on reduction, produced an 80% Cu/Al_2O_3 catalyst (w/w).

3.2.7 Gases

The 6% hydrogen-nitrogen mixture (B.O.C. Ltd.) used for catalyst reduction was specified by the manufacturers as being 99.98% pure.

Helium (B.O.C. Ltd.) was used for operation of the G.C., proportional counter and in a number of desorption experiments. Its stated purity was 99.9%.

Hydrogen (B.O.C. Ltd.) was specified as 99.9% pure.

Carbon monoxide (Air Products Ltd.) was specified as 99.5% pure.

All these gases were used directly from the cylinder without further purification. No impurities were detected in any of these gases by gas chromatography.

Both nitrous oxide (B.D.H.) and carbon dioxide (Air Products Ltd.) were added directly to the vacuum system from the cylinder and were further purified by cooling to -196^{o}C and pumping. After this, no impurities could be detected in either of these gases by gas chromatography.

3.2.8 Preparation of Radiolabelled Carbon Oxides

3.2.8.1 [14-C]Carbon Dioxide

[14-C]carbon dioxide was prepared by the addition of dilute hydrochloric acid to a sample of barium [14-C]carbonate (Radiochemical Centre, Amersham) whose specific activity was specified as 5m Ci mmol^{-1}. The [14-C]carbon dioxide generated was dried over silica gel and magnesium perchlorate and further purified by cooling to -196^{o}C and pumping. Small aliquots of the total batch were then removed, by expansion, into evacuated glass ampoules (Fig. 3.9). These allowed easy

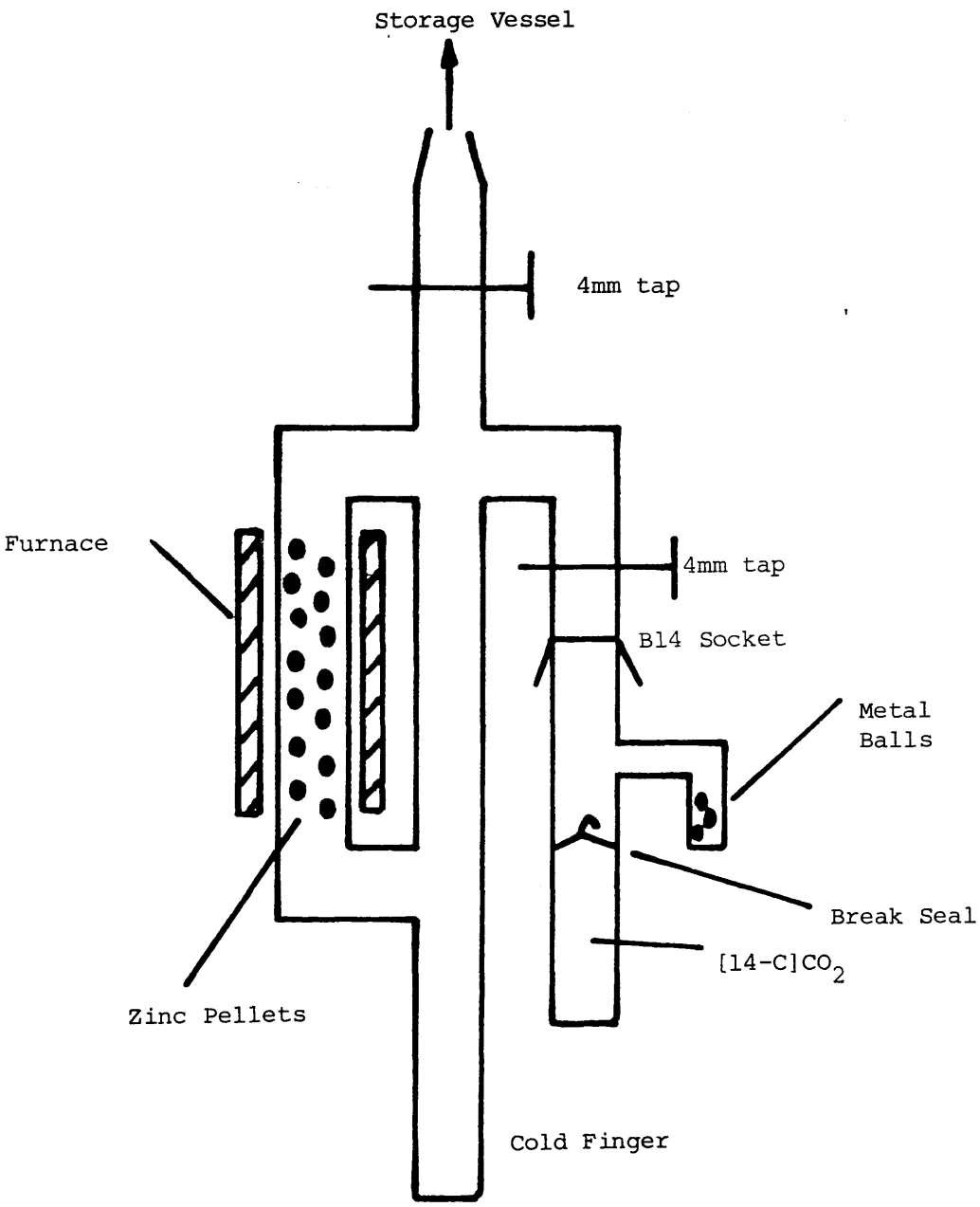

Figure 3.9. $[14\text{-}C]CO_2$ Reduction Apparatus and Associated Glass Ampoule

transfer of the radiolabelled dioxide into the storage bulb on the vacuum system via a break-seal mechanism. Further dilution of the [14-C]carbon dioxide with [12-C]carbon dioxide allowed preparation of radiolabelled material with a lower and more useful specific activity.

3.2.8.2 [14-C]Carbon Monoxide

This was prepared by reduction of [14-C]carbon dioxide. An ampoule of [14-C]carbon dioxide was attached, via a B14 socket, to the reaction system shown in Fig. 3.9. This system was connected to an evacuated 1 litre storage vessel on the vacuum system.

Dried zinc pellets, prepared from a moistened mixture of 95% zinc dust (analar) and 5% Aerosil silica (Degussa Ltd.), were contained in one arm of the Pyrex vessel. A small furnace surrounding this arm allowed the temperature of the pellets to be raised to 320^{o}C and held at this value whilst they were degassed by continuous pumping for 24 hours. The reaction vessel was then isolated from the vacuum system and the [14-C]carbon dioxide contained in the ampoule allowed to expand into this vessel and over the hot zinc pellets. Internal convection mechanisms ensured continual circulation of the carbon dioxide over the hot pellets. This reduction process was allowed to continue for 72 hours.

These conditions should ensure almost total reduction of dioxide to monoxide but, on completion of the process, any residual dioxide was trapped in the reaction vessel by placing liquid nitrogen around the cold finger (Fig. 3.9). The [14-C]carbon monoxide was then allowed to expand into the storage vessel and diluted to the required specific activity.

3.2.9 Experimental Procedure

3.2.9.1 Activation of CuO/Al_2O_3 Catalyst

The gas flow system which enabled control of the gas stream used for reduction purposes is shown in Fig. 3.7. To achieve catalyst activation, a 6% hydrogen-nitrogen stream was allowed to flow, via a Whitey switching valve (1), through a Negretti-Zambra flow control, which produced a constant flow rate of 25 ml min^{-1} through the rest of the system. After passing through the reference arm of the katherometer, the gas stream was diverted, via valve (2), through the main manifold and reaction vessel of the vacuum system. By manipulating valve (3) the eluting gas stream was redirected through the katherometer, before venting.

The CuO/Al_2O_3 catalyst was heated, over a period of 30 mins, to a temperature of 180°C and allowed to stand, in the hydrogen/nitrogen stream, at this temperature for a period of 12 hours. After this period hydrogen uptake, as monitored by the katherometer, had ceased. The temperature of the sample was then raised, over a very short time period, to 240°C, during which time further, slight, hydrogen uptake occurred. The reaction vessel was then evacuated and the Cu/Al_2O_3 sample allowed to cool, in vacuo, to ambient temperature.

3.2.9.2 Activation of Cupric Oxide

A 25 ml min^{-1} 6% hydrogen-nitrogen gas stream was allowed to flow over the cupric oxide sample using the procedure outlined in 3.2.9.1. When a stable gas flow had been produced, the temperature of the oxide was raised, slowly, over a period of 2 hours to 220°C. This temperature

was maintained for 12 hours and the copper metal generated by this procedure allowed to cool, in vacuo, to ambient temperature.

3.2.9.3 Determination of Copper Metal Surface Areas and Production of Partially Oxidised Surfaces

The chemistry relating to the reaction of nitrous oxide with copper metal surfaces is detailed in section 1.7.

In this study a chromatographic analysis of the nitrous oxide-copper reaction, in a static reaction system, was used to derive metal surface areas. This was achieved by admitting an excessive quantity of nitrous oxide, into the reaction vessel containing a freshly reduced copper sample, at a temperature of 80°C. Gas chromatographic analysis of the gas phase within the reaction vessel, together with a knowledge of the volume of the apparatus, enabled the quantity of reacted nitrous oxide to be determined. From this value the total copper metal surface area exposed in the reaction vessel could be calculated.

Further, by rereducing the oxidised metal (as in 3.2.9.2), the original reduced metal area could be regained. Admission of a previously calculated quantity of nitrous oxide into the reaction vessel containing the freshly reduced, but previously characterised sample, then produced an only partially oxidised copper surface.

In this reaction system, this procedure did not concentrate the oxidised species in any specific area of the catalyst bed, but rather produced a random scatter of oxidised species across the copper surface. The surfaces used for the experiments described in chapter 5 were generally oxidised to 50-60% of the maximal surface oxygen uptake.

3.2.9.4 Determination of Adsorption Isotherms

An adsorption isotherm was obtained by admitting small charges (0.5 - 1.0 torr) of radiolabelled material into the evacuated reaction vessel containing the copper sample. Each charge was allowed to equilibrate within the system for 10 minutes before using the G.M. counters to determine the quantity of adsorbed material.

Charges of radiolabelled carbon oxides could also be admitted to the reaction vessel containing a known pressure of a non-labelled adsorbate i.e. the isotherm could also be produced on surfaces pretreated with another gaseous species. Co-adsorption experiments, in which charges of gas containing equal mole fractions of radiolabelled and unlabelled adsorbates were admitted to the copper samples, could also be effected by premixing of the gases outwith the reaction vessel.

At any point during the adsorption processes, samples of the gas phase could be removed from the reaction vessel and purged through the combined G.C.-proportional counting system, allowing the chemical form of the gaseous species to be determined.

3.2.9.5 Radiotracer Temperature Programmed Desorption

On completion of an adsorption isotherm, the gas phase within the reaction vessel and any weakly adsorbed surface species were removed by an evacuation procedure. By manipulating Whitey valves (1) and (2) (Fig. 3.7) a 30 ml min^{-1} helium flow was then allowed to flow over the copper sample and then, via valve (3), through the proportional counting system. The boat containing the catalyst sample was then manoeuvred into the furnace region of the reaction vessel and heated,

linearly, to elevated temperatures (230°C). As the temperature increased, any desorbing radiolabelled material was swept through the proportional counting system. The data from the counter was continually monitored on a chart recorder and hence periods in which radiolabelled material was desorbing from the surface were seen as peaks on the recorder trace. The increasing temperature of the outside of the reaction vessel wall was followed simultaneously and this enabled the periods of maximal desorption rate to be characterised within certain temperature ranges. This technique did not allow any characterisation of the chemical form of the desorbing material.

3.3 On-line Mass Spectrometry

3.3.1 Apparatus

The apparatus used in this flow study is shown diagramatically in Fig. 3.10. This experimental arrangement allowed, for example, in situ surface area, temperature programmed reaction (T.P.Rn.) and temperature programmed desorption (T.P.D.) studies to be effected. The total apparatus can be considered as consisting of three separate, though wholly integrated, components.

3.3.1.1 The Feed System

Three parallel helium flows were required in the system - a katherometer reference stream, a reactant gas carrier stream and a stream to elute desorption products from the catalyst column to the analytical section. All three streams were produced from a single helium flow, the flow rate of each of the separate streams so produced being controlled by the combination of a pressure regulator

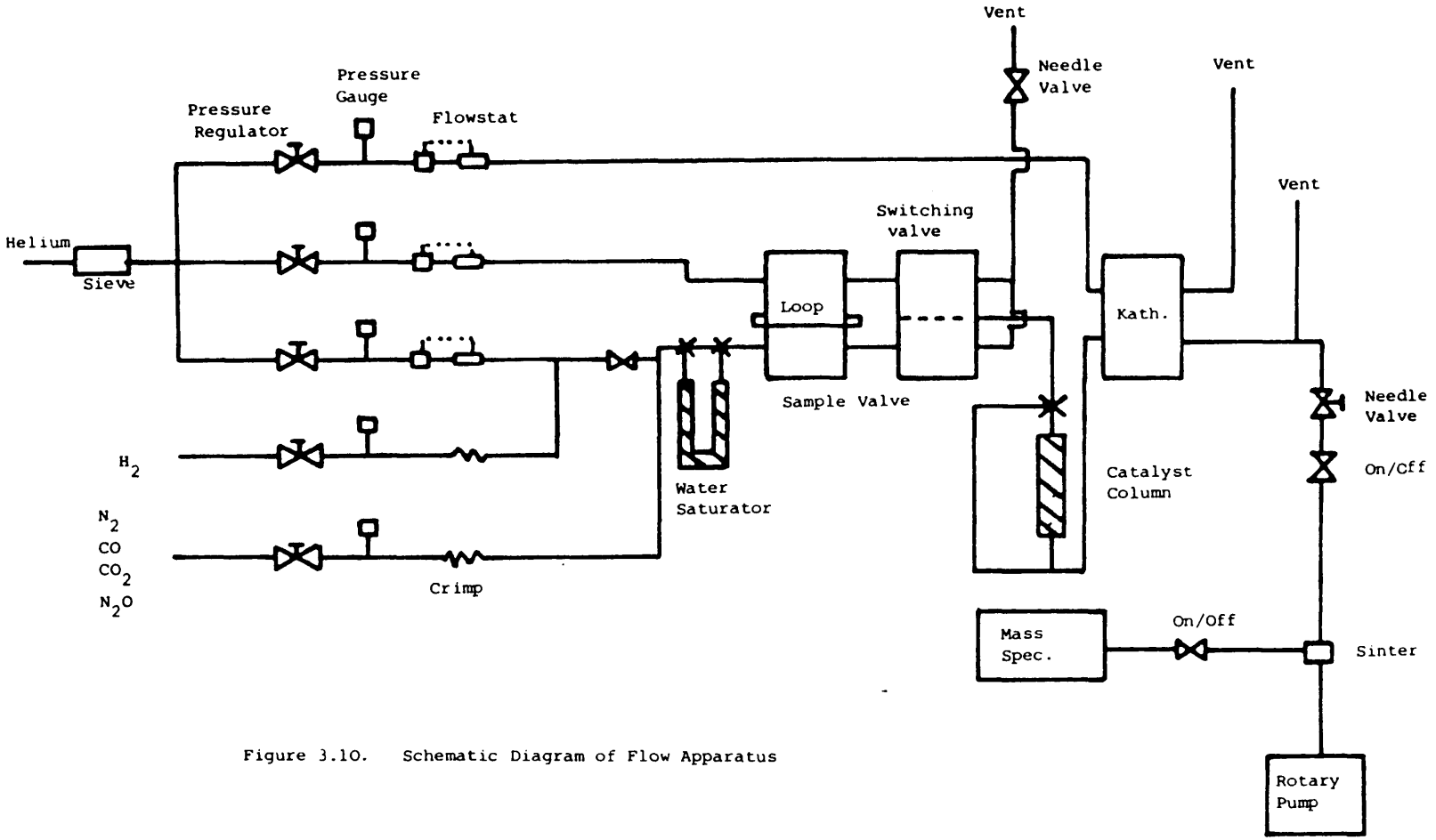

Figure 3.10. Schematic Diagram of Flow Apparatus

and flowstat.

A variety of gases (e.g. N_2O, CO, CO_2 or N_2) could be added directly to the helium carrier stream by connecting the relevant lecture bottle to the system via a pressure regulator and restrictor. This allowed total control of the helium-reactant gas ratio. Hydrogen could also be piped directly into the carrier stream via a similar regulator-restrictor combination.

To facilitate the introduction of water, in a controlled manner, to the copper catalyst, a water saturator was connected to the feed section. This consisted of a glass U-tube, packed with molecular sieves, which had been moistened by injection of a few ml. of distilled water. The helium 'carrier' stream could be diverted through this water column which, on elution, contained a small per cent of water vapour (1.5%). For experimental purposes the per cent water in this feed stream was often reduced to 0.5% by immersing the U-tube in an ice bath. These helium-water feed streams were found to contain an oxygen impurity, typically of the order of 0.016% of the total flow.

3.3.1.2 The Catalyst Column and Sampling System

A six port pneumatic flow switching valve, situated before the catalyst column, allowed either an eluting helium stream or the helium-reaction mixture to flow over the catalyst column as required. The presence of another six port pneumatic switching valve, with an associated sample loop of predetermined volume (0.42 cm^3), allowed calibration of the analytical system and hence a quantitative analysis

of both the mass spectrometer and katherometer outputs. These calibrations were confirmed by manual injection of nitrogen gas into an injection port situated between the catalyst column and the katherometer.

The cracking fractions of the gases of interest in the mass spectrometer were obtained by diverting the gas flow around the catalyst column via a by-pass.

The catalyst column itself consisted of a six inch (0.25 in. o.d.) length of stainless steel tubing housed in a chromatograph oven. This allowed controlled linear heating of the column to moderately elevated temperatures (ca. 250^{o}C). It should also be noted that the column could be cooled to sub-ambient temperatures by removal from the oven and immersion in e.g. a liquid nitrogen (-196^{o}C) or CO_2(s)/acetone (-60^{o}C) bath.

Both switching valves and all stainless steel (0.125 in. o.d.) tubing used in this and the analytical section were maintained at a temperature of 110^{o}C by heating in a chromatograph oven and by electrical heating tape respectively.

3.3.1.3 The Analytical System

Analysis of any products (or reactants) eluting from the catalyst column was achieved by utilising the combination of a Taylor Servomex Microcatherometer and an on-line Vacuum Generators Supavac mass spectrometer.

On elution from the catalyst column the complete gas flow passed through the heated katherometer (110^{o}C), the associated flux in the Wheatstone bridge circuit being recorded on a chart recorder.

The combination of a rotary pump and needle valve then ensured that a constant 5 ml min^{-1} portion of the total gas stream (25 ml min^{-1}) was diverted across a sinter associated with the mass spectrometer. With the flow rates through the katherometer and mass spectrometer constant, the deflection in the katherometer output which, from prior calibration, can be related to the percent reactant in the helium stream, was directly proportional to the increase in mass spectrometer signal. Hence quantitative analysis of the spectrometer output for any mass, was obtained by intercalibration with the katherometer.

3.3.2 Gases

The helium (B.O.C.) was purified by passing the flow through a rare gas purifier (B.O.C. Mk.3) which removes, to p.p.m. level, all traces of N_2, H_2, H_2O, CO_2 and hydrocarbon. From consideration of the amount of oxygen removed from the catalyst surface, by carbon monoxide reduction, following several hours in the helium stream, the oxygen impurity was calculated to be 0.116 p.p.m. which is within specification.

The hydrogen (Air Products Ltd.) was 99.99% pure; carbon monoxide (Matheson) was 99.997% pure; carbon dioxide (Distillers Co.) was 99.965% pure and the nitrous oxide (Air Products Ltd.) was 99.9% pure. All these gases were used directly from the cylinder without further purification.

3.3.3 Catalyst

The catalyst used in these studies was B.D.H. analar cupric oxide, which has been fully described in section 3.2.6.1. This experimental apparatus allowed the B.E.T. surface area of the oxide to be determined by nitrogen adsorption at -196°C (Section 4.4). The area was found to be 10.4 $m^2 g^{-1}$.

For experimental purposes 2g of the cupric oxide was thoroughly mixed with an equal quantity of acid washed glass beads (Mesh 85-100) before being poured into the stainless steel column. A thermocouple was positioned near the top of the catalyst bed (length ≈ 10 cm) and the catalytic mixture held in place by two (2.5 cm) plugs of glass wool.

3.3.4 Experimental Procedure

3.3.4.1 Activation of Cupric Oxide

A fully reduced copper surface was prepared by heating the copper surface, at a rate of 1°C min^{-1}, to 235°C, in a 25 ml min^{-1} 6% hydrogen-helium flow. Any residual oxygen was then removed from the sample by treatment, at this temperature, in a 5.5% carbon monoxide-helium stream (25 ml min^{-1}). This latter procedure generated a small quantity of carbon dioxide, corresponding to the removal of a few per cent of an oxygen monolayer from the copper surface. Any carbon monoxide remaining on the surface following this procedure was then allowed to desorb, from the hot copper surface, into a 25 ml min^{-1} helium stream. The copper catalyst was then cooled, in the helium flow, to the temperature required for experiment.

Following reaction of nitrous oxide, carbon dioxide or water with the copper sample, rereduction was effected by passing 6%

carbon monoxide - helium over the copper surface at 200°C. The amount of carbon dioxide generated (as monitored by the mass spectrometer or katherometer) could then be related to the oxygen coverage of the copper surface. It was found that these rather severe conditions caused some sintering of the copper, especially during removal of oxygen from the bulk of the copper sample.

3.3.4.2 Determination of Adsorption Isotherms by Gas-Adsorption Chromatography

The means by which gas-adsorption chromatography is used to generate adsorption isotherms is detailed in this section. The experimental technique is described in terms of the adsorption of nitrogen on copper oxide at -196°C, which was subsequently used to calculate the B.E.T. area of the oxide (section 4.4). However, an identical technique was also applied to study the adsorption characteristics of water on a reduced copper surface at a variety of elevated temperatures (section 6.4.4).

Gas-adsorption chromatography uses a katherometer to follow the adsorption of a gaseous species on the adsorbent and its subsequent desorption from the adsorbent surface in an eluting helium stream. The katherometer output which was obtained during the adsorption and desorption of nitrogen from cupric oxide, at -196°C, is shown in Fig. 3.11.

At point A, a 5.64% nitrogen-helium stream was switched through the column containing the cupric oxide sample. If no adsorption had occurred, the nitrogen flow would have been expected to cause a deflection on the katherometer signal after a time, T_o, which is the

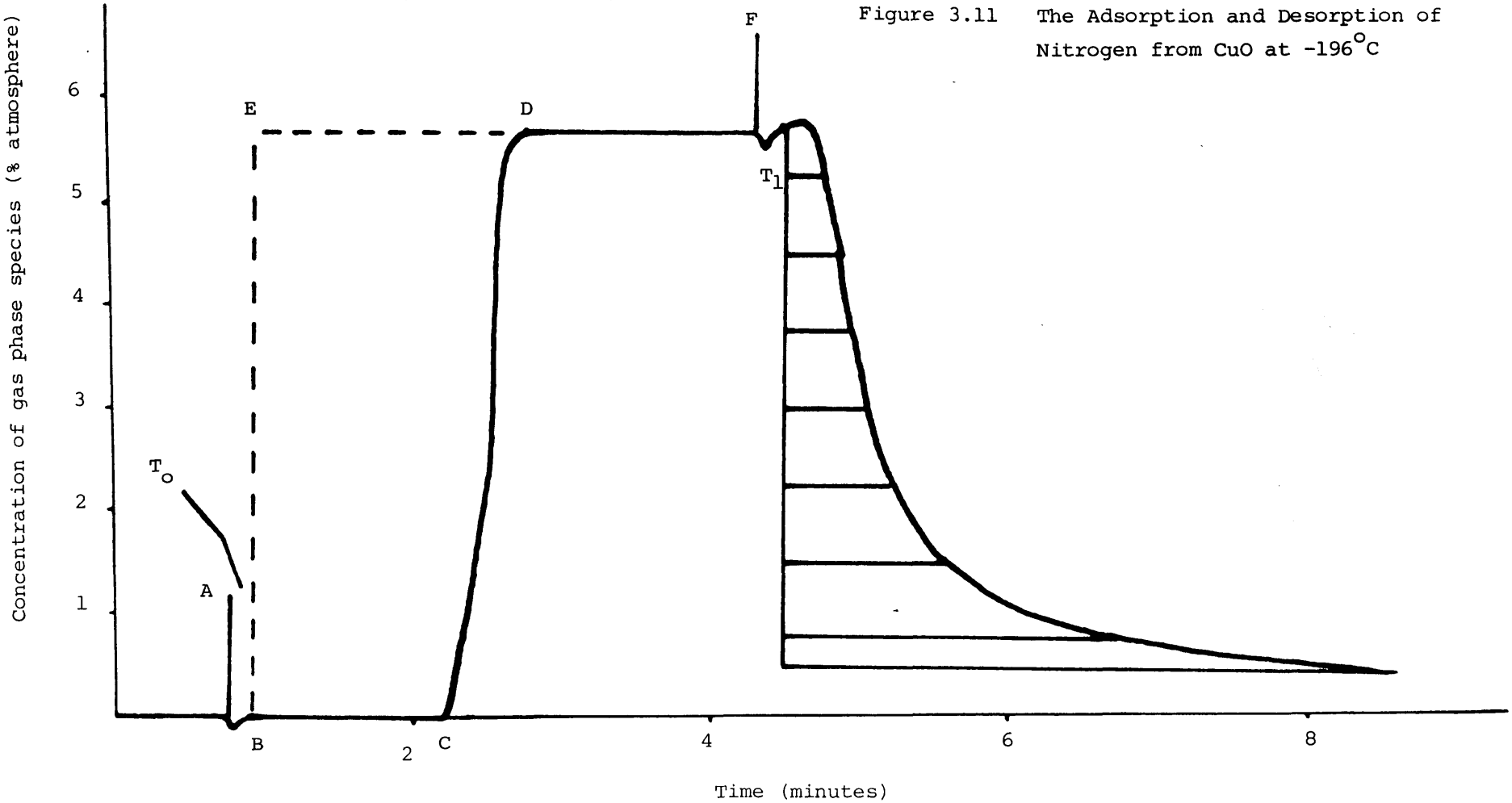

Figure 3.11 The Adsorption and Desorption of Nitrogen from CuO at -196°C

time taken for the nitrogen front to reach the detector. However, adsorption did occur, and the nitrogen front did not break through to the katherometer until the adsorption process was complete (Point C). The integral BCDE, therefore, gives the quantity of nitrogen adsorbed on the cupric oxide sample under the 5.64% nitrogen-helium flow. At point F the nitrogen-helium mixture was replaced by a pure helium stream. After another sweep-out time, T_1, the flowing helium entered the catalyst column and removed the gaseous mixture from the system. Thus, the diminishing nitrogen partial pressure allowed desorption to occur and the desorbing material was monitored on the katherometer. Stripwise integration of the desorption tail shape produced during this process, together with a knowledge of the total quantity of nitrogen originally adsorbed on the sample, allowed an adsorption isotherm to be generated (Fig. 3.12).

3.3.4.3 Copper Metal Surface Area Determination by Reactive Frontal Chromatography

A gas-chromatographic analysis of the reaction of nitrous oxide and copper metal surfaces has been described in section 3.2.9.3. The flow system used in these analyses does, however, allow a far more elegant means of determining copper metal surface areas.

The reaction of nitrous oxide with copper, at 60°C, is an extremely facile process (Sec. 1.7) and instant surface oxidation occurs on admission of nitrous oxide to a copper sample. Under these conditions a flow of 6% nitrous oxide in helium passing through a hot column of copper catalyst generates a nitrogen 'front' which enlarges until total surface oxidation has occurred down the catalyst

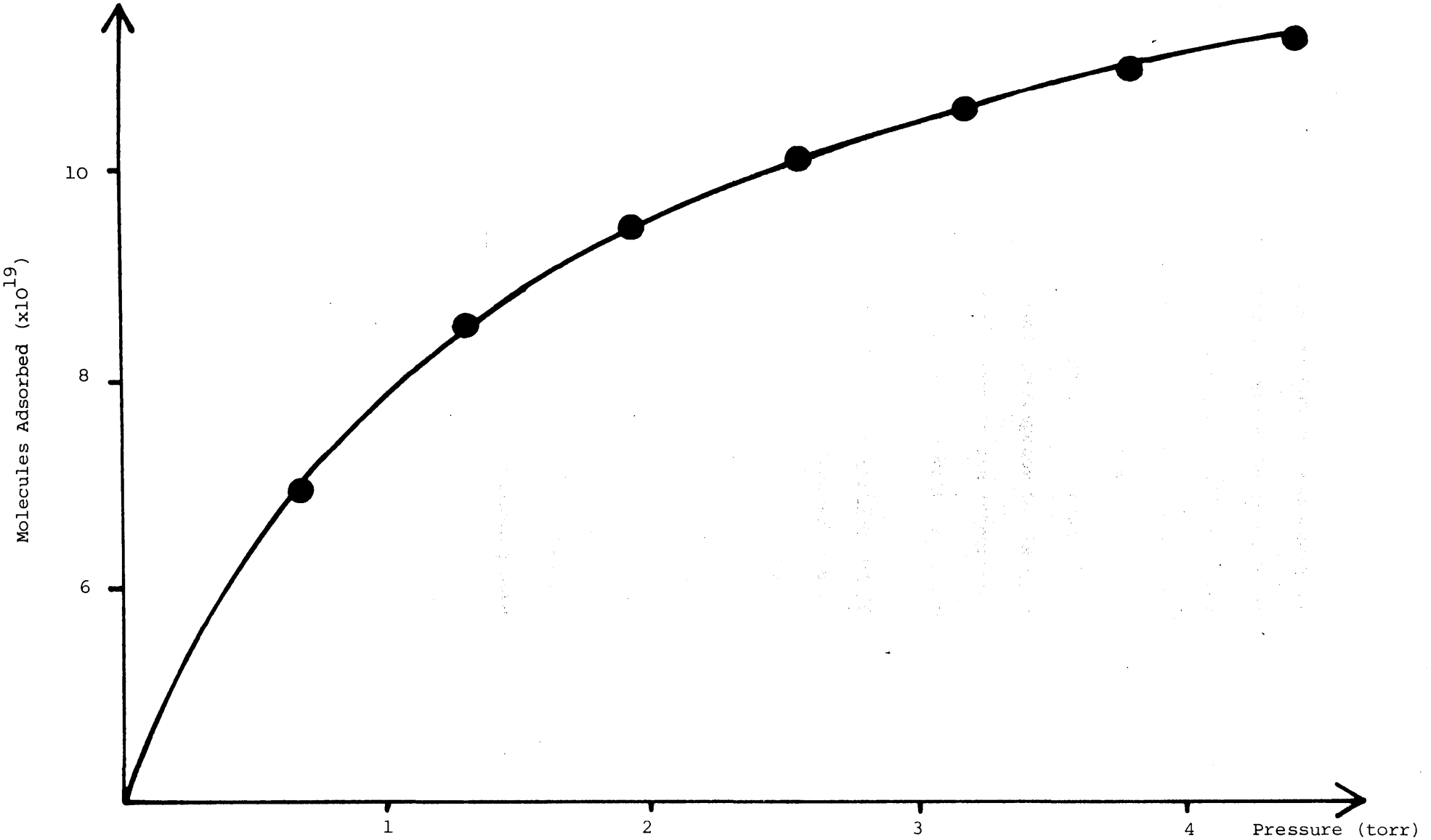

Figure 3.12. The Adsorption of N_2 on CuO (-196°C)

bed. At this point nitrogen evolution ceases and, immediately, a nitrous oxide front appears. Since the thermal conductivities of nitrogen and nitrous oxide are quite different, the evolution of these fronts is clearly seen by allowing the eluting gases to pass through a katherometer. Figure 3.13 shows a typical reactive frontal chromatogram produced by the reaction of nitrous oxide with copper metal at 60°C. The area ABCD corresponds to the quantity of nitrogen produced by the decomposition reaction and integration allows the exposed copper surface area to be accurately calculated.

3.3.4.4 Flow Studies and Subsequent Desorption Analysis

A mixed helium-reactant gas stream was allowed to pass over an activated copper surface (Sec. 3.3.4.1) for a predetermined length of time, during which the gases eluting from the catalytic column were monitored on the mass spectrometer. On completion of the flow study, the copper sample was cooled, if necessary, to ambient temperature, in the reactant gas stream. A pure helium stream was then used to flush the gaseous material and any weakly adsorbed surface species from the catalyst column, before heating the column, generally at a rate of $8^{\circ}C\ min^{-1}$, in the helium flow. Any material desorbing from the surface during this process was revealed by continuous scanning of a number of pre-set-masses by the mass spectrometer.

3.3.4.5 Temperature Programmed Reactions (T.P.Rn.)

A 25 ml min^{-1} helium stream containing a small per cent of a reactant gas mixture, was established through the catalyst column, which was maintained at ambient temperature until surface-gas

Figure 3.13 'Reactive Frontal Chromatogram' for the reaction of N_2O with Copper

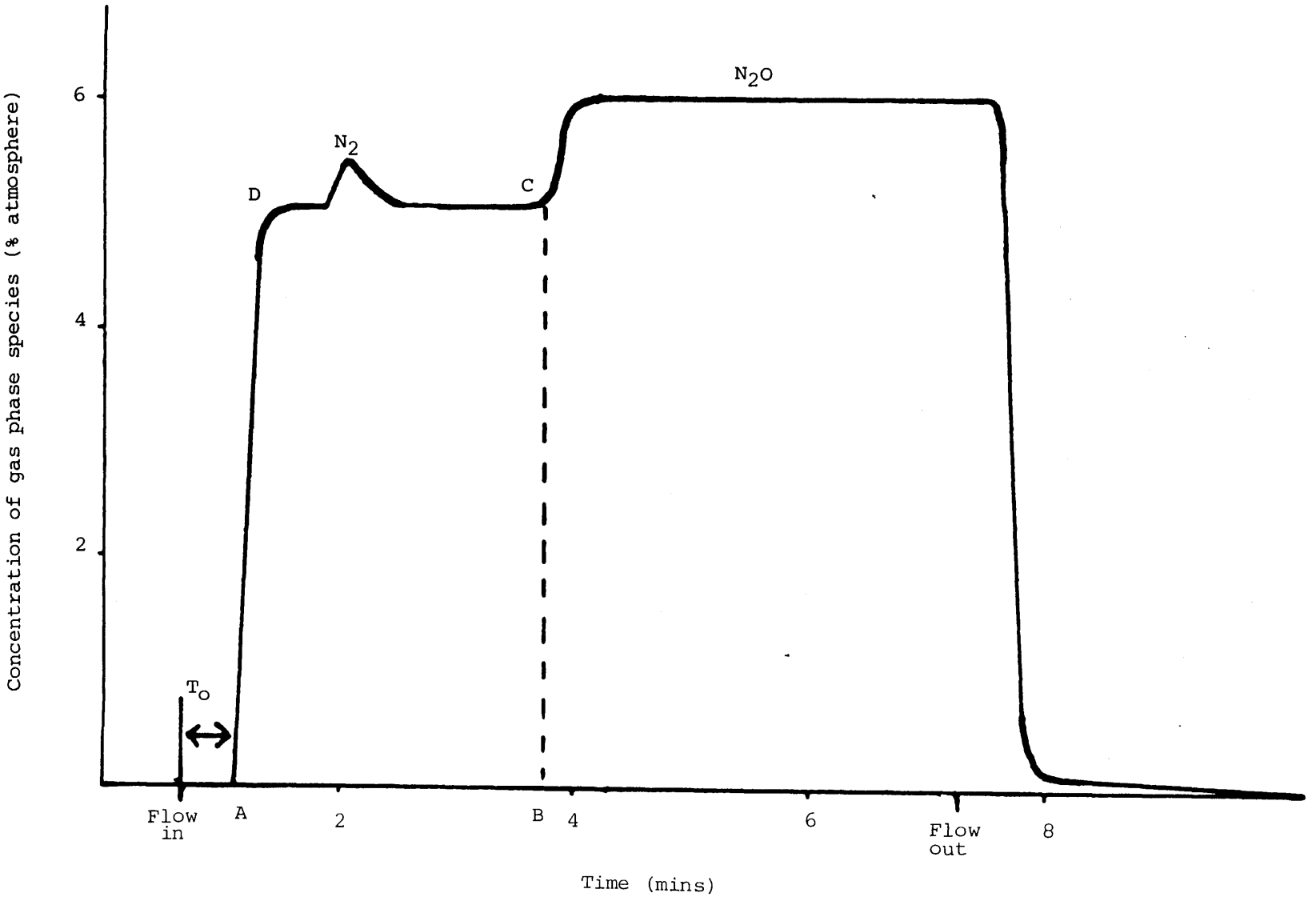

equilibrium had been obtained. Without disturbing this flow the temperature of the column was ramped, at $8^{o}C\ min^{-1}$, to a preset maximum of $250^{o}C$. During this period, the quantities of reactant and product gases eluting from the catalytic column were followed using the mass spectrometer. After cooling in the reactant gas stream, a T.P.D. study (Section 3.3.4.5) was then carried out.

3.3.4.6 Static Adsorption Studies and Subsequent Desorption Analysis

In order to mimic, as far as possible, the adsorption studies performed with the direct monitoring technique (Section 3.2.9.4) a number of adsorption systems were studied using a closed reaction vessel. This was achieved by allowing a reactant gas stream to flood the catalyst column and then switching the reactant flow through the reactor by-pass (Fig. 3.10). This produced an effectively closed reaction vessel containing a predetermined partial pressure of gaseous reactant. The effect of differing temperatures and reaction times upon this closed system was determined and the products of any reaction determined by mass spectroscopic analysis, after elution in a helium flow. A T.P.D. analysis was then performed as described in section 3.3.4.5.

C H A P T E R 4

EXPERIMENTAL ANALYSIS

EXPERIMENTAL ANALYSIS

4.1 Refinement of Radiochemical Analysis

4.1.1 Calibration of Radiochemical Data

It was noted in section 3.2.3 that the data collected on scaler-ratemeters during a radiochemical adsorption process was not used directly in the calculation of adsorption isotherms. A number of corrections were considered necessary to the experimental data and these factors were described in a qualitative manner in section 3.2.3. The means by which deadtime, background and intercalibration corrections were applied to the raw experimental data is presented below:

A(I) = total counts for GM1

B(I) = total counts for GM2

True count time for GM1

$$= T-A(I).S$$

True count time for GM2

$$= T-B(I).S$$

where T = Actual count time (secs)

S = Dead time (secs).

$$\text{GM1 count rate (c.p.s)} = \frac{A(I)}{T-A(I).S} = F(I).$$

$$\text{GM2 count rate (c.p.s)} = \frac{B(I)}{T-B(I).S} = G(I).$$

True GM1 count rate (c.p.s) = F(I)-W

True GM2 count rate (c.p.s) = G(I).Z-X

where w = background count for GM1 (c.p.s)

x = background count for GM2 (c.p.s)

z = intercalibration factor.

4.1.2 Errors Associated with Radiochemical Data

The errors on the calculated values of the deadtime, background count and intercalibration factors were small and, if combined in the calibration calculation shown in section 4.1.1, did not exceed the normal statistical error associated with the true count rates. The error on each of these values was, as with any other random process, the square root of the value itself.

4.1.3 Intercalibration of the Specific Count Rates of Radiolabelled Gases

Throughout the course of this study, batches of [14-C]carbon monoxide and [14-C]carbon dioxide were used which had distinctly different specific count rates. For ease of comparison and analysis, the different activities were, therefore, converted to a standard value of 2550 c.p.m. $torr^{-1}$. All the data presented in chapter 5 has been standardised in this manner.

4.2 Temperature Programmed Desorption Analysis

In this study, temperature programmed desorption (T.P.D.) analysis was effected by both radiochemical (section 3.2.9.5) and mass spectrometric (section 3.3.4.4) techniques. The total quantity of adsorbate desorbing from a catalytic surface during a T.P.D. analysis allows surface coverages to be determined. A number of mathematical treatments

can also be applied to enable calculation of the desorption activation energy ($E_{A(des)}$) of the adsorbed species. If the activation energy for adsorption is known, or is zero, the heat of adsorption of the species can then be calculated.

The mathematical treatment applied in this study is given below[144] :

$$\text{Rate of desorption} = -\frac{dn}{dt}$$

$$= \nu n^a \exp\left(\frac{-Ed}{RT}\right)$$

where n = surface coverage

ν = frequency factor

a = kinetic order

E_d = desorption energy.

In this analysis, linear temperature programming (at a rate of β deg.sec^{-1}) was applied and hence the rise in temperature of the catalyst can be calculated as

$$T = T_o + \beta t$$

where T_o = original catalyst temperature (K)

t = time (secs).

Therefore, $\frac{dT}{dt} = \beta$

and $\frac{dn}{dt} = \frac{dT}{dt}\ \frac{dn}{dT}$

$$= \beta \frac{dn}{dT}$$

Therefore,

$$\text{Rate of desorption} = \frac{-dn}{dT}$$

$$= \frac{\nu n^a}{\beta} \exp\left(\frac{-Ed}{RT}\right)$$

where β = heating rate ($deg.sec^{-1}$)

At the maximum rate of desorption (temperature = T_p)

$$\frac{-d^2n}{dT^2} = 0$$

By differentiation and substitution we obtain

$$\frac{\nu a n^{a-1}}{\beta} \exp\left(\frac{-Ed}{RT_p}\right) = \frac{Ed}{RT_p^2}$$

For <u>first-order</u> desorption, a = 1 and hence

$$\frac{E_d}{RT_p^2} = \frac{\nu}{\beta} \exp\left(\frac{-E_d}{RT_p}\right)$$

If $\nu = 10^{13}$ sec^{-1} (as proposed by transition state theory[145]) this equation allows a value of E_d to be obtained by iteration.

4.3 Line-shape Analysis

In this study, line-shape analysis of mass spectrometer data has proved a useful means of determining a variety of reaction activation energies.

(a) Consider $A_{(g)} + B_{(g)} \rightarrow C_{(g)} + D_{(g)}$

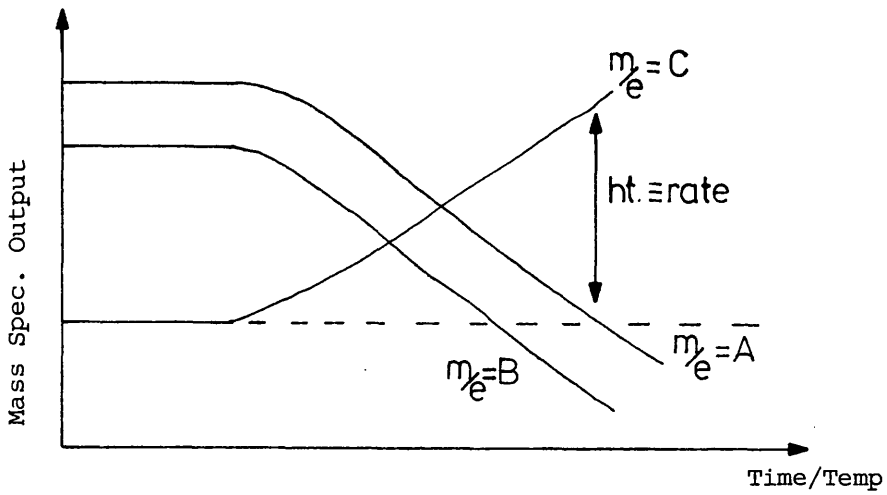

Figure 4.1. Line-shape Analysis of Reaction of $A_{(g)} + B_{(g)} \rightarrow C_{(g)}$

Rate of reaction = rate of production of $C_{(g)}$

≡ height of line C above background.

Now, rate = $k[A][B]$

where k = rate constant.

Therefore, $\ln(\text{rate}) = \ln k + \ln[A] + \ln[B]$

$$= \ln A - \frac{E_A}{RT} + \ln[A] + \ln[B]$$

At low percentage conversion, [A] and [B] are constant, therefore

$$\ln(\text{rate}) = -\frac{E_A}{RT} + \text{constant}$$

i.e. $$\ln(\text{height}) = -\frac{E_A}{RT} + \text{constant.}$$

Therefore, a plot of $\ln$ (height) against $\frac{1}{T}$ gives a straight line of gradient $-\frac{E_A}{R}$

(b) Consider $[A]_{ads} \rightarrow B_{(g)} + C_{(g)}$

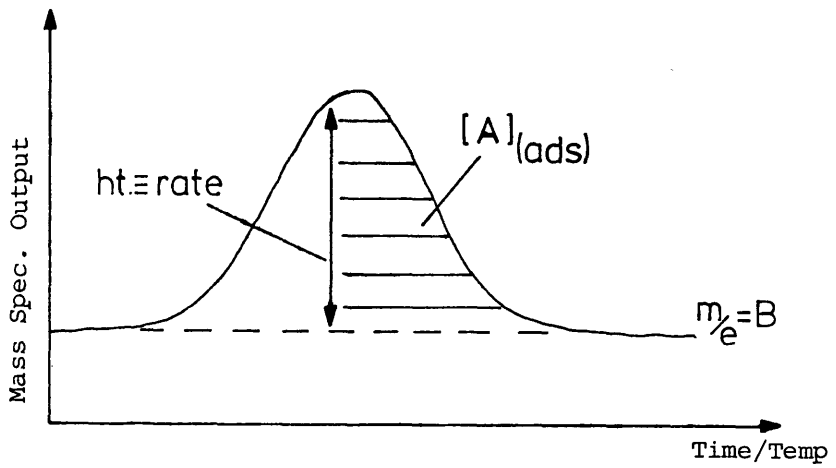

Figure 4.2 Line-shape Analysis of $[A]_{ads} \rightarrow B_{(g)} + C_{(g)}$

Rate of reaction = $k[A]_{ads}$.

= rate of production of B

= height of line B above background.

Therefore, height = $k[A]_{ads}$

and $\frac{\text{height}}{[A]_{ads}} = k$

Now, $[A]_{ads}$ = area of desorption peak.

Therefore, $\ln\left(\frac{\text{height}}{\text{area}}\right) = \ln A - \frac{E_A}{RT}$

and a plot of $\ln\left(\frac{\text{height}}{\text{area}}\right)$ against $\frac{1}{T}$ allows E_A to be determined from the gradient of the plot.

4.4 Calculation of Catalyst Surface Areas by N_2 Adsorption at $-196^{\circ}C$

The method by which gas-adsorption chromatography was used to determine the isotherm associated with the adsorption of nitrogen on copper oxide at $-196^{\circ}C$ (Fig. 4.3) is detailed in section 3.3.4.2.

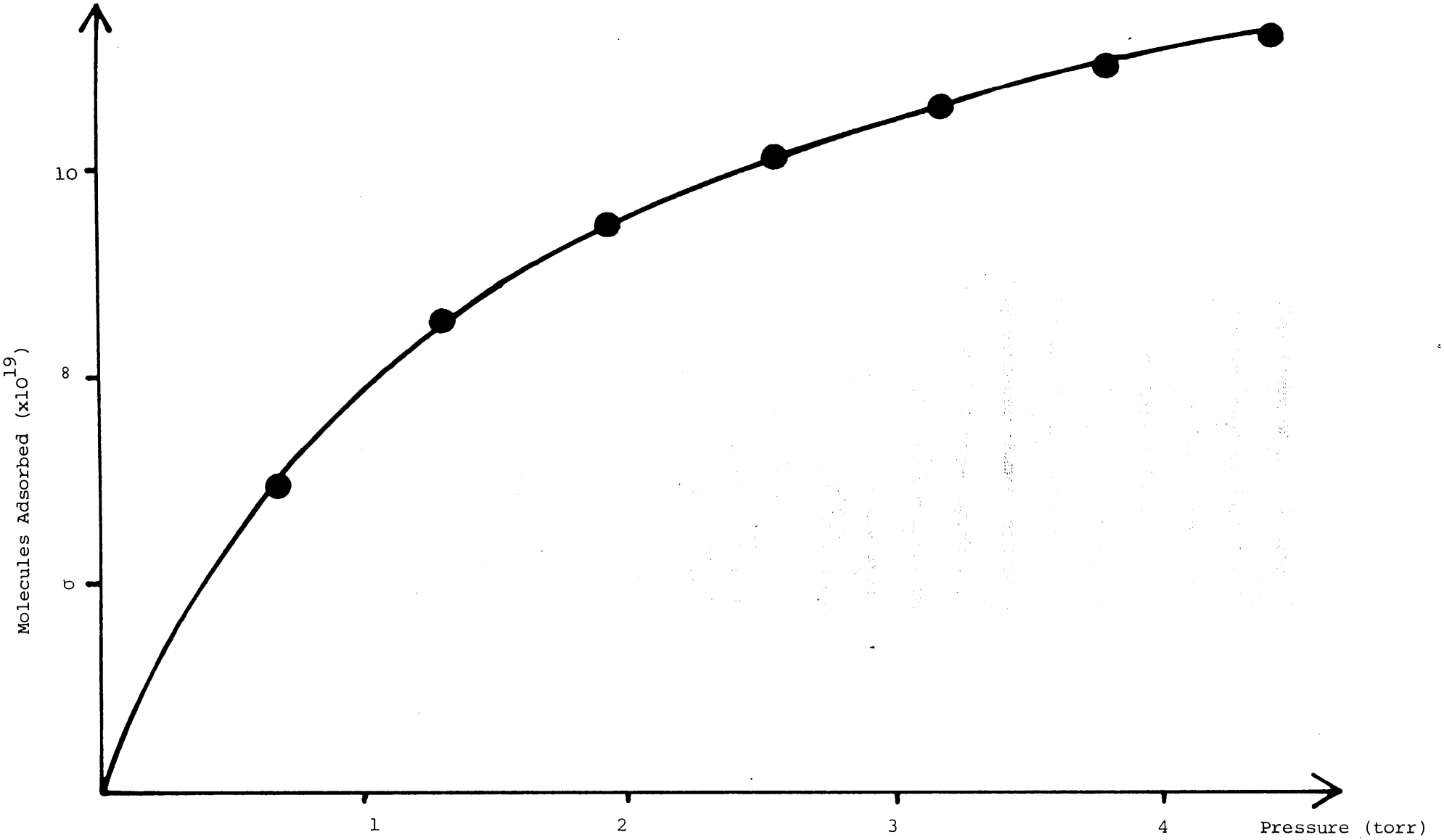

Figure 4.3 The Adsorption of N_2 on CuO (-196°C)

At -196°C, the adsorption of nitrogen on copper oxide, and many other substrates, is expected to produce S-shaped isotherms[146]. Figure 4.3 shows that, under the conditions used in this study, the linear portion of this type of isotherm had been reached. The beginning of this linear region corresponds to the presence of a unimolecular layer of adsorbed gas on the surface, that is point B on the isotherm as defined by Brunauer, Emmett and Teller [146]. It therefore follows that the total nitrogen uptake, under these flow conditions (area BCDE, Fig. 3.11), allows an estimate to be made of the total surface area of the sample. If the area covered by a nitrogen molecule is assumed to be $1.62 \times 10^{-19} m^2$, a cupric oxide total surface area of $10.3 m^2 g^{-1}$ is obtained.

This value can be ratified by linearising the isotherm with respect to the B.E.T. equation. This is possible since, with the B.E.T. equation in the form:

$$\frac{P}{V(P_O-P)} = \frac{1}{V_M C} + \frac{C-1}{V_M C} \cdot \frac{P}{P_O}$$

where P = pressure of gas

P_O = saturation vapour pressure

V = volume adsorbed

V_m = monolayer adsorbed volume

and C = constant,

a plot of $\frac{P}{V(P_O-P)}$ against $\frac{P}{P_O}$

allows V_m to be calculated from the gradient and intercept of the plot (Fig. 4.4). A surface area of $10.02\ m^2 g^{-1}$ is obtained using this

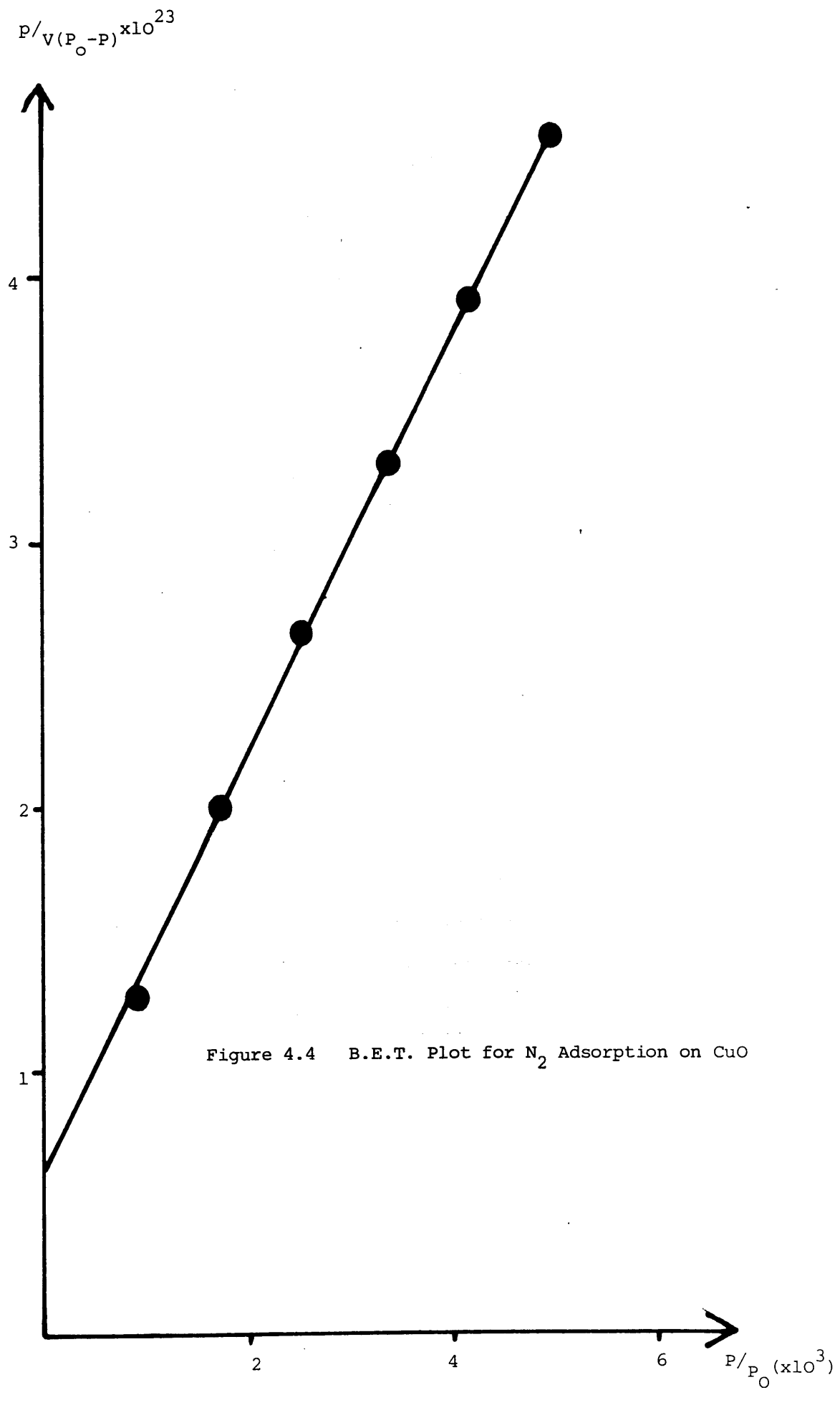

Figure 4.4 B.E.T. Plot for N_2 Adsorption on CuO

method. The value of the constant C, gathered from the B.E.T. equation, gives a heat of adsorption of 9.6 KJ mol^{-1} for nitrogen on this cupric oxide sample.

This procedure was also applied to determine the total surface area of a polycrystalline copper catalyst. The result obtained from this analysis is compared to that produced by nitrous oxide decomposition (section 3.3.4.3) in section 4.5.4.

4.5 The Calculation of Copper Metal Surface Areas by Nitrous Oxide Decomposition

A study of the nitrous oxide-copper system was considered necessary since, although the reaction is well documented (for example section 1.7), the analytical system described in section 3.2.9.3 is unique to this study. It was therefore essential to prove that, under the operating conditions inherent in our apparatus, this was a suitable method for copper metal surface area determination.

The specific surface areas determined for different polycrystalline copper samples were not constant, but rather lay in the range 4-6 m^2g^{-1}. This variation was due to the irreproducibility of the slurrying (section 3.2.2) and reduction (section 3.2.9.2) procedures utilised in this study.

4.5.1 The Effect of Reduction-Oxidation Cycles on Copper Surface Areas

0.2082g of cupric oxide was reduced as described in section 3.2.9.2. An excess quantity of nitrous oxide was allowed to interact with the copper surface, for 24 hours, at a temperature of 80°C. The surface

area of the sample was calculated to be 4.9 m^2g^{-1}. This reduction - oxidation cycle was then exactly reproduced. The surface area of the sample was found to be 5.1 m^2g^{-1}.

4.5.2 The Temperature Dependence of Nitrous Oxide Decomposition on Copper

A variety of redox cycles were effected on a 0.2065g sample of cupric oxide, in which only the temperature of the oxidation procedure was varied. The results presented in Table 4.1 show no significant effect of a temperature variation in the 40-80°C range.

Reaction Time	Temp.	Surface Area
15 mins.	80°C	4.2 m^2g^{-1}
15 mins.	60°C	4.1 m^2g^{-1}
15 mins.	40°C	4.2 m^2g^{-1}

Table 4.1. The Effect of Temperature on N_2O Decomposition.

4.5.3 The Time Dependence of Nitrous Oxide Decomposition on Copper

A fully reduced sample of cupric oxide (0.2162g) was allowed to interact with an excess quantity of nitrous oxide, for 15 mins, at 75°C. The surface area was found to be 5.6 m^2g^{-1}.

Upon re-reduction, and oxidation at 75°C for a period of 20 hours, the surface area was determined as 5.9 m $^2g^{-1}$. The reaction was evidently not time dependent at this temperature.

4.5.4 Comparison of Copper Surface Areas as Determined by Nitrous Oxide Decomposition and Nitrogen Adsorption

Following full reduction, the total surface area of a sample of polycrystalline copper was determined by nitrous oxide decomposition, at 60°C (section 3.3.4.3), to be 3.1 m^2. On rereduction the surface area was determined by nitrogen adsorption at -196°C and was found to be 3.3 m^2.

The low temperature adsorption of nitrogen, on copper, is, by its nature, a surface limited process. On the contrary, it has never been proven that only the exterior of a copper sample is oxidised by reaction with nitrous oxide. However, the close similarity of the above surface areas, determined by completely different techniques, proves that, at 60°C, nitrous oxide decomposition is a totally surface limited process, which acts to produce Cu(I), rather than Cu(II), species.

C H A P T E R 5

RADIOTRACER STUDIES INVOLVING THE CARBON-14 ISOTOPE

RADIOTRACER STUDIES INVOLVING THE CARBON-14 ISOTOPE

5.1 ADSORPTION ON POLYCRYSTALLINE COPPER

5.1.1 THE ADSORPTION OF [14-C]CARBON MONOXIDE

5.1.1.1 [14-C]Carbon Monoxide Adsorption

Figure 5.1 shows a typical isotherm produced by the adsorption of [14-C]carbon monoxide on 0.168g of freshly reduced polycrystalline copper. An equilibration period of 10 minutes, subsequent to the admission of a charge of radiolabelled material into the reaction vessel, was found to be sufficient to ensure complete gas-surface equilibration. Carbon monoxide was found to be the only species present in the gas phase during the build-up of the adsorption isotherm, as monitored by gas chromatographic analysis.

Some measure of the relative strength of the carbon monoxide-copper bond was gathered by exposing the catalyst to the pump section of the high vacuum apparatus. Following 15 minutes evacuation, the surface count rate had fallen from a saturation value of 2480 c.p.m. to 48 c.p.m. Only 2% of the total quantity of previously adsorbed carbon monoxide was therefore resistant to this evacuation.

Following evacuation, further charges of [14-C]carbon monoxide were admitted to the copper sample. This resulted in the production of an isotherm identical to that produced by the original carbon monoxide adsorption (Fig. 5.1). If the gas and surface count rates are considered as equivalent to the pressure resident within the system, P, and the adsorbed volume, V, respectively, a test of the Langmuir treatise of adsorption may be applied. Figure 5.2 shows that a plot of

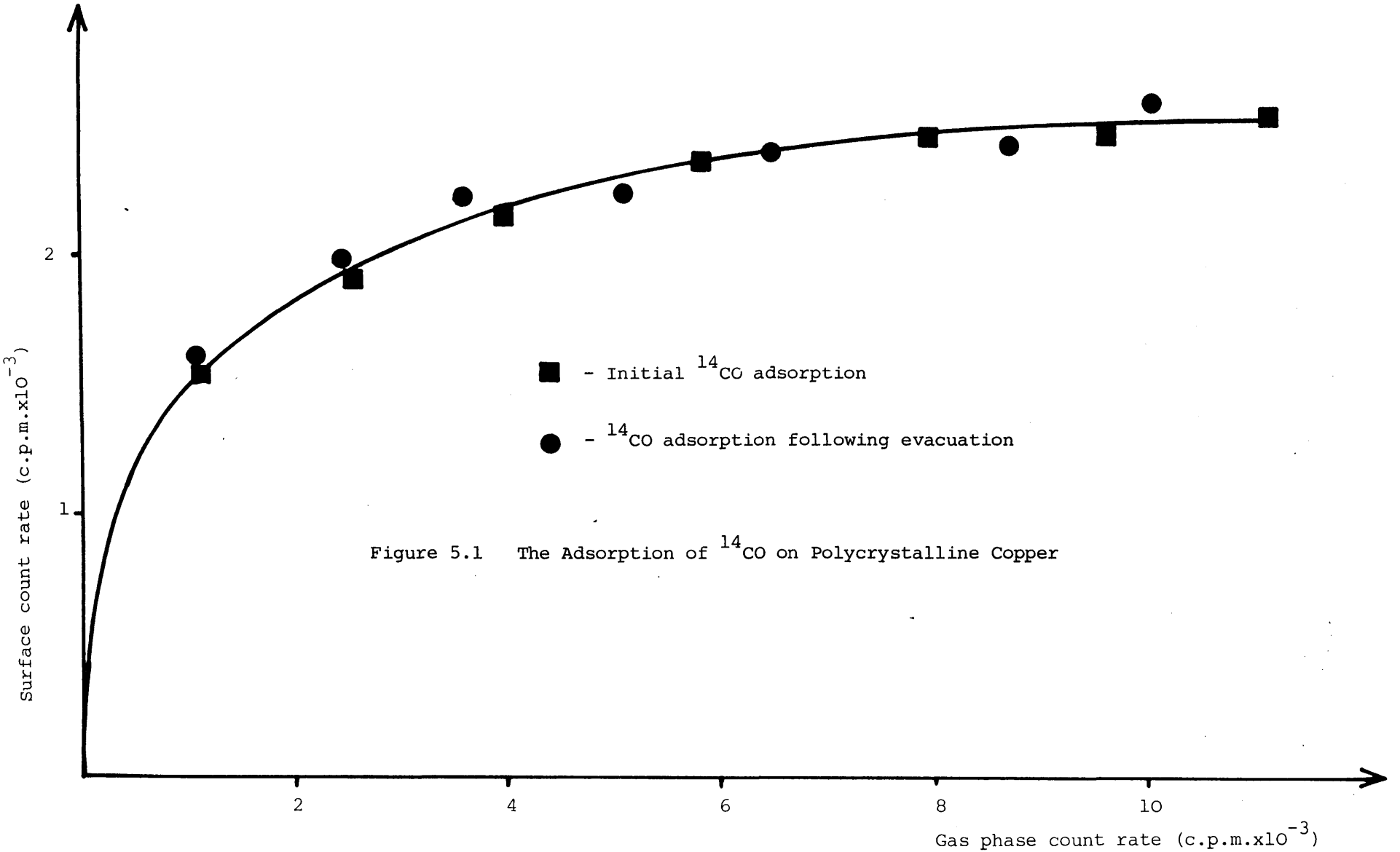

Figure 5.1 The Adsorption of ^{14}CO on Polycrystalline Copper

Figure 5.2 Langmuir plot for ^{14}CO adsorption on copper

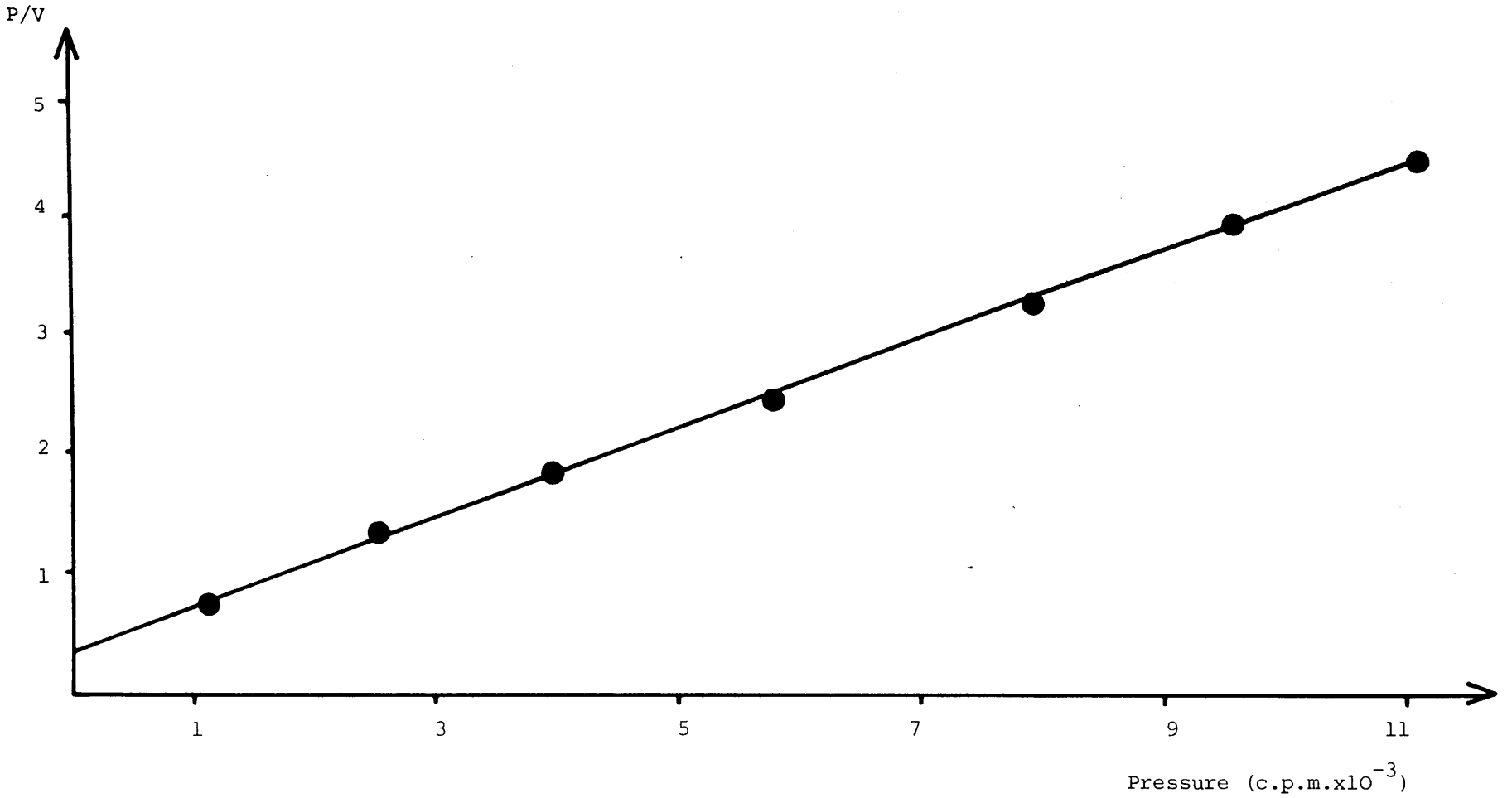

P/V against P gives a perfect straight line. From the gradient of the plot, the monolayer adsorbed volume is equivalent to a surface count rate of 2683 c.p.m. The fractional surface coverage, V/Vm, under the pressure and temperature conditions utilised in this study, may then be calculated. This allows an average value of the heat of adsorption of carbon monoxide on this surface to be calculated by substitution into Langmuir's original equation. A heat of adsorption of 43 KJ mol^{-1} is generated by this method.

5.1.1.2 Molecular Exchange

4.7 torr of [14-C]carbon monoxide was equilibrated for 30 minutes over a freshly reduced polycrystalline copper sample. The surface count rate after this period was determined as 2249 c.p.m. 4.7 torr of unlabelled carbon monoxide was then added to the reaction vessel, which caused the surface count rate to fall, instantly, to 1259 c.p.m. (44% decrease).

A 50% drop in the specific activity of the gas phase radioactivity would be expected to generate a 50% decrease in the measured surface activity, if all the adsorbed species were labile. In this case, it appears that 88% of the adsorbed carbon monoxide species will undergo a facile molecular exchange.

5.1.1.3 The Influence of Preadsorbed Material on [14-C]Carbon Monoxide Adsorption

(a) Preadsorbed [14-C]Carbon Dioxide

Small charges of [14-C]carbon dioxide were admitted to the reaction vessel, which contained 0.22g of copper, until a total pressure of 5.6 torr was resident in the system. Without evacuation,

charges of the [14-C]carbon monoxide were then added to the gas phase of the reaction vessel. Figure 5.3 details the adsorption processes that occurred in this experiment. Significant [14-C]carbon monoxide adsorption took place on the [14-C]carbon dioxide pretreated surface.

(b) Preadsorbed [12-C]Carbon Dioxide

Following the equilibration of 3.87 torr of unlabelled carbon dioxide on a copper sample, charges of [14-C]carbon monoxide were added to the adsorption system. A typical carbon monoxide-copper adsorption isotherm (e.g. Fig. 5.1) was generated by this procedure. After 7 minutes evacuation, it was found that only 0.5% of the previously adsorbed carbon monoxide species were still associated with the copper surface.

(c) Preadsorbed Hydrogen and [14-C]Carbon Dioxide

4.26 torr of hydrogen was equilibrated over a copper sample for 30 minutes. Without evacuation, charges of [14-C]carbon dioxide were added to the adsorption system. Again without evacuation, charges of [14-C]carbon monoxide were admitted to the reaction vessel. The changes in the surface and gas phase count rates are shown in Figure 5.4.

(d) Quantitative Analysis of Carbon Dioxide and Hydrogen Preadsorption Effects-Construction of [14-C]Carbon Monoxide Reference Isotherm

Figure 5.1 shows that two consecutive [14-C]carbon monoxide adsorptions on a copper surface, separated only by an evacuation procedure, generated identical isotherms. The initial adsorption process can therefore be considered to produce a reference isotherm for

Figure 5.3 The Adsorption of $^{14}CO_2$ and ^{14}CO on copper

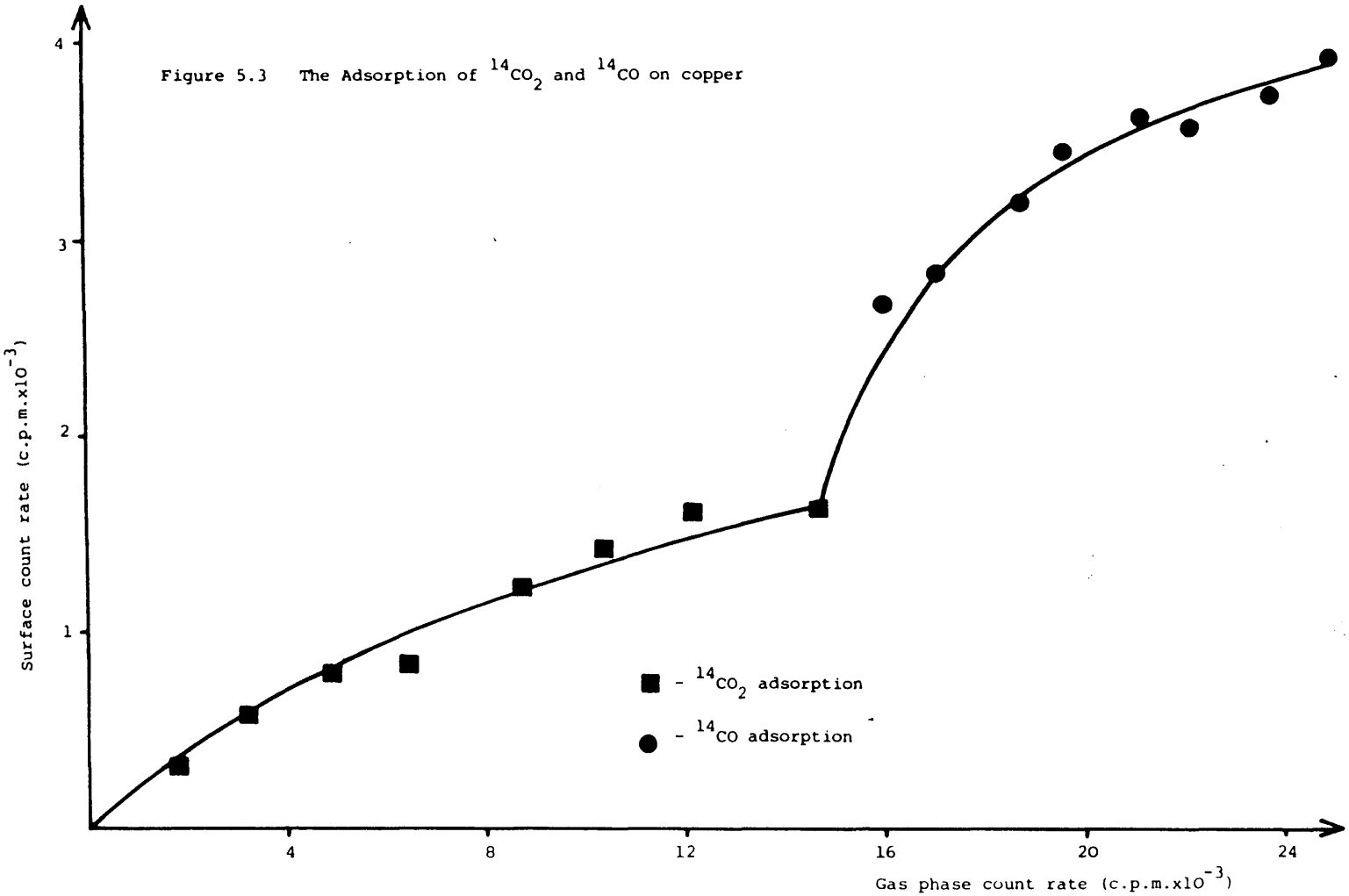

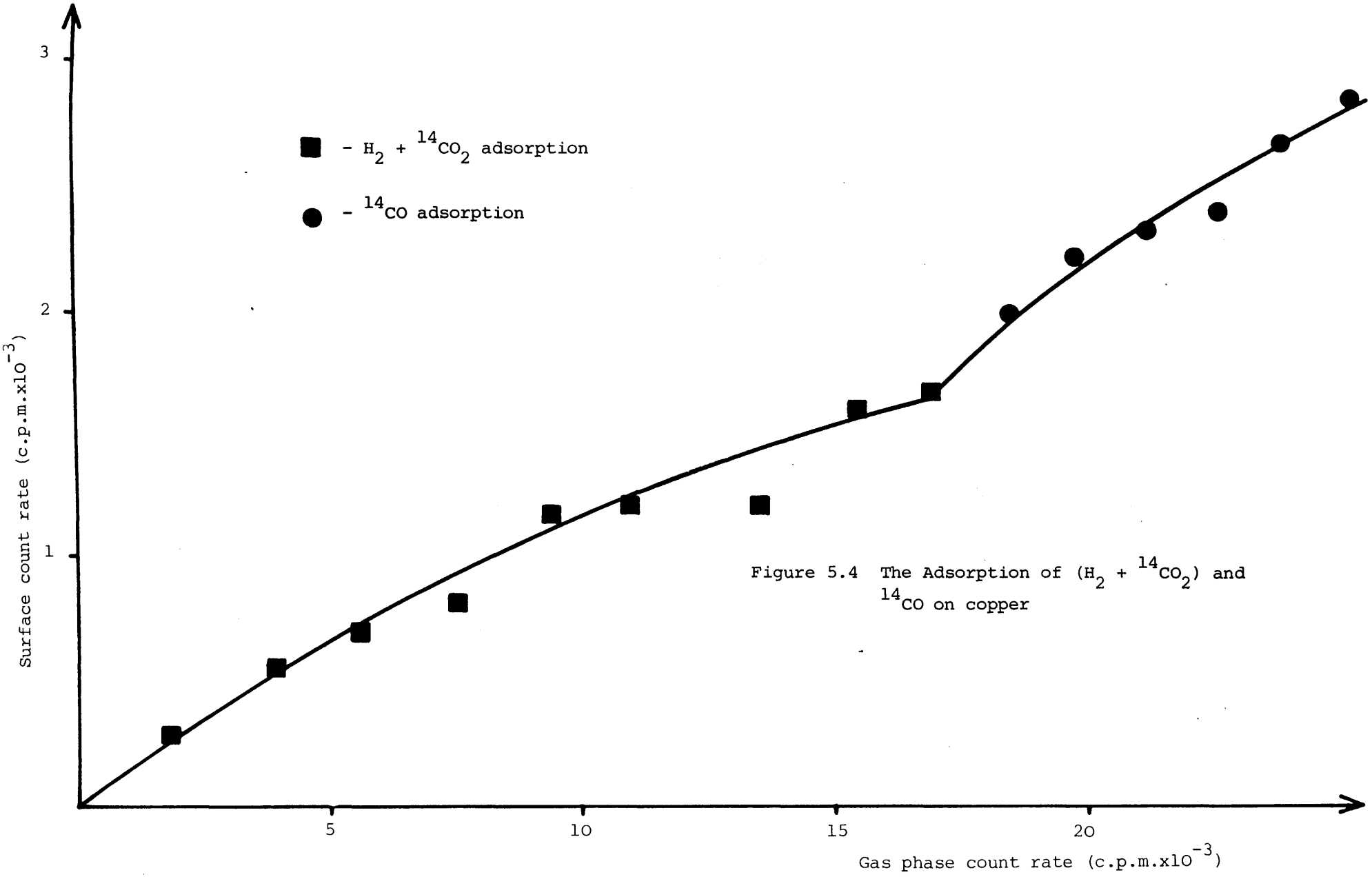

Figure 5.4 The Adsorption of (H_2 + $^{14}CO_2$) and ^{14}CO on copper

a particular copper sample.

Having created a reference isotherm specific to one copper surface, and, following subsequent evacuation, a charge of an unlabelled gaseous material may be admitted to the reaction vessel. If [14-C]carbon monoxide adsorption is unaffected by the presence of this material, adsorption should lead to the production of an isotherm identical to that of the previously constructed reference. Otherwise, any change in the isotherm must be related to the presence of the preadsorbed material.

The production of these reference isotherms allowed all the experiments to be completely self consistent and consequently independent of slight changes in counting geometry and the differing weights of catalyst used from experiment to experiment.

The effects of pretreating the copper surface with 5 torr carbon dioxide, 5 torr hydrogen and 10 torr carbon dioxide and hydrogen (equal mole fractions), for 30 minute periods, are shown in Figures 5.5, 5.6 and 5.7. A quantitative analysis of these experiments is given in Table 5.1.

Preadsorbed Species	Change in [14-C]CO Adsorption
CO_2	-34%
H_2	-21%
$CO_2 + H_2$	-29%

Table 5.1 Quantitative Analysis of [14-C]CO Preadsorption Experiments (Copper)

Figure 5.5 The Adsorption of ^{14}CO on a $^{12}CO_2$ pretreated copper surface

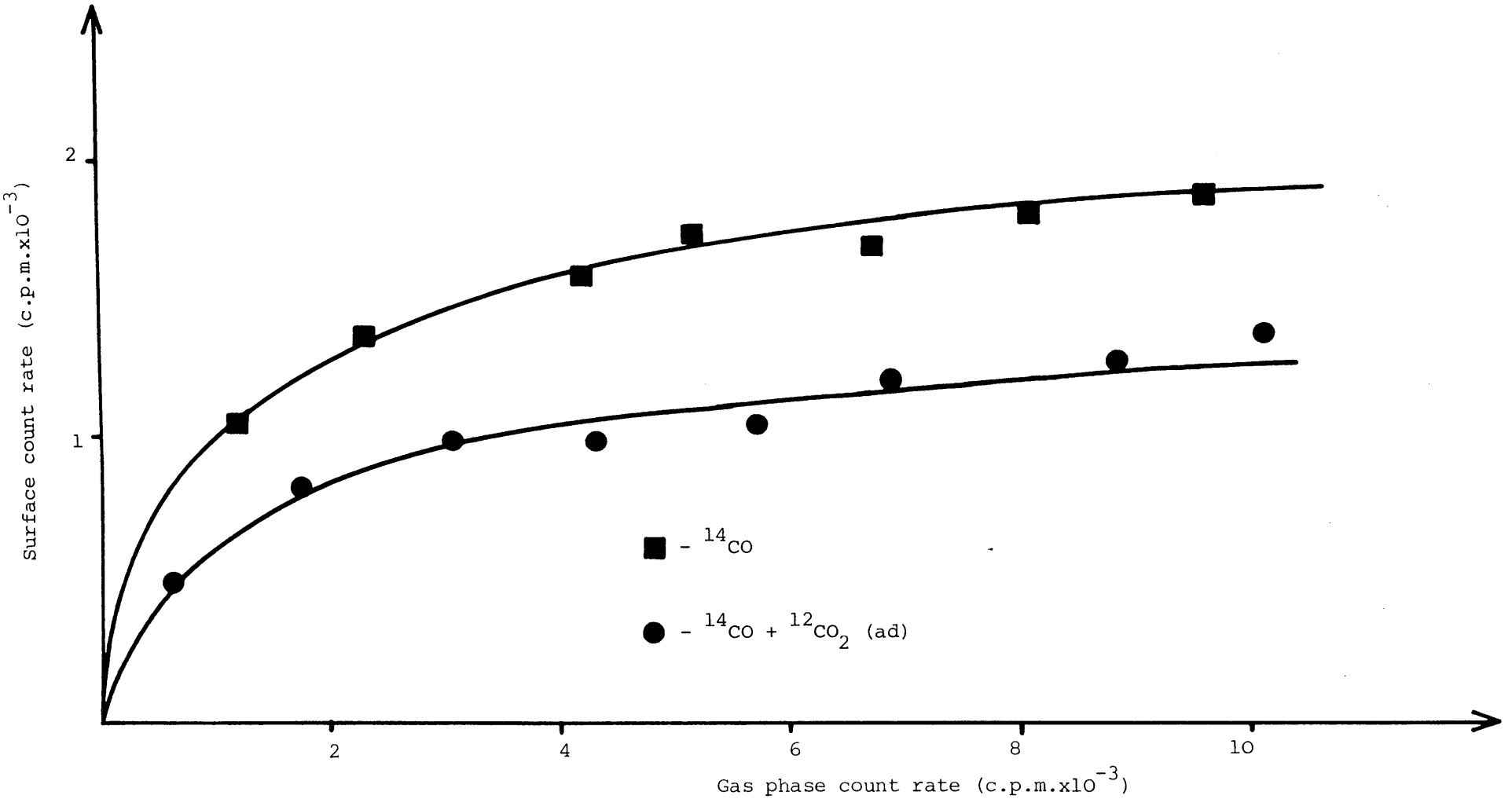

Figure 5.6 The Adsorption of ^{14}CO on H_2 pretreated copper surface

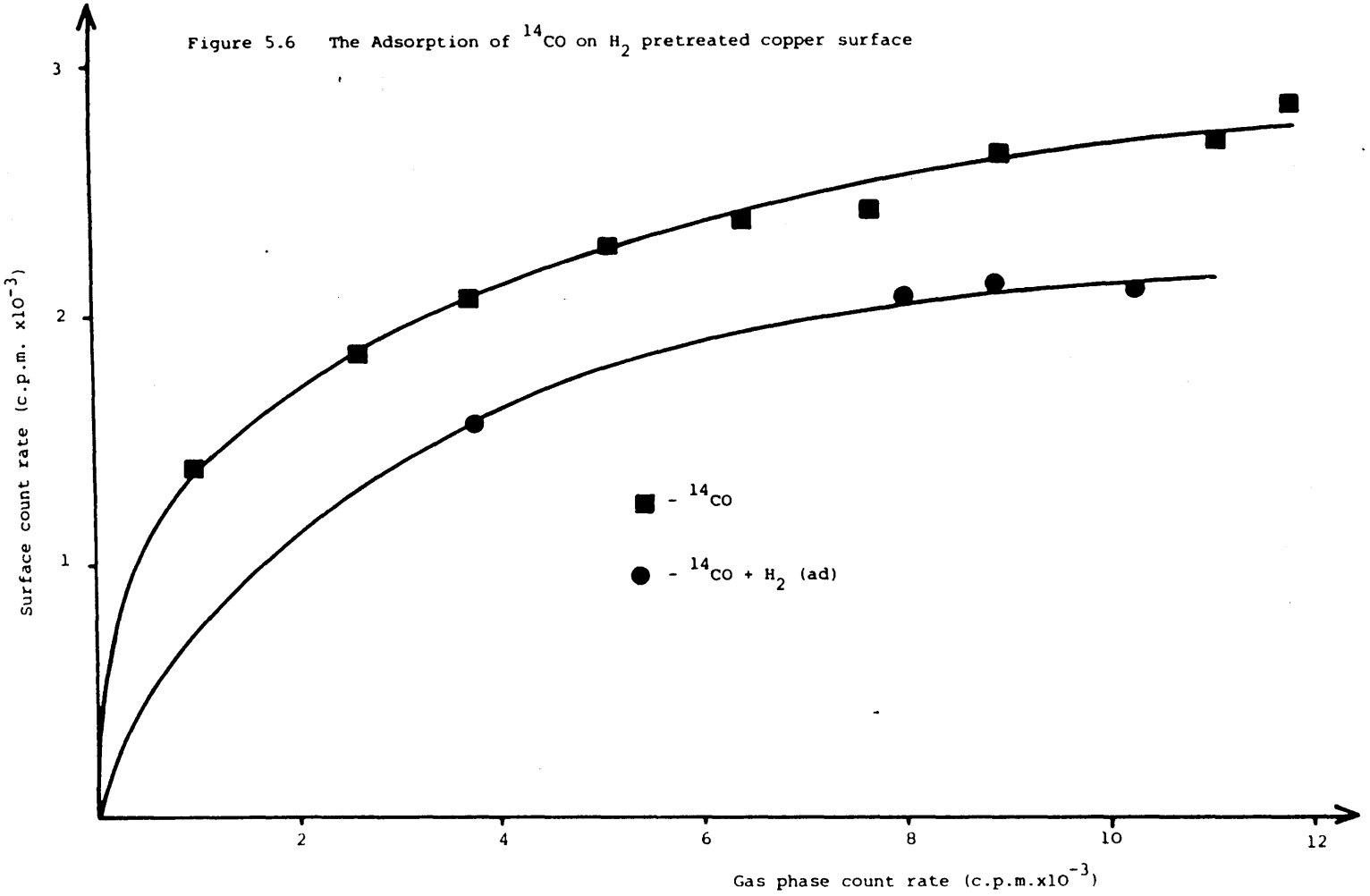

Figure 5.7 The Adsorption of ^{14}CO on a $^{12}CO_2 + H_2$ pretreated copper surface

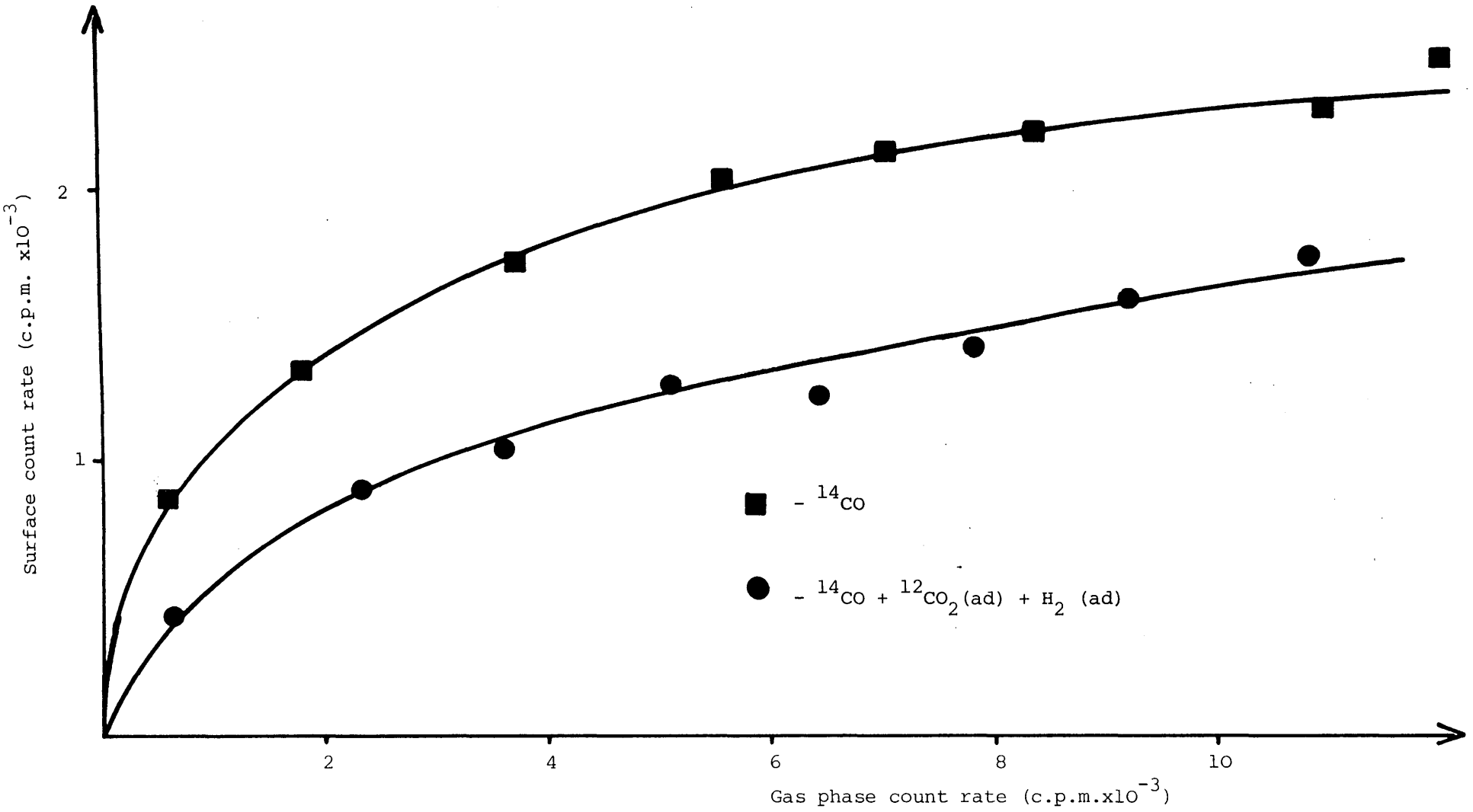

5.1.1.4 The Influence of Coadsorbing Material on [14-C]Carbon Monoxide Adsorption

The effect of coadsorbing species on [14-C]carbon monoxide adsorption was determined by admitting charges of gas, containing equal mole fractions of [14-C]carbon monoxide and a variety of unlabelled adsorbates, into the reaction vessel containing a copper surface which had previously been characterised by production of a [14-C]carbon monoxide reference isotherm.

The effects of coadsorbing carbon dioxide, hydrogen and carbon dioxide and hydrogen are shown in Figures 5.8, 5.9 and 5.10. A quantitative analysis of these experiments is given in Table 5.2.

Coadsorbate(s)	Change in [14-C]CO Adsorption
CO_2	-26% → -29%
H_2	-20%
$CO_2 + H_2$	-25%

Table 5.2 Quantitative Analysis of [14-C]CO Coadsorption Experiments (Copper)

5.1.1.5 Displacement of Adsorbed [14-C]Carbon Monoxide from the Copper Surface

(a) [12-C]Carbon Dioxide Displacement

Following the equilibration of 4.29 torr of [14-C]carbon monoxide over 0.16g of copper, small charges of [12-C]carbon

Figure 5.8 Co-adsorption of $^{14}CO + {}^{12}CO_2$ on copper

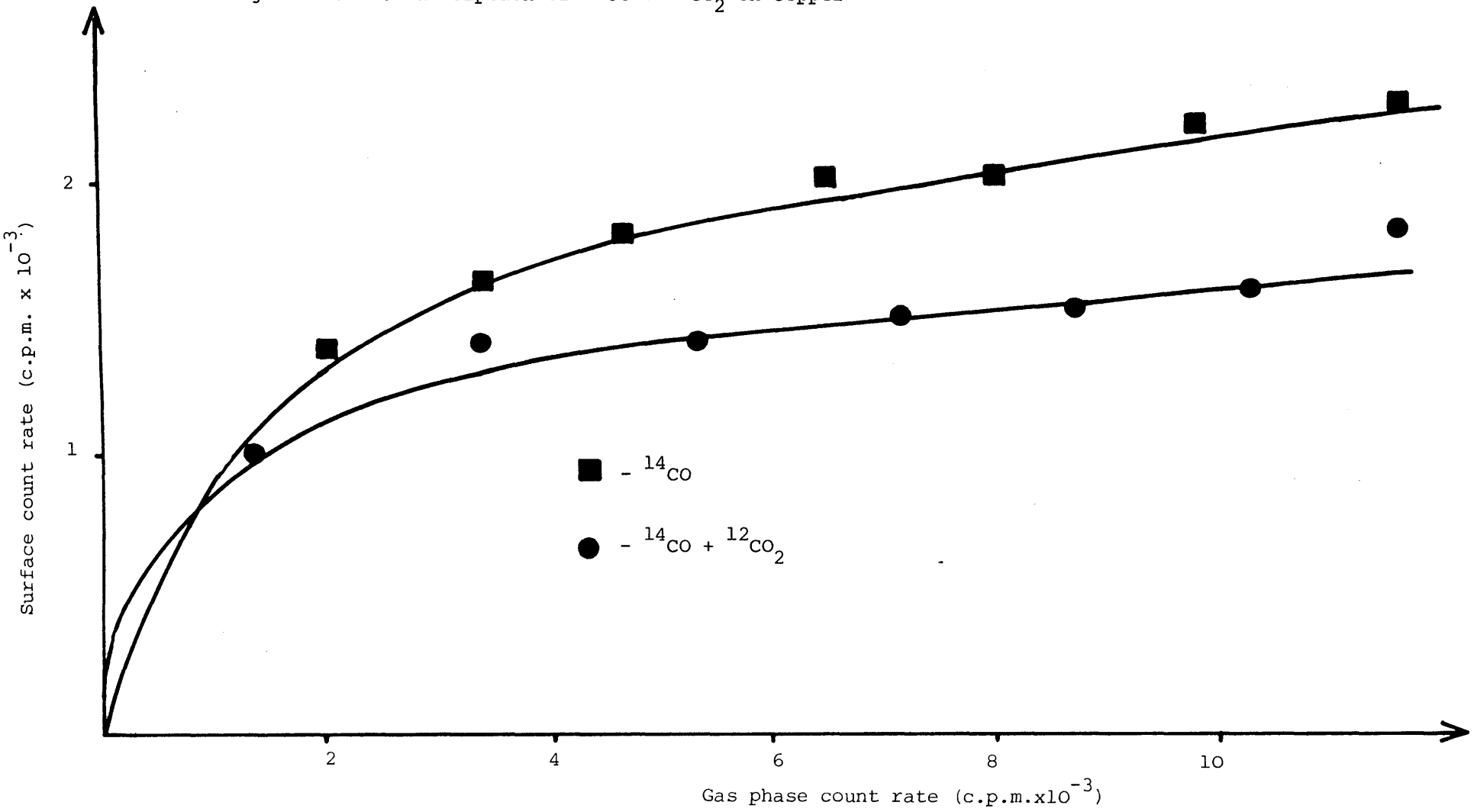

Figure 5.9 Co-adsorption of $^{14}CO + H_2$ on copper

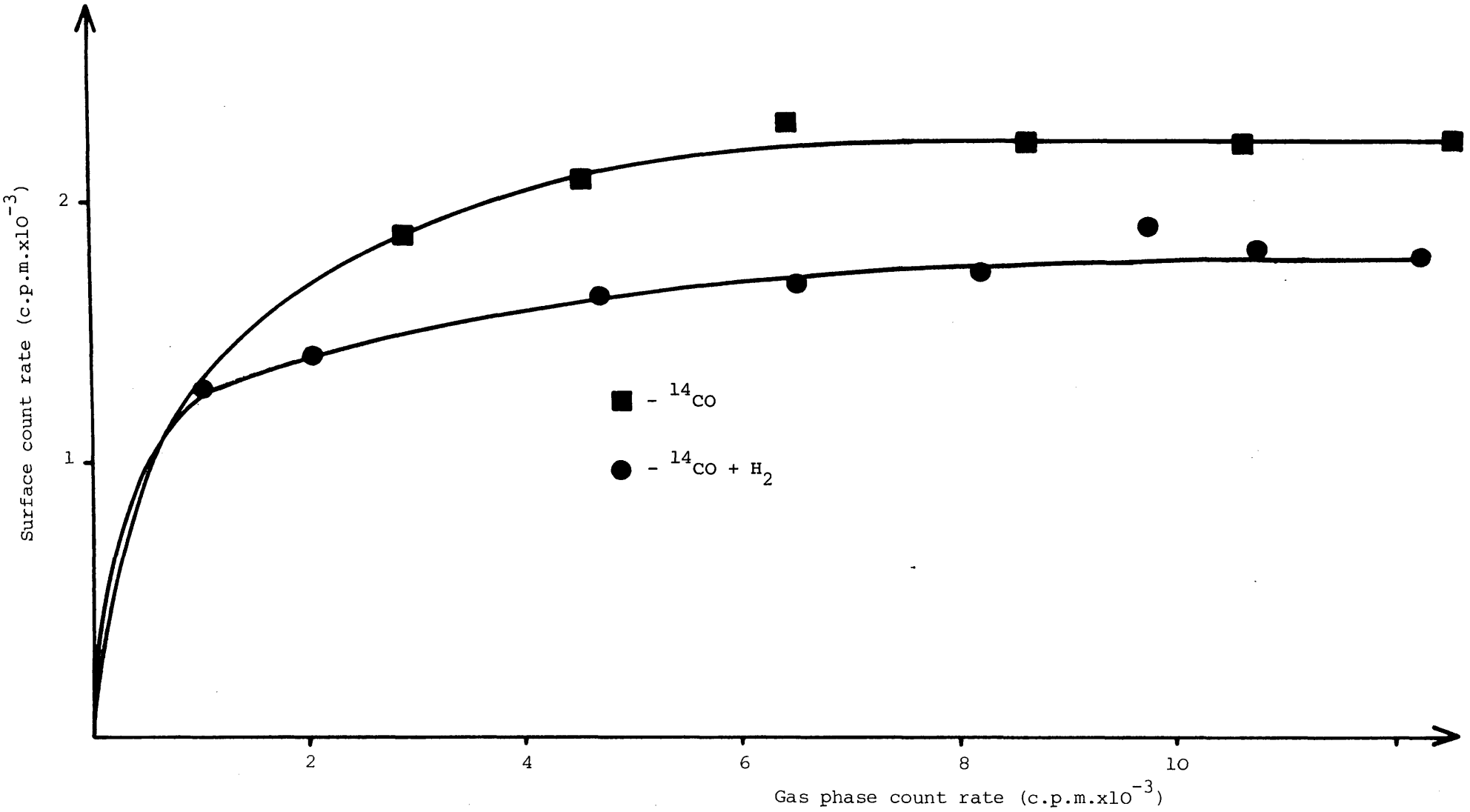

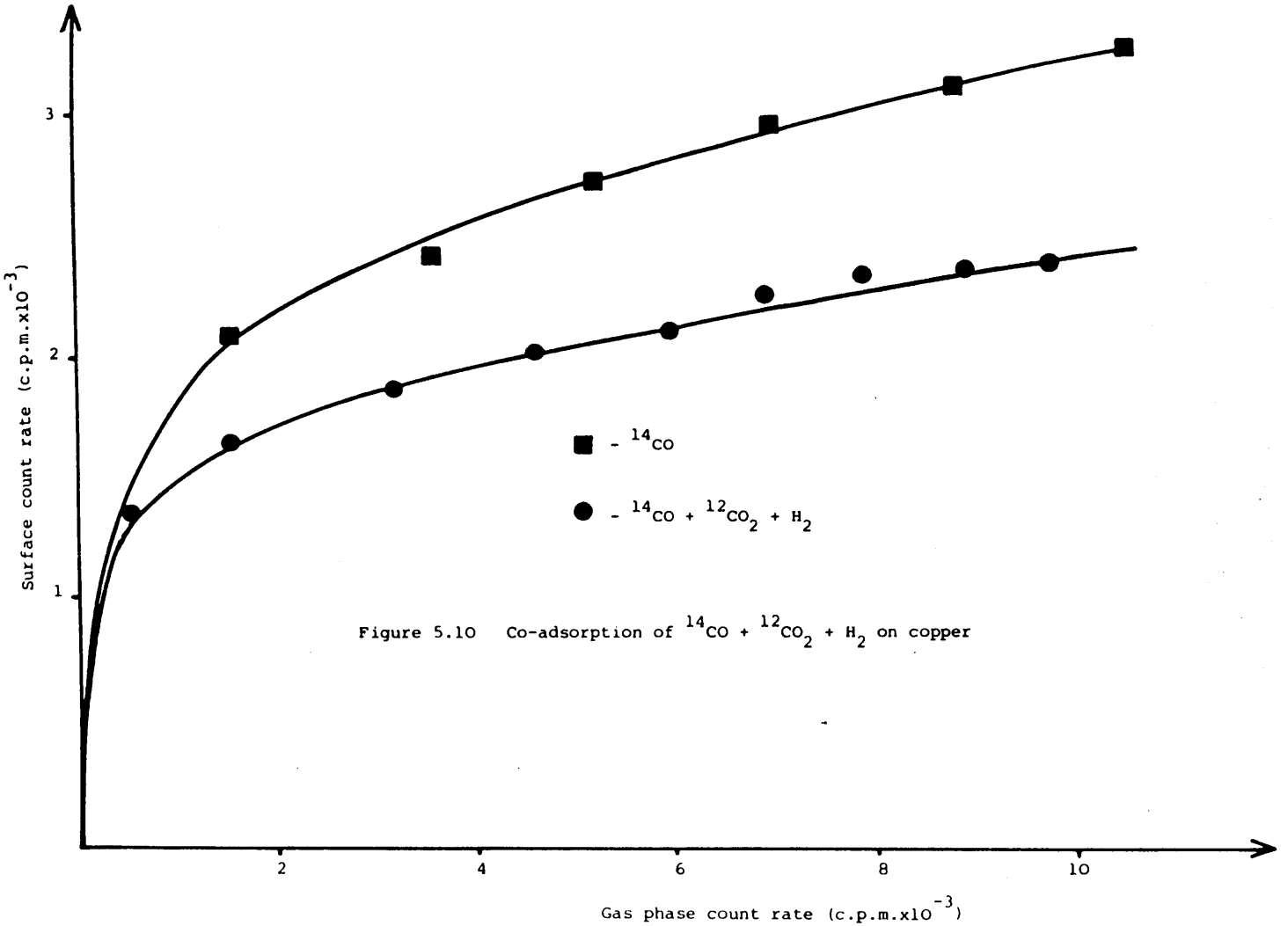

Figure 5.10 Co-adsorption of $^{14}CO + {}^{12}CO_2 + H_2$ on copper

dioxide were added to the reaction vessel until a total pressure of 8.42 torr was attained. Five minutes after the addition of each charge of carbon dioxide, the surface count rate was monitored. The results obtained are shown in Table 5.3.

Pressure [12-C]CO_2 (torr)	Surface Count Rate (c.p.m.)	% Change
0	2786	-
0.51	2636	-5.3
1.03	2639	-5.3
1.55	2592	-6.9
2.07	2513	-9.8
2.58	2469	-11.4
3.09	2560	-8.1
3.62	2465	-11.5
4.13	2339	-16.0

Table 5.3 Displacement of [14-C]CO by CO_2 (Copper)

0.56 torr of hydrogen was then added to this gaseous mixture. After 5 minutes the surface count rate had fallen, by a further 10.2%, to a value of 2101 c.p.m. The addition of further amounts of hydrogen had little effect on this value.

(b) Hydrogen Displacement

The equilibration of 4.38 torr of [14-C]carbon monoxide over 0.16g of copper produced a surface count rate of 2958 c.p.m. A small

charge of hydrogen (0.62 torr) was then added to the reaction vessel. This caused the count rate to drop, instantaneously, to a value of 2876 c.p.m. (2.8% decrease). Addition of further charges of hydrogen caused no significant change in this value.

5.1.2 THE ADSORPTION OF [14-C]CARBON DIOXIDE

5.1.2.1 [14-C]Carbon Dioxide Adsorption

Figure 5.11 shows a typical isotherm produced by the adsorption of [14-C]carbon dioxide on 0.171g of polycrystalline copper. Carbon dioxide was found to be the only species present in the gas phase during the build up of the adsorption isotherm.

After the addition of each charge of [14-C]carbon dioxide into the reaction vessel, 10 minutes was allowed to elapse before the gas and surface count rates were determined. This period was not considered adequate to allow gas-surface equilibrium to be attained, since previous studies had found that carbon dioxide interacted only very slowly with copper surfaces. Indeed, equilibrium was not expected until a period of several hours had elapsed. The surface count rates obtained after a 10 minute period were considered relatively stable within the time span of most of the experiments described in this section.

The above feature made it impossible to discuss the adsorption of carbon dioxide, on copper, in terms of saturation coverage. Rather, to facilitate a quantitative analysis of the [14-C]carbon dioxide adsorption isotherms, the surface count rate produced at a standing gas pressure of 4 torr [14-C]carbon dioxide was calculated. Whenever, in this section, a percentage change in the volume of adsorbed

Figure 5.11 The Adsorption of $^{14}CO_2$ on Polycrystalline Copper

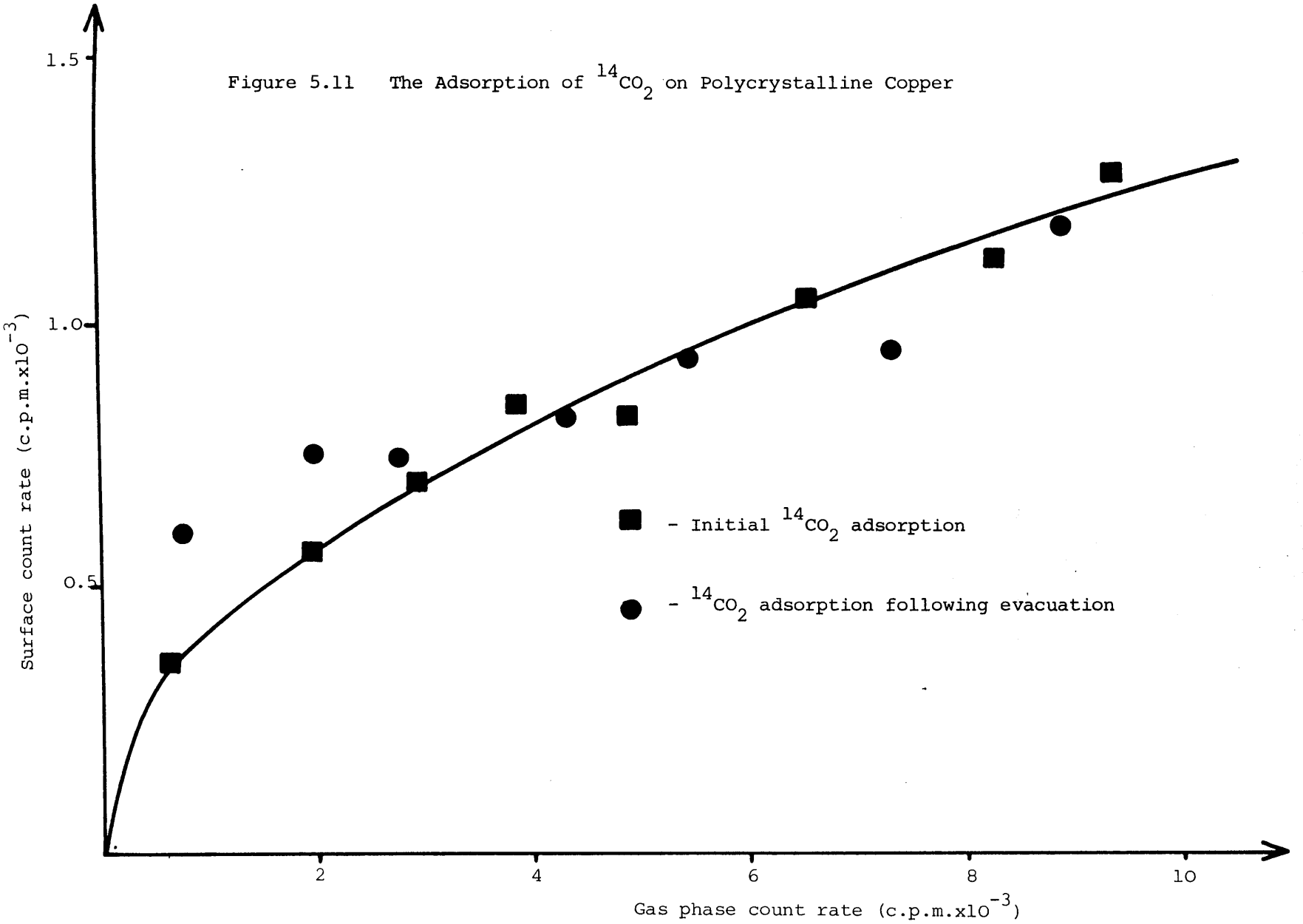

carbon dioxide is quoted, it has been calculated, from a reference isotherm, with respect to the original quantity adsorbed at 4 torr radiolabelled gas pressure.

On completion of the adsorption isotherm shown in Fig. 5.11, the reaction vessel was evacuated for 15 minutes. This resulted in a decrease in the surface count rate from 1290 c.p.m. (4 torr gas pressure) to 261 c.p.m., corresponding to the retention of 20% of the radiolabel on the copper surface. Subsequent admission of further charges of [14-C]carbon dioxide to the reaction vessel, resulted in the production of an isotherm virtually identical to that of the initial adsorption at gas pressures greater than 1 torr (2550 c.p.m.). Below this pressure, the presence of retained [14-C]labelled material created the appearance of an apparent increase in [14-C]carbon dioxide adsorption (Figure 5.11).

An attempt was made to linearise the carbon dioxide adsorption isotherm with respect to the Langmuir equation (Figure 5.12). A poor linear plot was obtained, but, at medium-high coverages, a best-fit line was drawn. This allowed the average heat of adsorption of carbon dioxide, on this polycrystalline copper sample, to be estimated as 36-40 KJ mol^{-1}. At low coverages the points showed considerable deviation from the extrapolated plot. This can be explained in terms of a small number of sites which give rise to a higher heat of adsorption than the bulk of the available copper surface.

5.1.2.2 Molecular Exchange

5.74 torr of [14-C]carbon dioxide was admitted to the reaction vessel, which contained 0.165g of copper, and equilibrated for

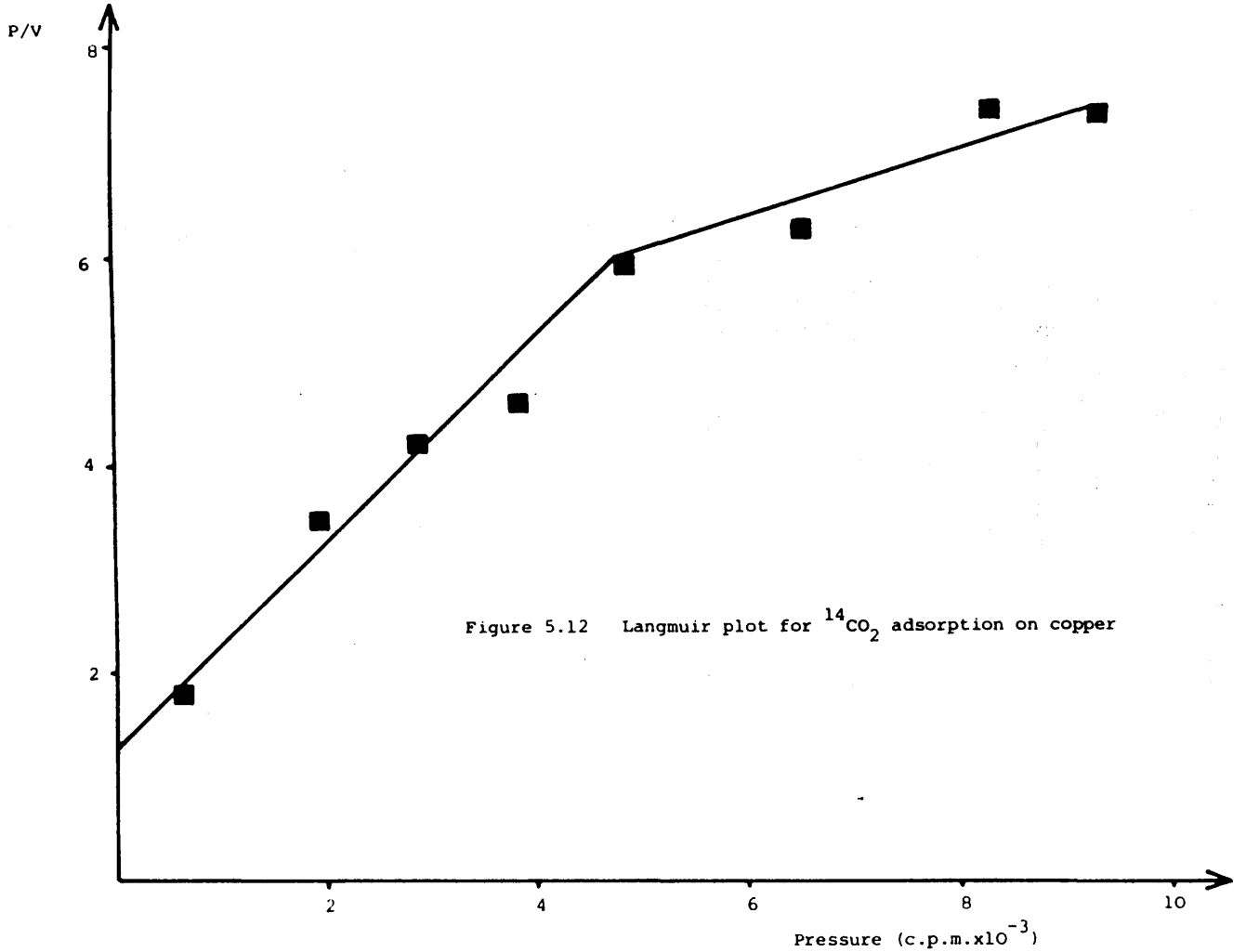

Figure 5.12 Langmuir plot for $^{14}CO_2$ adsorption on copper

30 minutes. A surface count rate of 1641 c.p.m. was obtained after this period. The specific activity of the gas phase within the vessel was then reduced, by 45%, by the admission of 4.65 torr of [12-C]carbon dioxide. After 10 minutes, the surface count rate had dropped to a value of 1323 c.p.m., which indicated that 44% of the adsorbed carbon dioxide species were undergoing facile molecular exchange.

5.1.2.3 The Influence of Preadsorbed Material on the [14-C]Carbon Dioxide Adsorption

(a) Preadsorbed [14-C]Carbon Monoxide

Charges of [14-C]carbon monoxide were allowed to adsorb on to a 0.161g sample of copper. This generated a typical carbon monoxide isotherm (e.g. Fig. 5.1) with a saturation surface count rate of 1556 c.p.m.

Without evacuation, charges of [14-C]carbon dioxide were added to the reaction vessel. After addition of the first charge of [14-C]carbon dioxide (0.75 torr), the surface count rate fell to a value of 1474 c.p.m. On addition of further charges of the radiolabelled carbon dioxide, no significant change in this value could be detected.

(b) Preadsorbed [12-C]Carbon Monoxide

3.82 torr of unlabelled carbon monoxide was equilibrated over 0.159g of copper for a period of 45 minutes. Charges of [14-C]carbon dioxide were then admitted to the reaction vessel and these readily adsorbed on the pretreated surface.

(c) Preadsorbed [14-C]Carbon Monoxide and Hydrogen

Small charges of gas, containing equal mole fractions of hydrogen and [14-C]carbon monoxide, were admitted to the reaction vessel which contained 1.6g copper, until a total pressure of 7.9 torr was obtained within the system. Charges of [14-C]carbon dioxide were then added to the system which, after an initial induction period, caused a significant increase in the total quantity of the adsorbed [14-C]radiolabel (Fig. 5.13).

(d) Quantitative Analysis of Carbon Monoxide and Hydrogen Preadsortion Effects

Figure 5.11 shows that two consecutive [14-C]carbon dioxide adsorptions on a copper surface, separated only by evacuation, leads to the production, at gas pressures greater than 1 torr, of identical isotherms. Reference isotherms may therefore be used to provide a quantitative analysis of preadsorption effects. (Section 5.1.1.3(d)).

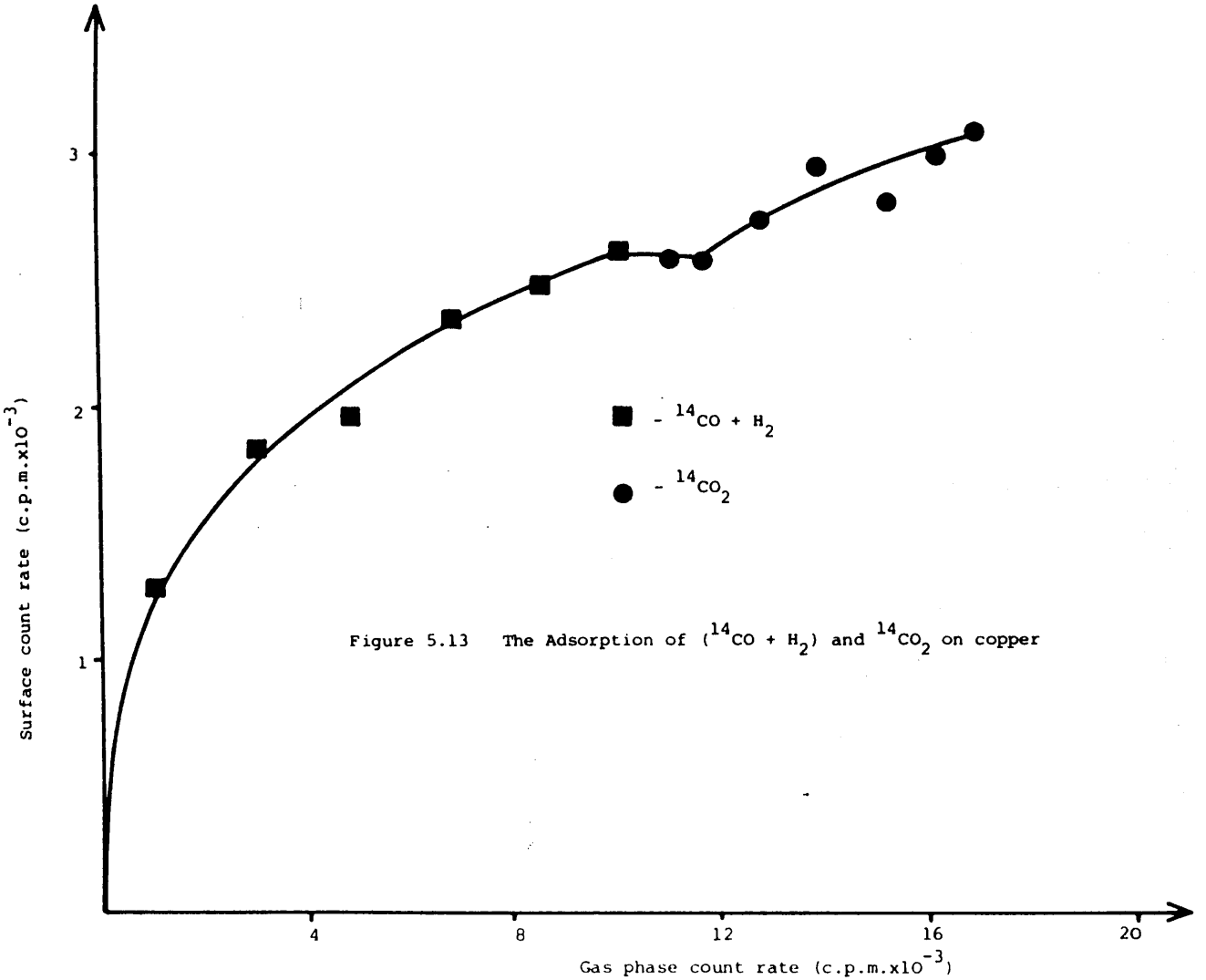

Figure 5.13 The Adsorption of ($^{14}CO + H_2$) and $^{14}CO_2$ on copper

The effects of pretreating the copper surface with 5 torr carbon monoxide, 5 torr hydrogen and 10 torr carbon monoxide and hydrogen (equal mole fractions), for 30 minute periods, are shown in Figures 5.14, 5.15 and 5.16. A quantitative analysis of these experiments is given in Table 5.4.

Preadsorbed Species	Change in [14-C]CO_2 Adsorption
CO	-37%
H_2	No change
CO + H_2	-44%

Table 5.4 Quantitative Analysis of [14-C]CO_2 Preadsorption Experiments (Copper)

5.1.2.4 The Influence of Coadsorbing Material on [14-C]Carbon Dioxide Adsorption

The effect of coadsorbing species on [14-C]carbon dioxide adsorption was determined by admitting charges of gas containing equal mole fractions of [14-C]carbon dioxide and a variety of unlabelled adsorbates, into the reaction vessel, which contained a copper surface previously characterised by production of a [14-C]carbon dioxide reference isotherm.

Figure 5.14 The Adsorption of $^{14}CO_2$ on a ^{12}CO pretreated copper surface

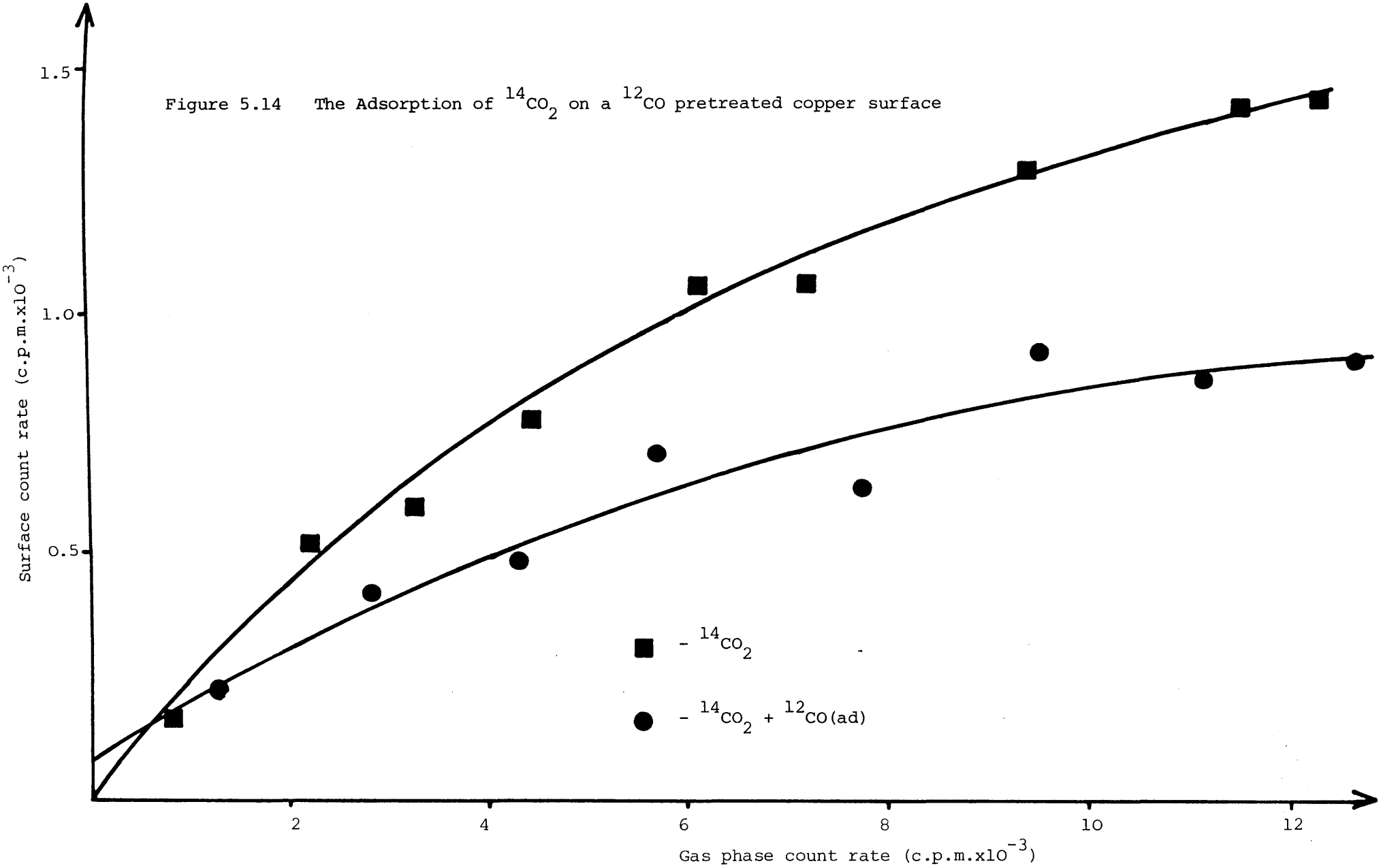

Figure 5.15 The Adsorption of $^{14}CO_2$ on a H_2 pretreated copper surface

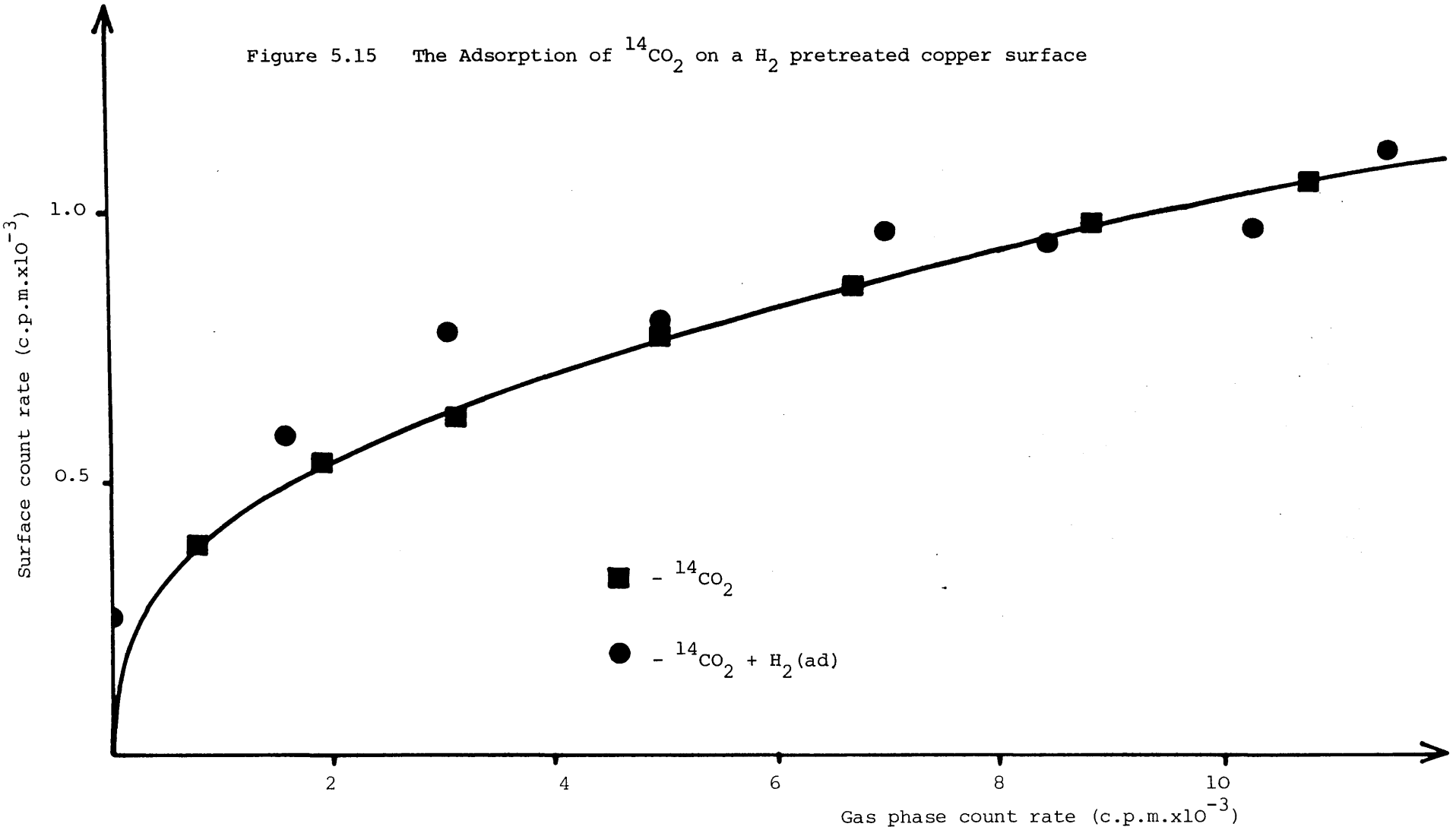

Figure 5.16 The Adsorption of $^{14}CO_2$ on a H_2 + ^{12}CO pretreated copper surface

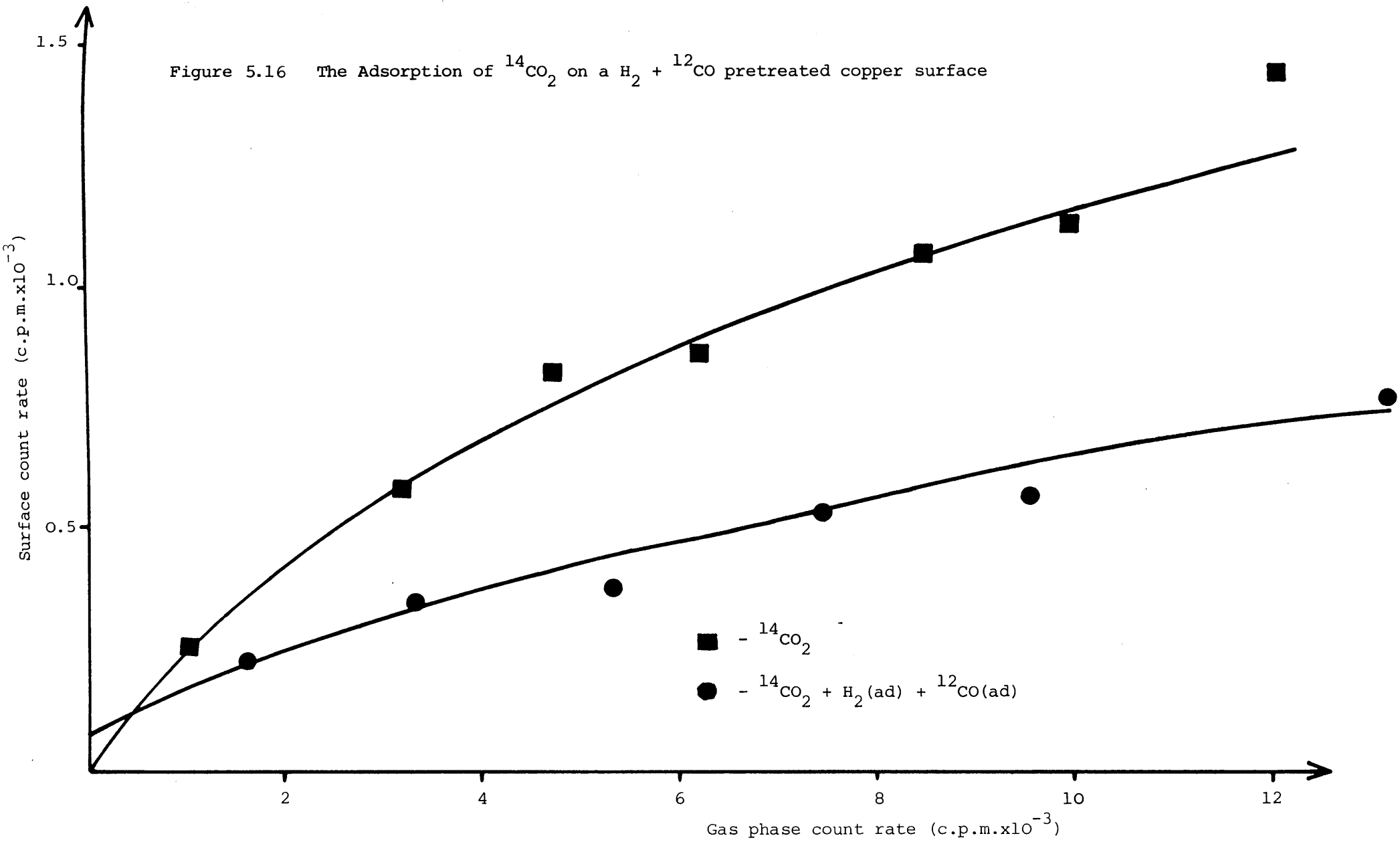

(a) Coadsorbing Carbon Monoxide or Hydrogen

The effects of coadsorbing carbon monoxide or hydrogen are detailed in Figures 5.17 and 5.18. It is clear that neither gas caused any significant change in the total quantity of [14-C]carbon dioxide adsorbed on the copper surface.

(b) Coadsorption of [14-C]Carbon Dioxide and Hydrogen on a [14-C]Carbon Monoxide Pretreated Surface

Small charges of [14-C]carbon monoxide were admitted to the reaction vessel, which contained 1.6g copper, until saturation surface coverage was attained. This corresponded to a surface count rate of 3070 c.p.m. Charges of gas containing equal mole fractions of [14-C]carbon dioxide and hydrogen were then added to the reaction vessel. No increase in the surface count rate was generated by this procedure. Rather, on addition of each charge of [14-C]carbon dioxide and hydrogen, a slight decrease in the surface count rate was observed.

(c) Coadsorption of [14-C]Carbon Dioxide and Hydrogen on a [12-C]Carbon Monoxide Pretreated Surface

5.2 torr of unlabelled carbon monoxide was equilibrated, over a 0.16g copper sample, for 60 minutes. Charges of gas containing equal mole fractions of [14-C]carbon dioxide and hydrogen were then added to the reaction vessel. The [14-C]radiolabel was readily adsorbed on the copper surface; this process generated an isotherm similar to that shown in Fig. 5.11.

Figure 5.17 Co-adsorption of $^{14}CO_2$ + ^{12}CO on copper

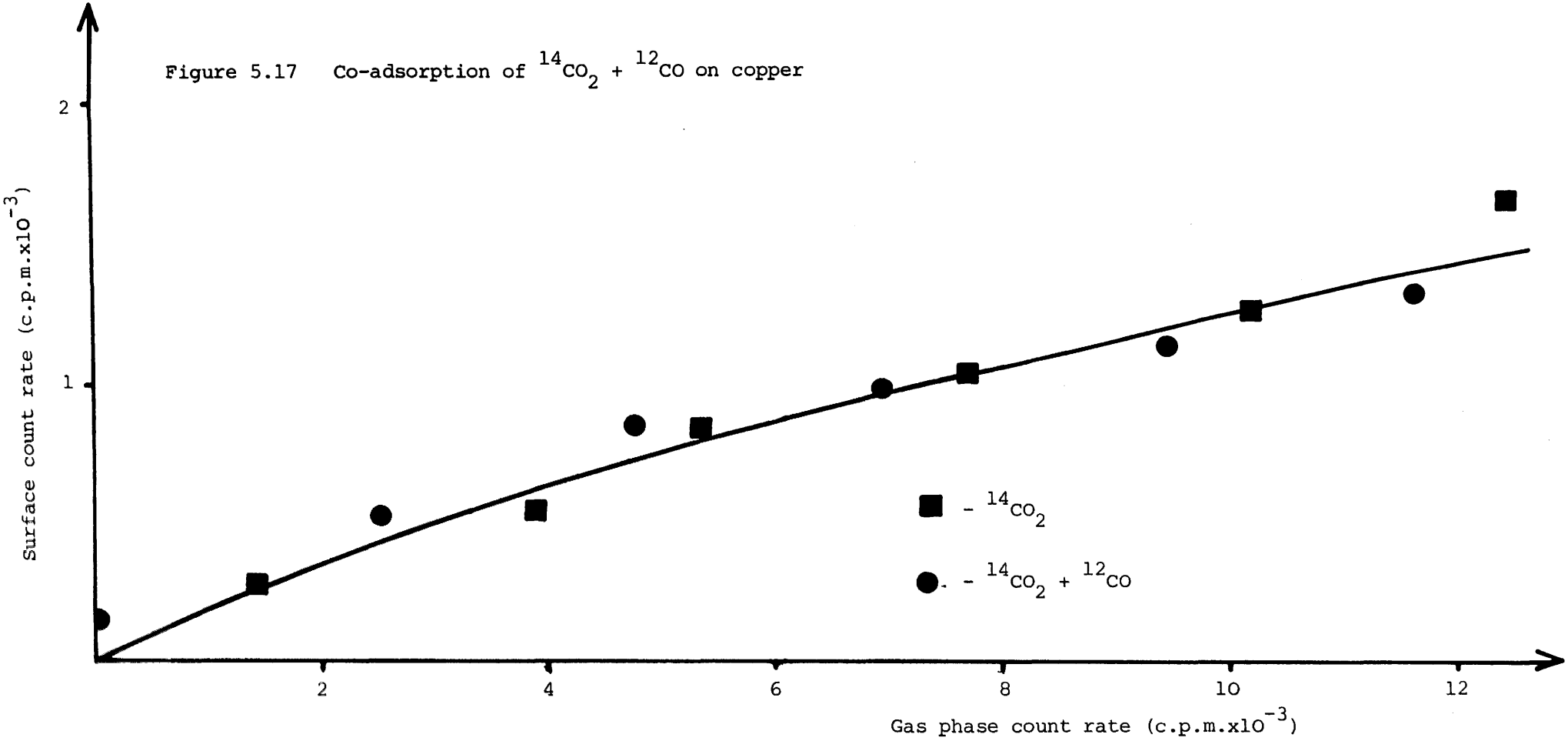

Figure 5.18 Co-adsorption of $^{14}CO_2 + H_2$ on copper

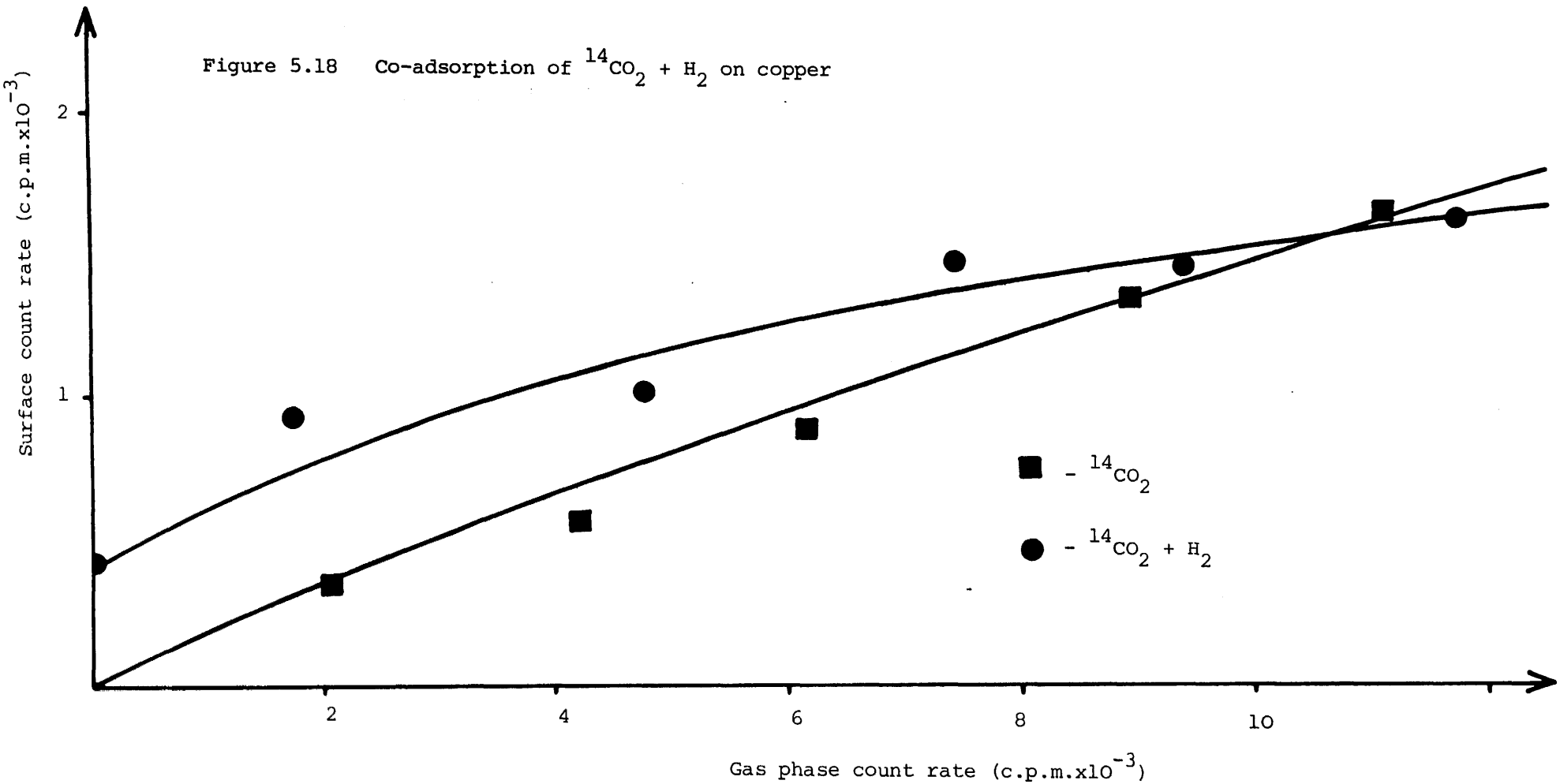

5.1.2.5 Displacement of Adsorbed [14-C]Carbon Dioxide from the Copper Surface

(a) [12-C]Carbon Monoxide Displacement

The equilibration of a 5.2 torr sample of [14-C]carbon dioxide over a 0.16g copper sample, for 60 minutes, produced a surface count rate of 1334 c.p.m. Charges of [12-C]carbon monoxide were then added to the reaction vessel and, 5 minutes after the addition of each charge of carbon monoxide, the surface count rate determined. The results obtained are shown in Table 5.5.

Pressure [12-C]CO (torr)	Surface Count Rate (c.p.m.)
0.82	1250
1.19	1444
1.81	1368
2.38	1419
3.25	1529
4.13	1383

Table 5.5 Displacement of [14-C]CO_2 by CO (Copper)

(b) Hydrogen Displacement

The equilibration of 5.01 torr [14-C]carbon dioxide, over a 0.16g copper sample, for 85 minutes, produced a surface count rate of 1463 c.p.m. Charges of hydrogen were then added to the reaction vessel and, five minutes after the addition of each charge of hydrogen, the surface count rate was determined.

The results obtained are shown in Table 5.6.

Pressure H_2 (torr)	Surface Count Rate (c.p.m.)
1.08	1374
2.12	1490
3.15	1503
3.67	1492
3.87	1626

Table 5.6 Displacement of [14-C]CO_2 by H_2 (Copper)

5.2 ADSORPTION ON PARTIALLY OXIDISED POLYCRYSTALLINE COPPER

5.2.1 The Adsorption of [14-C]Carbon Monoxide

Figure 5.19 shows a typical isotherm produced by the adsorption of [14-C]carbon monoxide on a 50% surface oxidised polycrystalline copper sample (0.173g). During the build up of the adsorption isotherm, gas chromatographic analysis of the gas phase within the reaction vessel revealed the presence of a significant quantity of carbon dioxide. The isotherm generated by the adsorption process, on this surface, is distinctly different to that obtained from carbon monoxide adsorption on a fully reduced copper surface (Fig. 5.1). It is obvious that saturation adsorption was not obtained under the conditions used in this experiment.

Subsequent exposure of the sample to 15 minutes evacuation resulted in the retention of 5% of the total quantity of previously

Figure 5.19 The Adsorption of ^{14}CO on 50% surface oxidised copper

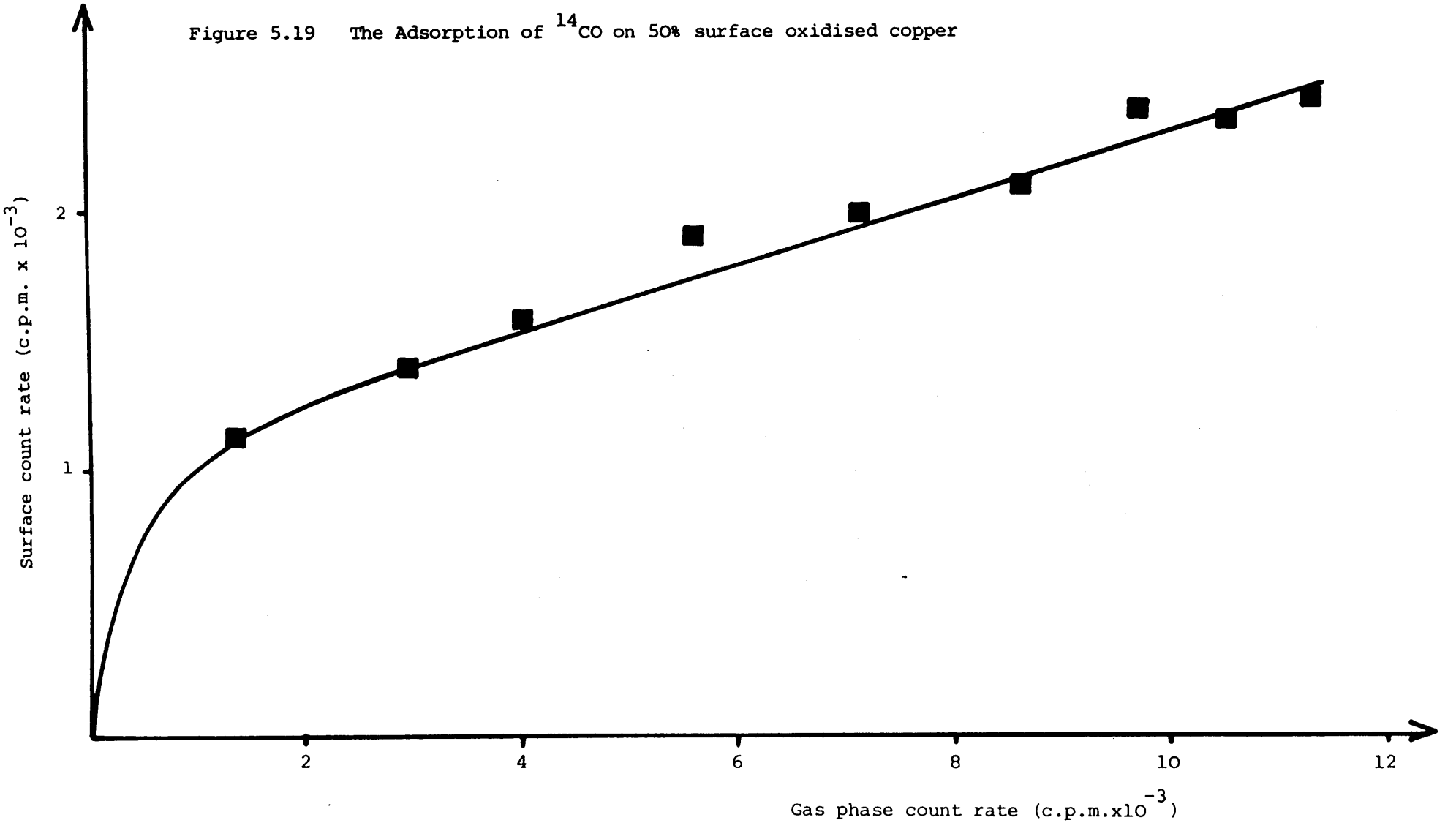

adsorbed radiolabel on the oxidised surface.

By linearising the adsorption isotherm with respect to the Langmuir equation, the monolayer adsorbed volume was found to be equivalent to a surface count rate of 3500 c.p.m. By substitution of this data into the Langmuir equation, the heat of adsorption of carbon monoxide on this surface was calculated to be 38 KJ mol^{-1}.

5.2.2 The Adsorption of [14-C]Carbon Dioxide

5.2.2.1 [14-C]Carbon Dioxide Adsorption

Figure 5.20 shows a typical isotherm produced by the adsorption of [14-C]carbon dioxide on a 50% surface oxidised copper sample (0.169g). During the build-up of the isotherm, carbon dioxide was found to be the only gas present in the gas phase of the reaction vessel.

Evacuation of the catalyst for 30 minutes resulted in a decrease of the surface count rate from 1820 c.p.m. (at 4 torr gas pressure) to 803 c.p.m. This represented retention of 44% of the radiolabel on the copper surface. Subsequent admission of further charges of [14-C]carbon dioxide to the reaction vessel produced similar behaviour to that described in section 5.1.2.1, that is, at gas pressures greater than 1 torr, the reference and second isotherms coalesced.

The Langmuir plot for this isotherm (Figure 5.21) showed excellent linearity except at very low coverages. The average heat of adsorption of carbon dioxide on the partially oxidised surface

Figure 5.20 The Adsorption of $^{14}CO_2$ on 50% surface oxidised copper

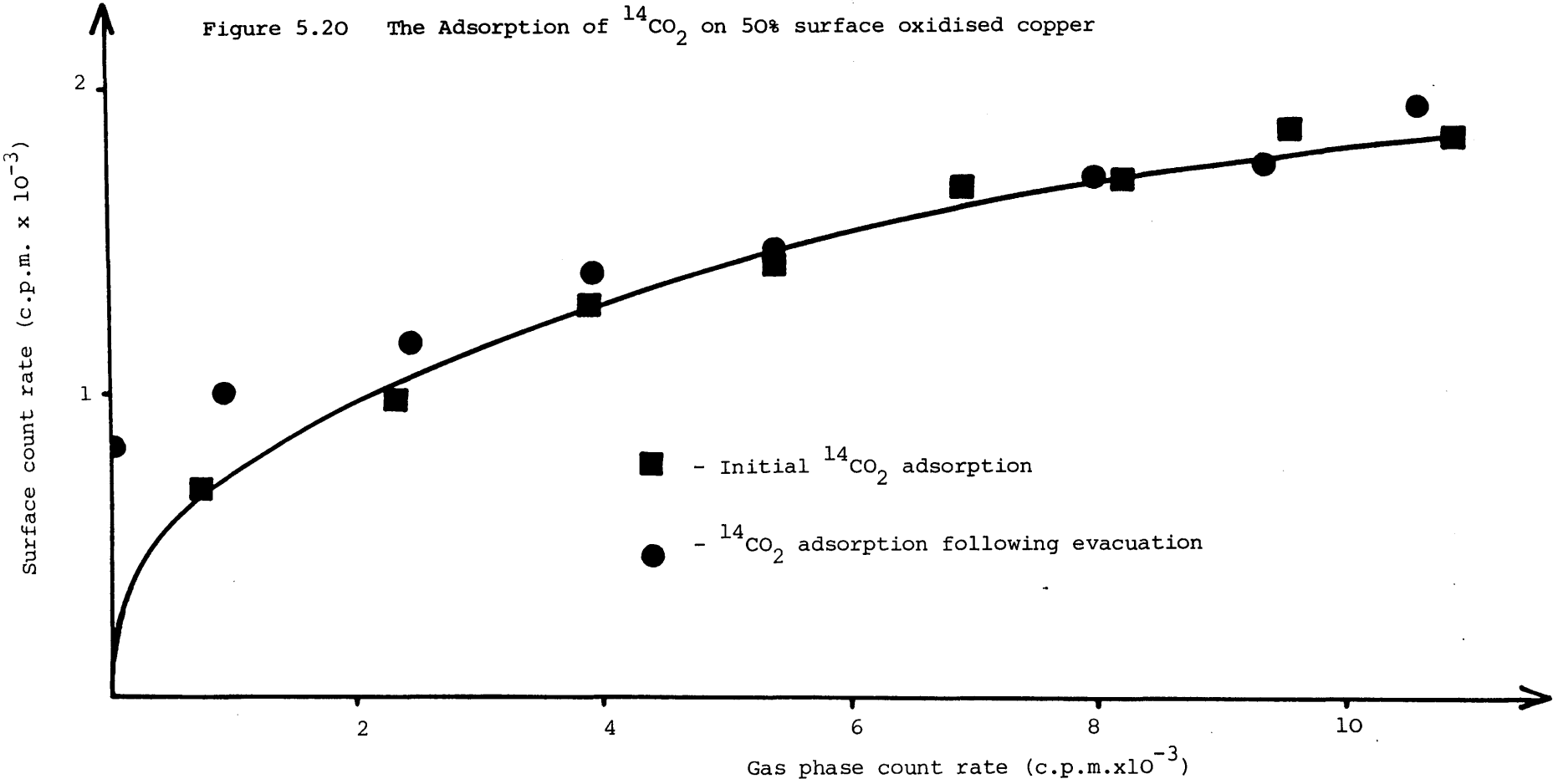

Figure 5.21 Langmuir plot for $^{14}CO_2$ adsorption on oxidised copper

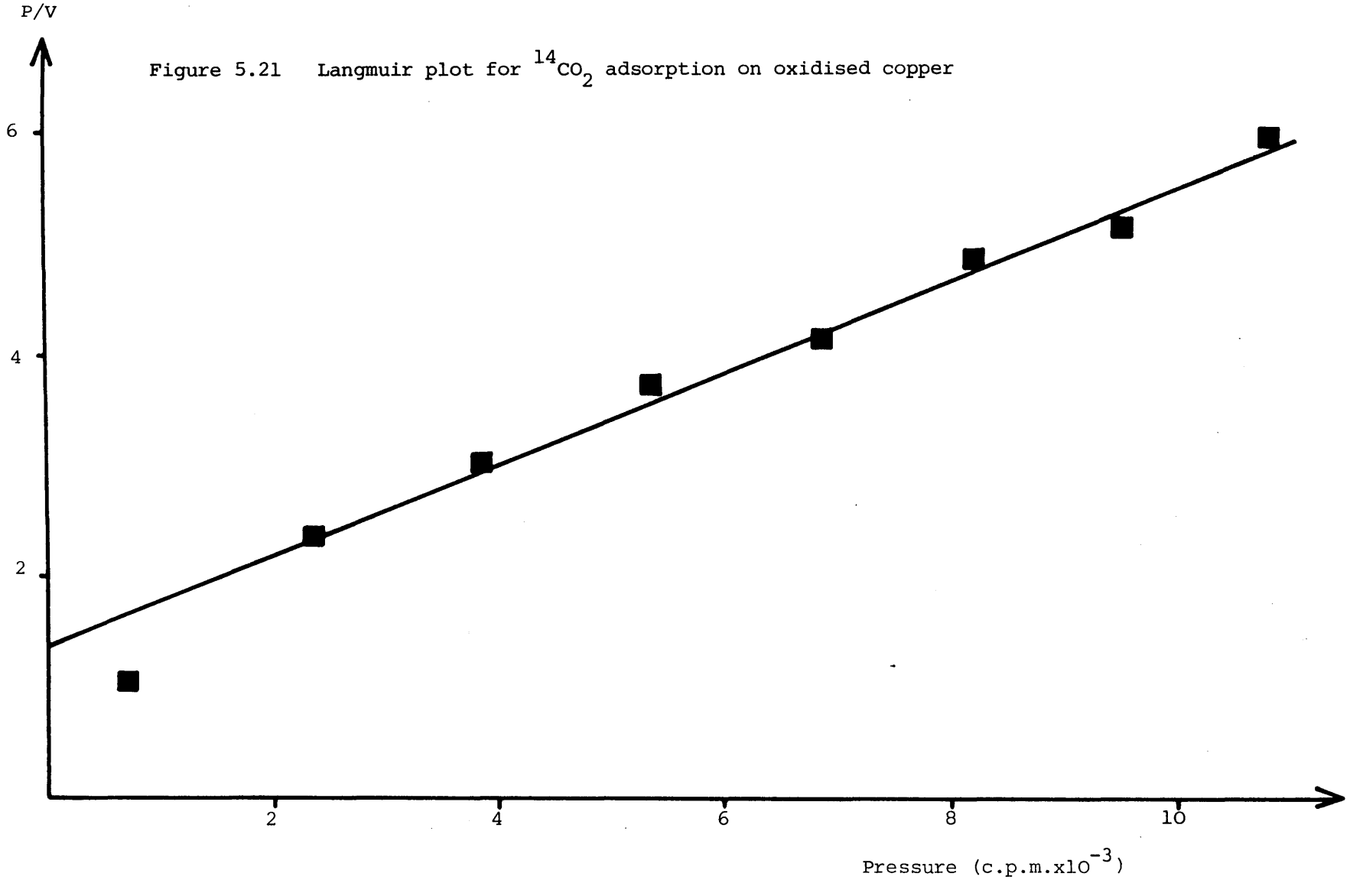

was calculated to be 40 KJ mol^{-1}.

5.2.2.2 The Influence of Preadsorbed Material on [14-C]Carbon Dioxide Adsorption

Figure 5.20 shows that two consecutive [14-C]carbon dioxide adsorptions on a partially oxidised copper surface, separated by 5 minutes evacuation, led to the production, at gas pressures greater than 1 torr, of identical isotherms. The use of reference isotherms (Section 5.1.1.3(d)) therefore allowed a quantitative analysis of a variety of preadsorption effects.

The effects of pretreating the oxidised surface with 5 torr carbon monoxide, 5 torr hydrogen and 10 torr carbon monoxide and hydrogen (equal mole fractions), for 30 minute periods,are shown in Figures 5.22, 5.23 and 5.24. A quantitative analysis of these experiments is given in Table 5.7.

Preadsorbed Species	Change in [14-C]CO_2 Adsorption
CO	-17%
H_2	+21%
CO + H_2	-22%

Table 5.7 Quantitative Analysis of [14-C]CO_2 Preadsorption Experiments (50% Oxidised Copper)

Figure 5.22 The Adsorption of $^{14}CO_2$ on a ^{12}CO pretreated oxidised copper surface

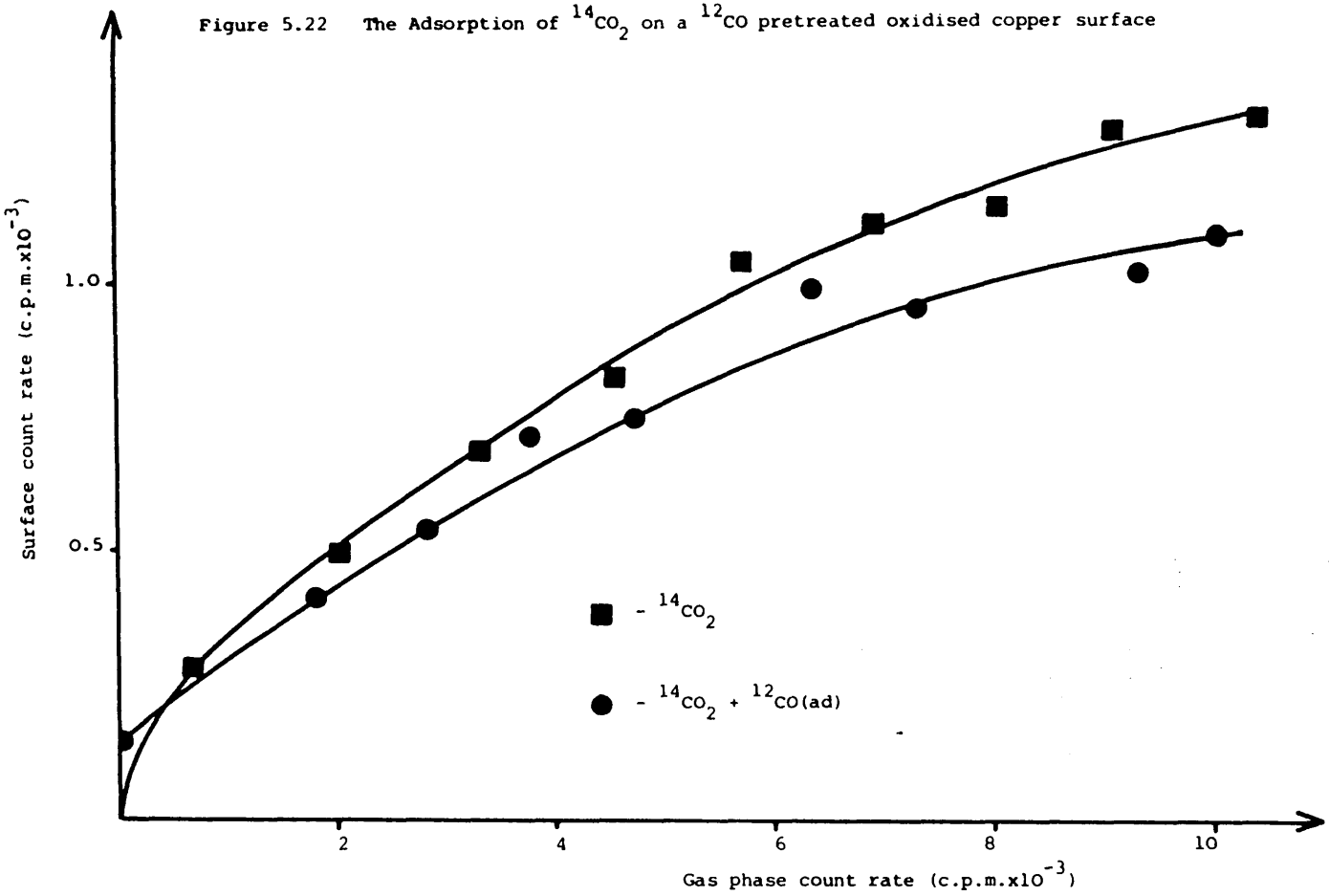

Figure 5.23 The Adsorption of $^{14}CO_2$ on a H_2 pretreated oxidised copper surface

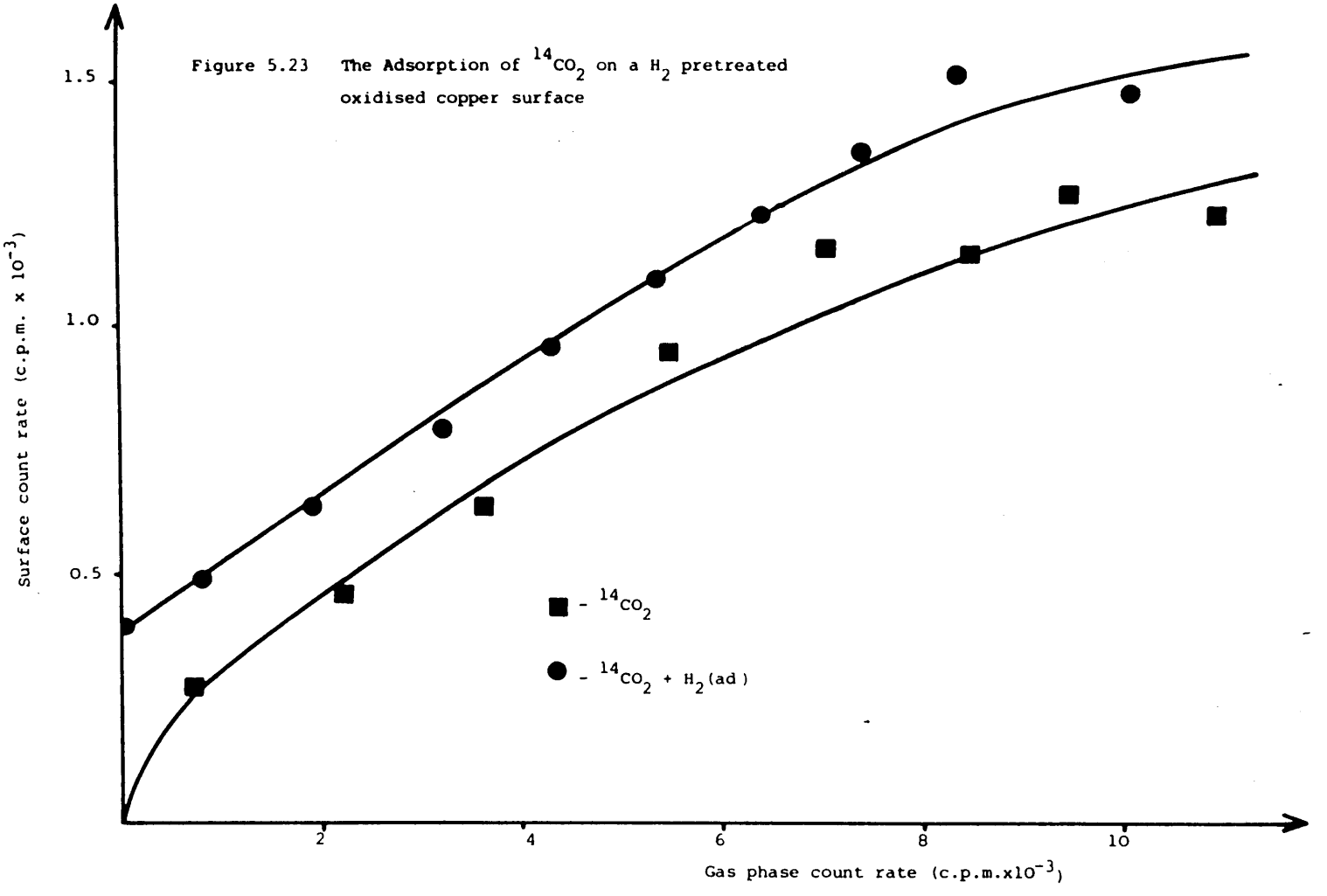

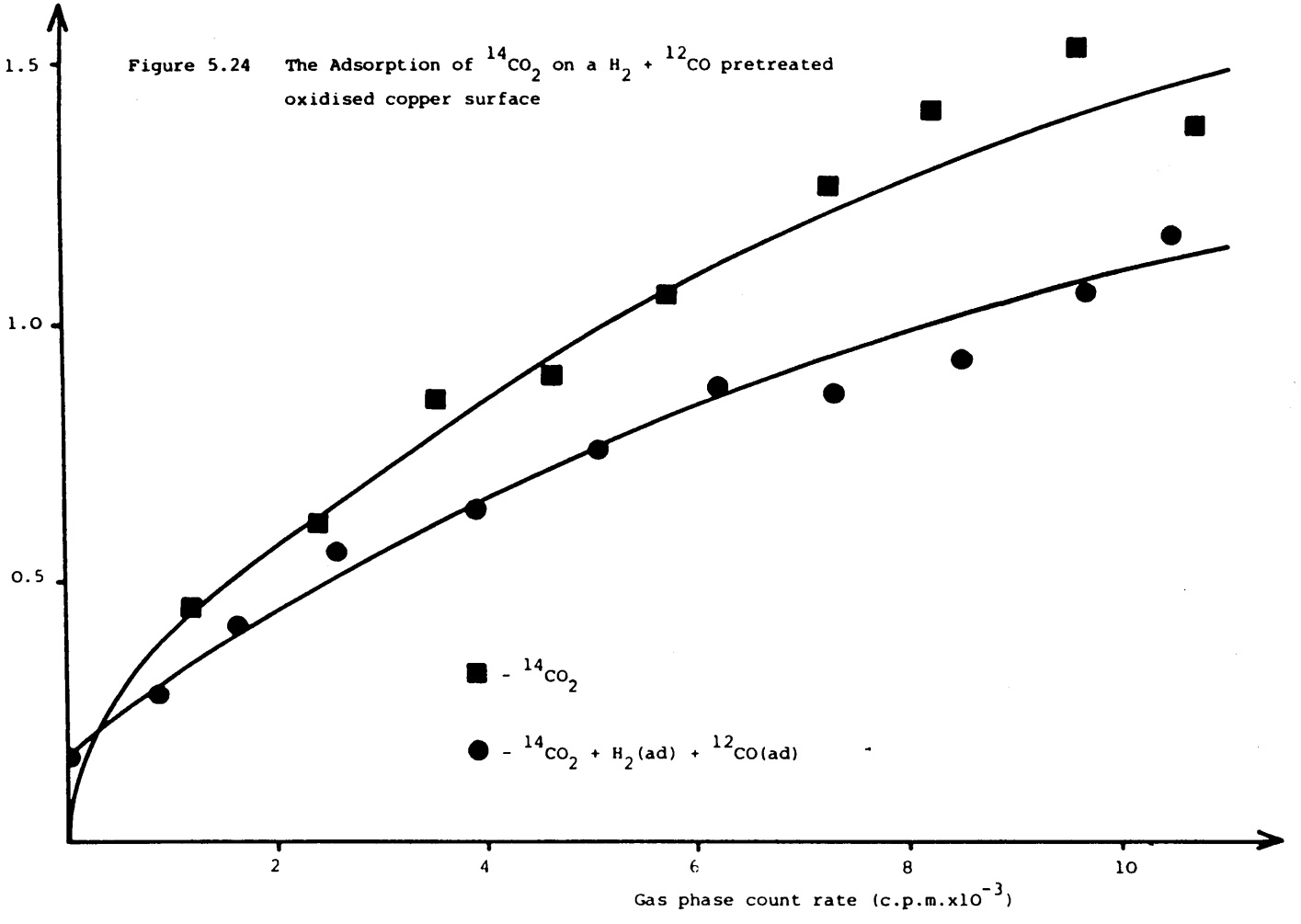

Figure 5.24 The Adsorption of $^{14}CO_2$ on a H_2 + ^{12}CO pretreated oxidised copper surface

5.3 ADSORPTION ON FULLY OXIDISED POLYCRYSTALLINE COPPER

5.3.1 The Adsorption of [14-C]Carbon Dioxide

(a) Fig. 5.25 shows a typical isotherm produced by the adsorption of [14-C]carbon dioxide on 0.18g of copper, whose surface had been completely oxidised by treatment with excess nitrous oxide, at 80°C, for 14 hours. After admission of each charge of radiolabelled adsorbate, a period of 10 minutes was found to be adequate to ensure that gas-surface equilibrium had been obtained.

Evacuation of the catalyst, for 15 minutes, resulted in a decrease in the surface count rate from 670 c.p.m. (at 4 torr gas pressure) to 34 c.p.m. This represented the retention of 5% of the radiolabelled species on the oxidised surface.

2.94 torr of unlabelled carbon monoxide was then admitted to the reaction vessel, for 60 minutes, and removed by pumping. Subsequent readmission of charges of [14-C]carbon dioxide to the reaction vessel, produced a greater [14-C]carbon dioxide coverage than was obtained on the freshly oxidised surface (Fig. 5.25).

(b) Fig. 5.26 details a typical isotherm produced by the adsorption of [14-C]carbon dioxide on 0.17g of copper, whose surface had been oxidised by treatment with excess nitrous oxide, at 40°C, for 15 minutes. Evacuation of the catalyst for 15 minutes resulted in the retention of 32% of the radiolabel on the oxidised surface.

Figure 5.25 The Adsorption of $^{14}CO_2$ on a fully oxidised and partially reduced copper surface

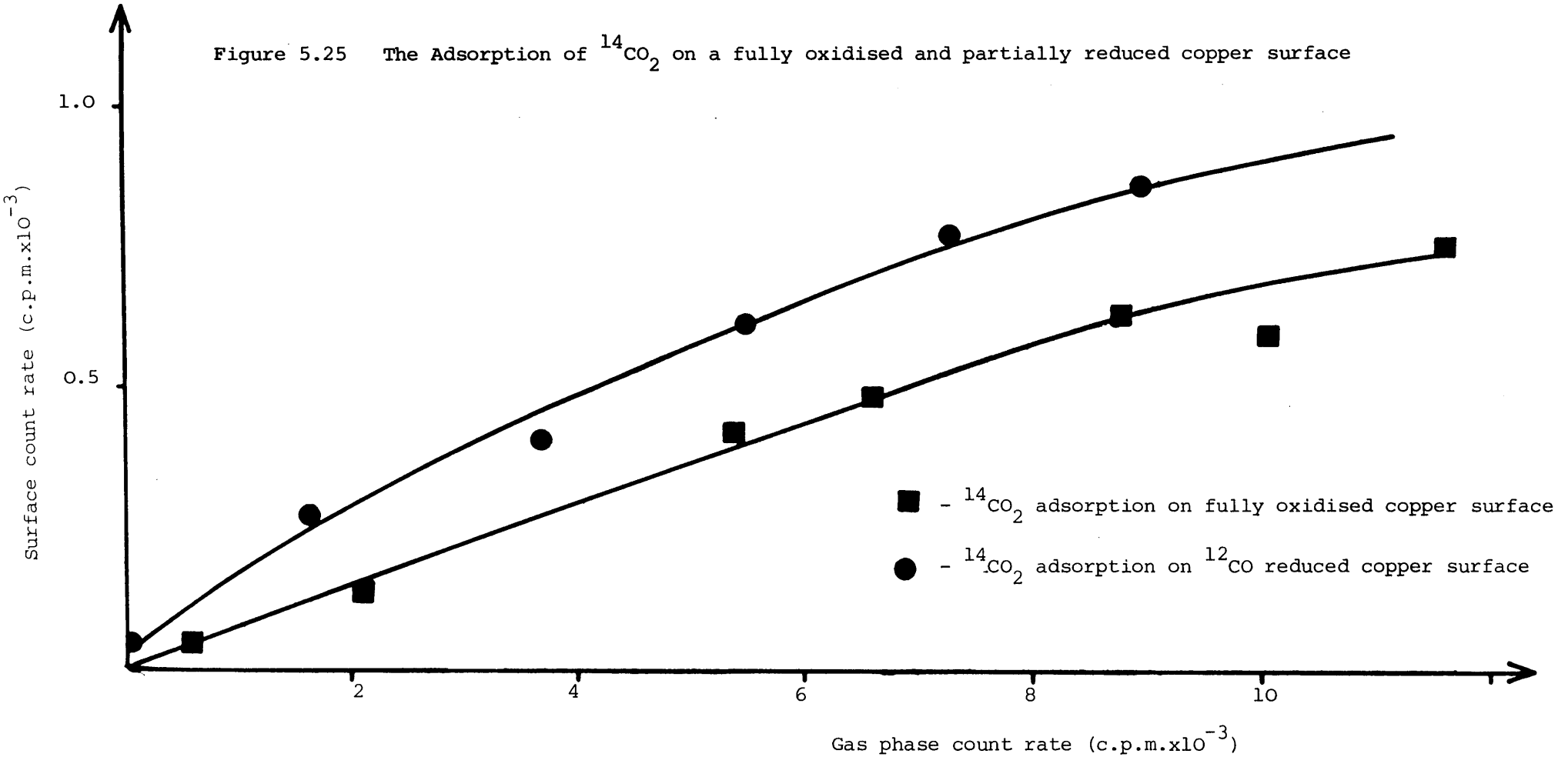

Figure 5.26 The Adsorption of $^{14}CO_2$ on copper, fully oxidised at 40°C

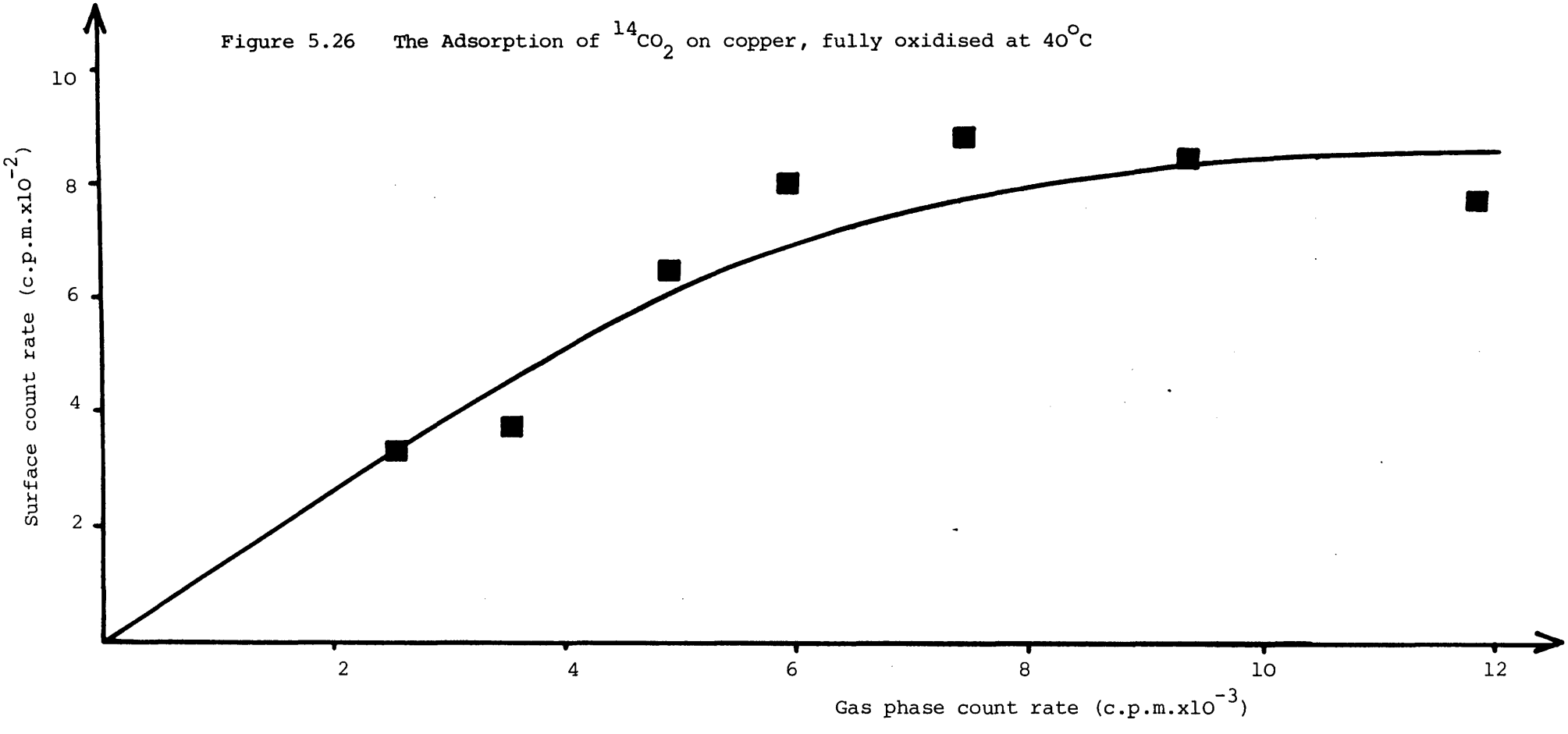

5.4 ADSORPTION ON COPPER-ALUMINA CATALYST

5.4.1 The Adsorption of [14-C]Carbon Monoxide

5.4.1.1 [14-C]Carbon Monoxide Adsorption

Figure 5.27 shows a typical isotherm produced by the adsorption of [14-C]carbon monoxide on 0.183g of freshly reduced copper-alumina catalyst. Following 15 minutes evacuation, it was found that only 5.5% of the total quantity of previously adsorbed carbon monoxide was resistant to this evacuation. Readmission of further charges of [14-C]carbon monoxide to the reaction vessel, exactly reproduced the previously determined reference isotherm. The data gave an excellent fit to the Langmuir equation (Figure 5.28) and, from this plot, the heat of adsorption of carbon monoxide on the copper-alumina catalyst was calculated to be 45 KJ mol^{-1}.

5.4.1.2 The Influence of Preadsorbed Material on [14-C]Carbon Monoxide Adsorption

The effects of pretreating the copper-alumina surface with 5 torr carbon dioxide, 5 torr hydrogen and 10 torr carbon monoxide and hydrogen (equal mole fractions), for 30 minute periods, are shown in Figures 5.29, 5.30 and 5.31. A quantitative analysis of these experiments is given in Table 5.8.

Figure 5.27 The Adsorption of ^{14}CO on Cu/Al_2O_3

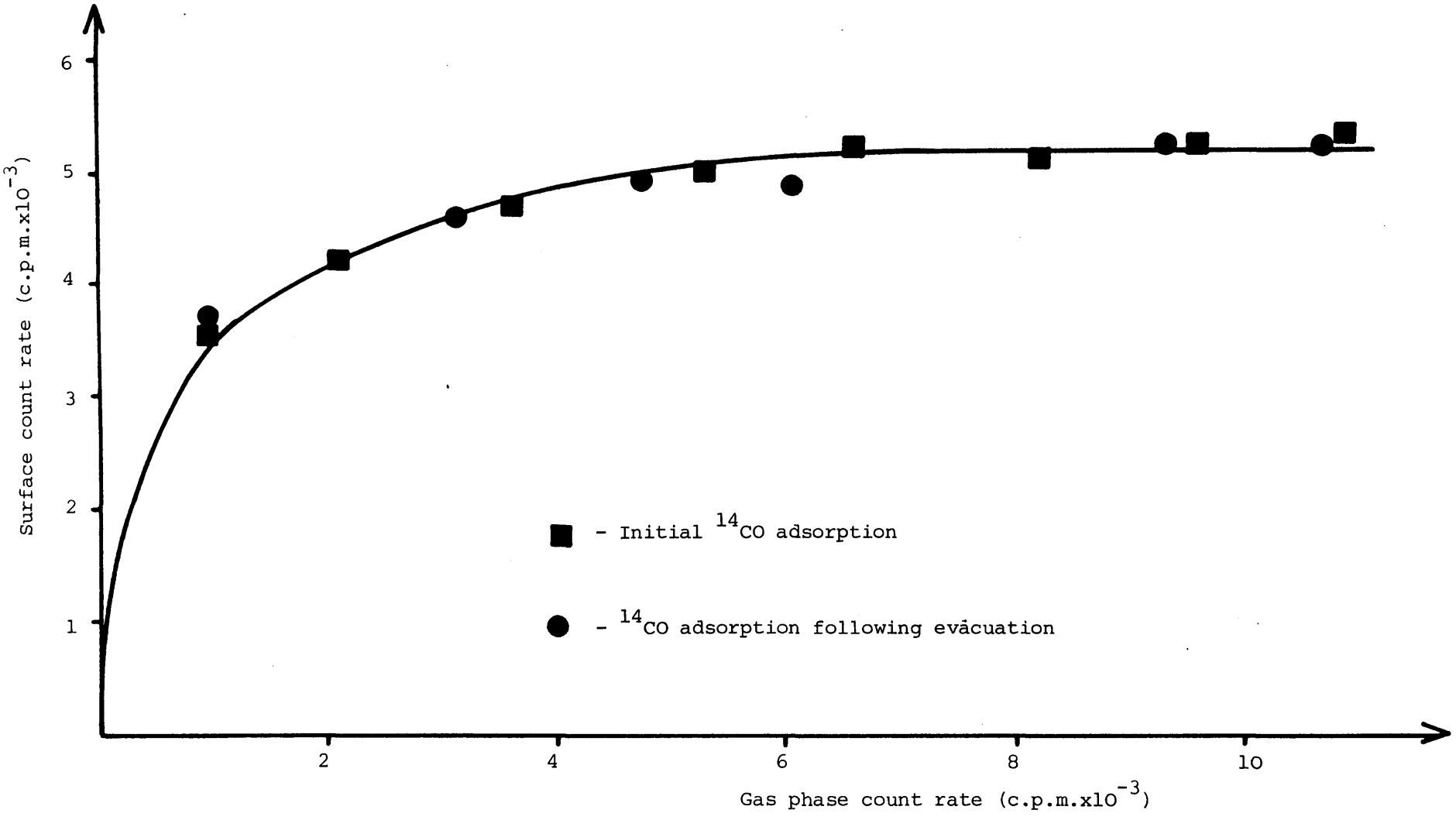

Figure 5.28 Langmuir plot for ^{14}CO adsorption on Cu/Al_2O_3

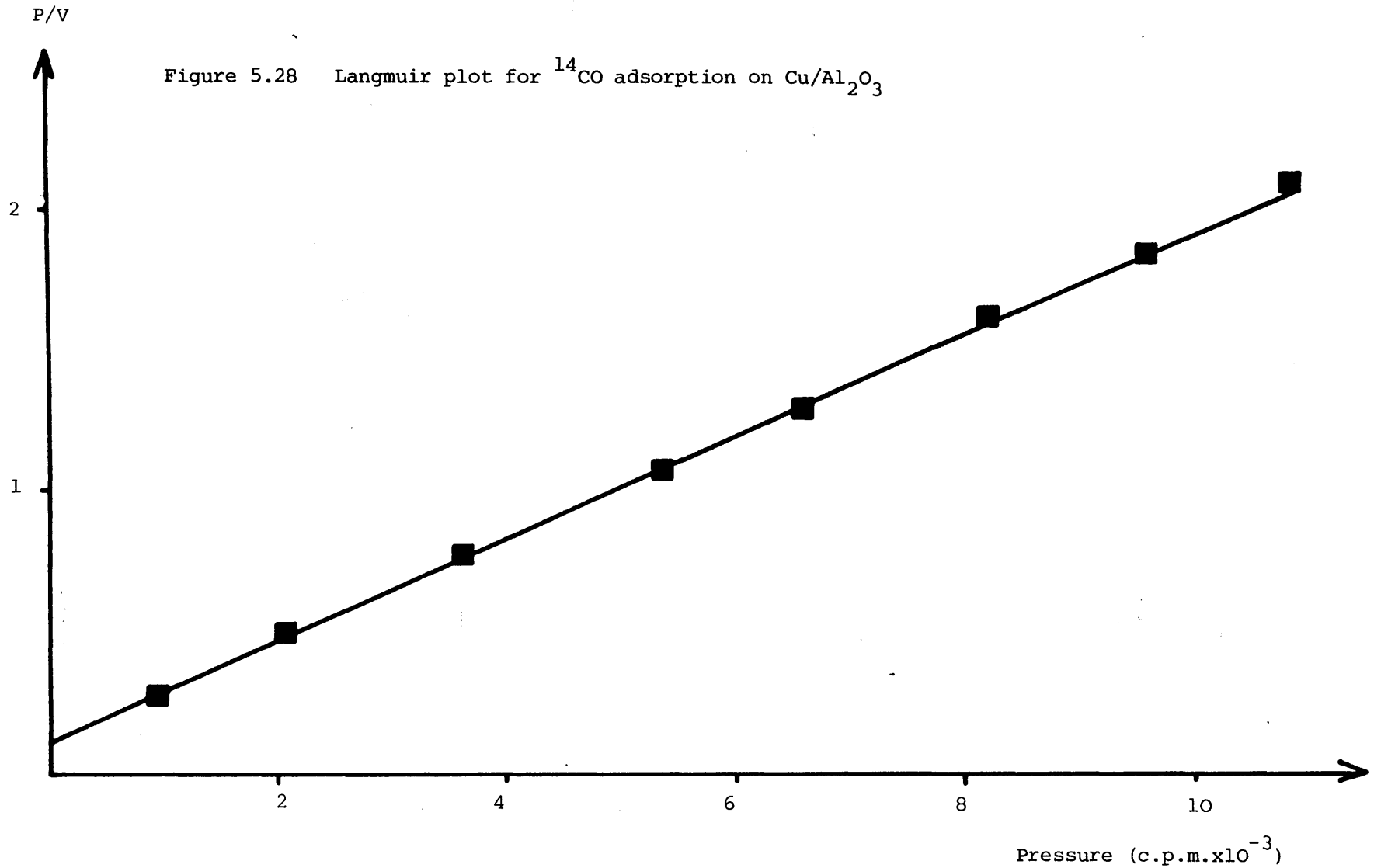

Figure 5.29 The Adsorption of ^{14}CO on $^{12}CO_2$ pretreated Cu/Al_2O_3

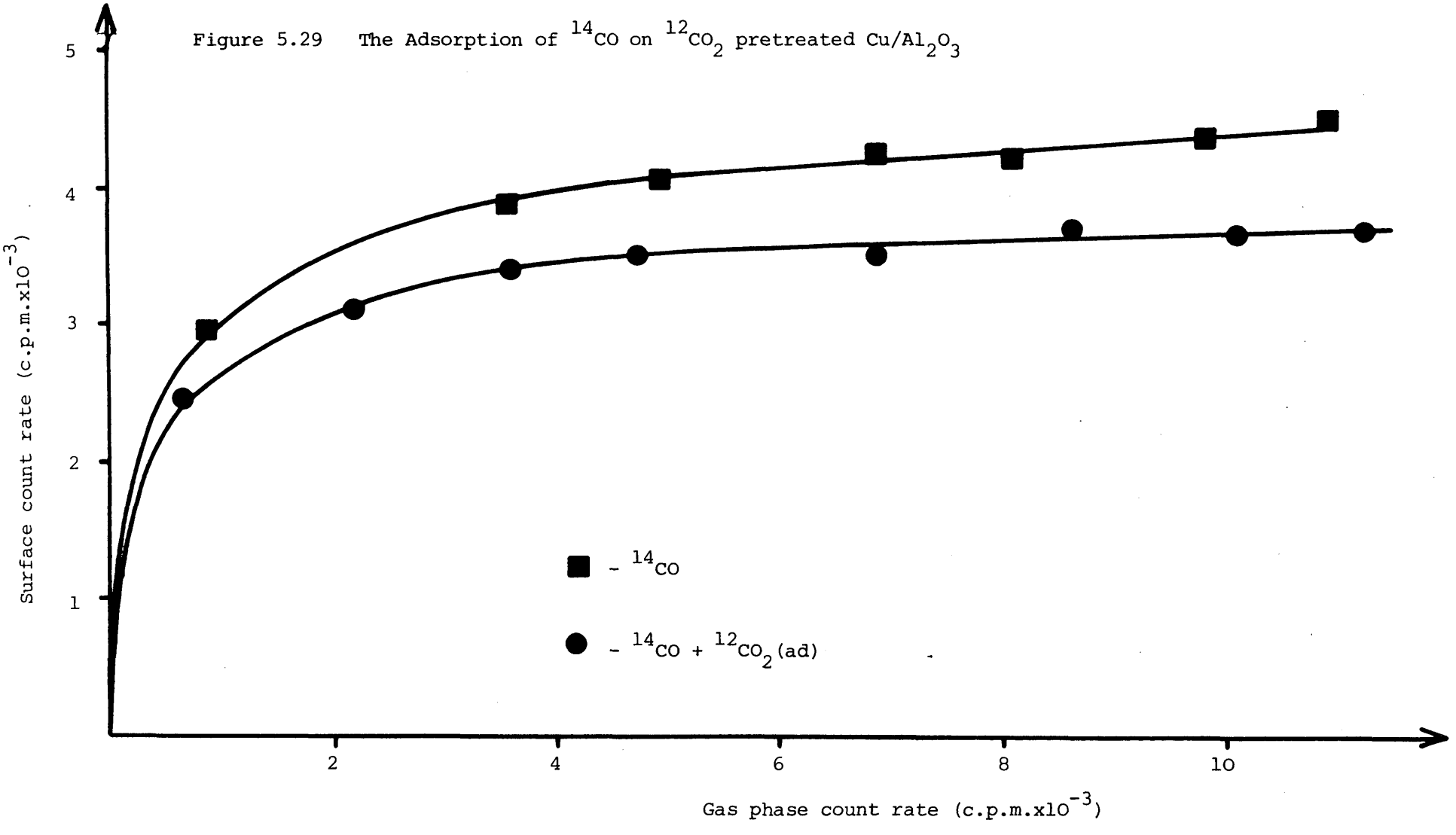

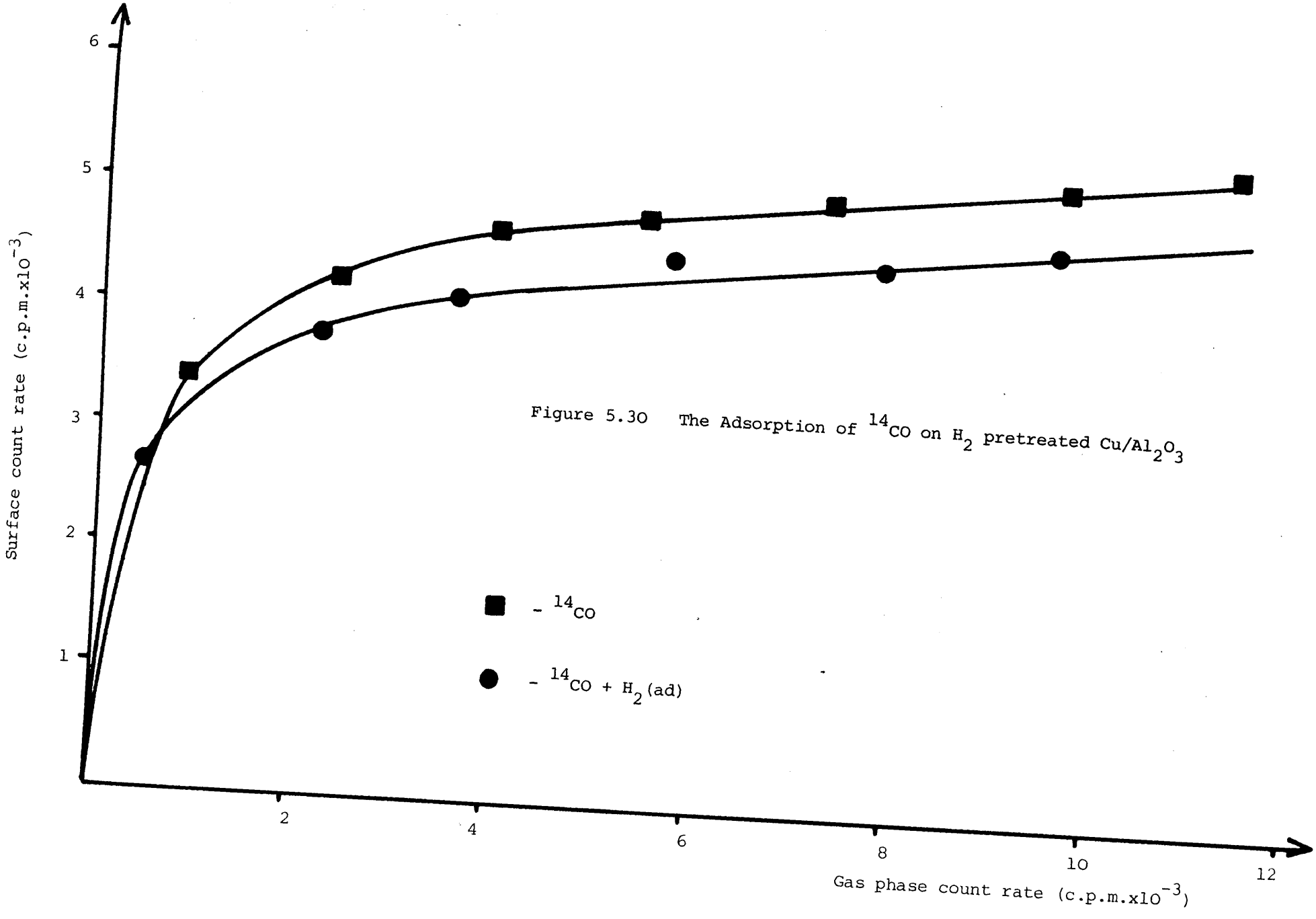

Figure 5.30 The Adsorption of ^{14}CO on H_2 pretreated Cu/Al_2O_3

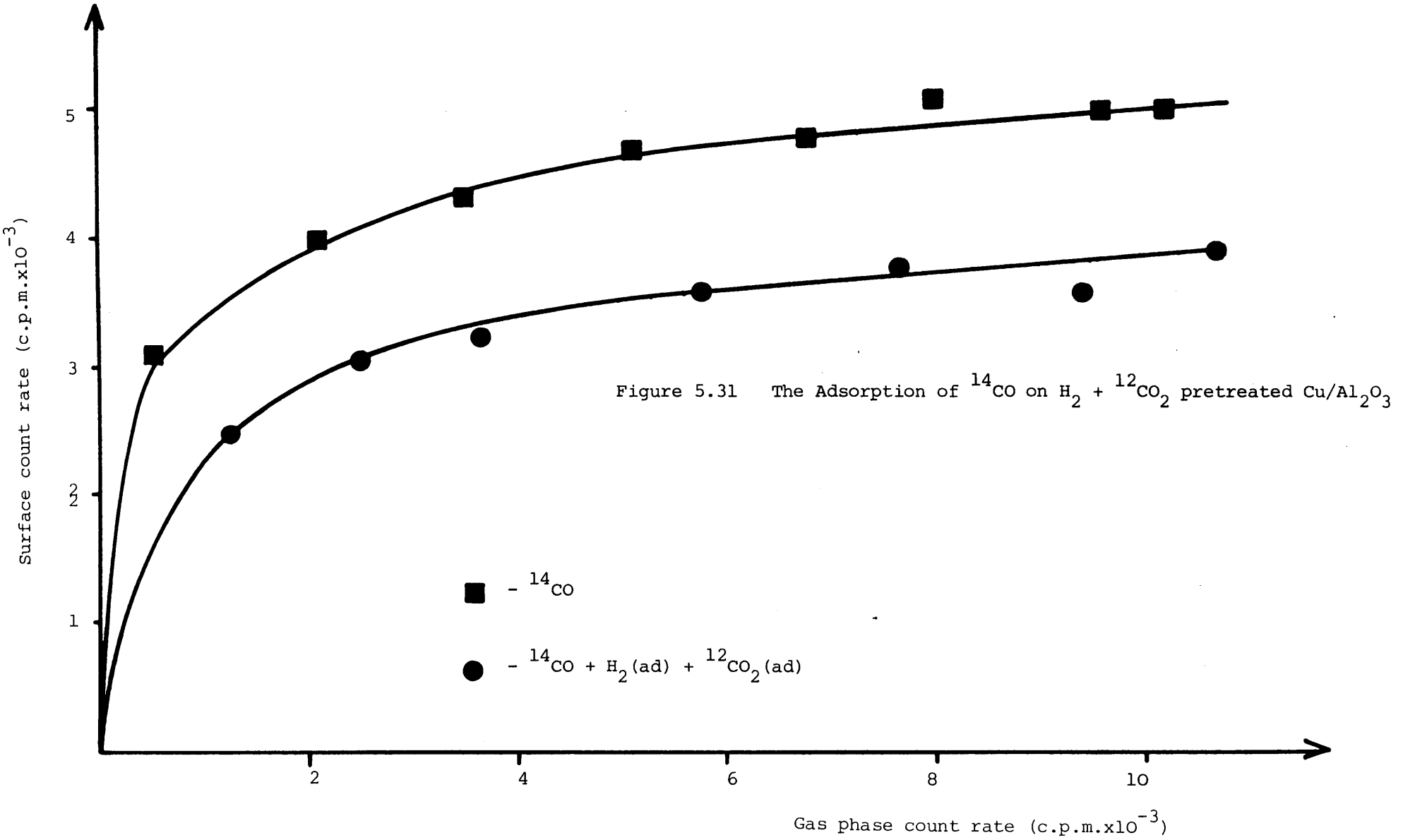

Figure 5.31 The Adsorption of ^{14}CO on H_2 + $^{12}CO_2$ pretreated Cu/Al_2O_3

Preadsorbed Species	Change in [14-C]CO Adsorption
CO_2	-16%
H_2	-10%
$CO_2 + H_2$	-23%

Table 5.8 Quantitative Analysis of [14-C]CO Preadsorption Experiments (Cu/Al_2O_3)

5.4.2 The Adsorption of [14-C]Carbon Dioxide

A typical isotherm produced by the adsorption of [14-C]carbon dioxide on a 0.185g sample of freshly reduced copper-alumina is shown in Figure 5.32 (Isotherm (1)). After evacuation, for 15 minutes, it was found that 50% of the previously adsorbed radiolabel remained associated with the copper surface. Readmission of further charges of [14-C]carbon dioxide did not reproduce the reference isotherm, but generated isotherm (2) (Fig. 5.32). This process was repeated until, on completion of isotherm (5), the copper-alumina surface appeared to be saturated with the [14-C]carbon dioxide adsorbate.

5.5 SCRAMBLING OF THE [14-C]RADIOLABEL

5.5.1 Reactions on Polycrystalline Copper

Following full reduction (Section 3.2.9.2), a 0.204g sample of copper was heated to 250°C in the reducing hydrogen-nitrogen flow. The system was then evacuated, for 30 minutes at this temperature.

Figure 5.32 The Adsorption of $^{14}CO_2$ on Cu/Al_2O_3

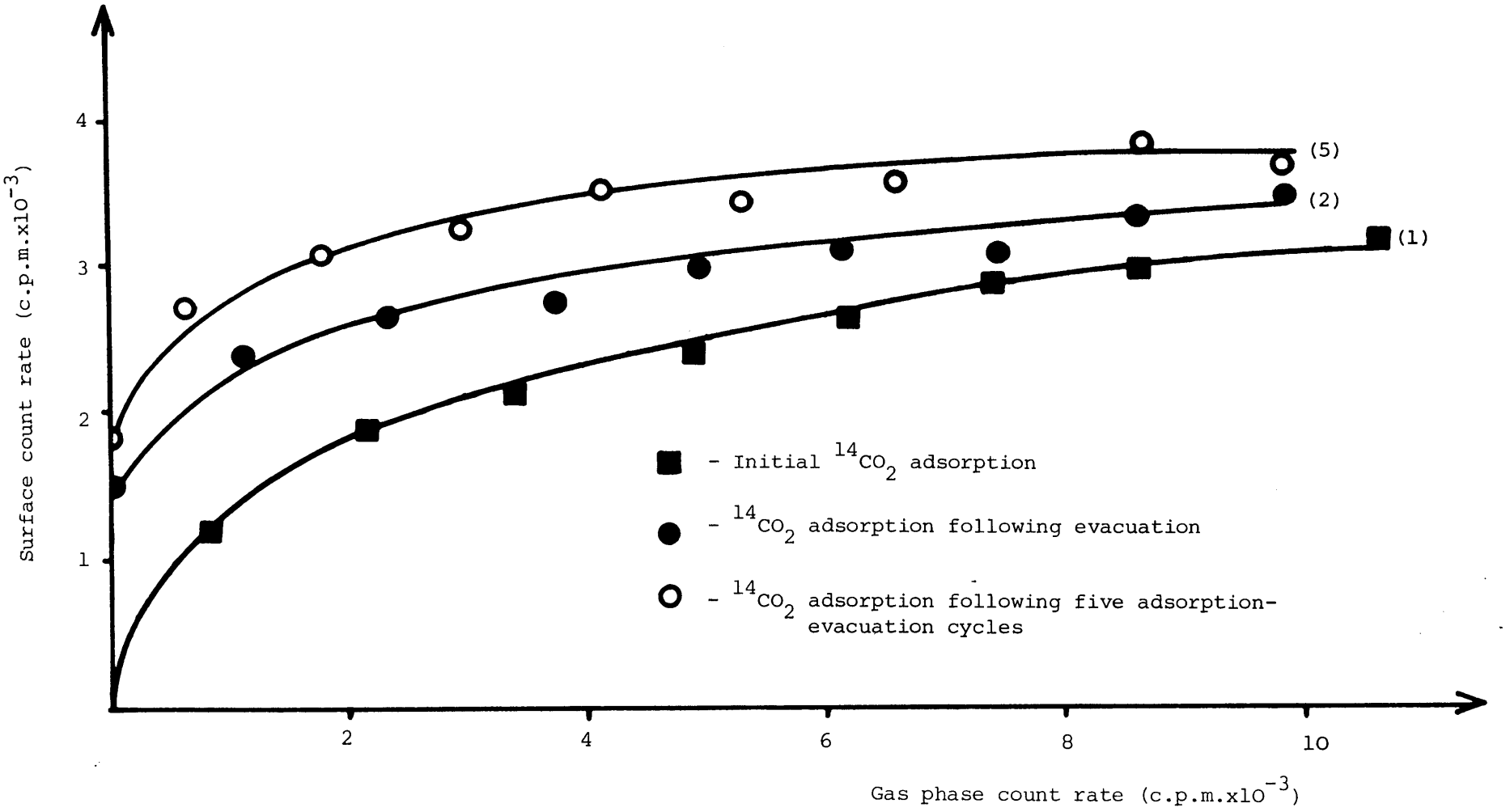

4.42 torr of [14-C]carbon dioxide was added to the reaction vessel and, after a period of 2 hours, samples of the gas phase were purged through the combined G.C. - proportional counter system. It was found that the gas phase of the reaction vessel contained a quantity of [14-C]carbon monoxide which, if adsorbed, would have produced 2% of monolayer coverage on the copper surface.

5.5.2 Reaction on Copper-Alumina Catalyst

A 0.23g copper-alumina sample was reduced as described in section 3.2.9.1. On completion of this procedure, the reducing mixture was removed by 30 minutes evacuation at 240°C. 4.13 torr of [14-C]carbon dioxide was added to the reaction vessel, at this temperature, and allowed to interact with the surface for 2 hours. After this time, [14-C]carbon dioxide was found to be the only species present in the gas phase of the reaction vessel. The [14-C]carbon dioxide was removed from the system by 30 seconds evacuation and 1.9 torr of [12-C]carbon monoxide then added to the reaction vessel. After a period of 15 minutes, a small amount of [14-C]carbon monoxide was evident in the gas phase of the reaction vessel.

5.6 RADIOTRACER TEMPERATURE PROGRAMMED DESORPTION

5.6.1 Desorption from Copper-Alumina

A 3.82 torr sample of [14-C]carbon dioxide was admitted to the reaction vessel, which contained a freshly reduced, 0.183g sample, of copper-alumina catalyst. After 60 minutes equilibration, at 20°C, the reaction vessel was evacuated for 5 minutes. On completion of this procedure, it was found that 55% of the previously adsorbed

material was still associated with the copper-alumina surface.

This radiolabelled material was desorbed from the surface by heating the sample, at a rate of 1.9 deg. min^{-1}, to 240°C, in a helium stream. Desorption occurred over a broad temperature range as is shown in Figure 5.33.

5.6.2 Desorption from Polycrystalline Copper

5.6.2.1 Desorption Subsequent to [14-C]Carbon Monoxide Adsorption

(a) [14-C]Carbon Monoxide Adsorption

A 4.2 torr sample of [14-C]carbon monoxide was allowed to interact with 0.17g of freshly reduced copper for 60 minutes. The temperature of the copper was 220°C. After cooling, to ambient temperature, the reaction vessel was evacuated for 5 minutes. This removed 95.5% of the previously adsorbed material from the copper surface. The remainder of the adsorbed radiolabel was desorbed from the surface by heating the sample, at a rate of 2.5 deg. min^{-1}, in a stream of helium; the desorption profile produced by this process is shown in Figure 5.34(a).

(b) Coadsorption of [14-C]Carbon Monoxide and Hydrogen

8.4 torr of a gaseous mixture which consisted of equal mole fractions of [14-C]carbon monoxide and hydrogen, was allowed to interact with 0.17g of copper for a period of 60 minutes. The temperature of the copper was 220°C. On evacuation, at ambient temperature, 4.5% of the total quantity of adsorbed radiolabel was found to be resistant to this procedure. The desorption profile produced on further heating of this sample, at a rate of 2.5 deg. min^{-1},

Figure 5.33 Radiotracer T.P.D. following $^{14}CO_2$ adsorption on Cu/Al_2O_3

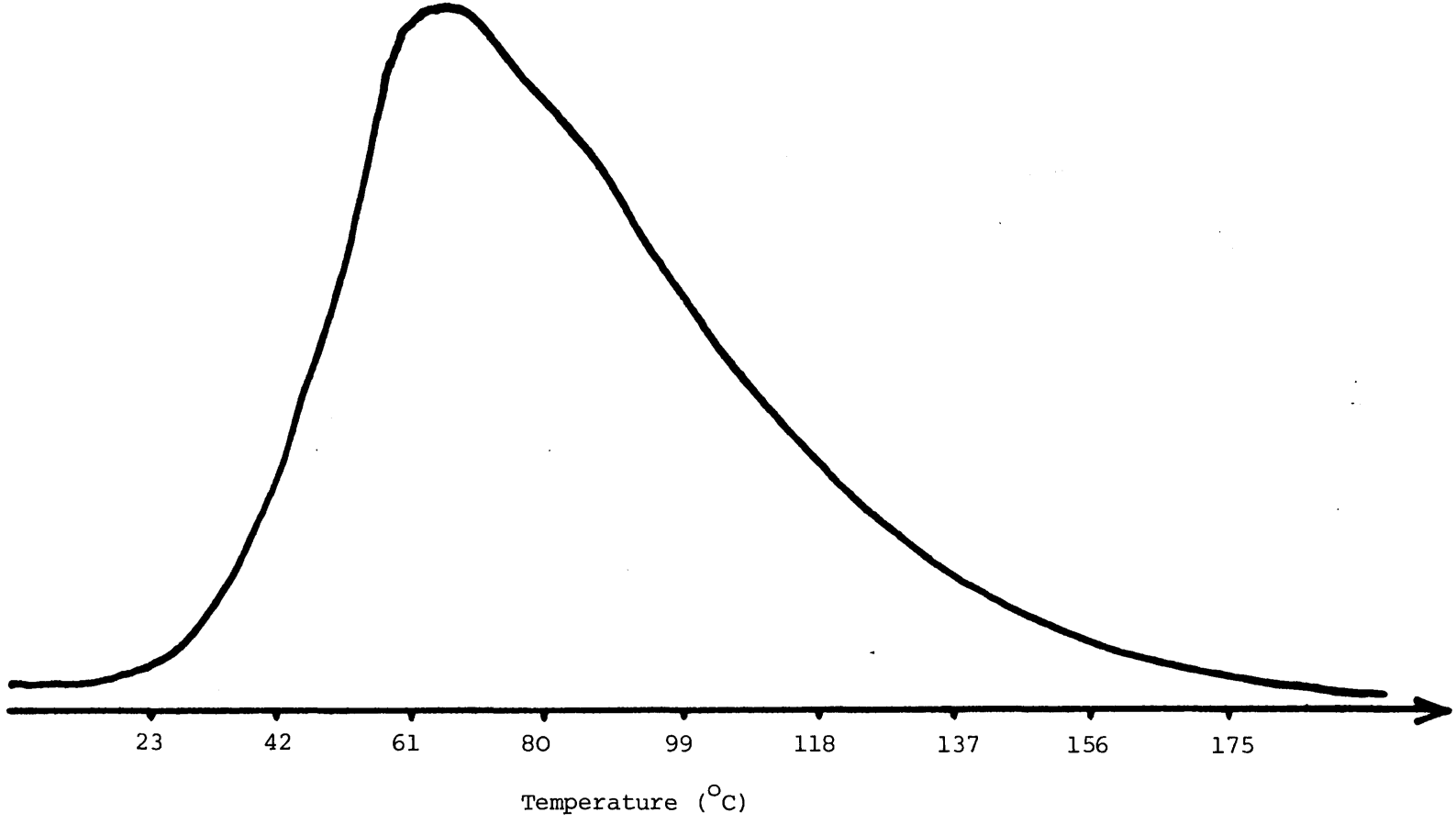

Figure 5.34 Radiotracer T.P.D. following the adsorption of
(a) ^{14}CO on copper
(b) $^{14}CO + H_2$ on copper

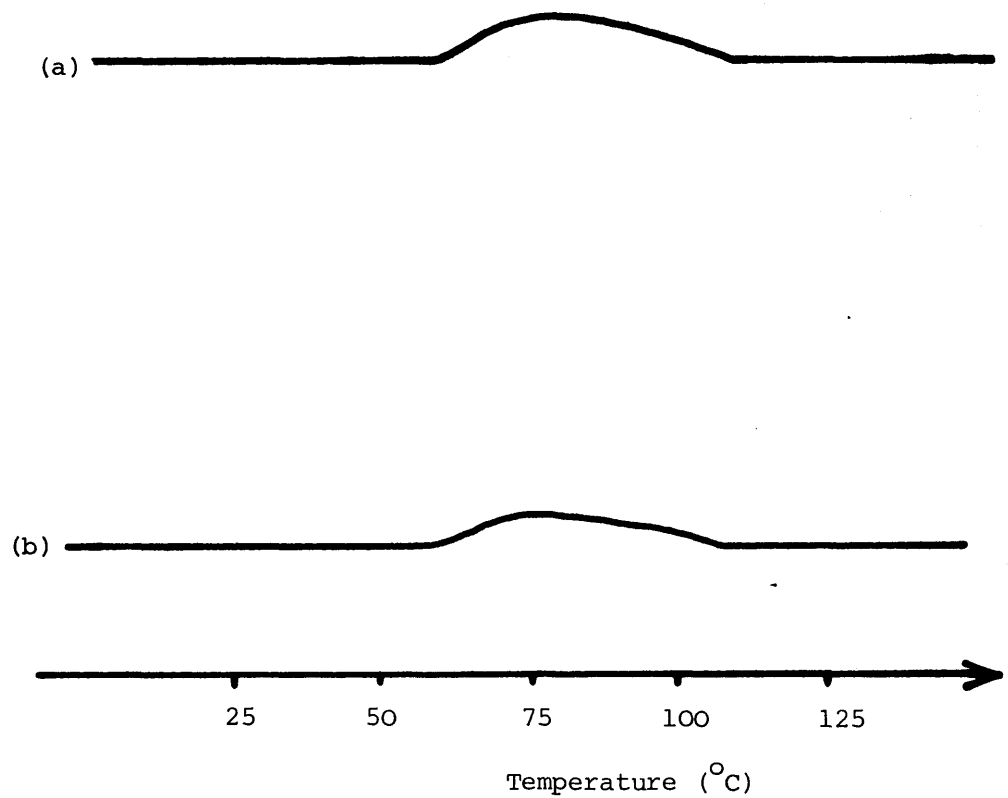

is detailed in Figure 5.34(b).

5.6.2.2 Desorption Subsequent to [14-C]Carbon Dioxide Adsorption

(a) [14-C]Carbon Dioxide Adsorption

Following the interaction of 3.89 torr [14-C]carbon dioxide with 0.32g of copper, at 23°C, for 60 minutes, 11% of the adsorbed radiolabel was found to be resistant to 5 minutes evacuation. On heating the copper, at a rate of 2.2 deg. min^{-1}, this material desorbed from the surface with a maximum rate at a temperature of 78°C (Figure 5.35).

(b) Coadsorption of [14-C]Carbon Dioxide and Hydrogen

Following the interaction of 3.8 torr of [14-C]carbon dioxide and 4.3 torr of hydrogen with 0.21g of copper, at 220°C, for 45 minutes, 63% of the adsorbed radiolabel was found to be resistant to 5 minutes, ambient temperature, evacuation. On heating the copper, at a rate of 3.6 deg. min^{-1}, this material was found to desorb from the surface with a maximum rate at a temperature of 141°C (Figure 5.36).

5.6.3 Desorption from Fully Oxidised Polycrystalline Copper

4.73 torr of [14-C]carbon dioxide was allowed to interact with a copper surface which had been fully oxidised by the reaction of nitrous oxide, for 15 minutes, at 70°C. Throughout the adsorption period (45 minutes) the temperature of the copper was maintained at 23°C. 26% of the adsorbed radiolabel was found to be resistant to 5 minutes evacuation. On further heating of the sample a desorption process occurred which showed a maximum rate at a temperature of 86°C (Figure 5.37).

Figure 5.35 Radiotracer T.P.D. following $^{14}CO_2$ adsorption on polycrystalline copper

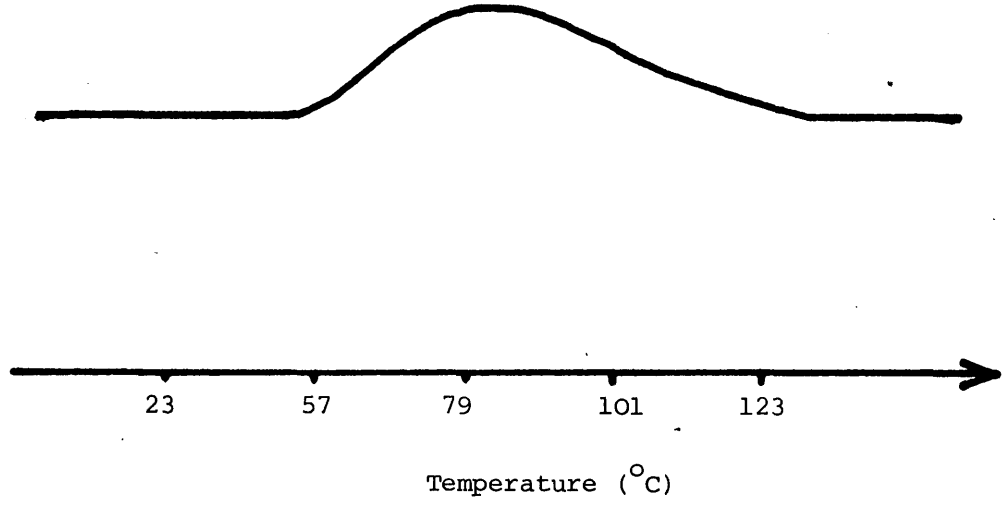

Figure 5.36 Radiotracer T.P.D. following $^{14}CO_2 + H_2$ adsorption on polycrystalline copper

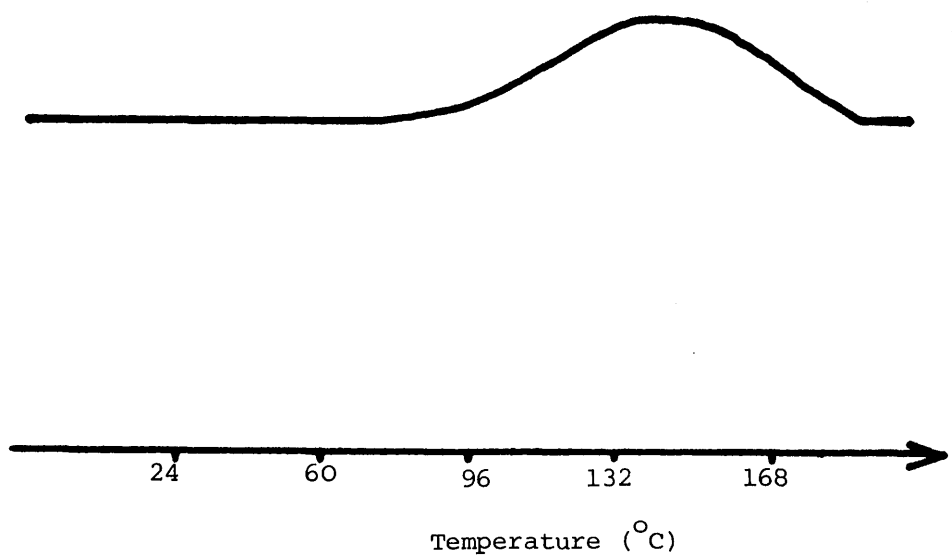

Figure 5.37 Radiotracer T.P.D. following $^{14}CO_2$ adsorption on a fully oxidised copper surface

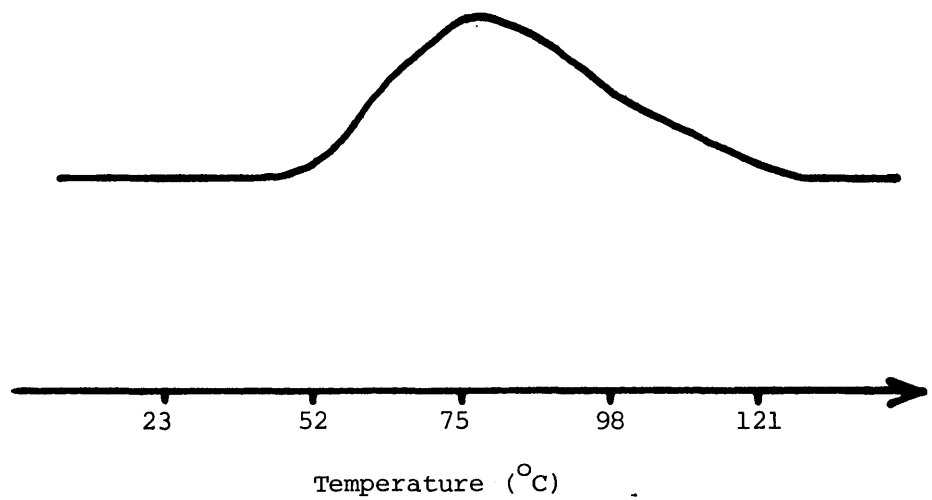

C H A P T E R 6

MASS SPECTROSCOPIC ANALYSIS OF ADSORPTION ON, AND DESORPTION FROM, POLYCRYSTALLINE COPPER

MASS SPECTROSCOPIC ANALYSIS OF ADSORPTION ON, AND DESORPTION FROM, POLYCRYSTALLINE COPPER

6.1 THE INTERACTION OF CARBON MONOXIDE WITH POLYCRYSTALLINE COPPER

A partially oxidised polycrystalline copper surface was reduced by reaction with a 25 ml min^{-1}, 6% carbon monoxide-helium flow at 219°C. When carbon dioxide production had ceased, the fully reduced surface was cooled, in the carbon monoxide-helium flow, to ambient temperature. After sweeping out the catalyst column for 10 minutes in a 25 ml min^{-1} helium stream, the temperature of the copper was raised, at a rate of 8 deg. min^{-1}, to 211°C. Carbon monoxide was found to desorb from the copper surface over a broad temperature range, but showed a maximum desorption rate at a temperature of 84°C (Figure 6.1). The total quantity of desorbed carbon monoxide was equivalent to 7% of maximum surface coverage.

In this study, the reaction of carbon monoxide with oxidised copper was the standard means of reducing polycrystalline samples (section 3.3.4.1). However, this experiment proved that this procedure did not produce a totally clean copper sample. Carbon monoxide which had become associated with a copper surface, during the reduction procedure, was therefore always desorbed from that sample before any carbon dioxide, water or hydrogen adsorption analysis.

Figure 6.1 T.P.D. following CO adsorption on copper

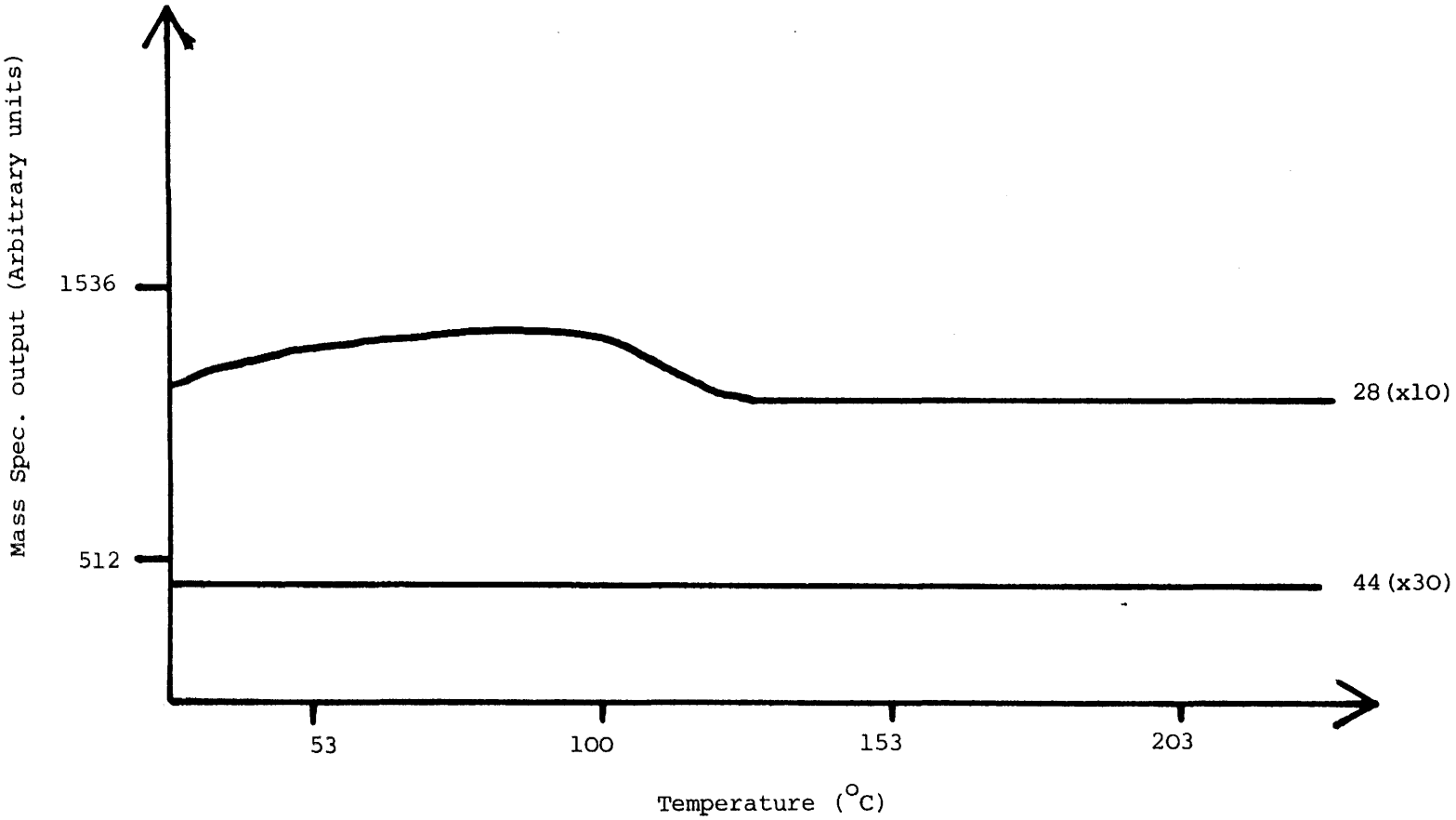

6.2 THE INTERACTION OF HYDROGEN WITH POLYCRYSTALLINE COPPER

A stream of 22% hydrogen-helium was flowed over freshly reduced copper powder for 15 minutes. The temperature of the column was 25°C. After this period, the catalyst column was immersed in liquid nitrogen, which caused the temperature to fall to -196°C. A helium flow was passed through the column for 5 minutes and the column then warmed to room temperature. Hydrogen was found to desorb from the copper at temperatures above -10°C (Figure 6.2). The column was then heated, at a rate of 8 deg. min^{-1}, to 200°C and any further desorption monitored (Figure 6.3). A slight hydrogen desorption was found to occur in the temperature range 34°C - 107°C.

6.3 THE INTERACTION OF CARBON DIOXIDE WITH POLYCRYSTALLINE COPPER

6.3.1 Continuous Flow Studies

6.3.1.1 Adsorption on Fully Oxidised Polycrystalline Copper

A 9% carbon dioxide-helium stream was flowed over a copper sample whose surface had been fully oxidised by treatment with excess nitrous oxide at 60°C. During the 10 minute adsorption period the temperature of the copper was maintained at 27°C. Carbon dioxide was the only gas eluted from the column during this time. Subsequent temperature programmed desorption (T.P.D.) revealed the presence of adsorbed carbon dioxide only (Figure 6.4). 9.2×10^{17} molecules of carbon dioxide desorbed in a broad feature with a maximum rate of desorption at a temperature, T_p = 54°C. Two slight shoulders on the tail of the peak were seen at temperatures of respectively, 128°C and 172°C.

Figure 6.2 Desorption of H_2 from copper at sub-ambient temperature

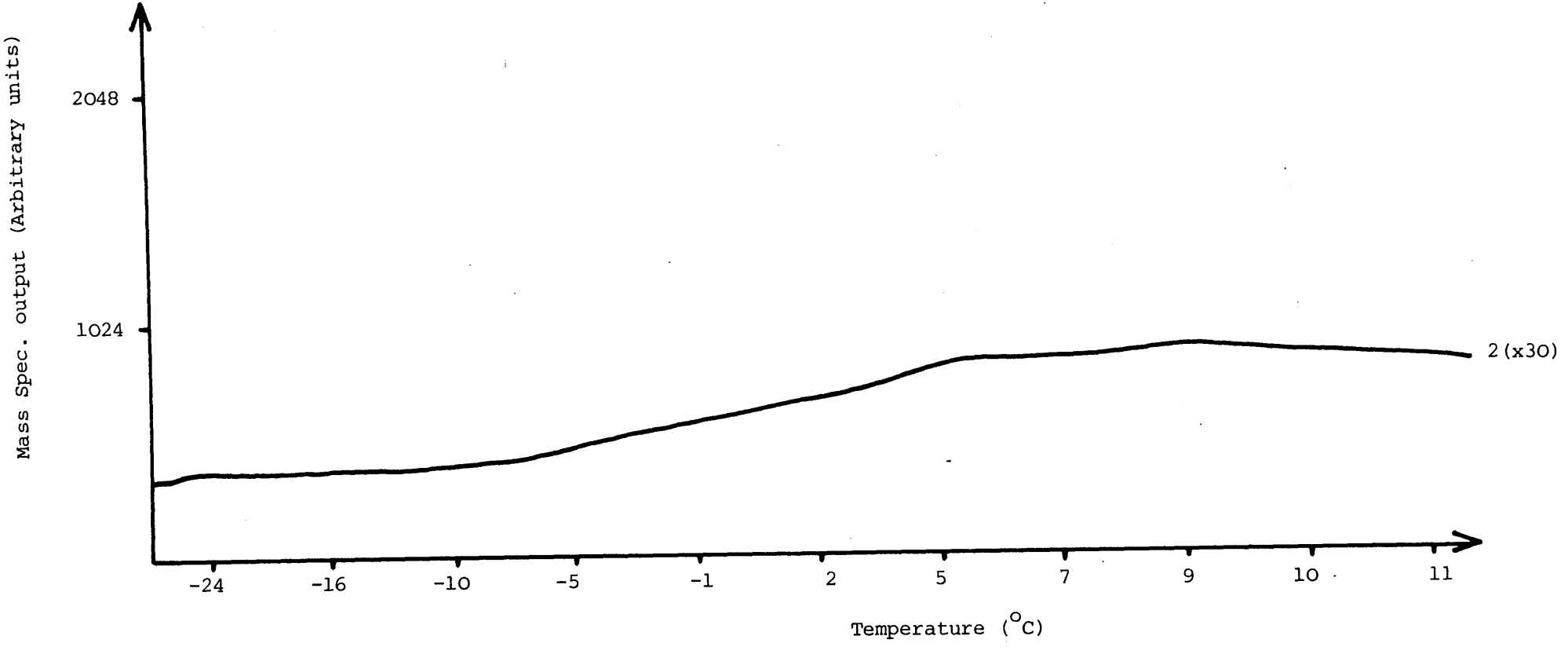

Figure 6.3 T.P.D. following H_2 adsorption on copper

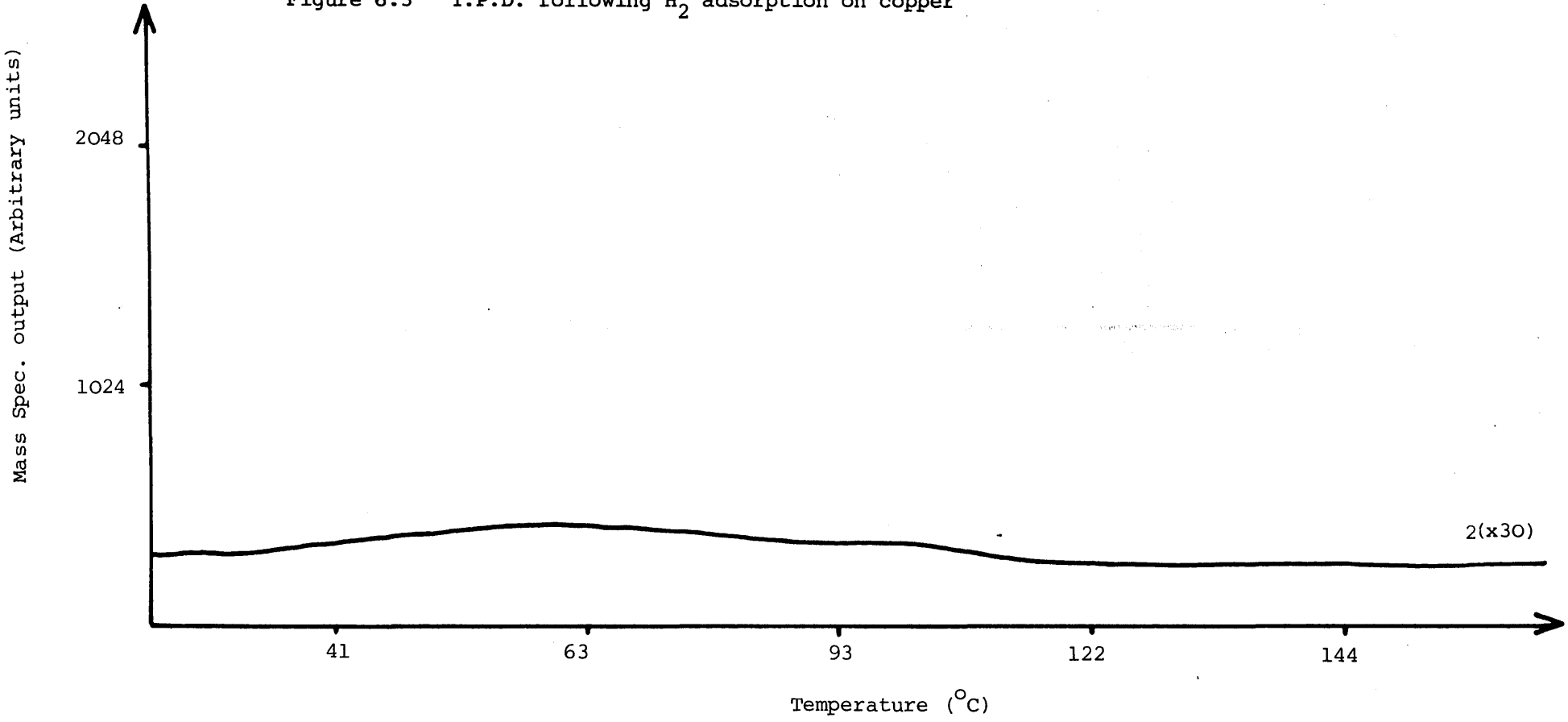

Figure 6.4 T.P.D. following CO_2 adsorption on fully oxidised copper

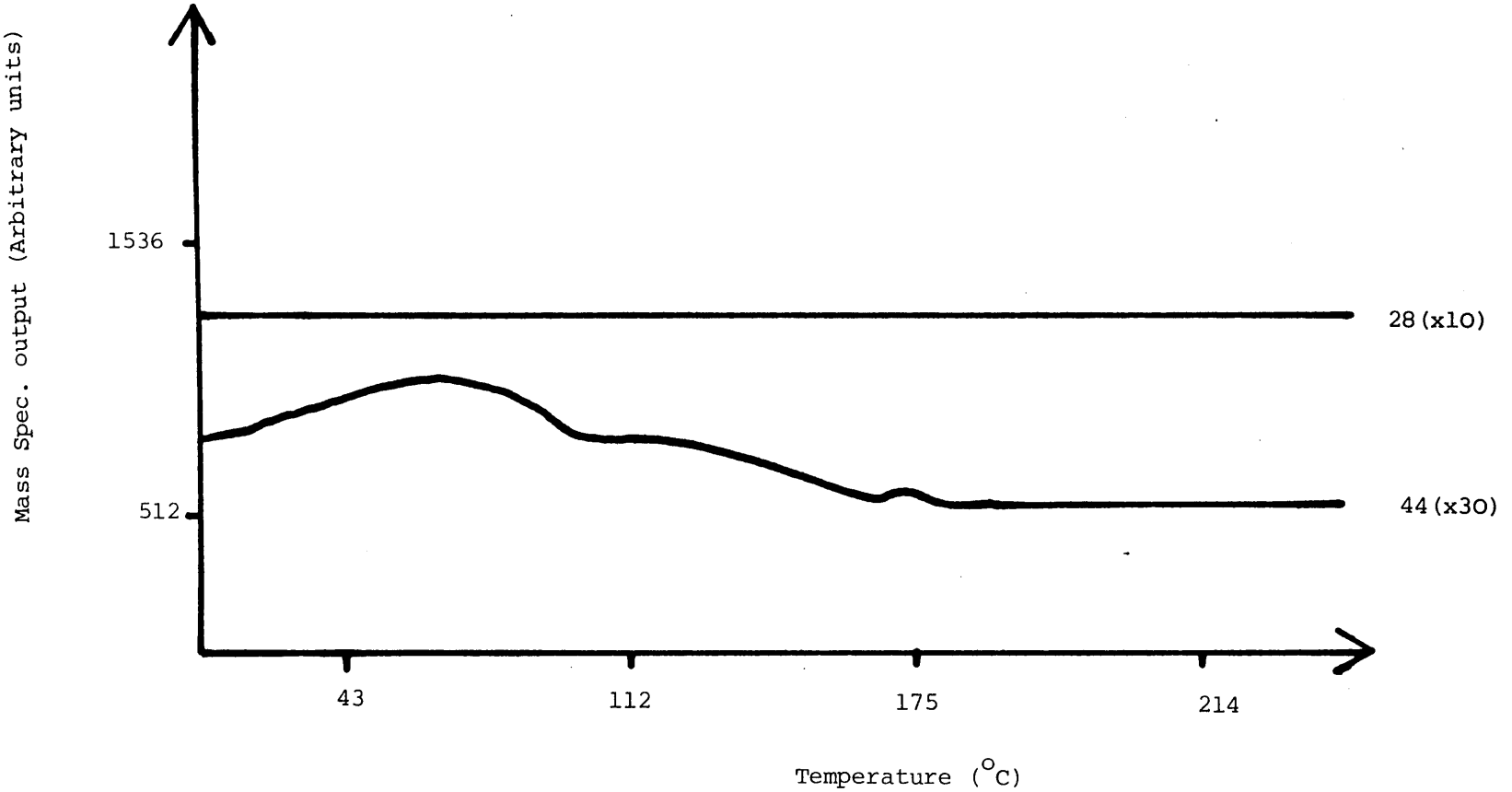

6.3.1.2 Adsorption on Partially Oxidised Polycrystalline Copper

A freshly reduced copper sample, maintained at a temperature of 60°C, was reacted with a quantity of nitrous oxide which was calculated to produce half monolayer coverage of oxygen on the copper surface. After cooling the copper sample to ambient temperature, a 9% carbon dioxide-helium stream was passed through the catalyst column for 10 minutes. Subsequent T.P.D. found no evidence of desorbing carbon monoxide species (Figure 6.5). Carbon dioxide was found to desorb with a maximum rate at a temperature of 57°C.

6.3.1.3 Adsorption on Reduced Polycrystalline Copper

In all the experiments described in this section, the analysis was concerned with those results pertaining from desorption studies and not with any data obtained during the original adsorption process. Variation in background reading, and hence inaccurate evaluation of mass spectrometer cracking fractions, rendered quantitative analysis of this data impractical.

(a) 225°C

A stream of 10% carbon dioxide-helium was flowed over a reduced copper sample, for 10 minutes, at a temperature of 225°C. The column was then cooled, in a helium flow, to ambient temperature. On further heating, at a rate of 8 deg. min^{-1}, 2.25×10^{18} carbon monoxide molecules were found to desorb from the surface with $T_p = 86°C$ (Figure 6.6). Small amounts of carbon dioxide were also released from the surface at temperatures of 123°C and 147°C. The subsequent reaction of a 6% carbon monoxide-helium stream with the copper sample, at 200°C, generated 5.53×10^{18} carbon dioxide molecules.

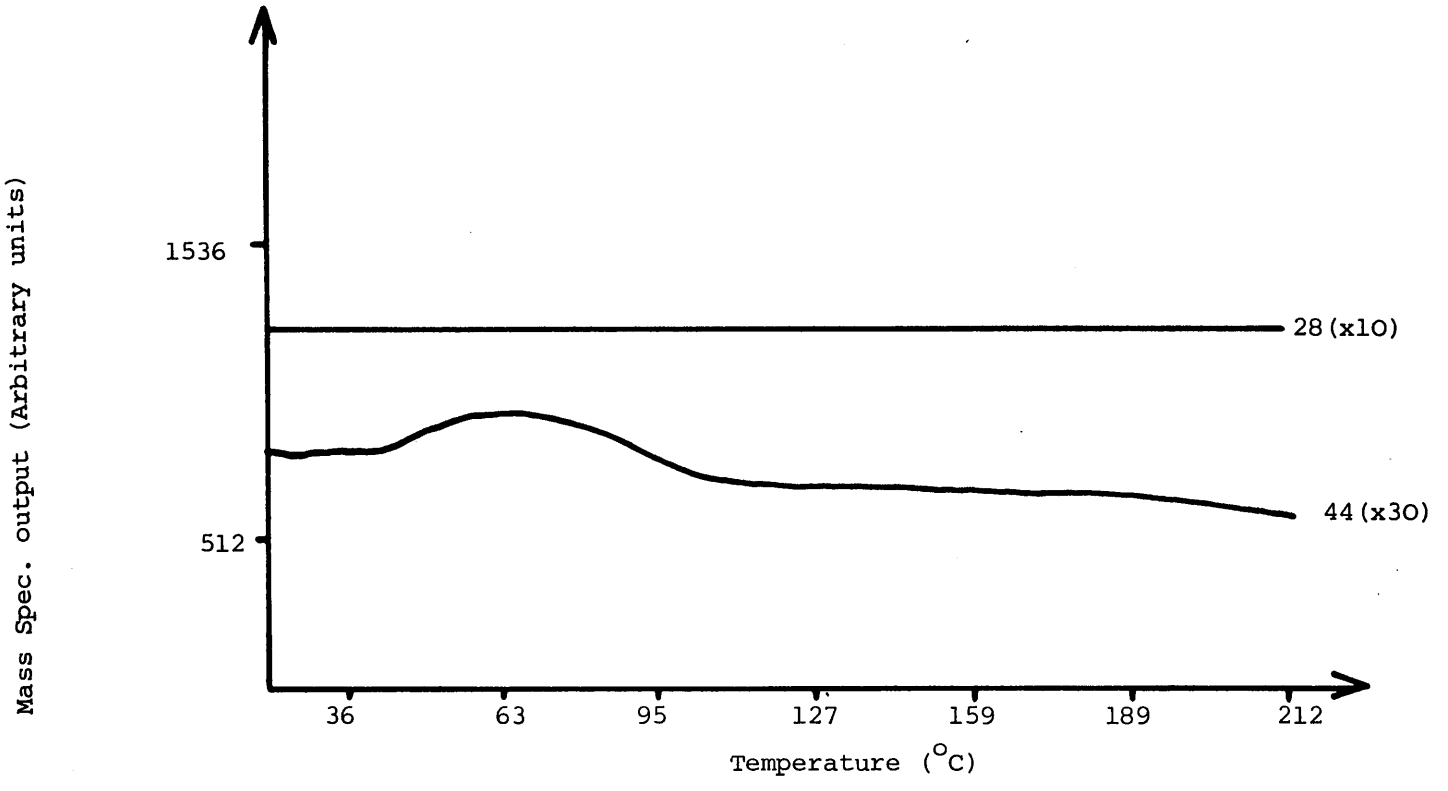

Figure 6.5 T.P.D. following CO_2 adsorption on partially oxidised copper

Figure 6.6 T.P.D. following CO_2 adsorption on copper at 225°C

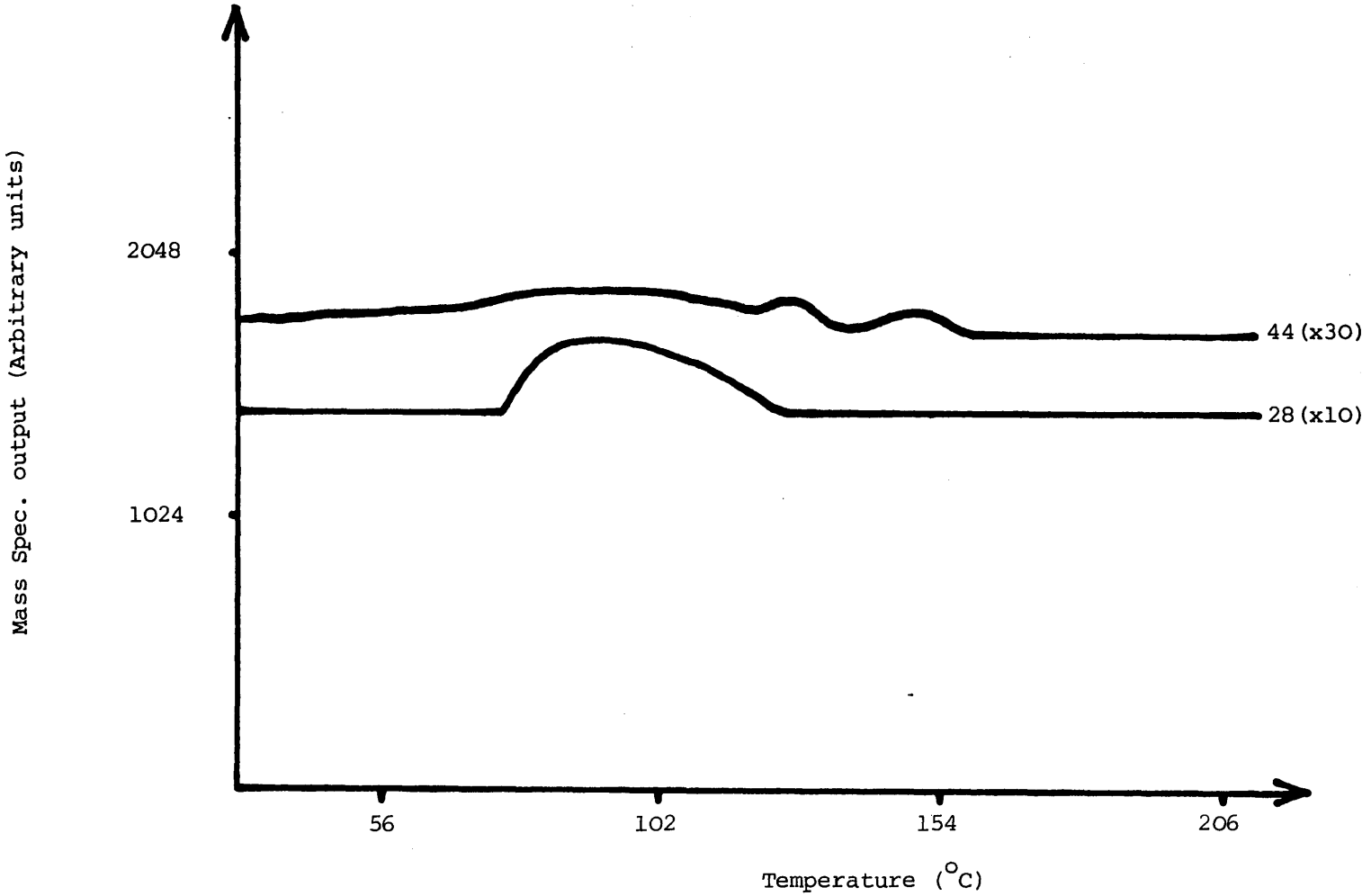

(b) 100°C

The above analysis was exactly reproduced for reaction at 100°C. T.P.D. revealed the presence of 1.79×10^{18} molecules of carbon monoxide, which desorbed with T_p = 91°C (Figure 6.7). Significant carbon dioxide desorption (1.0×10^{18} molecules) was also observed at more elevated temperatures (T_p = 153°C). The subsequent reaction of a 6% carbon monoxide-helium stream, with the copper sample, generated 1.09×10^{18} carbon dioxide molecules.

(c) 26°C

The desorption profiles produced following the reaction of a 10% carbon dioxide-helium stream with polycrystalline copper at 26°C, for 5 minutes and 65 minutes, are shown in Figures 6.8 and 6.9 respectively. It is apparent that the differing reaction times generated significantly different desorption profiles.

Following 5 minutes reaction, 1.77×10^{18} carbon monoxide molecules desorbed from the copper surface in a compact feature with T_p = 87°C. After 65 minutes reaction, 3.6×10^{18} carbon monoxide molecules were found to desorb in a far broader feature with T_p reduced to 66°C.

The two slight shoulders in the carbon dioxide desorption profile (T_p = 84°C and 150°C), produced following 5 minutes reaction, increased in size and showed slightly reduced T_p (66°C and 118°C) following the 65 minute reaction period.

Subsequent to the 5 minute reaction period, 2.79×10^{18} carbon dioxide molecules were produced by titration of the oxidised surface with carbon monoxide. Similar treatment, after the 65 minute reaction period, generated 8.04×10^{18} carbon dioxide molecules.

Figure 6.7 T.P.D. following CO_2 adsorption on copper at 100°C

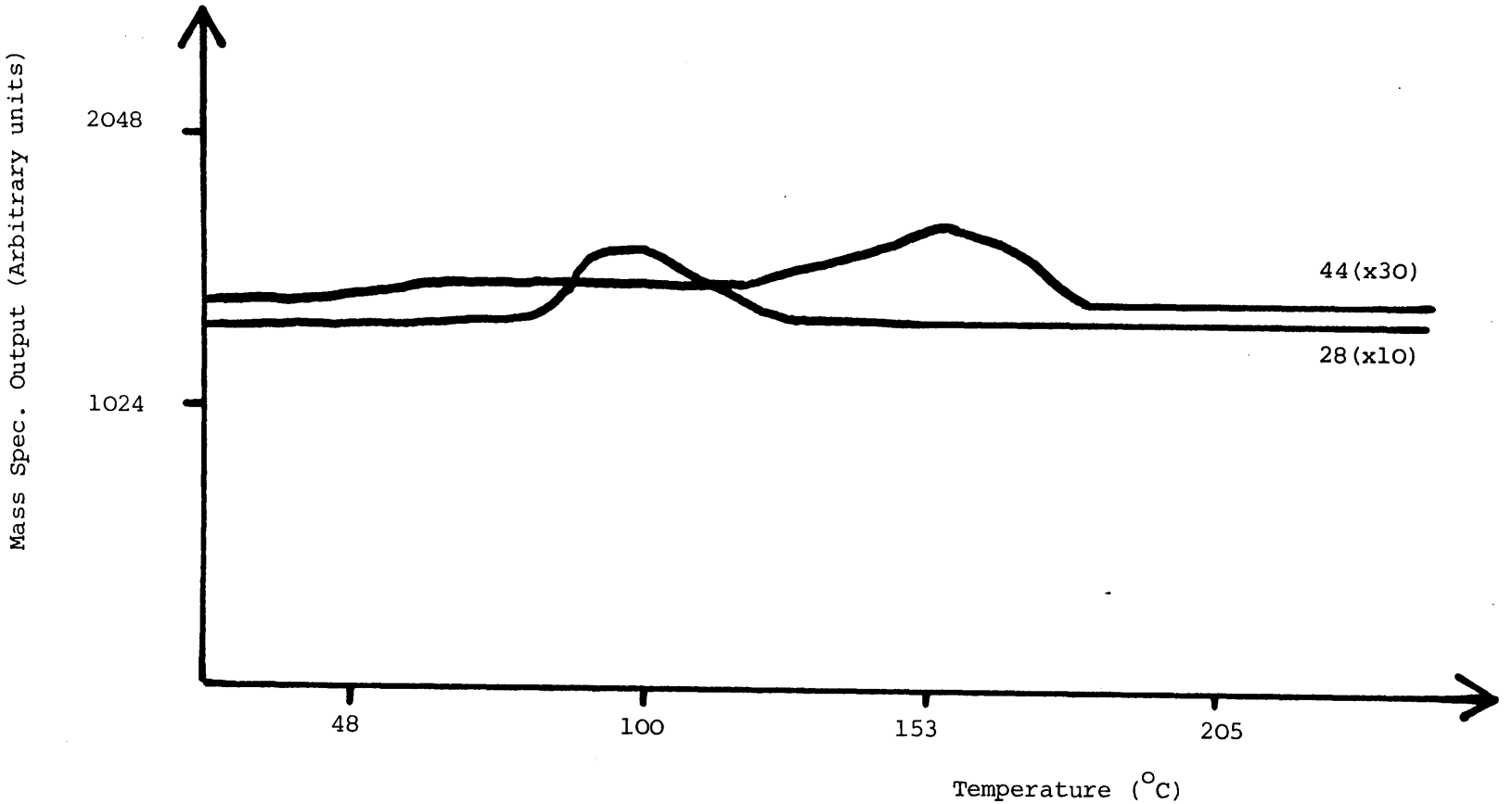

Figure 6.8 T.P.D. following CO_2 adsorption on copper at 26°C (5 mins)

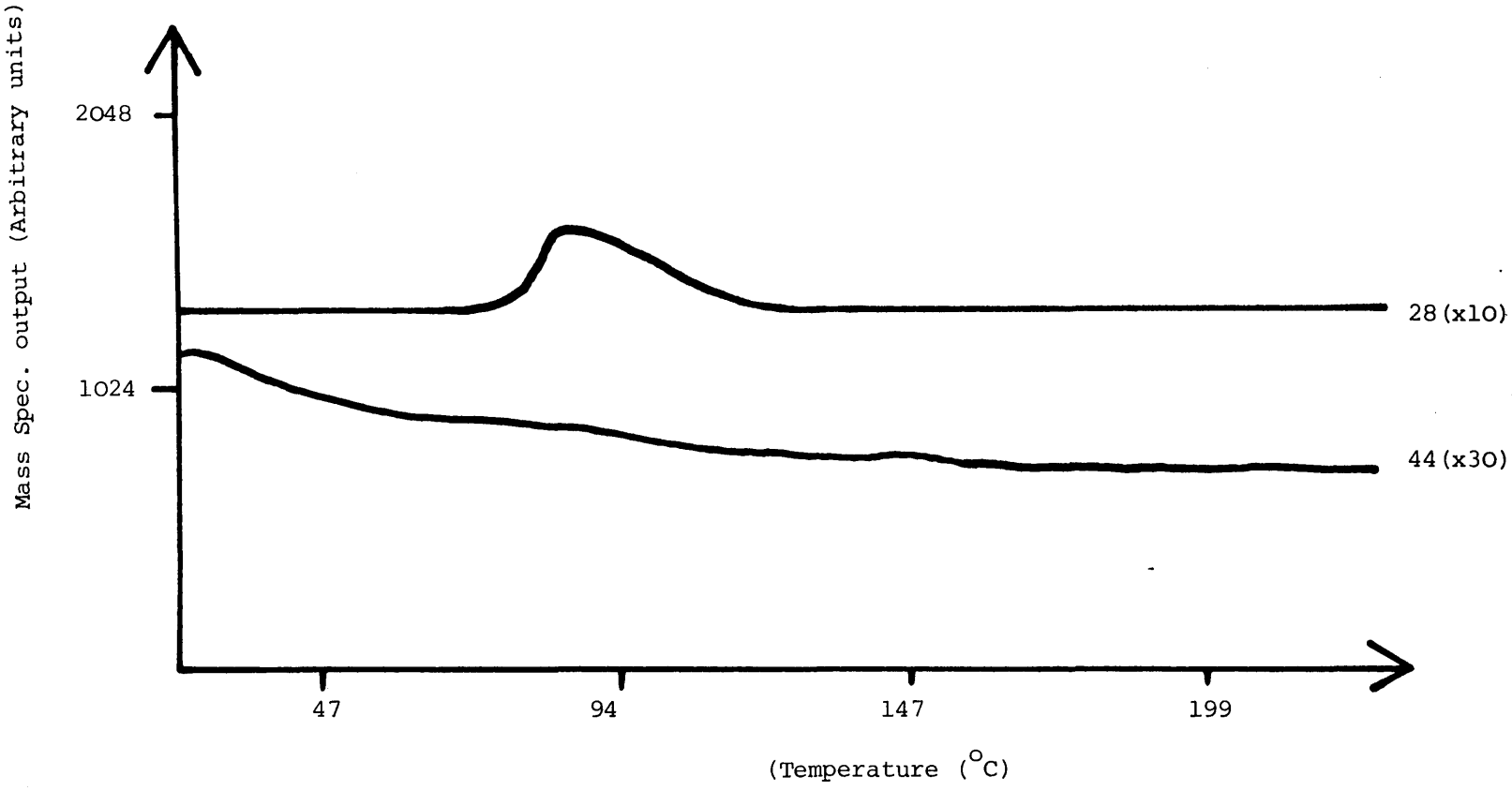

Figure 6.9 T.P.D. following CO_2 adsorption on copper at 26°C (65 mins)

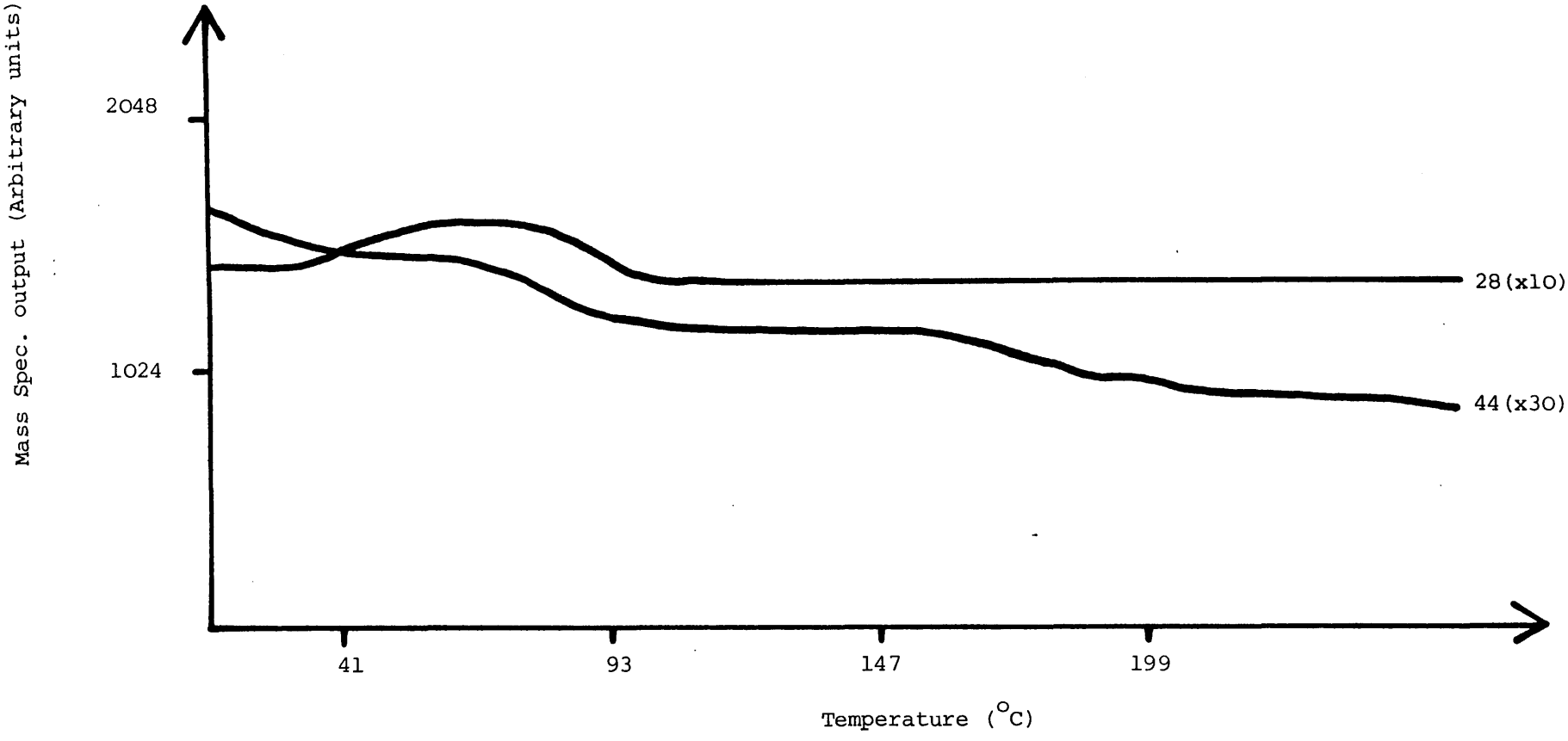

6.3.2 Static Adsorption Studies

6.3.2.1 Adsorption on Fully Oxidised Polycrystalline Copper

A 10% carbon dioxide-helium mixture (Pressure = 1 atm.) was allowed to stand, for 15 mins, within a closed reaction vessel which contained a sample of copper, whose surface had been fully oxidised by treatment with excess nitrous oxide at 60°C. The temperature of the oxidised sample was 26°C.

Subsequent T.P.D. gave rise to a broad carbon dioxide desorption feature (T_p = 67°C) and gave no evidence for adsorbed carbon monoxide species (Figure 6.10).

6.3.2.2 Adsorption on Reduced Polycrystalline Copper

(a) 216°C

A 10% carbon dioxide-helium mixture (Pressure = 1 atm.) was allowed to stand within a closed catalyst column, for 15 minutes, at a temperature of 216°C. A helium flow was then passed through the column at this temperature. This had the effect of removing the gas phase from the closed system and of allowing rapid desorption of any adsorbed species. A total of 5.3×10^{17} carbon monoxide molecules were eluted from the catalyst column by this procedure. The subsequent reaction of a carbon monoxide-helium stream with the copper surface produced no measurable quantity of carbon dioxide.

(b) 27°C

A mixture of 10% carbon dioxide-helium was allowed to stand within a closed catalyst column, for 15 minutes, at a temperature of 27°C. Subsequent T.P.D. gave rise to 1.12×10^{18} carbon monoxide

Figure 6.10 T.P.D. following CO_2 adsorption (static) on fully oxidised copper surface (26°C)

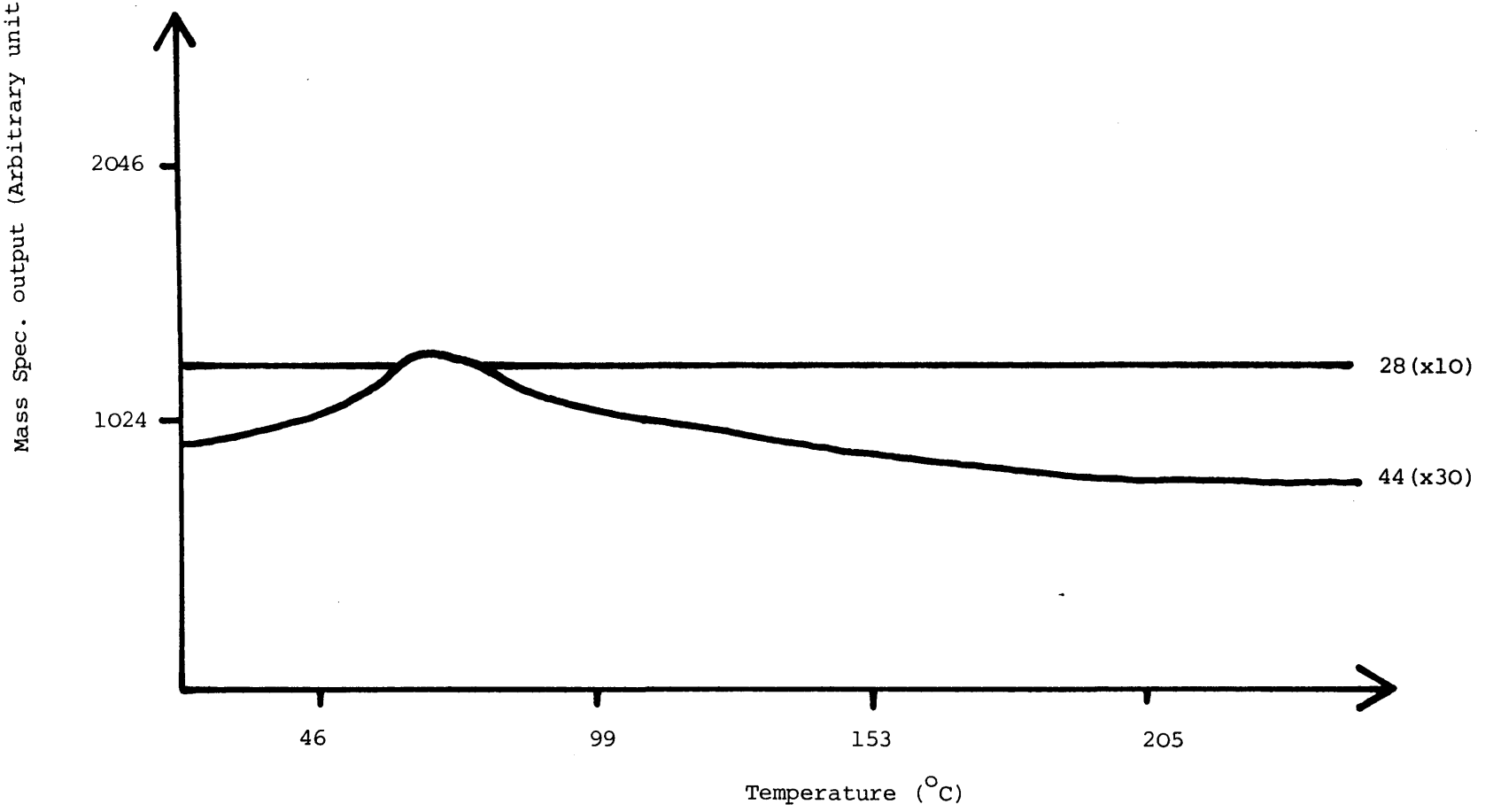

molecules, which desorbed in a compact feature with T_p = 109°C (Figure 6.11). A sharp carbon dioxide desorption feature, corresponding to the removal of 2.5 x 10^{17} carbon dioxide species, was observed at a temperature of 100°C and a broad feature noted at more elevated temperature (T_p = 160°C). Titration of the surface with 6% carbon monoxide-helium gave rise to 4.9 x 10^{17} carbon dioxide molecules.

The experiment was repeated, under identical conditions, with the carbon dioxide-helium mixture standing in the closed column for 65 minutes. On heating, 1.04 x 10^{18} carbon monoxide molecules desorbed with T_p = 109°C (Figure 6.12).

A pronounced desorption, corresponding to the production of 1.18 x 10^{18} carbon dioxide molecules, was observed with T_p = 100°C. A broad carbon dioxide desorption feature was also noted in the temperature range 130°C - 170°C. Titration of the surface with carbon monoxide gave rise to 5.6 x 10^{17} carbon dioxide molecules.

(c) <u>-60°C</u>

A mixture of 10% carbon dioxide-helium (Pressure = 1 atm.) was allowed to stand within a closed catalyst column, for 15 mins, at a temperature of -60°C. The column was warmed to room temperature, in a helium flow, during which time carbon dioxide was found to desorb from the copper surface (Figure 6.13). On further linear heating of the column to 214°C, 4.07 x 10^{18} molecules of carbon monoxide desorbed with T_p = 89°C (Figure 6.14). A small quantity of carbon dioxide desorbed as the temperature reached 81°C and a broad feature was obvious at temperatures between 140°C and 190°C.

Figure 6.11 T.P.D. following static adsorption of CO_2 on copper (15 mins at 27°C)

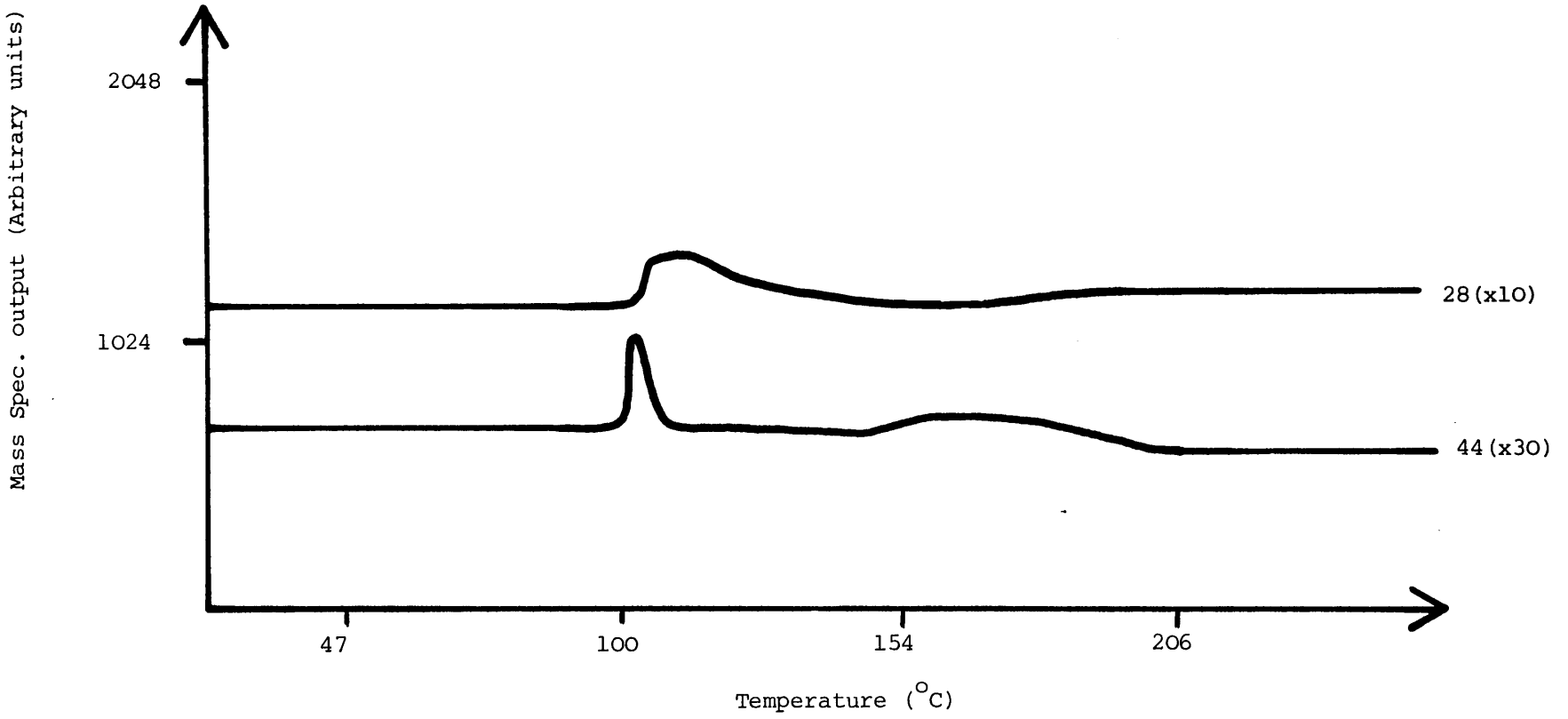

Figure 6.12 T.P.D. following static adsorption of CO_2 on copper (65 mins. at 27°C)

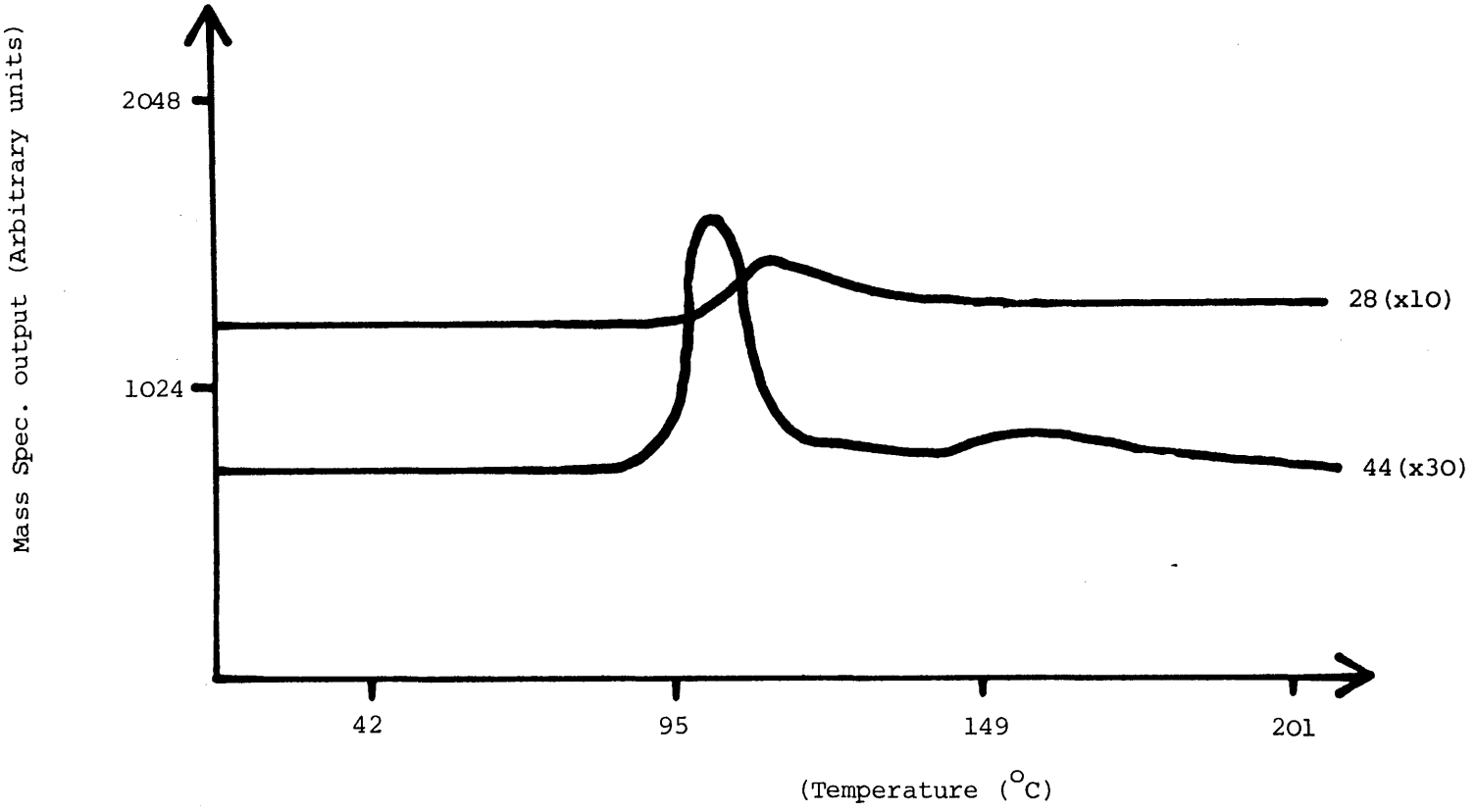

Figure 6.13 Desorption profile following static CO_2 adsorption on copper (15 mins at -60°C)

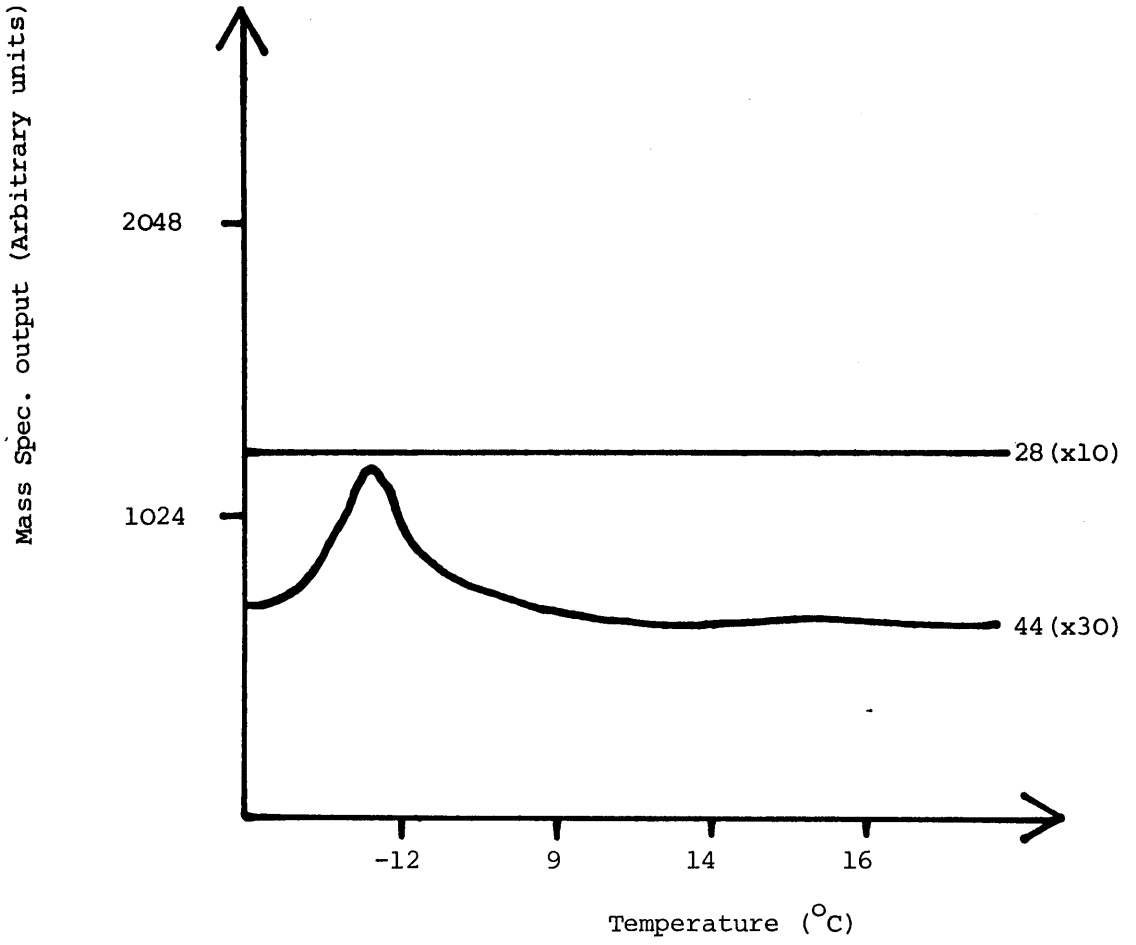

Figure 6.14 T.P.D. following static adsorption of CO_2 on copper (15 mins at -60°C)

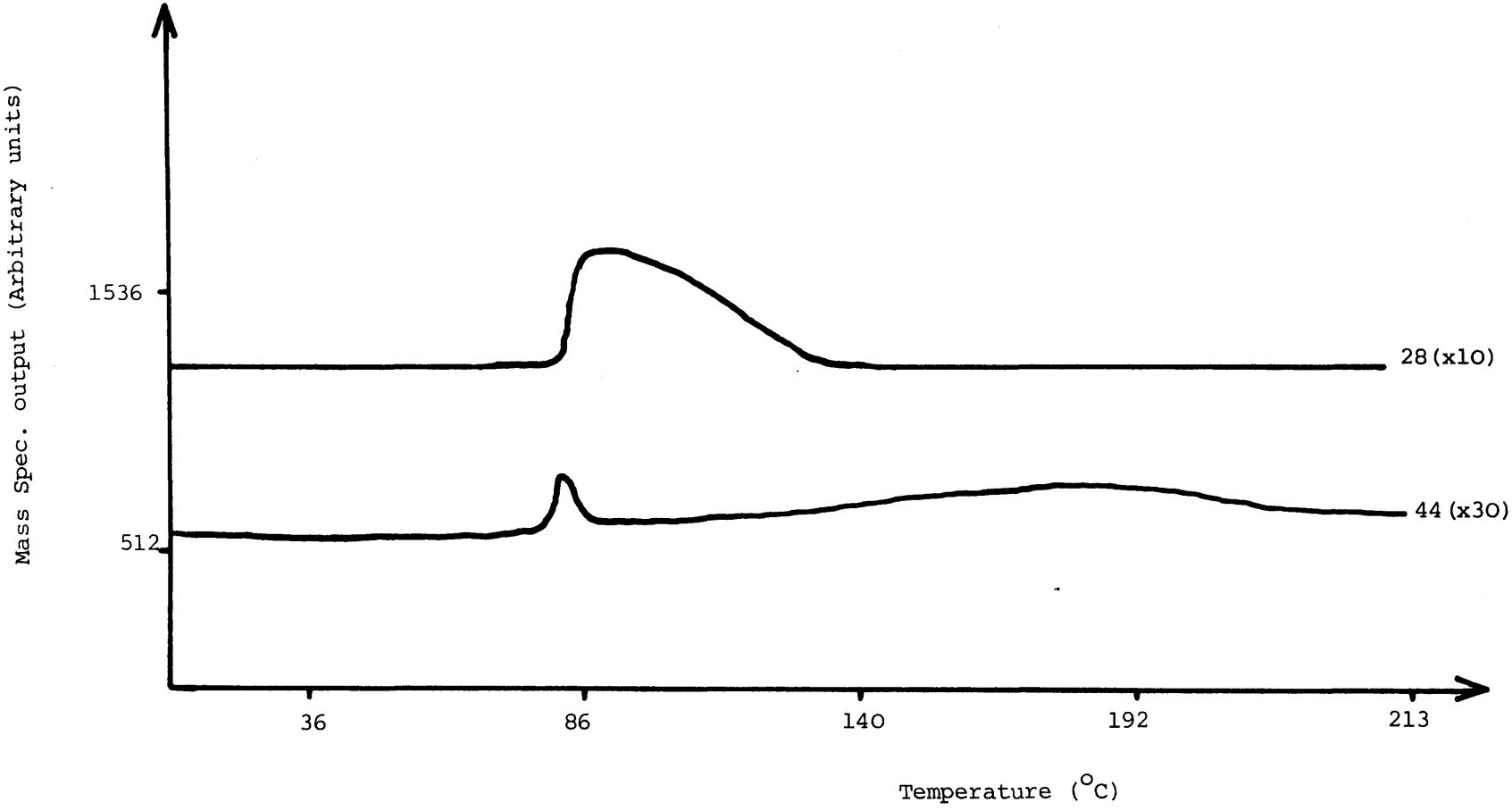

6.4 THE INTERACTION OF WATER WITH POLYCRYSTALLINE COPPER

6.4.1 Adsorption on Fully Oxidised Polycrystalline Copper

A 2.8% water-helium stream was flowed over a fully oxidised copper surface, for 10 minutes, at a temperature of 234°C. An instantaneous uptake of 1.12×10^{18} molecules of water (10% of a monolayer) was observed on the oxidised copper, but no hydrogen was evolved during this adsorption process (Figure 6.15). Thereafter a continual, though slight, adsorption of water occurred on the oxidised surface. Subsequent rereduction of the copper sample, in a 6% carbon monoxide-helium stream, resulted in the formation of an amount of carbon dioxide greater than that expected from the initial decomposition of nitrous oxide.

6.4.2 The Reactive Adsorption of Water on Polycrystalline Copper

The adsorption and reaction of a stream of 0.39% water-helium with copper was studied, over a wide range of temperature, by mass spectrometric analysis of hydrogen evolution during the adsorption process. Figure 6.16 shows the variation of the m/e = 2 peak during the passage of the water-helium stream through the catalyst bed at various temperatures. At relatively high reaction temperatures, a sharp pulse of hydrogen was eluted from the catalyst column after only 20-30 seconds reaction, while, at lower temperatures, a progressively more diffuse peak appeared after considerably elongated time intervals. At ambient temperature no clear hydrogen pulse was observed, although, after 15 minutes in the water stream, the amount of hydrogen being eluted from the column was slightly greater than that which

Figure 6.15 The Adsorption of H_2O on a fully oxidised copper surface

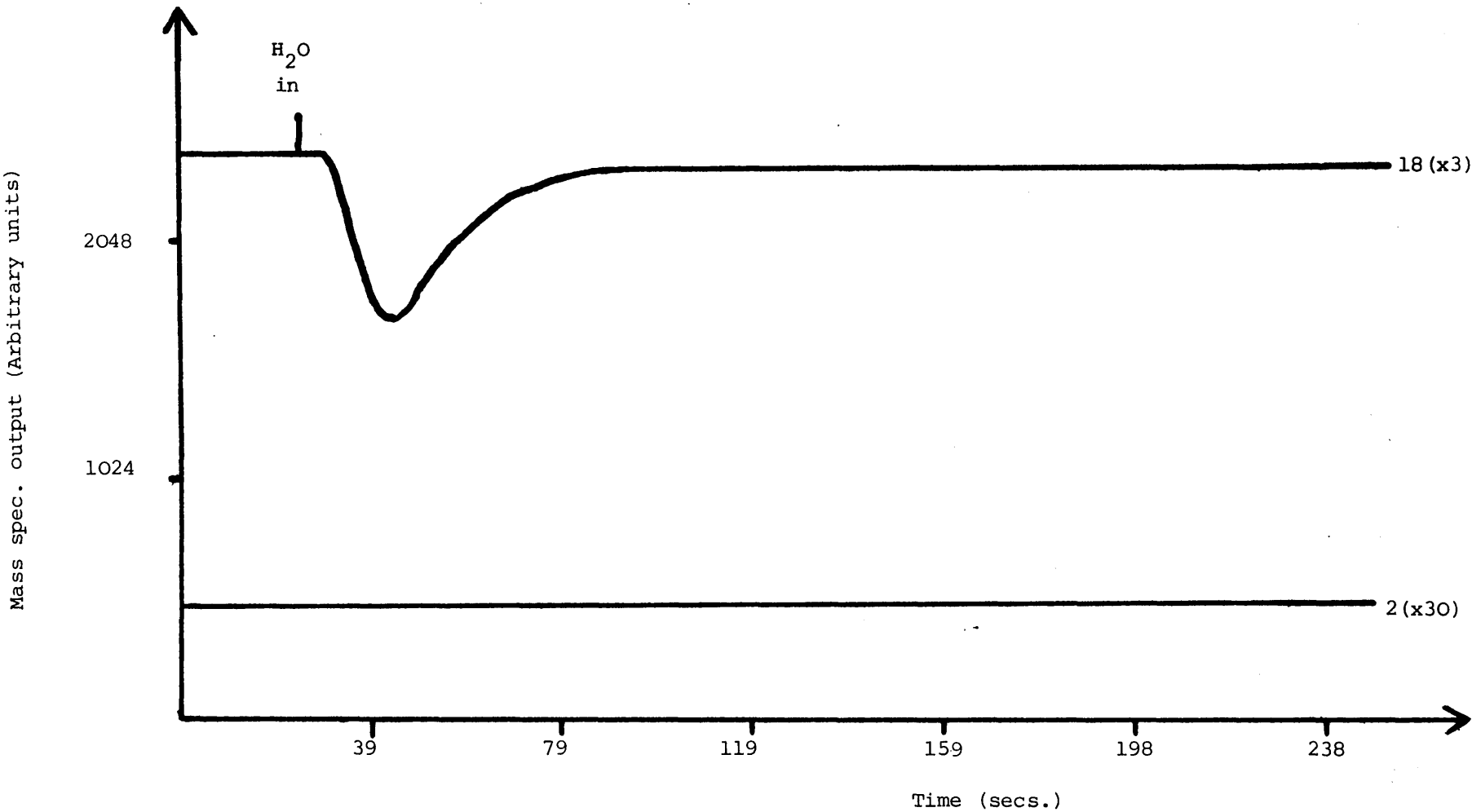

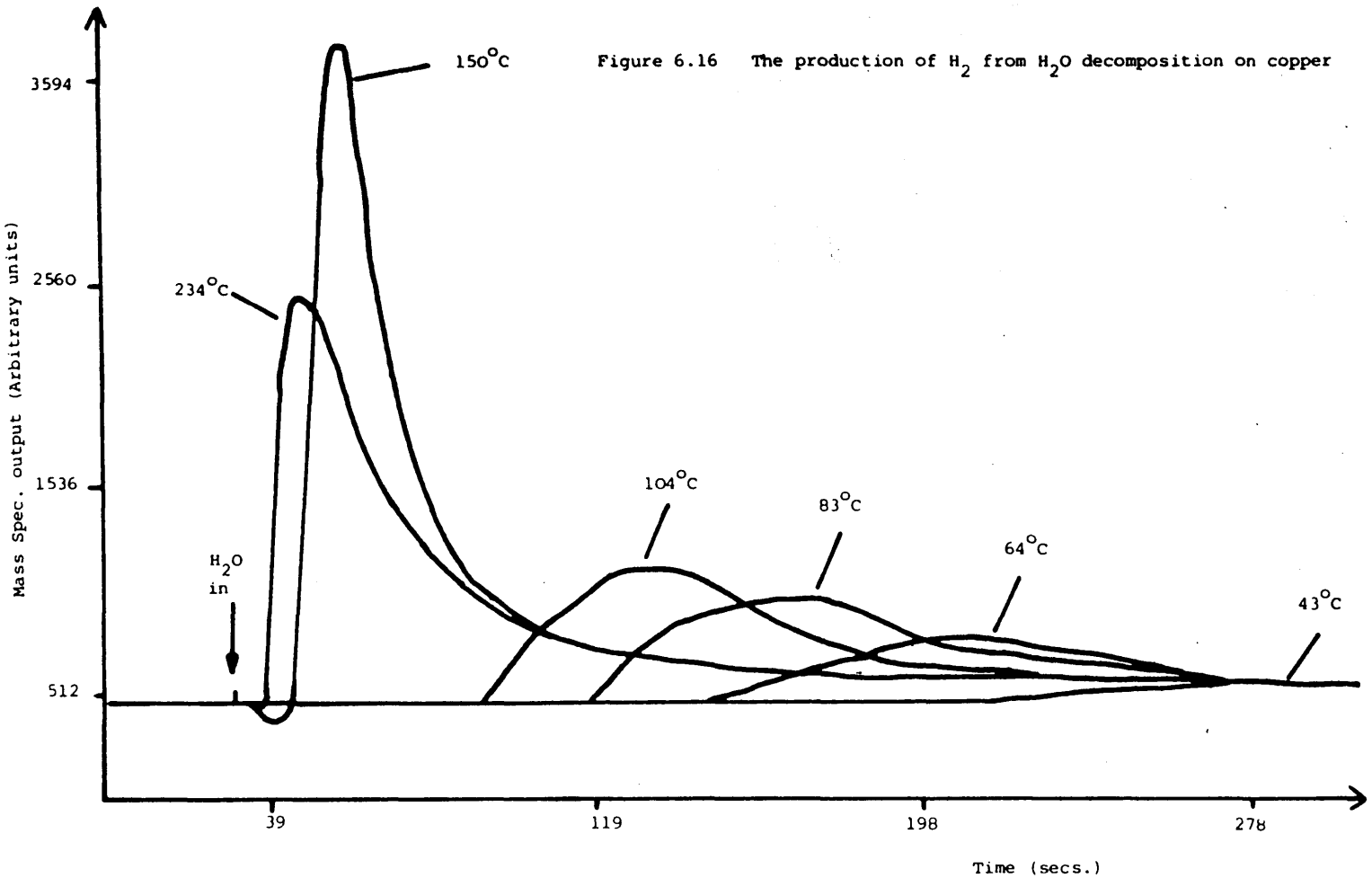

Figure 6.16 The production of H_2 from H_2O decomposition on copper

could be ascribed purely to the mass spectrometer water cracking fraction.

A full description of hydrogen evolution, at reaction temperatures between 24°C and 234°C is presented in Table 6.1. The quantity of hydrogen produced at each temperature is given as the oxygen coverage which should have acrued from the water decomposition process. These values were calculated relative to the maximum quantity of oxygen which could be produced on each surface by nitrous oxide decomposition at 60°C. At low temperatures, 'smearing' of the hydrogen pulse did not allow quantitative analysis of these features. While, at higher temperatures, maximum hydrogen production was observed at 150°C, which thereafter decreased slightly as the reaction temperature was increased to 234°C.

Table 6.1 also gives the quantity of oxygen titrated from the surface, by carbon monoxide reduction, at the end of each experiment. The surface oxygen coverages determined by this method showed little correlation with the quantity of hydrogen produced in each experiment.

The 0.016% oxygen impurity in the water-helium stream accounted for much of this inconsistency but a discrepancy was evident. For example, in reaction 7 the total quantity of adsorbed oxygen produced by hydrogen evolution and oxygen adsorption was expected to be 29% of a monolayer. Although, throughout the course of the experiment, hydrogen was continually eluted from the catalyst column, this quantity of hydrogen did not account for the 7% of a monolayer of oxygen which was extant on the copper surface.

Table 6.1 The Reactive Chemisorption of Water on Polycrystalline Copper

Reaction Number	Temp. (^{o}C)	Time in Flow (mins.)	Time of H_2 evolution (secs)[a]	Oxygen Coverage from H_2 evolution[b]	Total Oxygen Coverage[c] (%)	Oxygen Coverage from impurity (%)	Corrected Oxygen Coverage[d] (%)
1	24	22	-	-	51	31	20
2	43	10	340	-	33	14	19
3	52	10	230	-	28	14	14
4	64	14	160	-	21	20	1
5	83	10	125	4	28	14	14
6	104	10	90	5	28	14	14
7	150	15	32	8	36	21	15
8	234	15	21	7	>100	21	>100

a Time taken for peak maximum to be attained.

b Calculated as percentage of N_2O monolayer from yield of hydrogen desorbed.

c Calculated from subsequent CO titration, expressed as percentage of N_2O monolayer.

d CO titration values corrected for 0.016% oxygen impurity in feed gas, expressed as percentage of N_2O monolayer.

6.4.3 Temperature Programmed Desorption Following the Adsorption of Water on Polycrystalline Copper at 24°C

A 0.47% water-helium stream was flowed over a freshly reduced copper surface, for 22 minutes, at 24°C. Subsequent T.P.D. produced slight hydrogen desorption over a broad temperature range of 50°C - 160°C, while 1.39×10^{18} molecules of water desorbed from the surface at temperatures between 30°C and 160°C (Figure 6.17). This quantity corresponded to 10% of the maximum water uptake at ambient temperature.

6.4.4 The Thermodynamics of the Adsorption of Water, Accompanying its Decomposition, on Initially Clean Polycrystalline Copper

Gas adsorption chromatography (section 3.3.4.2) was used to determine the adsorption isotherms generated by the interaction of water with an initially fully reduced copper surface. Over the range of temperatures used in this study (43°C - 104°C) it was found that, following gas-surface equilibration in a 0.35% water-helium stream, a significant proportion of the adsorbed species only slowly desorbed from the copper surface in a helium flow. This fact, which was revealed by elongated tails on the desorption profiles, indicated the existence of strongly adsorbed water species. Adsorption isotherms (Fig. 6.18) were determined from the desorption profiles but, as a consequence of the elongated tails, little detail could be obtained in the low coverage range. This made an accurate determination of the isosteric heat of adsorption at these coverages impossible.

Figure 6.17 T.P.D. following the adsorption of H_2O on copper at 24°C

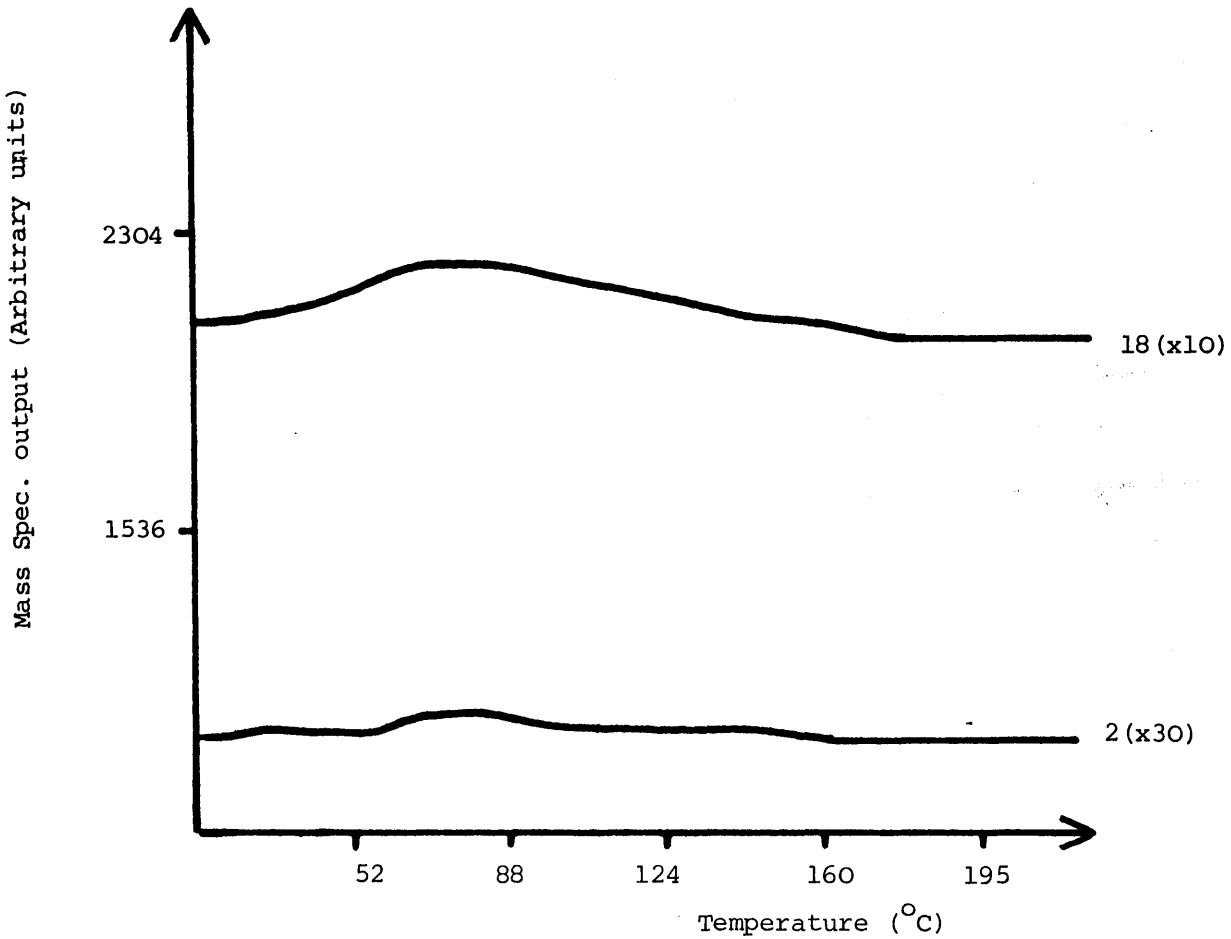

Figure 6.18 Isotherms for water adsorption on copper

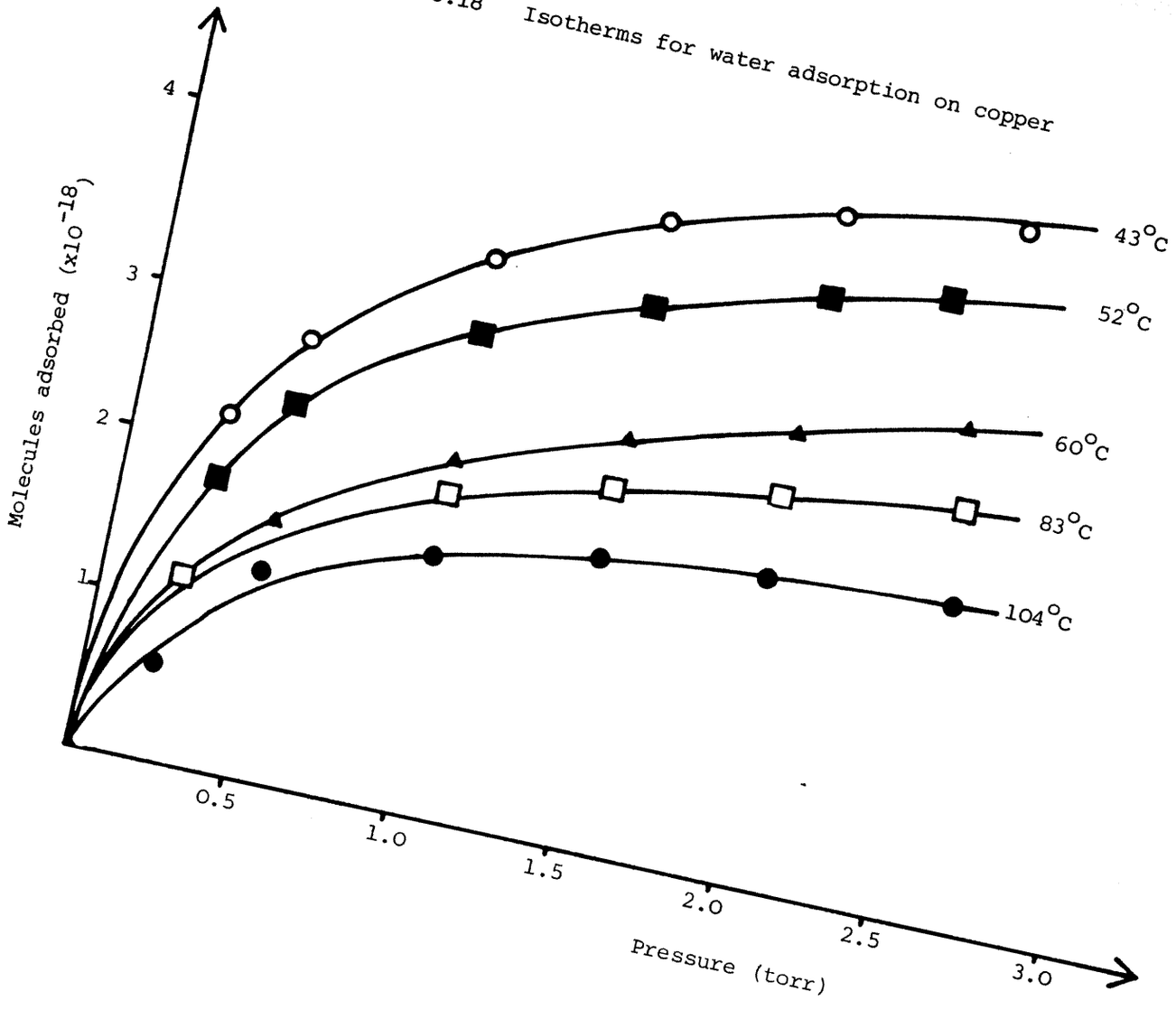

The Langmuir plots (Fig.6.19), calculated from the adsorption isotherms, show reasonable linearity at moderate-high ambient gas pressures. However, the monolayer adsorbate volumes, which were determined from the gradients of the plots, were not constant over the range of temperature used.

An estimation of the average heat of adsorption across the whole copper surface can be made from a knowledge of the fractional coverages of water, θ, at a variety of different temperatures and pressures. These coverages were calculated by dividing the total copper area of the catalyst by the total area occupied by adsorbed water molecules. For the purposes of this calculation the Van der Waals area of a water molecule was assumed to be $1.6 \times 10^{-19} m^2$. Substitution of the surface coverage, together with pressure and temperature data, into the Langmuir equation for non-dissociative adsorption gave the average heat of adsorption to be 45 KJ mol^{-1}.

6.5 TEMPERATURE PROGRAMMED REACTION OF CARBON MONOXIDE AND WATER ON POLYCRYSTALLINE COPPER

A 4.6% carbon monoxide-1.4% water-helium stream was flowed over a fully reduced copper surface, for 15 minutes, at 25°C (Fig. 6.20). Immediately on admission to the catalyst column (point A in Fig. 6.20), a negative deflection was noted in the carbon monoxide (m/e = 28) plot. This feature is indicative of the time to sweep out the dead volume of the catalyst bed and of adsorption on the copper surface. The water (m/e = 18) plot also showed a similar feature, although the time taken to achieve equilibrium in the water adsorption process indicated that this may have involved a significant activation energy.

Figure 6.19 Langmuir plots for water adsorption on copper

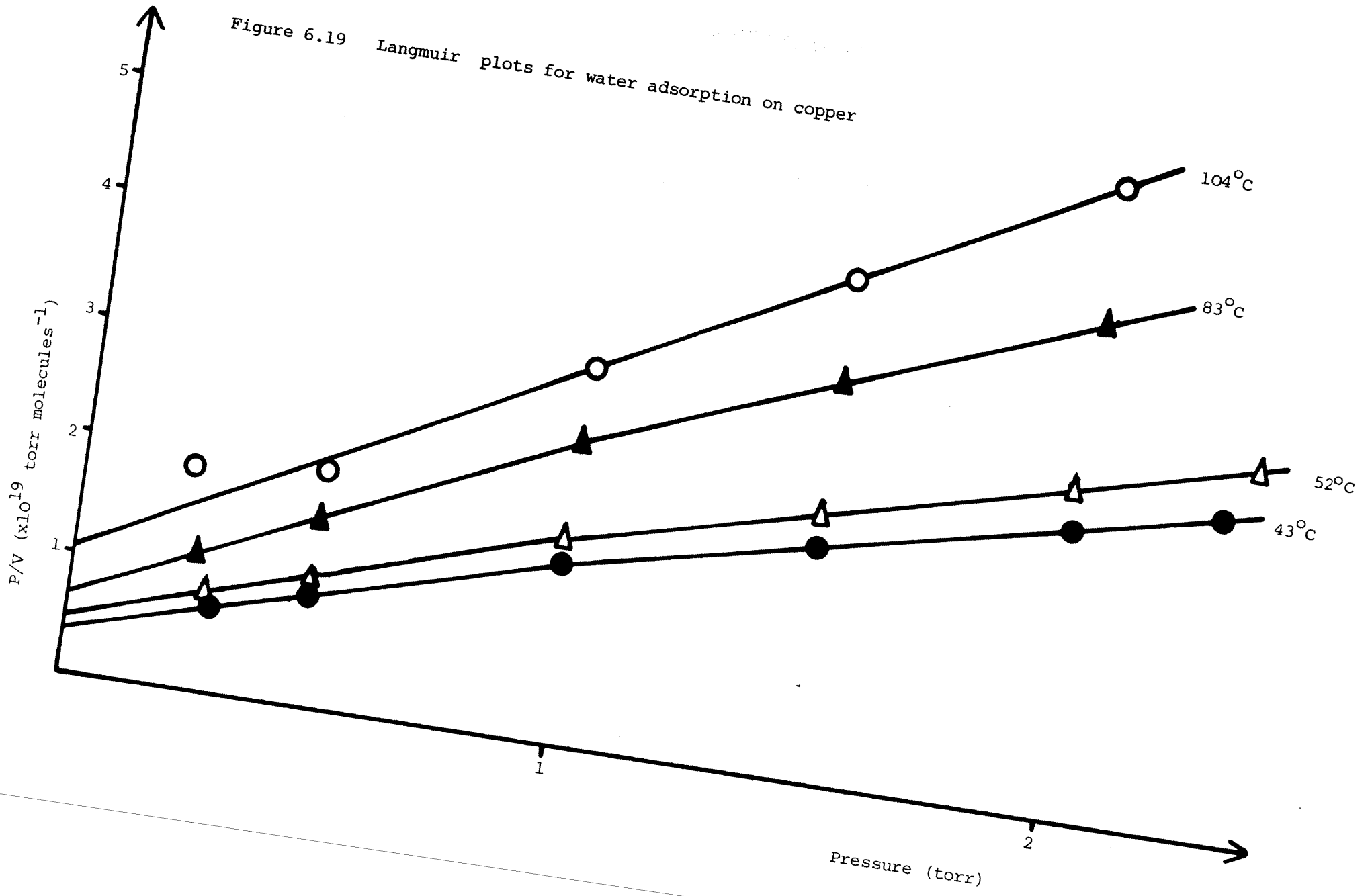

Figure 6.20 T.P.Rn. of CO and H_2O on copper

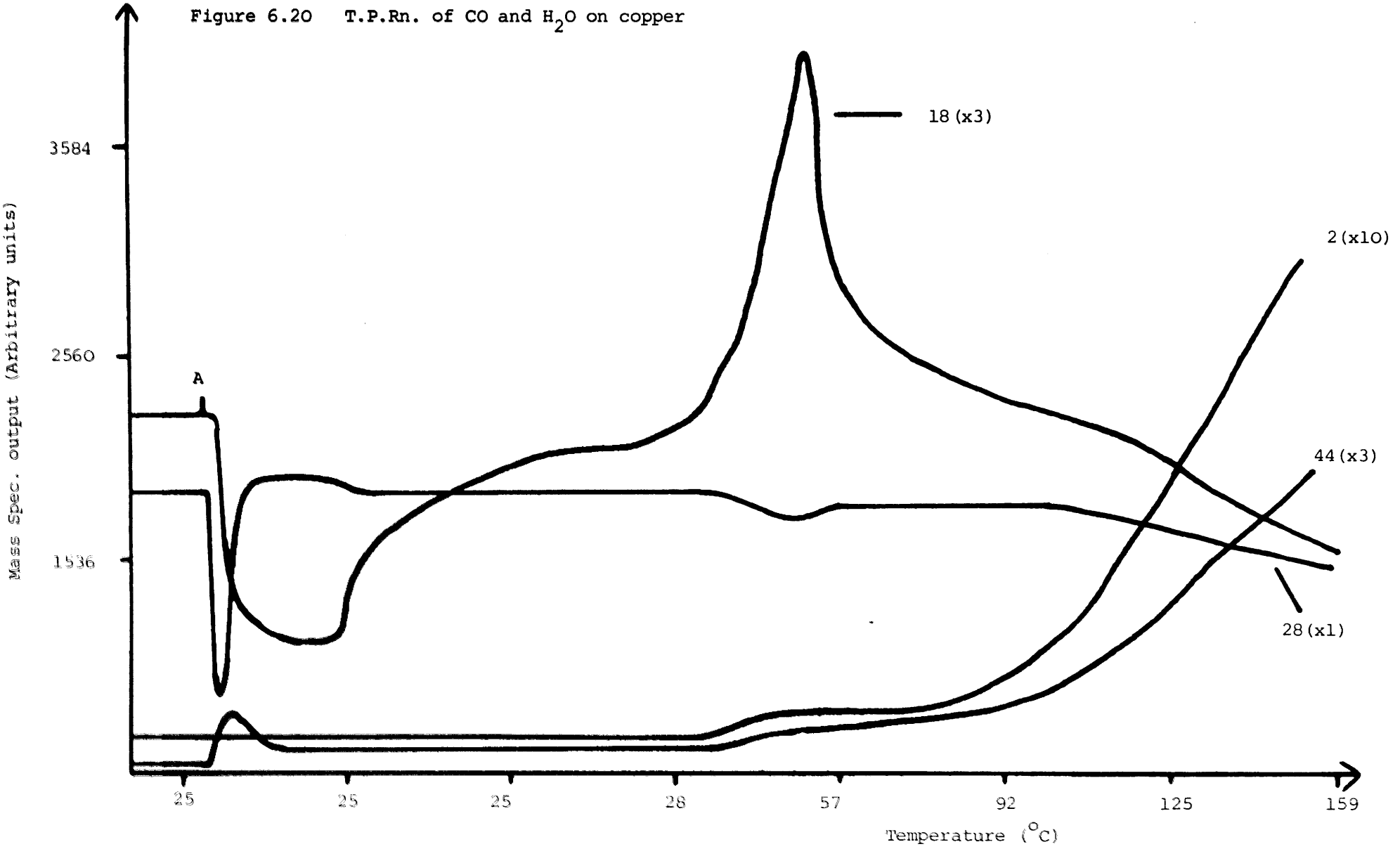

During the adsorption of water on to the copper surface, the carbon monoxide plot was found to be slightly greater than the reference value produced by flowing the reactant stream through the reactor by-pass. This positive deflection in the carbon monoxide plot can only be explained by assuming that adsorption of water on the copper surface displaced 13% of a monolayer of preadsorbed carbon monoxide from the adsorbent.

Figure 6.20 also clearly shows that, immediately the reactant mixture contacted the catalyst, a small quantity of carbon dioxide, corresponding to the removal of 4% of a monolayer of oxygen, was discharged from the catalyst column. No concomitant formation of gaseous hydrogen was detectable.

The temperature of the column was then raised, at a rate of 8 deg. min^{-1}, to a maximum temperature of $160^{o}C$. When heat was applied to the catalyst column gaseous hydrogen was instantly produced. Water desorption also occurred at moderately elevated temperatures while, at the same time, the negative deflection on the carbon monoxide plot indicated that 1.54×10^{18} carbon monoxide molecules (9% of a monolayer) had been adsorbed on to the copper surface.

At a temperature of $80^{o}C$-$90^{o}C$ the water gas shift reaction began to acrue a significant rate. At very low conversions (at which the concentration of both reacting species were considered invariant), analysis of the carbon dioxide and hydrogen line shapes gave an activation energy of 67-75 KJ mol^{-1} for the production of these species.

The catalyst column was then cooled to ambient temperature in the

carbon monoxide-water flow. After a brief helium flush the temperature of the column was raised, at 8 deg. min^{-1}, to 232°C. The desorption profile produced is detailed in Figure 6.21.

Water was found to desorb from the surface with a maximum rate at a temperature of 113°C. Hydrogen and carbon dioxide were found to desorb from the copper surface with a coincident T_p of 140°C.

6.6 THE REACTION OF CARBON MONOXIDE AND WATER ON POLYCRYSTALLINE COPPER AT 62°C

The reaction of a 4.48% carbon monoxide - 1.18% water-helium stream reached a steady state conversion of 2.7% after 2 minutes reaction, at 62°C, on a reduced copper sample. If all the exposed copper atoms are considered active in the reaction, the turnover frequency (T.O.F.) in the steady state region is found to be 2.78×10^{-4} molecules sec^{-1} $site^{-1}$. Before the attainment of the steady state conditions, a pulse of carbon dioxide was eluted from the catalyst column (Fig. 6.22), which was followed, after a further 48 seconds, by a similar hydrogen transient.

After 30 minutes reaction under these conditions, T.P.D. showed a broad water desorption with T_p = 73°C, a broad carbon dioxide desorption with T_p = 127°C and a slight hydrogen desorption in the temperature range 47°C - 108°C (Fig. 6.23).

6.7 TEMPERATURE PROGRAMMED REACTION OF NITROUS OXIDE AND HYDROGEN ON POLYCRYSTALLINE COPPER

A 8% nitrous oxide - 8% hydrogen-helium mixture was flowed over a reduced copper surface at 29°C. A large nitrogen transient was immediately observed indicating that, as expected, the copper surface

Figure 6.21 T.P.D. following CO/H_2O T.P.Rn.

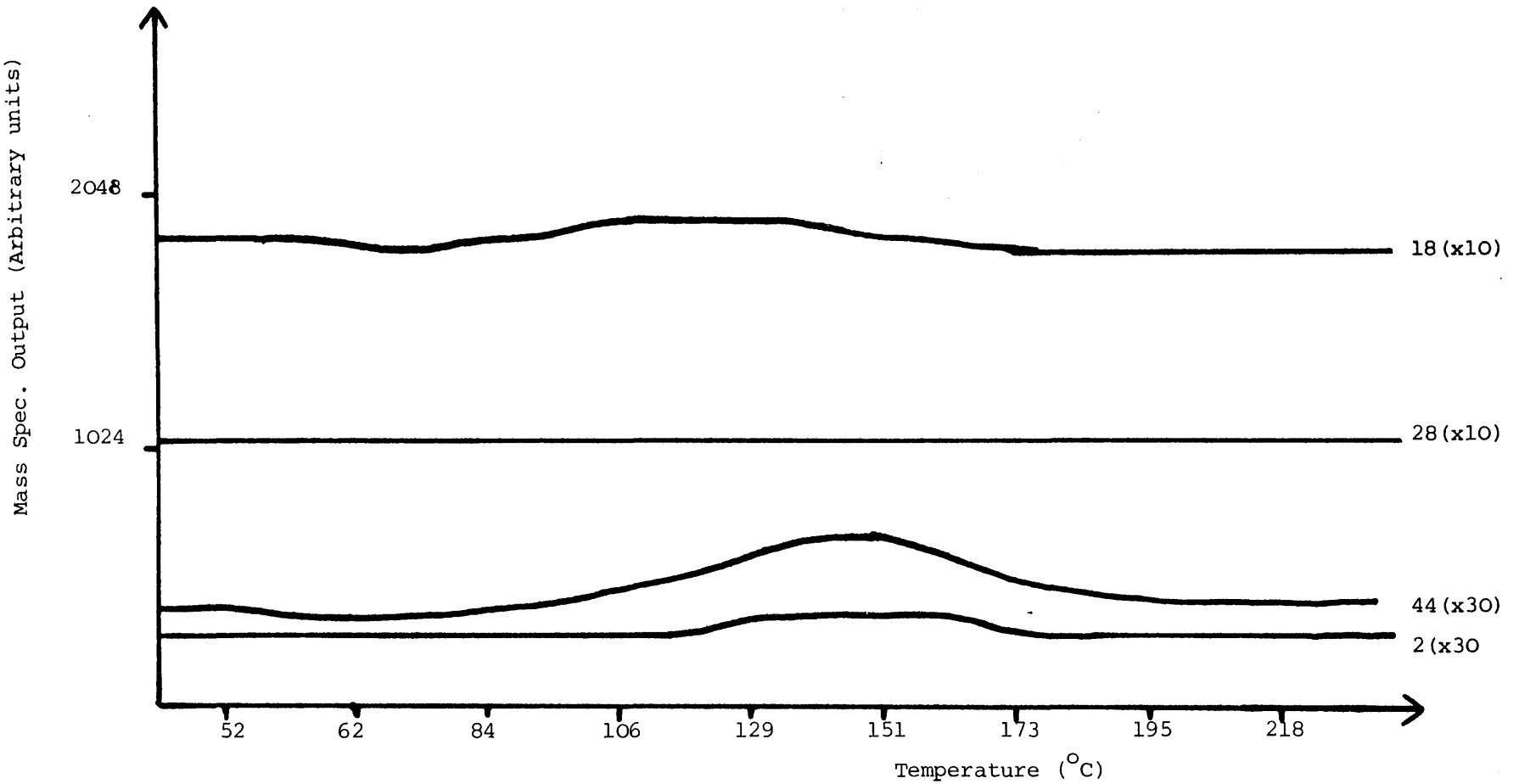

Figure 6.22 The shift reaction on copper at 62°C

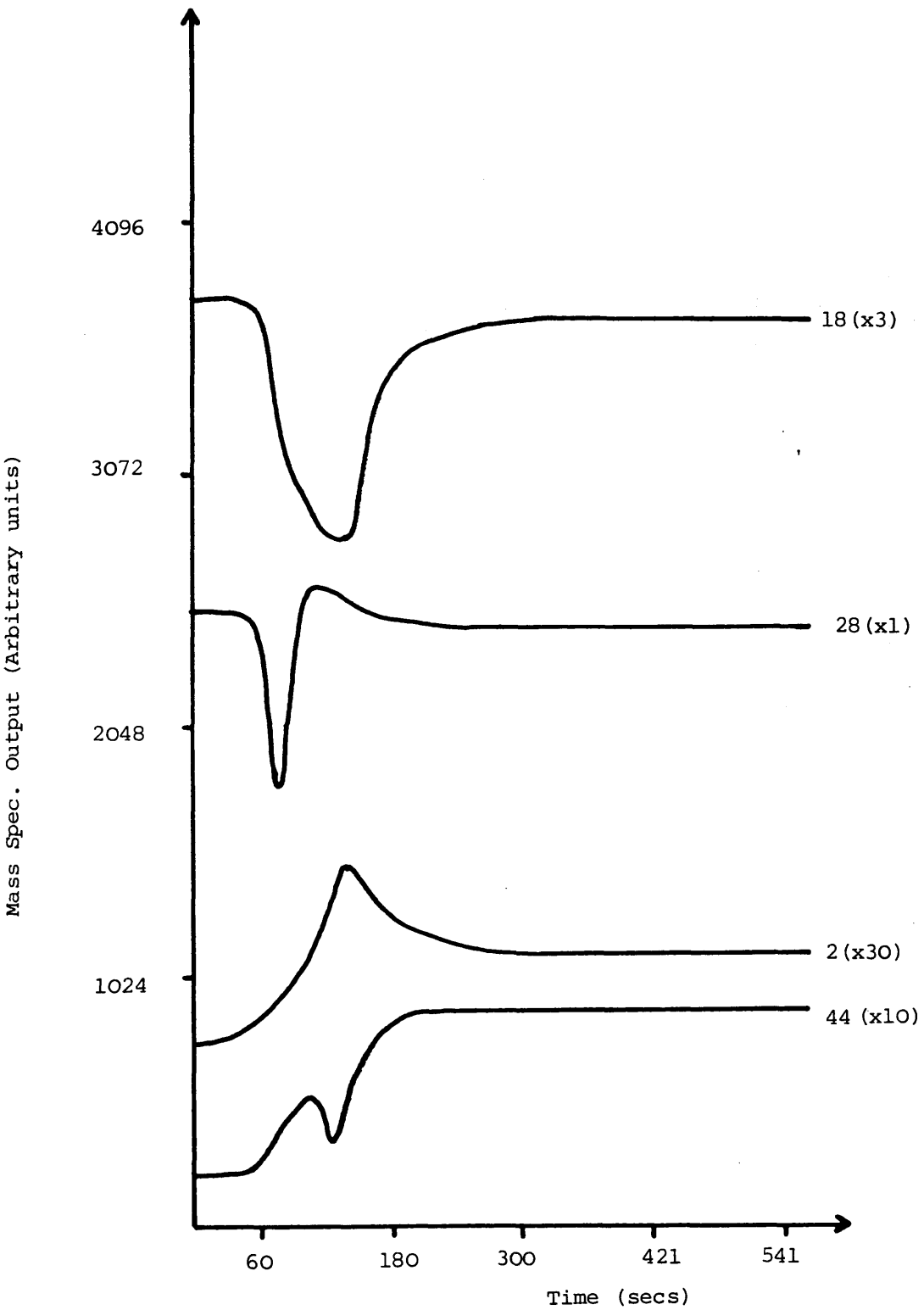

Figure 6.23 T.P.D. following CO/H_2O reaction on copper at $62^{\circ}C$

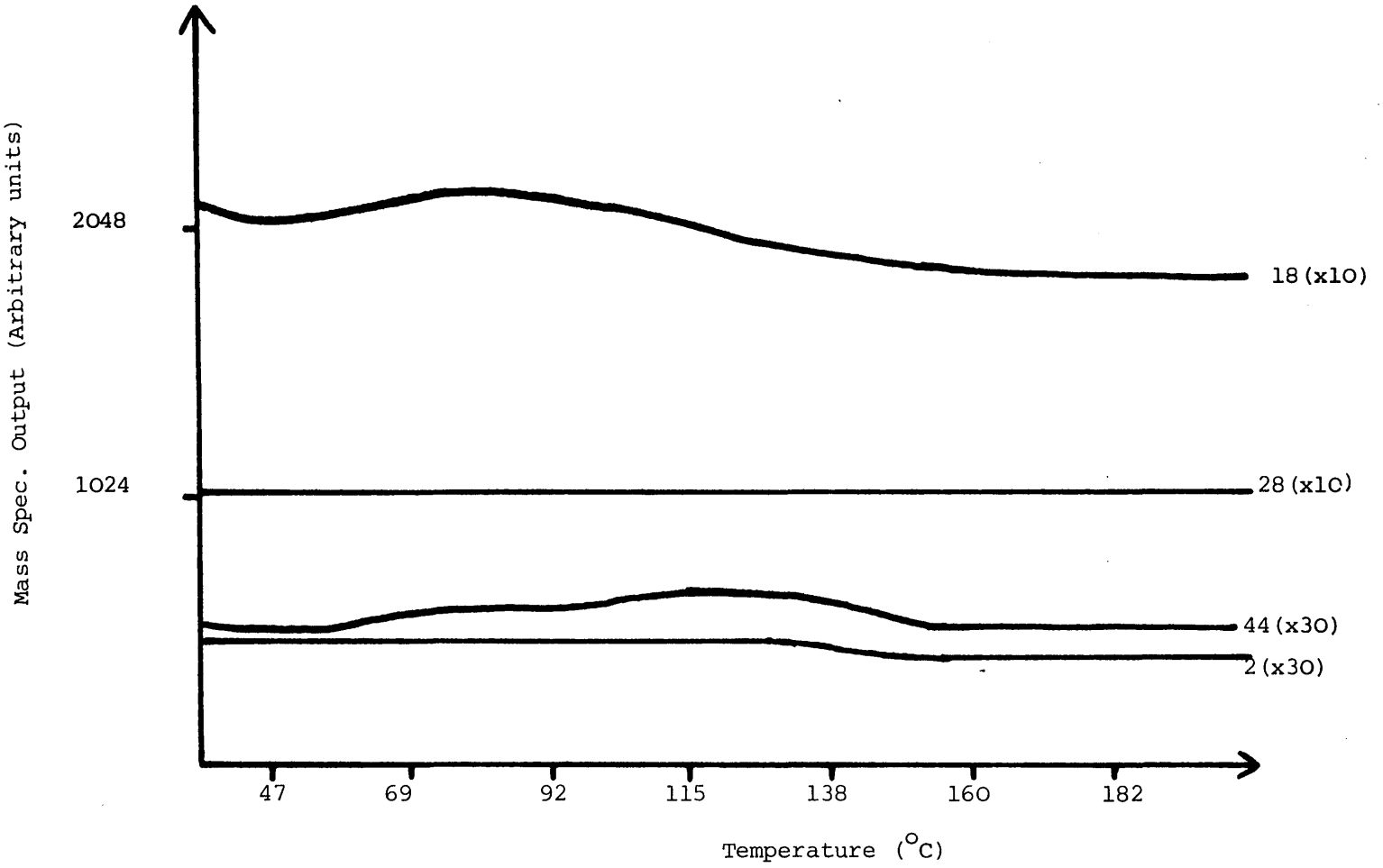

had become fully oxidised (θ = 0.5). The temperature of the catalytic column was then raised, at a rate of 8 deg. min^{-1}, from 29°C to 140°C (Fig. 6.24). The rates of water and nitrogen production were found to have the same temperature dependence and, from consideration of the respective leading edges, the activation energy of the hydrogen-nitrous oxide reaction was calculated to be 44 KJ mol^{-1}.

The onset of nitrogen production was not commensurate with that of water production. Indeed a delay time of 210 seconds, corresponding to the removal, by hydrogen, of 20% of the total oxygen coverage, was required before nitrous oxide decomposition occurred.

6.8 THE REACTION OF CARBON DIOXIDE AND HYDROGEN ON POLYCRYSTALLINE COPPER

6.8.1 The Reaction of Carbon Dioxide and Hydrogen on a Fully Oxidised Copper Surface

An 11% hydrogen - 11% carbon dioxide-helium stream was flowed over a fully oxidised copper surface for 10 minutes. The temperature of the column was 29°C. No gaseous species, apart from the carbon dioxide and hydrogen reactants, were eluted from the catalyst column during this period. Subsequent T.P.D. resulted in little hydrogen or carbon monoxide desorption (Fig. 6.25). Water desorption did occur over a wide temperature range (40°C - 160°C), while carbon dioxide was found to desorb with a maximum rate at a temperature of 66°C.

Figure 6.24 T.P.Rn. of H_2/N_2O on copper

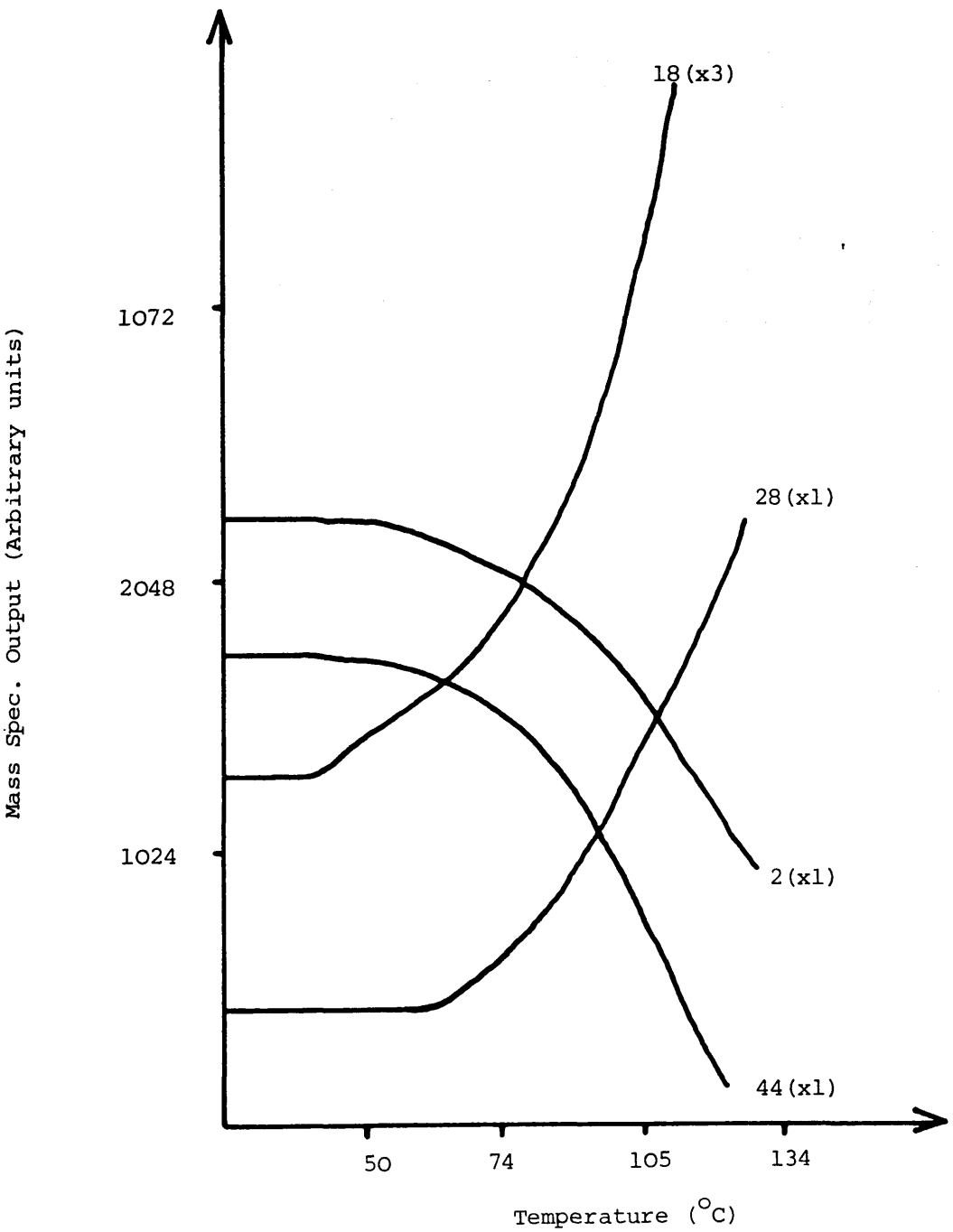

Figure 6.25 T.P.D. following CO_2/H_2 reaction on fully oxidised copper surface at 29°C

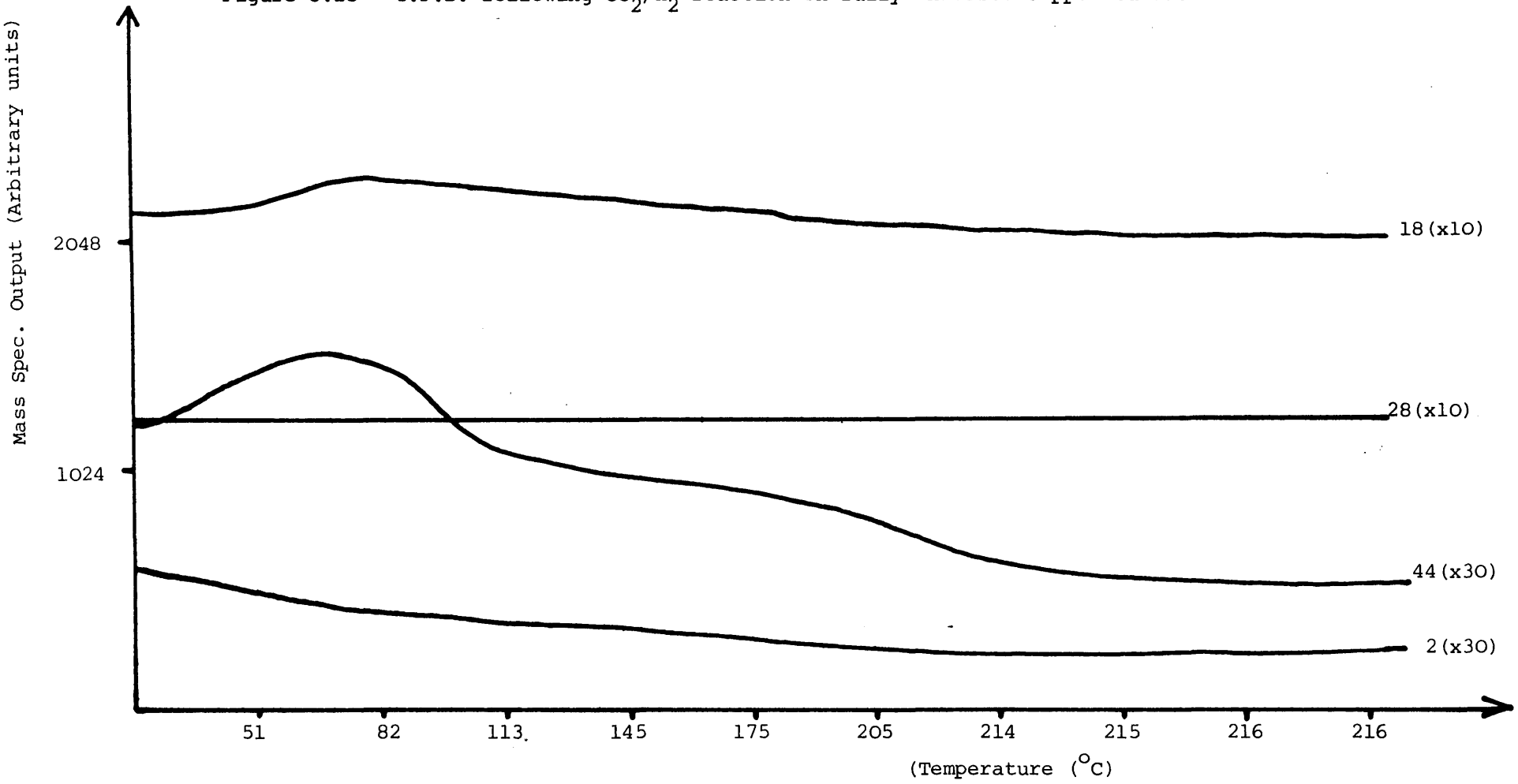

6.8.2 The Reaction of Carbon Dioxide and Hydrogen on Polycrystalline Copper at 32°C

A mixture of 8% hydrogen - 8% carbon dioxide-helium was flowed over a reduced copper surface, at 32°C, for 10 minutes. Analysis of the mixture eluted from the catalyst column during this period, revealed the presence of only the reactant species.

Three different species were found to desorb from the copper surface during subsequent T.P.D. (Fig. 6.26). Carbon monoxide desorbed at relatively low temperatures (T_p = 73°C), while hydrogen and carbon dioxide showed coincident maximum desorption rates at a temperature of 151°C. No water desorption was observed.

6.8.3 Temperature Programmed Reaction of Carbon Dioxide and Hydrogen on Polycrystalline Copper

A 25 ml min^{-1} stream of 9% carbon dioxide - 12% hydrogen-helium was flowed over a reduced copper sample, for 10 minutes, at ambient temperature. Without disturbing the gas flow, the temperature of the column was then raised, at a rate of 8 deg. min^{-1}, to 228°C. The temperature programmed reaction profile generated by this procedure is shown in Figure 6.27.

Carbon monoxide was liberated in two distinct temperature ranges. The first, at relatively low temperatures, produced a finite quantity of carbon monoxide (2.23×10^{18} molecules). Analysis of the carbon monoxide leading edge gave an activation energy of 130 KJ mol^{-1} for this process. Carbon monoxide production resumed at a temperature of 172°C and thereafter increased exponentially with temperature (E_A = 113 KJ mol^{-1}).

Figure 6.26 T.P.D. following CO_2/H_2 reaction on copper at 32°C

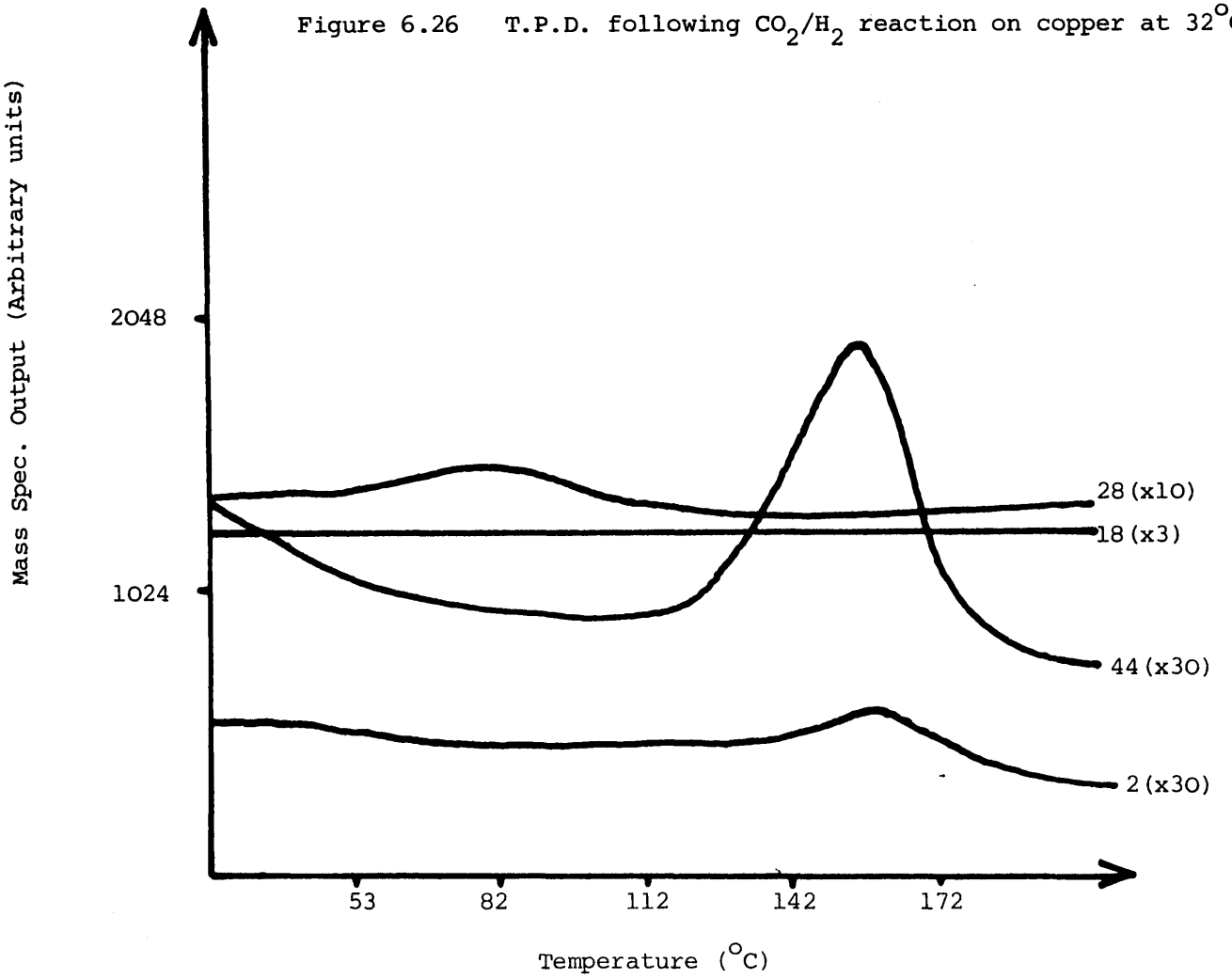

Figure 6.27 T.P.Rn. of CO_2/H_2 on copper

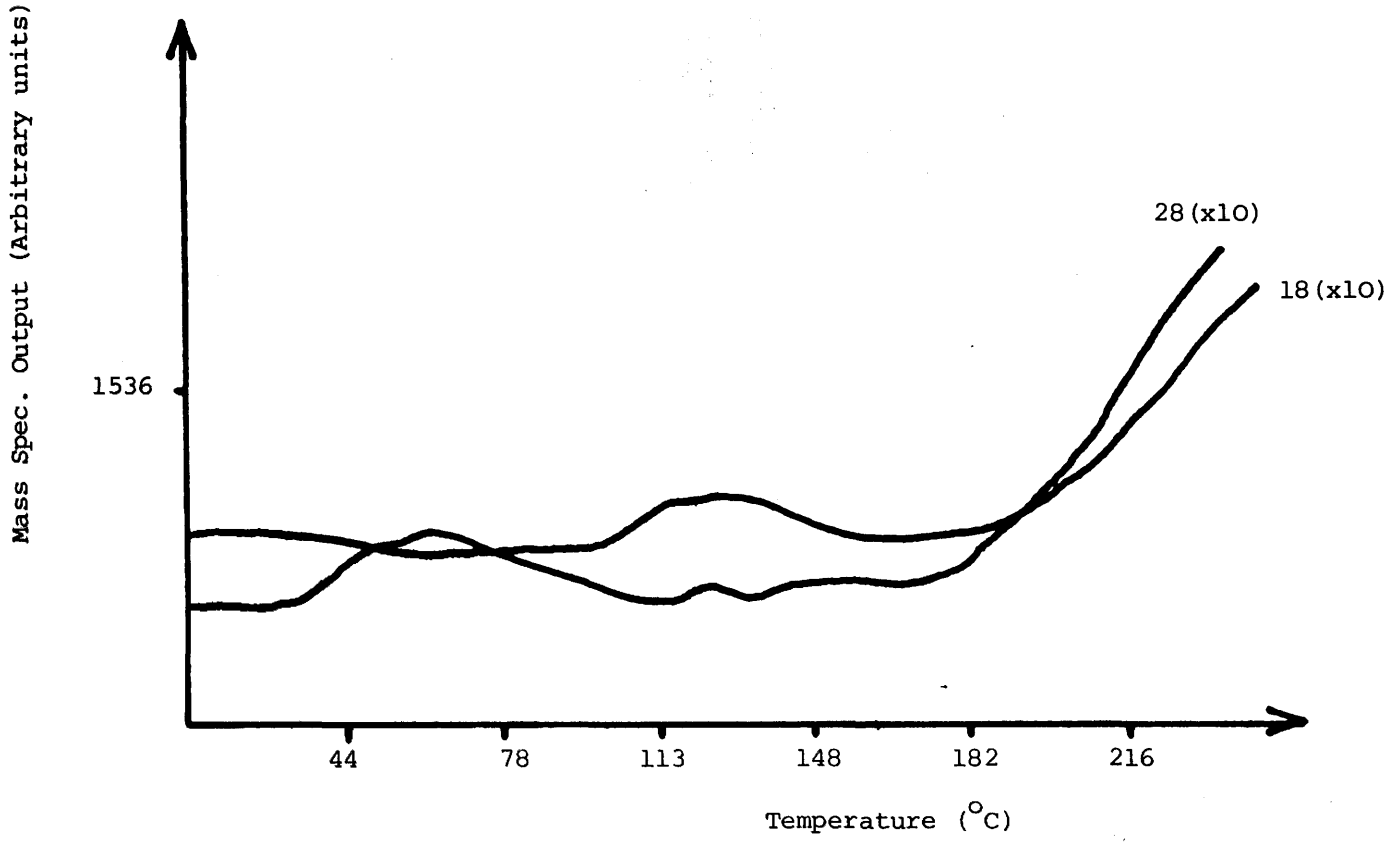

A similar pattern was observed for water production. A total of 1.1×10^{18} molecules of water were produced in the temperature range of $100^{\circ}C$ - $140^{\circ}C$. The activation energy of this process was 50 KJ mol^{-1}. When water production resumed at $188^{\circ}C$, the activation energy for the production of gaseous water vapour was calculated to be 113 KJ mol^{-1}.

The catalyst was then cooled to ambient temperature and T.P.D. carried out (Fig. 6.28). Hydrogen and carbon dioxide were both found to desorb from the copper surface with a maximum rate at $151^{\circ}C$. The activation energy for these desorptions was calculated to be 92 KJ mol^{-1}. Carbon monoxide was also desorbed from the surface at temperatures below $100^{\circ}C$.

6.9 THE ADSORPTION OF CARBON DIOXIDE ON PARTIALLY OXIDISED POLYCRYSTALLINE COPPER (OXYGEN CHEMISORPTION)

A copper sample, which had been fully reduced as described previously (section 3.3.4.1), was cooled to ambient temperature in a stream of helium. This flow was then diverted through the column by-pass for a period of 30 minutes. On readmission of the helium stream to the catalyst column, 3.11×10^{17} nitrogen molecules were eluted from the previously closed system. It was apparent that the flow switching procedure had allowed air to flood the catalyst column. This quantity of air could have allowed a maximum of 2% of an oxygen monolayer to be created on the copper surface.

A stream of 8% carbon dioxide-helium was flowed over this surface for 15 minutes. Subsequent T.P.D. revealed the presence of carbon monoxide ($T_p = 95^{\circ}C$) and carbon dioxide, which desorbed from the surface at a temperature of $87^{\circ}C$ (Fig. 6.29).

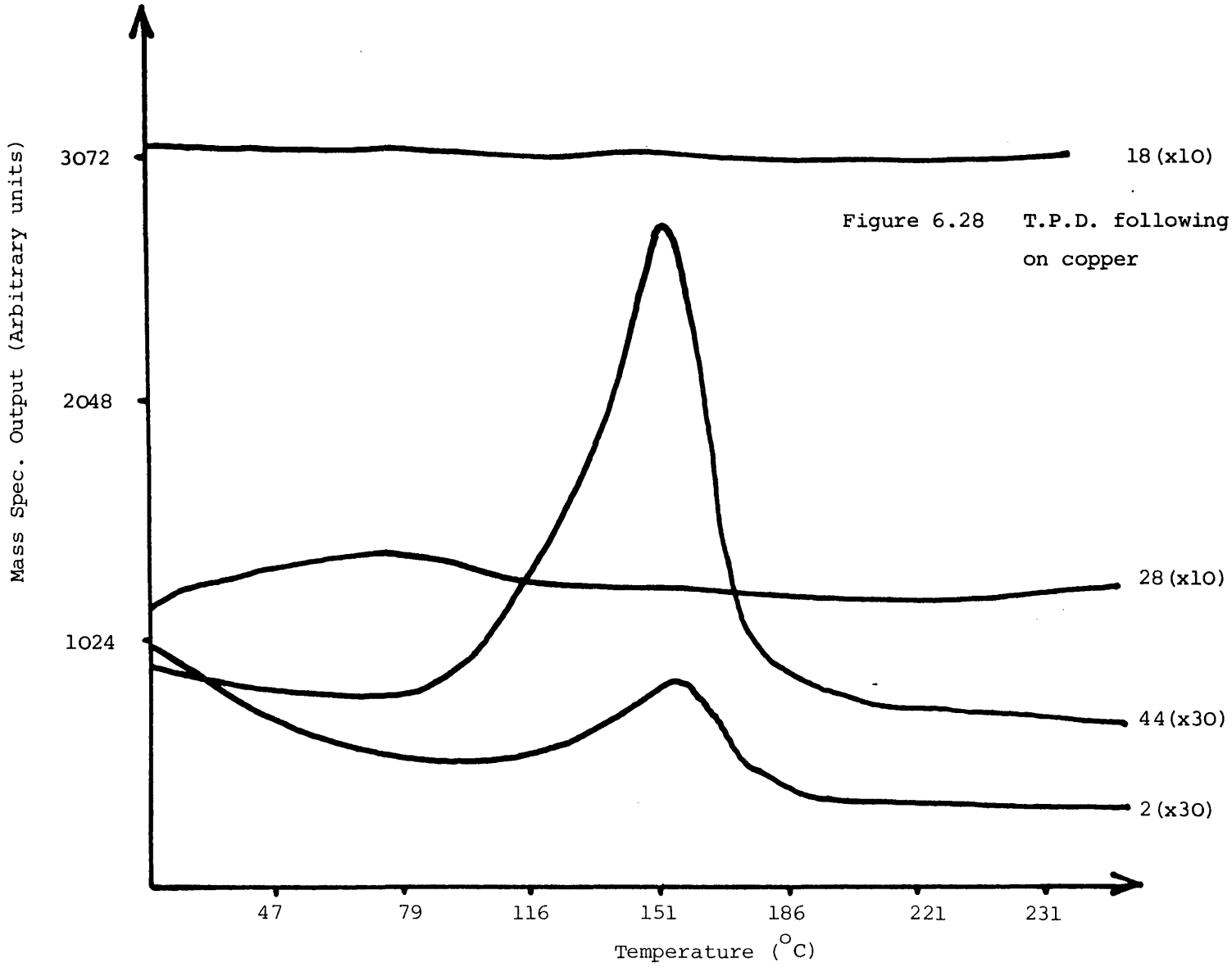

Figure 6.28 T.P.D. following T.P.Rn. of CO_2/H_2 on copper

Figure 6.29 T.P.D. following CO_2 adsorption on copper surface pretreated with O_2

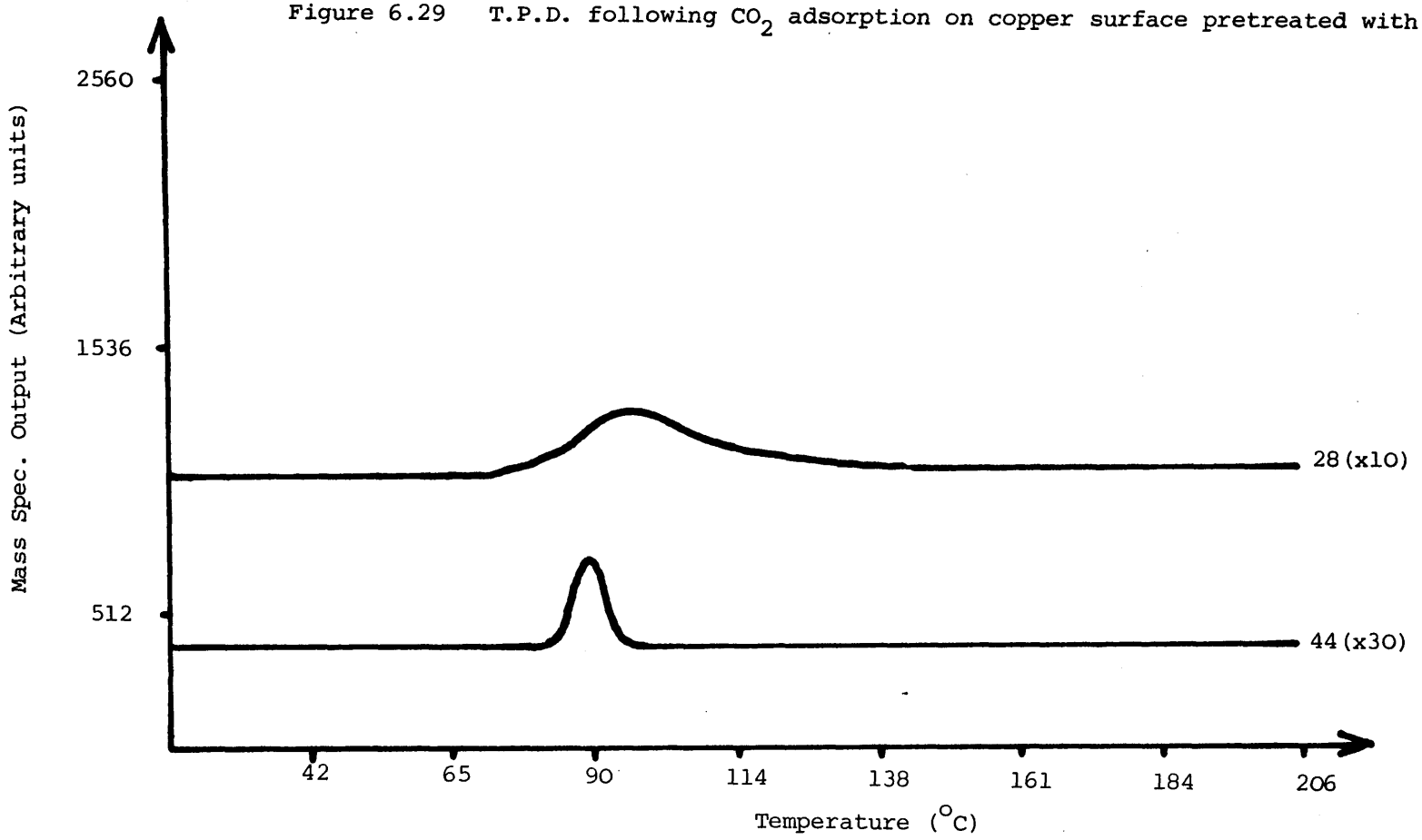

6.10 REACTION BLANKS

The catalyst column (section 3.3.1.2), which contained the copper catalyst, was removed from the flow system (3.3.1) and thoroughly cleaned. A 5 cm bed of glass beads was fixed in the centre of the stainless steel column and secured by two plugs of glass wool. The column was replaced into the flow system and a stream of 6% carbon monoxide-helium passed through the column, while the temperature was raised to 220^{o}C. This reduction procedure generated no carbon dioxide.

Separate flows of carbon dioxide, water and carbon monoxide were then admitted to the column over a range of temperatures. At no point during these flow studies was any material, other than the reactant gas, eluted from the catalyst column. T.P.D. revealed that the stainless steel and glass surfaces did not allow adsorption and/or decomposition of carbon dioxide, water or carbon monoxide.

CHAPTER 7

DISCUSSION

DISCUSSION

7.1 The Copper Surface

It would be scientifically unsound to embark on a discussion concerning the adsorptive properties of polycrystalline copper without giving some consideration to the role that surface, or sub-surface, impurities may play in modifying the adsorption characteristics of pure copper metal. The copper oxide precursor utilised in these studies has been described previously (Section 3.2.6.1) and would be considered by many surface scientists as a 'dirty' material. Upon reduction, segregation of a variety of trace metal impurities must be considered as a feasible possibility. Unfortunately the extent of this segregation mechanism remains unclear, since no *in situ* surface analysis of the reduced adsorbent was possible. However, the generation of 50% of a monolayer of undesirable material on a reduced copper substrate, which is calculated to be the maximum possible impurity level (Section 3.2.6.1), appears rather unlikely, simply due to the close similarity of many of the results obtained from this copper adsorbent and those produced by adsorption on scrupulously clean metal surfaces.

In contrast to these ill-defined poisoning or promotional effects, a quantitative analysis of the extent of oxygen availability on the reduced adsorbents was accomplished. It was clear that a fully reduced copper surface could only be obtained by a combination of hydrogen *and* carbon monoxide reductions. These successive treatments were performed on all samples used in the flow-microreactor system and hence these copper surfaces can be considered as, initially, 100% metallic copper. However, the copper samples prepared in the reaction

vessel of the high vacuum apparatus could be subjected to a 'hydrogen-only' reduction and are all likely to have retained a few percent of a monolayer of oxygen.

7.2 The Adsorption of Carbon Monoxide on Polycrystalline Copper

The main points of the experimental observations described in sections 5.1.1, 5.1.2, 5.2.6.1 and 6.1 can be summarised as follows:

Carbon monoxide adsorbed on polycrystalline copper in two distinct forms. The bulk of the adsorbate was resident with a heat of adsorption of ca. 43KJ mol^{-1}, while a few percent of a monolayer of a far more strongly adsorbed species was also evident. No evidence for carbon monoxide decomposition was obtained. The interaction of carbon monoxide with oxidised copper generated carbon dioxide and a small quantity of a strongly adsorbed surface species.

Gaseous carbon monoxide interacts with polycrystalline copper in a manner which fits, almost perfectly, the Langmuir treatise of adsorption. The isotherm generated by this adsorption process (Fig. 5.1) gives a perfect straight line plot when linearised with respect to the Langmuir equation (Fig. 5.2). The data extracted from these plots gives saturation coverage as corresponding to 92% of a carbon monoxide monolayer (section 5.1.1.1). The fact that the calculated monolayer adsorbed volume, V_m, is not obtained on the copper surface may indicate the presence of bridge-bonded carbon monoxide species. The adsorption of these species, which are known to exist on copper surfaces [49], involves an interaction with two copper atoms and will therefore reduce the total number of sites available for linear carbon monoxide bonding.

The effect of evacuation on a carbon monoxide saturated surface was to remove 98% of the adsorbed species. The residence time of the 2% of the material retained on the surface (>15 minutes at 10^{-4} torr) allows the activation energy of desorption of these species to be calculated as ca. 90 KJ mol^{-1}, by substitution into the Frenkel equation. This is confirmed by the radiotracer T.P.D. study of this particular system which, following the adsorption of carbon monoxide on a copper sample at 220°C, showed radiolabelled desorption from near ambient temperature to 110°C (Fig. 5.34). This corresponds to a range of activation energies of desorption of 80-105 KJ mol^{-1}. However, the calculated average heat of adsorption across the whole surface was found to be only 43 KJ mol^{-1}, which gives good evidence for a polycrystalline surface which appears heterogeneous with respect to carbon monoxide adsorption. It should be stressed that this calculated value of the average heat of carbon monoxide adsorption, as with all other calculated heats quoted in this discussion, was obtained by inserting data into a simplified form of the Langmuir equation (section 5.1.1.1). In order to facilitate these calculations, the ratio of adsorption and desorption rate constants was considered as unity, thereby allowing the adsorption-desorption equilibrium constant in the Langmuir equation to be expressed as $\exp\left(\frac{\Delta H}{RT}\right)$.

The fact that two broadly different forms of adsorbed carbon monoxide exist on a polycrystalline copper surface is clearly shown by a molecular exchange experiment (section 5.1.1.2). While the bulk of adsorbed carbon monoxide (88%) underwent a facile exchange process, a small fraction (12%) was found to be far less labile. In summary,

the bulk of the carbon monoxide species associated, by adsorption, with a polycrystalline copper surface, are resident with a heat of adsorption of ca. 43 KJ mol^{-1}. This is similar to that found in a variety of other studies e.g. 39 KJ mol^{-1} on evaporated films [4], 50 KJ mol^{-1} on polycrystalline samples [56] and 50 KJ mol^{-1} on a Cu(111) single crystal [52]. A few percent of a monolayer of carbon monoxide is, however, far more strongly bound on the polycrystalline surface. The heat of adsorption of these species can be as high as 105 KJ mol^{-1}. This value is similar to that found by Joyner et al. [35], following carbon monoxide adsorption on a Cu(100) single crystal at 22°C. Beebe and Wildner [58] determined heats of adsorption as high as 85 KJ mol^{-1} on polycrystalline samples, while Kleir [59] also found a small fraction of adsorbed carbon monoxide resistant to evacuation.

The radiotracer desorption analysis described above does not give definitive proof that the desorbing radiolabelled material was [14-C]carbon monoxide. (This technique cannot distinguish chemically unique [14-C]labelled species). However, direct comparison of this experiment with that described in section 6.1, in which mass spectrometry was used to detect thermal desorption products,proves that the desorbing radiolabelled material was indeed carbon monoxide. Subsequent to the adsorption of carbon monoxide on the copper sample, only carbon monoxide was found to desorb from the copper surface (Fig. 6.1). The lack of any desorbing carbon dioxide, which could have formed via the Boudouard reaction ($2CO \rightarrow C + CO_2$),effectively rules out the possibility that any dissociative carbon monoxide adsorption had occurred. It is interesting to note that a quantitative

analysis of this desorption study showed that 7% of a carbon monoxide monolayer was irreversibly adsorbed on the polycrystalline surface. This is rather more than that observed in the direct monitoring analysis and may be explained, in terms of a site blocking mechanism, by a few percent of an oxygen monolayer, on the 'hydrogen-only' reduced copper samples. Since no carbon dioxide was found in the gas phase of the reaction vessel at any time during the room temperature adsorption of carbon monoxide on these copper samples, it is evident that this oxygen species was not readily removed from the surface to the gas phase. This does not however rule out the possibility of a carbon monoxide-adsorbed oxygen interaction.

Figure 5.19 details the adsorption isotherm produced by the interaction of [14-C]carbon monoxide with a 50% surface oxidised polycrystalline copper sample. This isotherm is distinctly different to that produced by carbon monoxide adsorption on a reduced copper sample and, therefore, indicates a modification of the adsorption process by the pre-adsorbed oxygen. The removal of oxygen from the surface by carbon monoxide [87,96], and coincident adsorption site creation, is the likely cause of the distinctive slope associated with this adsorption isotherm. This feature is apparently characteristic of a carbon monoxide-adsorbed oxygen interaction [147,148].

The direct interaction of carbon monoxide with adsorbed oxygen, or a long range effect of the adsorbed oxygen species, causes the estimated average heat of adsorption of carbon monoxide to fall from ca.43 KJ mol^{-1}, on the reduced copper, to ca. 38 KJ mol^{-1} on the oxidised surface (section 5.2.1). A direct interaction of carbon

monoxide and oxygen, possibly leading to carbonate formation [47], may be the cause of the increased portion (5.5%) of the irreversibly bound radiolabel on these partially oxidised samples (section 5.2.1).

7.3 The Adsorption of Carbon Monoxide on a Copper-Alumina Catalyst

The adsorption of carbon monoxide on a sample of reduced copper-alumina catalyst showed very similar behaviour to that observed on reduced copper powders. In general, Langmuir -type adsorption isotherms were observed (Fig. 5.28) and the average heat of adsorption across the whole surface was estimated to be ca.45 KJ mol^{-1}. This behaviour is not surprising, since it has previously been shown that carbon monoxide effects no interaction with the alumina component of this catalyst [148]. The slight increase in the average heat of adsorption, and the correspondingly increased fraction of irreversibly adsorbed material (section 5.4.1.1), as compared to the reduced copper powder, can therefore be attributed to slightly differing percentages of the various exposed crystalline faces, on these structurally dissimilar surfaces.

7.4 The Adsorption of Carbon Dioxide on Polycrystalline Copper

The main points of the experimental observations described in sections 5.1.2, 5.2.2, 5.3.1, 5.5.1, 5.6.2.2 and 6.3 can be summarised as follows:

Carbon dioxide was found to chemisorb on the copper surfaces used in this study. This involved, at least in part, a decomposition of molecularly adsorbed carbon dioxide which led to the formation of

carbon monoxide and adsorbed oxygen. This reaction was promoted under conditions of relatively low temperature. The production of oxygen, by carbon dioxide decomposition, allowed both low and high energy forms of molecularly adsorbed carbon dioxide to exist on the copper surface. Preadsorption of oxygen considerably modified the adsorbed state of carbon dioxide.

A number of studies have proposed that the interaction of gaseous carbon dioxide with copper metal produces a non-perturbed, physically adsorbed, carbon dioxide moiety (31,33,56). It has also been suggested that carbon dioxide will not interact, in any manner, with metallic copper surfaces [85,86]. However, direct monitoring of a [14-C]carbon dioxide-polycrystalline copper system produces an adsorption isotherm (Fig. 5.11) which proves, beyond all reasonable doubt, that substantial carbon dioxide chemisorption takes place on the polycrystalline copper sample.

Perhaps not surprisingly, considering the apparent time dependency of this adsorption process (Section 5.1.2.1), the Langmuir plot, derived from the adsorption isotherm (Fig. 5.12), is not linear over the full range of surface coverages. However, at medium-high coverages, the average heat of carbon dioxide chemisorption appears to lie between 36 and 40 KJ mol^{-1}. The substantial deviation of the low coverage points from the best-fit plots does indicate that a number of copper sites, or ensembles, exist which allow a far higher heat of chemisorption. This becomes obvious when a carbon dioxide covered copper sample is subjected to a brief evacuation. On average, 20% of the adsorbed radiolabel is resistant to vacuum pumping. The bulk of this material is found to desorb from the copper surface only when the temperature is

raised to at least 60°C (Fig. 5.35). Desorption is not complete until far higher temperatures (120°C) are attained.

To explain these adsorption-desorption features in terms of a simple carbon dioxide-metallic copper interaction would, however, be rather simplistic. As previously discussed, the presence, and effect, of a few percent of a monolayer of oxygen on these copper samples cannot be ignored. Further complicating features arise when data obtained from use of the internal flow proportional counter is considered (section 5.5.1). This reveals that, at elevated temperatures (250°C), the interaction of carbon dioxide with copper produces a small, but significant, quantity of gaseous carbon monoxide. The fact that relatively high temperatures are required to produce gaseous carbon monoxide may imply a significant activation energy for the carbon dioxide decomposition process. Alternatively, the production of gas phase carbon monoxide may be limited by a significant activation energy of desorption of the adsorbed carbon monoxide species. It is, therefore, entirely possible that, even at ambient temperature, carbon dioxide, by its own adsorption process, renders any discussion of carbon dioxide-metallic copper interactions completely irrelevant.

Clearly it is important to attempt to separate the potentially modifying role of oxygen in this system from those adsorption characteristics ascribable to oxygen-free copper adsorbents. There is ample evidence to suggest that the presence of adsorbed oxygen, from any source, does modify the adsorption characteristics of carbon dioxide [87,115,116]. Indeed, it has been determined that

partial oxidation of a copper surface effectively doubles the quantity of adsorbed radiolabel which remains resistant to a brief evacuation procedure (section 5.2.2). The Langmuir plot (Fig. 5.21), constructed from the isotherm produced by the adsorption of carbon dioxide on to this 50% oxidised copper surface (Fig. 5.20), shows excellent linearity (except at very low surface coverages), in complete contrast to that derived from the carbon dioxide-reduced copper interaction (Fig. 5.12).

A dissociative carbon dioxide chemisorption would destroy the linearity of these plots and it is therefore possible that the straight line plot obtained from the partially oxidised surface is generated because of oxygen poisoning of many of the metallic ensembles which facilitated the dissociative mechanism. This is confirmed by reference to Figs. 6.10 and 6.4 which show the desorption products eluted from a fully oxidised copper surface subsequent to the adsorption of carbon dioxide, at ambient temperature, in both static and flow reaction systems. No carbon monoxide desorption is evident, while carbon dioxide exists on the oxidised surface in a variety of molecular states which desorb from the surface over a continuous broad range of temperatures ($30^{o}C$ - $160^{o}C$). Fig. 6.4 shows that maximum desorption rates were reached at temperatures of 54, 128 and $172^{o}C$, corresponding to desorption activation energies of 88, 109 and 124 KJ mol^{-1}. These values are in close agreement with previously published desorption data by Chinchen *et al.* [115].

This wide range of adsorbed carbon dioxide species fully accounts for the large quantities of irreversibly adsorbed carbon dioxide (32% of all adsorbates), which the direct monitoring

technique reveals as being produced on contact of [14-C]carbon dioxide with a completely oxidised copper surface (section 5.3.1(b)). This particular oxidised surface was generated by the reaction of a copper sample with an excess quantity of nitrous oxide, for 15 minutes, at 40°C, which is similar to the oxidation procedure used in the flow-microreactor system (section 3.3.4.3). However, if an excess quantity of nitrous oxide was allowed to interact with the copper sample for 14 hours at 80°C, the adsorption characteristics of the radiolabelled carbon dioxide were drastically modified (section 5.3.1(a)). Analysis of the associated adsorption isotherm (Fig. 5.25) revealed a very limited carbon dioxide adsorption on this oxidised copper, while subsequent exposure to vacuum pumping removed 95% of the adsorbed material. It is obvious that, in complete contrast to the copper samples used in the experiments described in section 5.3.1(b), and in the flow-microreactor system (section 6.3.2.1), irreversible carbon dioxide adsorption occurred to only a very limited extent on this oxidised sample. However, a more extensive adsorption was obtained subsequent to partial reduction of the surface with carbon monoxide.

It is tempting to explain these effects in terms of the presence of a bulk copper oxide, formed by the more severe oxidation conditions used in the experiment described in section 5.3.1(b). However, the results detailed in sections 4.5.3 and 4.5.2 clearly show that the total quantity of nitrous oxide reacted with the copper surface is independent of the length of the oxidation treatment and of the temperature at which it is carried out.

There is one possible explanation as to why a copper surface which

is oxidised, by nitrous oxide decomposition, at 80°C for 14 hours, does not adsorb carbon dioxide to the same extent as that of a copper sample which was treated with nitrous oxide for 15 minutes at 40°C. A number of studies [99,100] have documented the fact that oxidation of a copper surface can lead to geometric disruption and surface reconstruction. These effects, which seem to occur more readily at elevated temperatures, could lead to the production of an oxidised copper surface which is not geometrically suited to carbon dioxide adsorption.

It is interesting to note that mass spectrometric analysis proves that only 50% oxidation of a copper surface is sufficient to completely poison the surface with respect to carbon dioxide dissociation (Fig. 6.5). This infers that a relatively large ensemble is required to allow the carbon dioxide decomposition pathway, or that the chemical nature of the whole copper surface is completely altered by the dissociative adsorption of sub-monolayer doses of nitrous oxide.

Having confirmed that metallic copper is necessary to effect a dissociative chemisorption of carbon dioxide, further analysis can be made of the reaction of a flow of carbon dioxide with an initially oxygen-free copper surface.

Figure 6.8 clearly shows that, following the reaction, at 26°C, of a 10% carbon dioxide-helium flow with metallic copper for a five minute period, significant quantities of carbon monoxide were produced from the adsorbent during temperature programmed desorption. The maximum rate of carbon monoxide removal from the surface, which occurred at 87°C, was equivalent to an activation energy of desorption of 100 KJ mol^{-1}. The experimental procedure utilised in this desorption analysis demanded

that, after the adsorption process and prior to temperature-programming, the copper sample was briefly exposed to a helium flow. In this time desorption could occur and hence the total quantity of carbon monoxide observed during temperature-programming was unlikely to correspond to that quantity originally associated with the polycrystalline copper. However, titration of residual oxygen from the copper surface, on completion of the desorption analysis, allowed a good estimate to be made of the total quantity of carbon monoxide formed by the carbon dioxide decomposition pathway. In the above experiment, the removal of 2.79×10^{18} atomic oxygen species confirmed that 9% of a monolayer of carbon monoxide had originally been associated with the copper catalyst. The existence of this quantity of carbon monoxide, after a very short reaction period at temperatures as low as ambient, may indicate that a small fraction of the copper surface is comprised of metallic ensembles, which readily facilitate decomposition of molecular carbon dioxide. The desorption activation energy of the carbon monoxide species produced by this adsorption ($100\,KJ\,mol^{-1}$) indicates that these may be rather similar in chemical nature to the adsorbent produced by carbon monoxide adsorption on only a small fraction of the metallic copper surface (section 7.2).

Carbon dioxide was also found to desorb from the copper adsorbent over a wide temperature range (Fig. 6.8). The form of the desorption process appears similar to that described in Figures 6.4 and 6.10, which show carbon dioxide desorption from oxidised copper, and hence it is concluded that these carbon dioxide species are associated with the

oxygen generated by the dissociative chemisorption of carbon dioxide. This is confirmed by reference to the experiment described in section 6.3.1.3(c) in which, following the reaction of a 10% carbon dioxide-helium stream with copper, at 26°C, for 65 minutes, a total of 8.04×10^{18} carbon monoxide molecules were produced on the copper surface. The corresponding quantity of adsorbed oxygen (50% of a monolayer) can be seen to have allowed a more extensive molecular carbon dioxide adsorption (Fig. 6.9) than was obtained on the less oxidised surface (Fig. 6.8). The physical nature of these carbon dioxide species cannot be deduced from the data produced by this experimental technique. However, it is proposed that the highest energy desorption states are related to the presence of carbonate-type species. These states are only slightly populated following reaction at ambient temperatures (Figs. 6.8 and 6.9), although 10 minutes reaction at 100°C allows more extensive carbon dioxide adsorption in this form (Fig. 6.7). An activated copper-carbonate formation, similar to that observed on zinc oxide [149], may explain this phenomena.

The extent of carbon dioxide decomposition, at ambient temperature, is a distinctly time-dependent phenomena, since reaction of the carbon dioxide stream for 5 minutes produced 9% of a carbon monoxide monolayer, while 25% coverage was obtained after 65 minutes reaction (section 6.3.1.3(c)). The surface potential diagram shown in Fig. 7.1 shows that, making no assumptions concerning the adsorbed state of the molecular carbon dioxide species, an activation energy of between 34-99 KJ mol^{-1} is calculated for the production of adsorbed carbon monoxide and oxygen from gaseous carbon dioxide. These values were

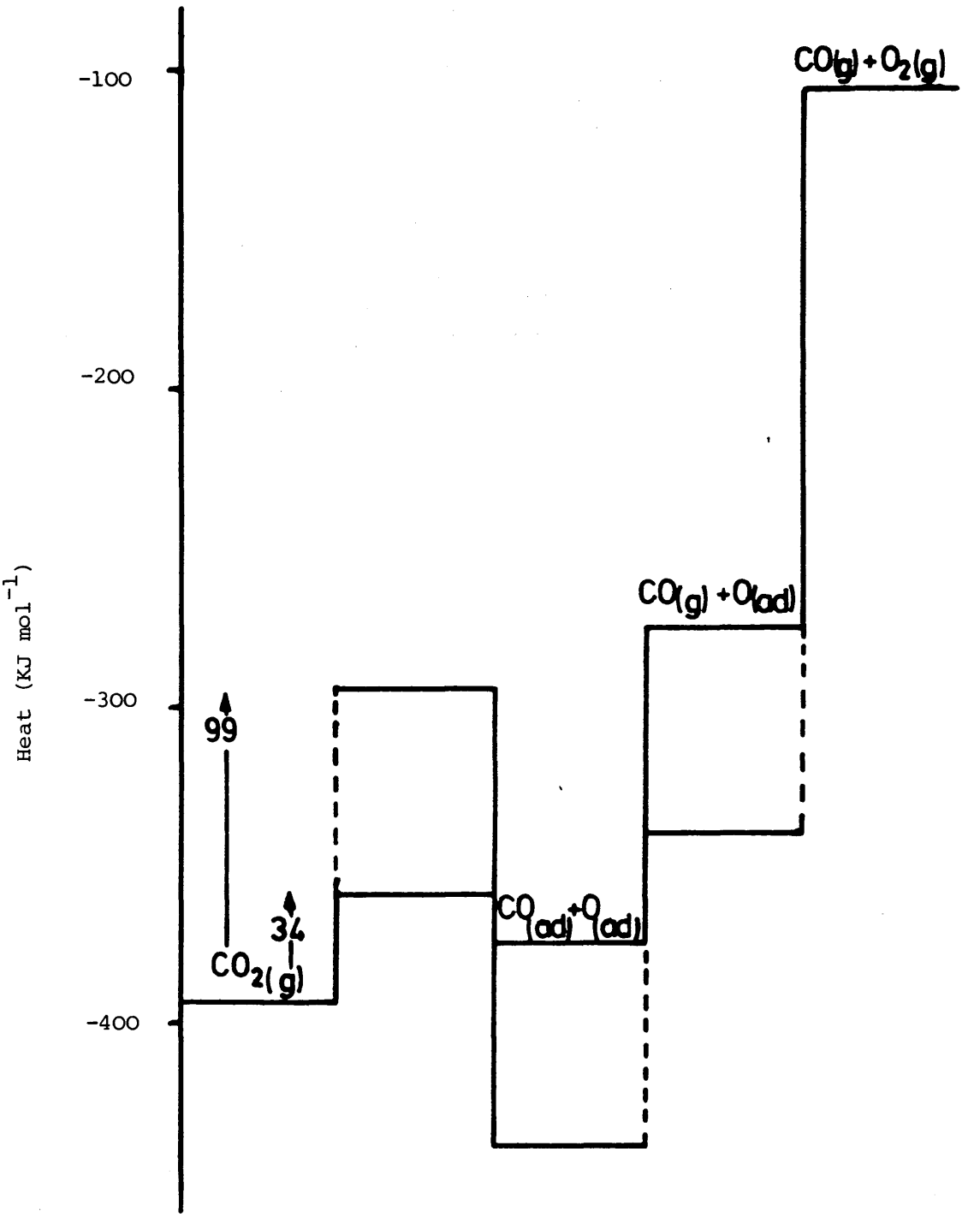

Figure 7.1 Energy plot for the formation of $CO_{(ad)}$ and $O_{(ad)}$ from $CO_2(g)$.

obtained by assuming the heat of adsorption of carbon monoxide to be 100 KJ mol^{-1} (Fig. 6.8) and the activation energy for the surface catalysed carbon monoxide-adsorbed oxygen reaction as 80 KJ mol^{-1} [96]. The heat of adsorption of oxygen was considered to lie in the range 340-470 KJ mol^{-1} [57,150], yet it is entirely possible that, if a number of very active copper sites allow oxygen to adsorb with a higher heat of adsorption, a limited number of carbon dioxide molecules will require little or no activation energy for dissociation.

The kinetic barrier shown in Figure 7.1 satisfactorily explains the time-dependency of the carbon dioxide decomposition pathway. However, it is surprising that, following the reaction of carbon dioxide with copper for 10 minutes at 225°C, no more than 18% of a carbon monoxide monolayer was produced on the copper surface (section 6.3.1.3(a)). The suggestion [151] that molecular carbon dioxide adsorption, stimulated by carbon dioxide dissociation, acts to limit the extent of oxidation of the copper surface appears to be confirmed by this data.

Without doubt, these studies confirm the general characteristics associated with the carbon dioxide-copper adsorption system, which were obvious from the radiotracer direct monitoring technique. However, it is possible that the fine details of the adsorption of carbon dioxide on the copper samples used for mass spectrometric and direct monitoring analyses may differ, simply because of the slight degree of oxidation associated with copper samples prepared by 'hydrogen-only' reduction. Somewhat fortuitously, the mechanics of the flow switching procedure utilised to create a static reaction vessel inside a flow microreactor (section 3.3.4.6 and section 6.9), caused a very slight air oxidation of the previously oxygen-free copper surfaces. The

static adsorption studies, and corresponding mass spectrometric analysis, are therefore concerned with the adsorption of carbon dioxide on a slightly oxidised copper surface, which is likely to be similar in nature to those 'hydrogen-only' reduced surfaces used in radiotracer direct monitoring analysis.

Figure 6.29 reveals that the presence of a few percent preadsorbed oxygen on a copper surface, was not enough to prevent the production of carbon monoxide by reaction, at ambient temperature, of an 8% carbon dioxide-helium stream. However, a unique molecular carbon dioxide desorption state appeared in the desorption profile (α'-carbon dioxide). This surface moiety must be associated with preadsorbed oxygen, since none of the continuous flow studies detailed in section 6.3.1 produced an adsorbed carbon dioxide species which desorbed from the surface in such a distinctive manner. As is shown in Figure 6.29, the desorption peak was remarkably sharp and showed a maximum desorption rate at a temperature of $87^{o}C$.

The adsorption of carbon dioxide, in a static system, for 15 minutes, on a pre-oxidised surface at ambient temperature, also allowed formation of the unique molecular carbon dioxide adsorbate (Fig. 6.11). It is fascinating to note that, despite oxidation of the copper sample by carbon dioxide dissociation, the expected wide range of carbon dioxide desorption states were not observed (cf. Fig. 6.9). Only the very 'sharp' desorption feature (at $100^{o}C$) and a very high energy state can be distinguished. A longer adsorption period, at the same temperature, did not, in contrast to the flow studies, allow more extensive carbon dioxide dissociation (section 6.3.2.2(b) and 6.3.2.2(c)). However, a substantial increase in the total quantity of α'-carbon dioxide which

desorbed at 100°C, was observed. It appears that the growth of this species did not allow carbon dioxide adsorption in those forms which, previously, were seen to desorb between ambient temperature and 100°C. The highest energy desorption state (150°C-180°C), which, by comparison with Figure 6.7, is likely to consist of carbonato-complexes, did not appear to be reduced by the growth of the other unique molecular entity.

There are two pieces of experimental evidence which allow the physical nature of α'-carbon dioxide to be deduced. First, the desorption peaks associated with this species are remarkably sharp and symmetrical. This is normally characteristic of a second order desorption event [152]. Second, the temperature at which α'-carbon dioxide desorbs from the copper surface, during temperature-programming, appears to be dependent only on the surface coverage of carbon monoxide. For example, in Figure 6.11 it can be seen that, when carbon monoxide began to desorb from the copper surface, at 100°C, α'-carbon dioxide was coincidently desorbed. However, when a larger carbon monoxide coverage was extant on the copper surface (Fig. 6.14) and desorption correspondingly commenced at a significantly lower temperature (81°C), the desorption of α'-carbon dioxide was again found to coincide with the desorption of the lowest energy carbon monoxide species from the copper surface.

These results are consistent with a mechanism in which preadsorbed oxygen allows the production of adsorbed α'-carbon dioxide, which exists as a partially dissociated carbon dioxide molecule. On temperature-programming, the carbon monoxide and oxygen components of this species recombinatively desorb and therefore show desorption features

attributable to a second-order event. The time dependency of the growth of this species on the copper surface (section 6.3.2.2(b)) may also indicate that, when partially dissociated from the carbon monoxide species, the oxygen component of α'-carbon dioxide functions as the original preadsorbed oxygen and allows the formation of another partially decomposed carbon dioxide molecule. In this manner the adsorption process will appear self-perpetuating.

The dependence of the desorption temperature of α'-carbon dioxide on carbon monoxide coverage, may be explained by assuming that, before moving into the gas phase, any desorbing carbon monoxide molecule will gain a measure of mobility in the adsorbed state. On migration across the surface, reaction with oxygen and subsequent carbon dioxide desorption will ensue (Fig. 7.2).

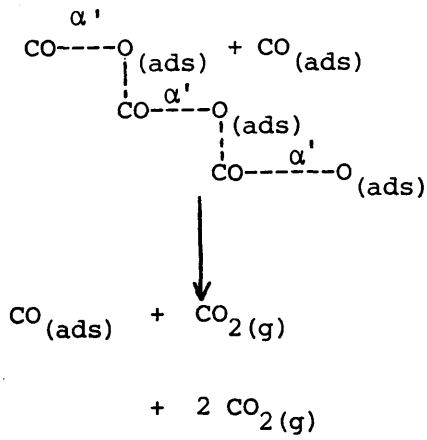

Fig. 7.2 Carbon monoxide 'catalysed' desorption of α'-carbon dioxide.

Removal of an oxygen 'keystone' from the matrix of partially dissociated adsorbates forces a rapid reintegration and desorption of these species. The leading edge of the carbon monoxide desorption profile will, therefore, determine the temperature at which the molecular carbon dioxide species desorb from the copper surface. The production of α'-carbon dioxide, and its subsequent reaction with carbon monoxide, provides a route by which a direct carbon monoxide-carbon dioxide interconversion may occur. The mechanics of this process are evidently completely independent of those associated with the water gas shift reaction. It is interesting to note that, an [18-O]tracer study of the hydrogenation of carbon monoxide and carbon dioxide on a copper-zinc oxide catalyst [135], has provided evidence for a direct carbon monoxide-carbon dioxide interconversion on the catalytic surface.

The formation of α'-carbon dioxide, together with that of adsorbed carbon monoxide and carbonato species, fully explains the time dependency of carbon dioxide adsorption on copper, as was determined by the radiotracer direct monitoring technique. These adsorbates also account for the 20% retention of adsorbed radiolabel on these surfaces. The remaining 80% has a lower heat of adsorption, 36-40 KJ mol^{-1}, (section 5.1.2.1), which did not allow detection by thermal desorption analysis, but does fully account for the observed carbon dioxide coverages under the conditions utilised in the radiotracer adsorption studies (θ_{CO_2} = 0.62 at $20^{o}C$, 5 torr pressure and ΔH = 38KJ mol^{-1}).

Sub-ambient desorption analysis clearly revealed the presence of a weakly bound carbon dioxide species (Fig. 6.13). The adsorption

of this molecular species is likely to depend on interaction with the copper surface and the variety of more strongly held adsorbates, since gas adsorption chromatography [56] has previously revealed that the interaction of molecular carbon dioxide species with a metallic copper surface generates a heat of adsorption of only 17 KJ mol^{-1}. Under the conditions operative in the static adsorption studies (P_{CO_2} = 76 torr, temperature = 25°C), this heat of adsorption would allow only 0.04% of a monolayer of this species to form on the copper surface. Hence, physically adsorbed carbon dioxide can be considered of little consequence to the total adsorption process. However, adsorption at -60°C (section 6.3.2.2(c)) would, theoretically, allow up to 7% of a monolayer of 17 KJ mol^{-1} carbon dioxide to be resident on the copper adsorbent. Remarkably, this low temperature adsorption process facilitated the production of 13% of a monolayer of carbon monoxide (Fig. 6.14), as compared to the 4% coverage which was attained, under identical conditions, at ambient temperature (Fig. 6.11). Therefore, it is possible that, under favourable temperature and pressure conditions, a physically adsorbed carbon dioxide species (ΔH = 17 KJ mol^{-1}) acts as a precursor to carbon dioxide dissociation on polycrystalline copper surfaces.

7.5 The Adsorption of Carbon Dioxide on a Copper-Alumina Catalyst

Previous studies [153] have revealed that carbon dioxide undergoes a slow adsorption on alumina, probably leading to extensive carbonate formation. Thus, the adsorption of carbon dioxide on a sample of copper-alumina will show rather complex behaviour, characteristic of

that on both copper (section 7.4) and alumina.

The isotherm produced by the adsorption of [14-C]carbon dioxide on a freshly reduced sample of copper-alumina (Fig. 5.32) showed, as expected, little tendency to reach saturation coverage. Indeed, it was only subsequent to the completion of five separate adsorption studies that the copper-alumina surface became saturated with carbon dioxide. Large quantities of the adsorbed radiolabel could not be removed by evacuation at ambient temperature. However, all the adsorbed species were eventually desorbed by raising the temperature to 180°C. (Fig. 5.33). This material is likely to consist of both carbon dioxide, generated from carbonate decomposition on the alumina surface, and carbon monoxide, produced by carbon dioxide dissociation on the metallic copper surface.

The [14-C]scrambling experiment described in section 5.5.2, clearly showed that, at elevated temperature, carbon monoxide was a product of molecular carbon dioxide chemisorption. However, it is interesting to note that, unlike studies involving unsupported copper surfaces (section 5.5.1), the adsorbed carbon monoxide did not undergo thermal desorption at 240°C but did undergo rapid gas-surface exchange with [12-C]carbon monoxide. This indicates that the surfaces of the polycrystalline powder and the alumina-supported copper metal are, as previously postulated (section 7.3), intrinsically different.

7.6 The Adsorption of Hydrogen on Polycrystalline Copper

In contrast to a variety of studies which conclude that hydrogen undergoes no ambient temperature interaction with copper powders, films

or single crystals [4,14,53,78,79], the studies described in section 6.2 reveal that a variety of adsorption states are induced by adsorption on polycrystalline copper powders at 25°C. Thermal desorption analysis revealed the presence of relatively weakly bound hydrogen, which desorbed at sub-ambient temperature (Fig. 6.2), and a more strongly held species which recombinatively desorbed on elevation of the surface temperature to between 34°C and 107°C (Fig. 6.3). Previous studies [18,21,80,81] have generally found the heat of adsorption of hydrogen on a variety of copper surfaces to lie within the range 40-49 KJ mol^{-1}, although a heat of 146 KJ mol^{-1} [14] has also been reported.

In this study no attempt has been made to calculate the heat of adsorption of hydrogen from the T.P.D. studies. The second order nature of the hydrogen desorption process does not allow the Redhead equation (section 4.2) to be applied in this case, and uncertainty also exists as to the true value of the pre-exponential factor for a second order desorption process [53,154]. However, studies of the coadsorption of hydrogen and [14-C]carbon monoxide on polycrystalline copper (section 5.1.1.4) indicate that the average heat of adsorption of hydrogen on the polycrystalline copper surface is 43 KJ mol^{-1} (section 7.8.3).

7.7 The Adsorption of Water on Polycrystalline Copper

The main points of the experimental observations described in sections 6.4 and 6.5 can be summarised as follows:

The molecular adsorption of water on polycrystalline copper occurred with an average heat of adsorption of 45 KJ mol^{-1}.

A small section of the copper surface allowed a facile decomposition of water. The evolution of hydrogen, by this reaction, was evidently an activated process. The total quantity of adsorbed oxygen, produced by water decomposition, did not correlate with the amount of gaseous hydrogen produced by the same reaction. An oxidised copper surface allowed significant water adsorption and the formation of a surface species, which desorbed as molecular water over a broad range of temperature.

The production of hydrogen by the adsorption and reaction of water on polycrystalline copper, as shown in Fig. 6.16, is convincing evidence for the occurrence of a dissociative chemisorption of water on the copper surface. Throughout the temperature range studied, the maximum initial quantity of hydrogen evolved was equivalent to the production of 7-8% of a monolayer of adsorbed oxygen. Thereafter, a far slower production of hydrogen and, consequently, adsorbed oxygen, was evident. These facts suggest that, as previous single crystal studies had indicated [2,67,68], the adsorption and reaction of water on copper is a distinctly surface sensitive process.

Further evidence for heterogeneity of the polycrystalline surface with respect to water adsorption, comes from an examination of the Langmuir plots shown in Figure 6.19. These plots were derived from adsorption isotherms (Fig. 6.18) which were produced by gas-adsorption chromatography. However, these isotherms cannot be considered as representing water adsorption on metallic copper since, as is shown in Figure 6.16, a coincident adsorption and dissociative chemisorption of water occurred on the copper surface.

The Langmuir plots show good linearity in the medium-high pressure range and allow a heat of adsorption of 45 KJ mol^{-1} to be calculated (section 6.4.4). This compares well with the values of 34 and 42 KJ mol^{-1}, which have previously been associated with the adsorption of molecular water on a Cu(111) surface [67,68].

At lower surface coverages a distinct deviation in the Langmuir plots was evident. The increased gradient in this region indicated that the P/V values were less than expected from a simple extrapolation of the high coverage plots. This implies larger adsorbed volumes, V, in the lower coverage regions, than predicted for the major part of the adsorption process. Although the isosteric heat of adsorption could not be determined at low surface coverages (section 6.4.4), it must be much larger than the value of 45 KJ mol^{-1} derived from the linear portion of the Langmuir plots.

Some indication of the strength of the chemisorption process can be obtained by considering the T.P.D. profile shown in Figure 6.17. This shows that, following the adsorption of water on copper at 24°C, 10% of the total quantity of adsorbed material did not desorb from the surface until temperatures of 30°C-160°C were attained.

Figure 6.17 also shows that significant quantities of hydrogen were desorbed from the polycrystalline surface over a broad temperature range. This could indicate the presence of atomic hydrogen on the copper surface, following water adsorption at 24°C, yet, as is shown in Figure 6.16, the reaction of water and copper at ambient temperature, was slow to evolve any hydrogen gas. Indeed, the temperature dependence of the form of the hydrogen 'transients' shown

in Figure 6.16 indicates a considerable energy barrier to the formation of hydrogen. Further evidence that this is the case is obtained by considering the effect of the addition of carbon monoxide to the water-copper system.

Figure 6.20 shows that reaction of a stream of carbon monoxide and water hydrogen, at ambient temperature, did not produce gaseous hydrogen. However, immediately on contact of the carbon monoxide-water mixture with the copper surface, a finite quantity of carbon dioxide was evolved. Before commencing the experiment, the copper surface was fully reduced, by reaction with carbon monoxide at 200°C, and can, therefore, be considered to be free of oxygen before the carbon monoxide-water mixture entered the catalyst column.

The carbon monoxide-water feedstream was known to contain a 0.016% oxygen impurity, which would readily allow carbon dioxide formation. However, the quoted figure of 4% of a monolayer of oxygen removed by carbon monoxide was calculated to take account of the oxygen impurity in the feedstream. Since no evidence has been obtained for the occurrence of the Boudouard reaction ($2CO \rightarrow CO_2 + C_{(ads)}$) on polycrystalline copper (section 7.2), the carbon dioxide must be formed by reaction of carbon monoxide with oxygen generated by a facile water decomposition process. This dissociation is, however, limited to only a small fraction of the total copper area and, since only a finite quantity of carbon dioxide was evolved at ambient temperature, appears to be self-poisoned by the adsorption of atomic hydrogen species.

The fact that atomic hydrogen species, which are produced by water decomposition, are strongly chemisorbed on the polycrystalline copper

surface is not unexpected, since total hydrogen desorption, from copper, is not achieved until temperatures of ca. 107°C are reached in T.P.D. experiments (Fig. 6.3). The form of the hydrogen transients shown in Figure 6.16 suggests that an activation energy exists for the production of gaseous hydrogen from the reaction of water on polycrystalline copper. It is likely that this activation energy is not associated with the decomposition of water on the copper surface, but is attributable to the recombinative desorption of atomic hydrogen.

The thermodynamics of water decomposition (Fig. 7.3), show that an activation barrier of 27-92 KJ mol^{-1} does exist for the dissociative chemisorption. These values are calculated by assuming the heat of adsorption of oxygen on copper to be 340-470 KJ mol^{-1} (57,150) and the activation energy for gaseous water formation, from gaseous hydrogen and adsorbed oxygen, to be 44 KJ mol^{-1} (section 6.7). However, as previously noted when carbon dioxide dissociation was considered (section 7.4), the presence of a small number of copper sites, which allow a far higher heat of adsorption of oxygen, could eliminate the activation barrier to decomposition.

The continuous slight, although not inconsiderable, production of hydrogen, which followed the elution of the hydrogen 'transients' shown in Figure 6.16, suggests that a substantial energy barrier exists to the water decomposition process on the majority of the copper surface. However, in section 6.4.2 it was noted that this continual hydrogen elution did not fully account for the total quantity of oxygen which could be titrated from the copper surface at the end of an experimental run (Table 6.1). This indicates the

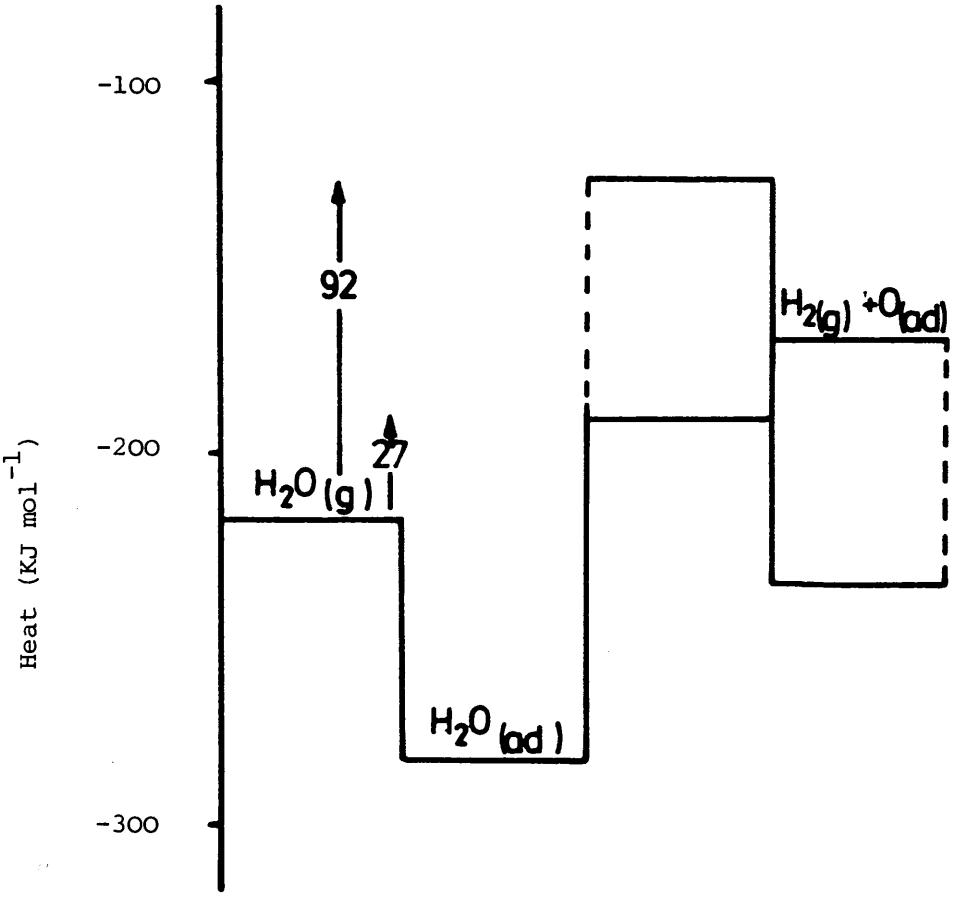

Figure 7.3 Energy plot for the formation of $H_2(g)$ and $O_{(ad)}$ from $H_2O(g)$

existence of a route which permits water dissociation on copper, yet by which hydrogen remains associated with the catalytic surface.

There are two means by which hydrogen retention may occur. Reaction of atomic hydrogen with adsorbed oxygen will produce hydroxyl species, which are likely to have a significant lifetime on the catalytic surface [148]. This will delay, or prevent, any hydrogen desorption process. Recent LEED and atomic diffraction studies [155] have shown that it is also possible that surface atomic hydrogen species can travel into the subsurface of the copper metal. In so doing, subsurface and, eventually, surface reconstruction effects are induced. Subsequent adsorption on these reconstructed regions will act to lock these hydrogen atoms in the bulk of the copper and prevent hydrogen desorption. A similar hydrogen trapping mechanism is postulated to occur in a copper-zinc oxide-alumina catalyst under methanol synthesis conditions [156].

The adsorbed oxygen produced by these decomposition processes is likely to modify subsequent molecular water adsorption. A number of single crystal studies [2,67,69,70] all reveal a tendency for oxygen to induce hydroxyl formation. Surface oxidised polycrystalline copper has been found to accommodate a degree of water adsorption (Fig. 6.15) and this is likely to involve hydroxylation of the surface. An activated disproportionation of these species, leading to the formation of molecular water and adsorbed oxygen, is proposed to account for the observed desorption of water molecules, subsequent to the ambient temperature reaction of water with polycrystalline copper samples (Fig. 6.17).

The presence of oxygen on the copper surface also explains the fact that the monolayer adsorbate volunes, V_m, calculated from Langmuir plots of water adsorption on polycrystalline copper (section 6.4.4), were not constant over the temperature range used in the study ($43^{o}C$-$104^{o}C$). If the copper surface was unchanging over this temperature range, then this data could not be satisfactorily explained. However, the copper surface is likely to be oxidised to a different extent at each temperature and, since different bonding modes of water have been observed on reduced and oxidised copper surfaces [70], this is sufficient to explain the variations in the calculated values of V_m.

7.8 The Combined Adsorption of Carbon Monoxide, Carbon Dioxide and Hydrogen on Polycrystalline Copper

The main points of the experimental observations described in sections 5.1, 5.2, 5.6.2 and 6.8 can be summarised as follows:

The adsorption of [14-C]carbon dioxide on polycrystalline copper was found to be limited by preadsorption of carbon monoxide, but unaffected by coadsorption of the same material. In contrast, both preadsorbed and coadsorbing carbon dioxide severely limited the extent of [14-C]carbon monoxide adsorption. The addition of [14-C]carbon monoxide to a [14-C]carbon dioxide precovered surface caused a significant increase in the total quantity of adsorbed radiolabel. In contrast, the addition of [14-C]carbon dioxide to a [14-C]carbon monoxide precovered surface did not affect the concentration of adsorbed radiolabel.

The adsorption of hydrogen caused a 20% decrease in the extent of carbon monoxide adsorption, but did not affect the desorption profile of the adsorbed carbon monoxide. The extent of carbon dioxide adsorption was found to be unaffected by the presence of hydrogen, but dramatic changes were observed in the carbon dioxide desorption profile. No such effect was observed on a fully oxidised copper surface.

7.8.1 The Role of Carbon Monoxide in Modifying Carbon Dioxide Adsorption

Figure 5.17 clearly shows that coadsorption of carbon monoxide with [14-C]carbon dioxide, on polycrystalline copper, did not block the adsorption of the radiolabelled species. In complete contrast, it was found that preadsorption of carbon monoxide substantially reduced (37%) the total quantity of [14-C]carbon dioxide associated with the copper surface (Fig. 5.14). This dramatic difference in behaviour can be explained by considering the possible interaction of carbon monoxide with those adsorbates retained on the copper surface subsequent to production of the [14-C]carbon dioxide reference isotherm. It should be remembered that these materials (fully dissociated carbon dioxide molecules, partially dissociated carbon dioxide molecules and carbonato complexes) are considered as essential in promoting the adsorption of a molecular, 38 KJ mol^{-1}, carbon dioxide species on the copper adsorbent (section 7.4). The uninhibited interaction of carbon monoxide with these adsorbates, as in the carbon monoxide preadsorption experiment, will allow a variety of redox reactions of the type:

$$CO_{(ad)} + CO_{3(ad)}^{2-} \rightarrow 2CO_2(g) \quad (87).$$

By this means the copper surface is partially cleansed of oxygen

containing species and thereby subsequent carbon dioxide adsorption will be inhibited. Under coadsorption conditions, these surface reduction processes are themselves hindered by the adsorption of a protective 'envelope' of carbon dioxide around the reducible adsorbates. This protective mechanism allows carbon dioxide adsorption to continue apparently undisturbed by the presence of carbon monoxide.

A seemingly strange aspect of the combinative adsorption of carbon monoxide and carbon dioxide is detailed in section 5.1.2.3(a). In this experiment it was found that, following the adsorption of [14-C]carbon monoxide on a copper sample, and with no intervening evacuation, admission of charges of [14-C]carbon dioxide caused no further increase in the total quantity of radiolabelled species associated with the catalyst. Indeed, a slight reduction in the amount of surface radioactivity was quickly established. That carbon dioxide adsorption does not occur under these conditions is not a feasible proposition, as is clear by the judicious use of [12-C]carbon monoxide, as detailed in section 5.1.2.3(b). Rather, the conclusion is reached that carbon dioxide adsorption occurs at the expense of carbon monoxide, which had previously been associated with the copper metal.

This displacement mechanism is clearly revealed by the addition of charges of [12-C]carbon dioxide to a system containing a [14-C]carbon monoxide precovered surface (Table 5.3). In this experiment the surface count rate was observed to decrease upon addition of unlabelled carbon dioxide. The addition of [14-C]carbon dioxide also caused a slight decrease in the surface count rate (section 5.1.2.3(a)), simply due to displacement of the [14-C]carbon monoxide, which had a higher specific

activity than that of the replacing [14-C]carbon dioxide gas.

7.8.2 The Role of Carbon Dioxide in Modifying Carbon Monoxide Adsorption

Subsequent to the adsorption of [14-C]carbon dioxide on a freshly reduced copper surface, and without any evacuation, it was found that the addition of [14-C]carbon monoxide to the static system dramatically increased the total quantity of radiolabelled material in the adsorbed state (Fig. 5.3). Substantial [14-C]carbon monoxide adsorption was obviously occurring, which did not necessarily involve coincident desorption of the preadsorbed [14-C]carbon dioxide species. Indeed, as is detailed in section 5.1.2.5, little evidence exists for any mechanism which allows significant displacement of adsorbed carbon dioxide by gaseous carbon monoxide. The bulk of those copper sites which facilitate the adsorption of carbon monoxide are, therefore, totally inert with respect to sorption of gaseous carbon dioxide. This supports the thesis that, while carbon monoxide will readily adsorb on single metal atoms, the larger carbon dioxide molecule may require a particular ensemble of metal atoms to facilitate a significant interaction.

As was noted in section 7.8.1, there is some overlap of the area of carbon monoxide and carbon dioxide adsorption on a polycrystalline copper surface. That competition for co-ordinatively unsaturated high energy sites exists is made apparent by reference to section 5.1.1.3(b). In this experiment it was found that preadsorption of unlabelled carbon dioxide effectively poisoned those areas of the copper surface which had previously allowed the formation of a relatively strong carbon monoxide-copper chemisorption bond.

The total area of adsorption overlap appears to extend over ca. 34% of the region of maximum carbon monoxide adsorption (Table 5.1). The largest competitive effects are generated by preadsorption of carbon dioxide (Fig. 5.5), while coadsorption of [14-C]carbon monoxide with [12-C]carbon dioxide forced the total quantity of adsorbed [14-C]carbon monoxide to fall, initially, by 26% (Fig. 5.8). However, over a long time period, the total quantity of [14-C]carbon monoxide associated with the copper surface showed a further slight decrease (Table 5.2). This is attributable to the slow adsorption of carbon dioxide on an area of the catalyst which had previously adsorbed [14-C]carbon monoxide.

7.8.3 The Role of Hydrogen in Modifying Carbon Monoxide Adsorption

The preadsorption and coadsorption of hydrogen with [14-C]carbon monoxide (Figs. 5.6 and 5.9) had a delitereous effect on the extent of [14-C]carbon monoxide adsorption on the polycrystalline surfaces. A 20% reduction in the total quantity of adsorbed carbon monoxide was obvious in both experiments. If Langmuir kinetics are assumed for the competitive carbon monoxide and hydrogen adsorption processes then, using the previously calculated heat of adsorption of carbon monoxide of 43 KJ mol^{-1} (section 5.1.1.1) and the Langmuir equation for surface coverage determination in this competitive adsorption system

$$\theta_A = \frac{K_A C_A}{1+K_A C_A+K_B^{\frac{1}{2}} C_B^{\frac{1}{2}}}$$

it can be calculated that a 20% decrease in carbon monoxide adsorption will be expected if the heat of adsorption of hydrogen is 43 KJ mol^{-1}. This is in good agreement with previous studies which have found the heat

of adsorption of hydrogen to be 43-49 KJ mol^{-1} on copper powder [21], 40 KJ mol^{-1} on copper films [18] and 40 KJ mol^{-1} on a Cu(311) single crystal surface [81].

The kinetic features of the recombinative desorption of atomic hydrogen from copper are unclear (section 7.6) and hence no estimate can be made of the lifetime of these species on copper under, for example, the conditions of the water gas synthesis process. However, thermal desorption studies (Figs. 6.2 and 6.3) have shown that desorption of atomic hydrogen from a polycrystalline copper surface is not complete until surface temperatures in the region of 100°C are attained.

In contrast to the preadsorption and coadsorption effects, it has been found that, if a monolayer of [14-C]carbon monoxide is formed on polycrystalline copper, hydrogen will displace only 2.8% of the adsorbed radiolabel (section 5.1.1.5(b)). This may indicate a significant attractive interaction between the adsorbed carbon monoxide species [44,60].

The possibility of an interaction between adsorbed atomic hydrogen and carbon monoxide, leading to the formation of an adsorbed complex, must also be considered. If formed, this complex would be expected to reveal differing adsorption characteristics to that of the separate carbon monoxide and hydrogen constituents. However, two pieces of evidence, from radiotracer analyses, fail to give any support for this proposition. First, Figure 5.14 reveals that preadsorbed carbon monoxide caused a 37% decrease in [14-C]carbon dioxide adsorption on a copper adsorbent. It has also been found that the preadsorption of both hydrogen and carbon monoxide (Fig. 5.16) generated a 44% decrease

in [14-C]carbon dioxide adsorption, which indicates that little or no enhancement in carbon monoxide adsorption is produced by the presence of the atomic hydrogen adsorbate. Second, radiotracer T.P.D. found no evidence of a carbon monoxide-hydrogen interaction. Comparison of Figures 5.34(a) and 5.34(b), which are thermal desorption profiles generated subsequent to the reaction of [14-C]carbon monoxide and a [14-C]carbon monoxide-hydrogen mixture with polycrystalline copper at 220^{o}C, reveals no significant difference in the temperature of desorption of the radiolabelled adsorbate. [14-C]carbon monoxide adsorption was, therefore, completely unaffected by coadsorption with hydrogen. This fact appears to rule out any mechanistic route by which a combination of carbon monoxide and hydrogen may form methanol on unsupported copper catalysts.

7.8.4 The Role of Hydrogen in Modifying Carbon Dioxide Adsorption

In complete contrast to the adsorption characteristics of [14-C]carbon monoxide, the preadsorption (Fig. 5.15) or coadsorption (Fig. 5.18) of hydrogen with [14-C]carbon dioxide did not reduce, in any way, the total quantity of radiolabel associated with the copper catalyst. It has also been found (section 5.1.2.5(b)) that charges of hydrogen are incapable of displacing adsorbed [14-C]carbon dioxide from the polycrystalline surface. By itself, this data indicates a total poisoning of those sites reactive towards hydrogen chemisorption by the carbon dioxide adsorbate. This does, however, presuppose the analysis of a variety of other adsorption data.

It has previously been noted, in section 5.1.2.3(a), that the

adsorption of [14-C]carbon dioxide on a [14-C]carbon monoxide precovered surface caused no increase in the total quantity of radiolabelled material associated with the copper surface. The adsorption of [14-C]carbon dioxide, by a displacement mechanism, was suggested to account for this behaviour (section 7.8.1). In a similar experiment, a mixture of hydrogen and [14-C]carbon monoxide was dosed on to a copper sample, before admission of [14-C]carbon dioxide (Fig. 5.13). In this case, the adsorption of [14-C]carbon dioxide caused a significant increase in the total quantity of adsorbed [14-C]containing material. This behaviour can be explained by assuming that, besides displacing [14-C]carbon monoxide from the copper surface, [14-C]carbon dioxide adsorbed on those sites which were associated with an adsorbed hydrogen species. Coadsorption of hydrogen and carbon monoxide has been found to allow a significant coverage of atomic hydrogen species on polycrystalline copper (section 7.8.3).

Further evidence of carbon dioxide adsorption on hydrogen adsorption sites can be gathered from an analysis of a variety of competitive [14-C]carbon monoxide preadsorption experiments. Table 5.1 shows that the separate preadsorption of carbon dioxide and hydrogen, on copper, reduced subsequent [14-C]carbon monoxide adsorption by 34% and 21% respectively. If hydrogen and carbon dioxide adsorb on totally discrete metallic sites, preadsorption of both hydrogen and carbon dioxide would block over 50% of [14-C]carbon monoxide adsorption. In reality, a reduction of only 29% was produced. These results, together with identical coadsorption analyses (Table 5.2), give

definitive evidence of the interaction of carbon dioxide with hydrogen-bearing copper ensembles at ambient temperature.

Having ascertained this adsorption mechanism, it is behoveful to question the fate of the atomic hydrogen species following carbon dioxide adsorption. Displacement and recombinative desorption is possible, though the possibility of a carbon dioxide-hydrogen interaction cannot be overlooked. Indeed, following the reaction of carbon dioxide and hydrogen at 220°C, on a polycrystalline copper surface, a remarkable radiotracer desorption profile was obtained (Fig. 5.36). There is no similarity between this profile and that generated by the adsorption of carbon dioxide alone on a copper surface (Fig. 5.35). The relatively high temperatures required to effect desorption of the radiolabel in the presence of hydrogen (T_p = 141°C), indicates a substantial modification, and energetic stabilisation, of adsorbed carbon dioxide.

The form of the stabilised carbon dioxide species is made clear by the use of a mass spectrometer in the desorption analysis (section 6.8.2). In this experiment, a stream of 8% hydrogen - 8% carbon dioxide-helium was allowed to interact with a freshly reduced sample of copper metal, which was maintained at a temperature of 32°C. Subsequent T.P.D. revealed a coincident desorption of carbon dioxide and hydrogen from the copper surface (Fig. 6.26). The maximum desorption rate of both hydrogen and carbon dioxide, which occurred at a temperature of 151°C, substantiates a promotional effect of hydrogen on the carbon dioxide adsorption process. This is likely to involve the formation of a surface formate species [157].

A reasonable criticism of T.P.D. experiments is the fact that

the technique cannot distinguish between an adsorbate which is formed on the catalyst surface at dosing temperatures, and any adsorbate which may be formed, by reaction of surface species, during subsequent temperature-programming. For example, in the above discussion, it has been assumed that a formate species was formed, on polycrystalline copper, by co-dosing of carbon dioxide and hydrogen at 32°C. In this case, this assumption is justified, since radiotracer adsorption studies, which are carried out at ambient temperature, also provide evidence for a carbon dioxide-hydrogen interaction. For example, hydrogen, by itself, has been found to displace 2.8% of a monolayer of preadsorbed [14-C]carbon monoxide from polycrystalline copper (section 5.1.1.5(b)), while the combination of carbon dioxide and hydrogen immediately removes 10.2% of preadsorbed [14-C]carbon monoxide (section 5.1.1.5(a)). This enhanced displacement suggests a significant carbon dioxide-hydrogen interaction.

The mechanics of formate formation are not clarified by this study. What is apparent is the fact that carbon monoxide adsorption does not poison a copper surface with respect to the adsorption of formate species (sections 5.1.1.5 and 5.1.2.4). In contrast, the adsorption of a monolayer of oxygen on polycrystalline copper removes all possibility of a carbon dioxide-hydrogen interaction (Fig. 6.25). It is possible that the interaction of carbon dioxide with hydride-type species, which are created by hydrogen adsorption on metallic copper [18], provides the route by which surface formate is evolved.

Although energetically favourable, it is clear that formation of formate species is not ubiquitous across the whole of a polycrystalline copper surface. The data presented in Figure 5.4 clearly shows that,

subsequent to the adsorption of [14-C]carbon dioxide and hydrogen on copper, extensive [14-C]carbon monoxide adsorption was still possible. The formation of carbon monoxide, by carbon dioxide decomposition, in the presence of a substantial surface coverage of formate species (Fig. 6.26), also shows that the mechanism of carbon dioxide decomposition remains unperturbed by any adjacent interaction of carbon dioxide and hydrogen.

Hydrogen has also been found to modify the extent of carbon dioxide adsorption on a partially oxidised copper surface (section 5.2.2.2). In sharp contrast to preadsorbed carbon monoxide, which caused a 17% decrease in the extent of carbon dioxide adsorption, preadsorbed hydrogen significantly increased (21%) the concentration of adsorbed carbon dioxide (Table 5.7 and Fig. 5.23). This effect is likely to involve the production of hydroxyl species on the copper surface [148], which may promote carbon dioxide adsorption by formation of novel surface complexes.

7.9 The Combined Adsorption of Carbon Monoxide, Carbon Dioxide and Hydrogen on Copper-Alumina Catalysts

A number of references have already been made to the fact that significant differences are apparent between the surface structure of polycrystalline and supported copper samples (sections 7.3 and 7.5). This is not surprising, since the polycrystalline

material can be described as an infinite array of different crystal faces separated only by imperfections and boundary edges, while the supported metal exists as relatively small metallic islands in a 'sea' of refractive aluminium oxide.

A direct comparison of Table 5.1 and Table 5.8, which detail quantitative analyses of [14-C]carbon monoxide preadsorption experiments on polycrystalline copper and copper-alumina respectively, shows significant differences between the two copper adsorbents. The most obvious difference is the fact that, on the supported copper samples, the effect of the separate preadsorption of carbon dioxide and hydrogen was effectively half of that on the polycrystalline material. In simplistic terms, this suggests that the adsorptions of carbon dioxide and hydrogen are surface sensitive and are less favoured on the supported copper catalyst than on the polycrystalline copper adsorbent.

In section 7.8.4 evidence was presented which clearly revealed that, on polycrystalline copper surfaces, preadsorption of both carbon dioxide and hydrogen did not effect any combinative effect on the total quantity of adsorbed [14-C]carbon monoxide. However, reference to the same experiment on the copper-alumina catalyst (Table 5.8) reveals that, on this adsorbent, the situation is considerably more complex. While, separately, carbon dioxide and hydrogen caused 16% and 10% reductions in the quantity of adsorbed [14-C]carbon monoxide, a combination of the two resulted in a 23% reduction in carbon monoxide adsorption.

This discrepancy, as compared to the polycrystalline copper data (Table 5.1), could indicate the involvement of the alumina support in these experiments. It is possible that atomic hydrogen adsorbed on copper metal, near the metal-support interface, may interact with carbon dioxide resident on the alumina support. Subsequent formation of a formate species at the metal-support interface will act to block carbon monoxide adsorption sites which were previously unaffected by the separate adsorption of carbon dioxide or hydrogen.

7.10 The Mechanism of the Water Gas Shift Reaction on Polycrystalline Copper

The main points of the experimental observations described in sections 6.4, 6.5, 6.6 and 6.8 can be summarised as follows:

The activation energies of the forward and reverse shift reactions have been determined as 67-75 KJ mol^{-1} and 113 KJ mol^{-1} respectively. T.P.D. has shown that a significant concentration of formate species exists on the copper surface under reaction conditions. The activation energy for the production of carbon dioxide and hydrogen, by formate decomposition, was calculated to be 92 KJ mol^{-1}. Both carbon dioxide and water are found to readily oxidise a fraction of the polycrystalline copper surface. In contrast, desorption

of the carbon monoxide and hydrogen species, produced by these decomposition reactions, is not facile. Adsorbed oxygen may be removed from a copper surface by reaction with carbon monoxide or hydrogen.

A number of studies [128,134,139] have proposed that the production of carbon dioxide and hydrogen, from a carbon monoxide-water reactant mixture, is effected by production of a formate intermediate on the surface of the copper catalyst:

$$CO(g)+H_2O(g) \rightarrow [HCOO^-]_{(ad)} \rightarrow CO_2(g)+H_2(g)$$

There is no doubt that this species does exist on the catalytic surface during the shift reaction since, following the reaction of carbon monoxide and hydrogen at a maximum temperature of 160°C on polycrystalline copper, T.P.D. (Fig. 6.21) showed coincident desorption of carbon dioxide and hydrogen from the copper surface. The maximum rate of desorption of these species (at 140°C) is characteristic of the presence of a copper-formate species [157]. However, the indisputable presence of this surface species does not necessarily prove that it has any function as an intermediate in the shift reaction.

If the associative mechanism is considered necessary to the mechanics of the forward shift reaction, then one of the steps in the synthesis will

involve the production of carbon dioxide and hydrogen by decomposition of the formate intermediate. From line shape analysis of the carbon dioxide and hydrogen plots shown in Figure 6.28, the activation energy of this process was calculated to be 92 KJ mol^{-1} . This is considerably lower than values calculated by Boudart and Iglesia [158], which show a range of 116-133 KJ mol^{-1} on a variety of copper surfaces.

However, in Boudart's studies, the formate species were produced by formic acid adsorption while, in these experiments, carbon dioxide and hydrogen were the precursor materials. Therefore, in this study, oxidation of the copper surface, by carbon dioxide decomposition, will occur coincidently with formate production. This may be of vital significance, since a recent theoretical study of copper-formate bonding [159] has concluded that π-electron donation, from the formate species to the copper substrate (which is increased by oxygen chemisorption), weakens the C-O bond in the formate species. This weakening effect can be expected to manifest itself in a lowering of the activation energy associated with the formate decomposition process.

The activation energy of the forward shift reaction, which was determined by analysis of the carbon dioxide and hydrogen line shapes shown in Figure 6.20, is 67-75 KJ mol^{-1}. It is, therefore, evident that the coincident evolution of carbon dioxide and hydrogen from formate decomposition, which has an activation energy of 92 KJ mol^{-1}, cannot be the rate determining step in the forward shift reaction. If the associative mechanism is operative, it can be concluded that the production of a surface formate species, from carbon monoxide and water, must be rate determining in the water gas shift reaction.

By this mechanism, it is obvious that production of carbon dioxide should then be coincident with that of hydrogen.

However, when the forward shift reaction was studied at a temperature of 62°C (Fig. 6.22), it was evident that, in the period before the reaction reached a steady-state conversion, the rate of production of carbon dioxide was distinctly different from the rate of hydrogen evolution. This is irrefutable evidence that formate production is not rate-determining in the shift reaction. These deductions lead to the proposal that a carbon monoxide-hydroxyl interaction, which appears unlikely on copper surfaces [62], is of no relevance to the mechanism of the shift reaction on polycrystalline copper.

The formate species, which was found to be extant on the copper surface following the reaction of carbon monoxide and water (Fig. 6.21) may, therefore, have been formed by interaction of carbon dioxide and hydrogen, which were products of the forward shift reaction. This is known to be a very facile reaction (section 7.8.4). It is interesting to note that, under low conversion conditions, where product concentrations and/or readsorptions are not expected to be significant, no coincident desorption of carbon dioxide and hydrogen could be distinguished (Fig. 6.23). The desorption profile was as expected by a combination of the separate adsorptions of hydrogen (Fig. 6.3) and water (Fig. 6.19) on reduced copper, and carbon dioxide (Fig. 6.4) on an oxidised copper surface.

Having determined that no symbiotic interaction of carbon monoxide and water is essential to the mechanics of the forward shift reaction, the role of the redox mechanism:

$$H_2O(g)+S \rightarrow H_2(g)+O_{(ad)}$$

$$CO(g)+O_{(ad)} \rightarrow CO_2(g)+S$$

must now be discussed. It was noted in section 7.7 that water will readily oxidise a small percentage of a polycrystalline copper surface. Evidence was also presented to show that, while carbon monoxide would effect a facile reduction of the water oxidised surface, the further oxidation of these copper sites did not ensue until a recombinative desorption of hydrogen had occurred. This process evidently involved a significant activation energy and proceeded only very slowly at ambient temperature. Consequently, it can be stated that, at ambient temperature, the forward shift reaction will occur on a small number of active copper ensembles, but is limited by hydrogen desorption from these sites.

At a reaction temperature of 62^{o}C a very similar situation was encountered. On contact of a carbon monoxide-water stream with polycrystalline copper, carbon dioxide was evolved (Fig. 6.20). Comparison of the m/e = 2 and m/e = 44 plots in Figure 6.20 shows that, in the early stages of the reaction, the rate of carbon dioxide production was greater than that of hydrogen evolution. This data is consistent with a mechanism in which the slow, or rate-determining, step in the forward shift reaction is the recombinative desorption of atomic hydrogen. The activation energy of this process lies within the range 67-75 KJ mol^{-1}.

Further evidence that the sequential oxidation and reduction of copper surfaces can fully account for the activity of copper based catalysts in the low temperature shift reaction, can be obtained from a

brief analysis of the turnover frequency (T.O.F.) of the reaction on polycrystalline copper, compared to that obtained on well defined copper single crystals. From the data of Campbell *et al.* [68], the T.O.F. on a Cu(111) surface, at 62°C, was calculated to be 2.29×10^{-6} molecules $sec.^{-1}$ $site^{-1}$, assuming all the copper atoms to be active. In comparison, on the polycrystalline copper catalyst, assuming that 8% of the copper atoms, which are highly active in the dissociative chemisorption of water, are active in the shift reaction, a T.O.F. of 5.56×10^{-3} molecules $sec.^{-1}$ $site^{-1}$ was obtained. Clearly it would be of interest to determine the nature of the sites on the polycrystalline copper, which are three orders of magnitude more active than those on a smooth Cu(111) single crystal surface.

The experimental data compiled in this study is consistent with a theory in which the forward shift reaction is considered to proceed by a sequential redox mechanism. Therefore, by the principle of microscopic reversibility, the reverse water gas shift should also be sequential.

In this study, direct experimental evidence has been obtained which proves that the redox steps involved in a sequential reverse shift mechanism, are feasible on polycrystalline copper.

$$CO_2(g) + S \rightarrow CO_{(ad)} + O_{(ad)} \quad \text{(Figure 6.8)}$$

$$H_2(g) + O_{(ad)} \rightarrow H_2O(g) \quad \text{(Figure 6.24)}$$

If this redox mechanism is operative, the overall activation energy of 113 KJ mol^{-1}, which was determined by line shape analysis of the m/e = 18 and m/e = 28 plots shown in Fig. 6.27, is likely to be associated

with the production of gaseous carbon monoxide by carbon dioxide decomposition:

$$CO_2(g)+S \rightarrow CO_{(ad)}+O_{(ad)}$$

$$CO_{(ad)} \rightarrow CO(g)+S$$

This is a reasonable assumption, since line shape analysis has allowed the activation energy of the reaction

$$H_2(g)+O_{(ad)} \rightarrow H_2O(g)$$

to be calculated as only 44 KJ mol^{-1}.

The question remains as to whether the rate of the reverse shift reaction is limited by the decomposition of carbon dioxide or by the desorption of carbon monoxide. In section 7.4 it was noted that, on the bulk of a polycrystalline copper surface, the decomposition of carbon dioxide is likely to be an activated process. However, as in the case of water decomposition, adsorption on ca. 7% of the available copper sites readily allows dissociation of carbon dioxide. The activation energy of desorption of the carbon monoxide species, produced by carbon dioxide decomposition on these sites (ca. 100 KJ mol^{-1}), is similar to that determined for the overall reverse shift reaction (113 KJ mol^{-1}).

It is therefore proposed that, on polycrystalline copper, the reverse water gas shift reaction proceeds by a redox mechanism on a small number of highly active sites. The turnover rate of the reaction appears to be limited by carbon monoxide desorption. However, in these circumstances, it is surprising that the reverse shift reaction does not 'take-off' until a temperature of 172°C is

reached in T.P.Rn. experiments (Fig. 6.27). If the reaction is self-poisoned by carbon monoxide, then this effect should be overcome at temperatures of ca. 80°C-100°C, since desorption of carbon monoxide is normally complete in this temperature range (Fig. 6.8). Indeed, the T.P.Rn. profile shown in Figure 6.27 does show a desorption of 2.23×10^{18} carbon monoxide molecules (6.3% of a monolayer) at temperatures below 100°C. However, Figure 6.27 also shows that water evolution was not coincident with the production of carbon monoxide. Therefore, at these temperatures, the reaction of gaseous hydrogen with adsorbed oxygen, which normally proceeds between 50°C and 70°C (Fig. 6.24), did not occur and, consequently, constrained the shift reaction to a single turnover on each of the active sites.

Between 100°C and 140°C, hydrogen reduction, and hence production of gaseous water, was observed. It is possible that the adsorption of carbon dioxide around the oxygen adsorbate, possibly leading to carbonate formation, protected the oxygen species from hydrogen reduction. It would only be on desorption of the carbon dioxide 'envelope' that unrestricted reduction could proceed. At temperatures in the region of 170°C, it is likely that the limited residence time of the carbon dioxide adsorbate on the catalyst and, possibly, a reduced sticking probability of adsorption, rendered these restrictions on the rate of the reverse shift inconsequential.

In conclusion, it is therefore proposed that, despite the presence of copious quantities of adsorbed formate on a polycrystalline

copper catalyst during the shift reaction (Figs. 6.21 and 6.28), the mechanism of the reaction involves a facile oxidation (by water or carbon dioxide) and subsequent reduction (by carbon monoxide or hydrogen) of a small fraction of the total copper surface. The rates of both the forward and reverse shift reactions appear to be desorption limited.

7.11 The Mechanism of the Methanol Synthesis Reaction on Polycrystalline Copper

The study reported in this thesis has not been concerned with any direct mechanistic analysis of the methanol synthesis reaction. However, the data generated by the separate and competitive adsorption of carbon monoxide, carbon dioxide and hydrogen on polycrystalline copper, together with a number of previously published studies, does allow consideration of the mechanism of the methanol synthesis reaction from carbon monoxide-carbon dioxide-hydrogen synthesis gas mixtures.

It has previously been proposed that formate species, generated by the interaction of carbon dioxide and hydrogen on copper based catalysts [115], undergo an activated hydrogenolysis, which leads to the formation of an adsorbed methoxy species and then, by further hydrogenation, to gaseous methanol formation. Although the data generated in this study allows no comment to be made on the latter components of this mechanism, it is clear that an adsorbed formate species is produced, on a polycrystalline copper surface, by the interaction of carbon dioxide and hydrogen, at far lower temperatures than had previously been thought possible. For example,

Amenomiya et al.[133] produced good spectroscopic evidence for formate formation at 100°C, while, in this study, T.P.D. and radiotracer adsorption studies have revealed that the surface species is produced at ambient temperature (section 7.8.4).

Methanol formation, from these formate species, obviously involves an oxidation of the metallic copper surface. Indeed, it has been found that, under industrial synthesis conditions, the copper surface is in a partially oxidised state [127]. These oxidised copper sites are likely to play an invaluable role in methanol synthesis on polycrystalline copper, since they allow a 'stock' of adsorbed carbon dioxide to exist on the copper surface (Fig. 6.4). Many of these species will have a considerable residence time on the copper adsorbent, even at the temperatures used for methanol synthesis (220°C).

The promotional effect of adsorbed oxygen, on the activity of the copper catalyst, must be considered in relation to the fact that oxidation of the copper surface acts to hinder formate production (section 7.8.4). The possible role of carbon monoxide in a synthesis gas mixture is, therefore, to maintain the redox balance on the copper surface, which will allow maximum methanol synthesis activity.

This study has also produced good evidence to show that, by themselves, carbon monoxide and hydrogen can effect no surface interaction which is likely to lead to methanol formation on polycrystalline copper catalysts (section 7.8.3). However, in the presence of carbon dioxide, water may be introduced in to the

adsorption system, via the reverse water gas shift reaction, which will allow hydroxyl formation on the copper surface (section 7.7). This study cannot rule out the possibility that, on supported copper catalysts, a carbon monoxide-hydroxyl interaction may provide a feasible pathway to the formation of methanol.

It is evident from this study that, under industrial methanol synthesis conditions, a catalytic copper surface will be dominated by a large surface coverage of formate species. However, a variety of molecular carbon dioxide species will co-exist on the adsorbent, together with species, of varying lifetime, generated by the adsorption of carbon monoxide, hydrogen and water.

It has also become clear that the water gas shift reaction occurs in parallel to the methanol synthesis reaction on a polycrystalline copper catalyst. The sites which facilitate the shift reaction, via a redox mechanism, are highly active, though small in number (section 7.10) and are completely unrelated to those which allow formate adsorption and subsequent methanol formation.

REFERENCES

1. O. Beeck, A.E. Smith and A. Wheeler, Proc. Roy. Soc. A, 177, 62 (1940).
2. A. Spitzer, A. Ruth and H. Luth, Surface Sci., 152/153, 543 (1985).
3. L. Pauling, J. Am. Chem. Soc., 69, 542 (1947).
4. B.M.W. Trapnell, Proc. Roy. Soc. A, 218, 566 (1953).
5. D.A. Dowden, J. Am. Chem. Soc., 1, 242 (1950).
6. W.G. Bragg, Phil. Mag. (6), 28, 355 (1914).
7. E.A. Owen and B. Pickup, Z. Krist., 88, 116 (1934).
8. P.W. Reynolds, J. Am. Chem. Soc., 1, 265 (1950).
9. G.C. Bond and R.S. Mann, J. Chem. Soc., 3566 (1959).
10. P. Sabatier and J.B. Senderens, Compt. Rend., 114, 1429 (1892).
11. W.G. Palmer, Proc. Roy. Soc. A, 98, 13 (1920).
12. V. Ponec, Z. Knor and S. Cerny, J. Catal., 4, 485 (1965).
13. A. Sieverts, Zeit. Phys. Chem., 60, 140 (1907).
14. T. Kwan, J. Res. Inst. Catalysis (Hokkaido), 1, 96 (1949).
15. R.J. Mikovsky, M. Boudart and H.S. Taylor, J. Am. Chem. Soc., 56, 540 (1960).
16. J.C.P. Mignolet, J. Chim. Phys., 54, 19 (1957).
17. J. Pritchard and F.C. Tompkins, Trans. Farad. Soc., 56, 540 (1960).

18. C.S. Alexander and J. Pritchard, J. Chem. Soc. Farad. Trans. (1), 68, 202 (1972).

19. D.A. Dowden, Bull. Soc. Chim. Belges, 67, 439 (1958).

20. G. Natta, Catalysis vol. III, p.349 (Ed. P.H. Emmett, Reinhold, 1955).

21. R.A. Beebe, G.W. Low, E.L. Wildner and S. Goldwasser, J. Am. Chem. Soc., 57, 2527 (1935).

22. R.N. Pease, J. Am. Chem. Soc., 45, 1196 (1923).

23. G.C.A. Schuit and L.L. van Reijen, Adv. Catal., 10, 242 (1958).

24. R.J. Weiss and J.J. de Marco, Rev. Mod. Phys., 30, 59.

25. G.C. Chinchen, P.J. Denny, D.G. Parker, G.D. Short, M.S. Spencer, K.C. Waugh and D.A. Whan, Prepr. Am. Chem. Soc. Div. of Fuel Chem., 29, 178 (1984).

26. K. Kleir, Appl. Surf. Sci., 19, 267 (1984).

27. C.L. McCabe and G.D. Halsey, J. Am. Chem. Soc., 74, 2732 (1952).

28. J. Cunningham, G.H. Al-Sayyed, J.A. Cronin, C. Healy and W. Hirschwald, Appl. Catal., 25, 129 (1986).

29. G. Blyholder, J. Phys. Chem., 68, 2772 (1964).

30. L.H. Jones, J. Mol. Spectr., 9, 130 (1962).

31. A.B. Anderson, Surface Sci., 62, 119 (1977).

32. D.L. Roberts and G.L. Griffin, Appl. Surf. Sci., 19, 298 (1984).

33. P.R. Norton and R.L. Tapping, Chem. Phys. Letts., 38, 207 (1976).

34. A.M. Bradshaw and J. Pritchard, Proc. Roy. Soc. A, 316, 169 (1970).

35. S.A. Isa, R.W. Joyner and M.W. Roberts, J. Chem. Soc. Farad. Trans. (1), 74, 546 (1978).

36. J. Pritchard and P. Hollins in 'Vibrational Spectroscopies for Adsorbed Species', ACS Symp. Series No. 137, p.51.

37. F. Boccuzzi, G. Ghiotto and A. Chiorino, Surface Sci., 156, 933 (1985).

38. A.W. Smith and J.M. Quets, J. Catal., 4, 163 (1965).

39. J. Pritchard and M.L. Sims, Trans. Farad. Soc., 66, 427 (1970).

40. J. Pritchard, Trans. Farad. Soc., 59, 437 (1963).

41. J. Pritchard, Surface Sci., 79, 231 (1979).

42. M.A. Chesters, J. Pritchard and M.L. Sims in 'Adsorption-Desorption Phenomena', Ed. F. Ricca, Academic Press 1972, p.277.

43. K. Horn and J. Pritchard, Surface Sci., 55, 701 (1976).

44. K. Horn, M. Hussain and J. Pritchard, Surface Sci., 63, 244 (1977).

45. M.A. Chesters and J. Pritchard, Surface Sci., 28, 460 (1971).

46. J. Pritchard, J. Vac. Sci. Technol., 9, 895 (1972).

47. G. Ghiotto, F. Boccuzzi and A. Chiorino, Surface Sci., 178, 553 (1986).

48. S. Anderson, Surface Sci., 89, 477 (1979).

49. M.A. Chesters, S.F. Parker and R. Ramal, Surface Sci., 165, 179 (1986).

50. R. Rydberg, Surface Sci., 89, 627 (1982).

51. D.P. Woodruff, B.E. Hayden, K. Prince and A.M. Bradshaw, Surface Sci., 123,397 (1982).

52. J. Pritchard and P. Hollins, Surface Sci., 89, 486 (1979).

53. I.E. Wachs and R.J. Madix, J. Catal., 53, 208 (1978).

54. W.K. Kirstein, B. Kruger and F. Thieme, Surface Sci., 176, 505 (1986).

55. E. Giamello, B. Fubini and V. Bolis, Appl. Catal., (in press).

56. K.C. Waugh, R.S.C. Catalysis meeting, London, October 1985.

57. R. Dell, F. Stone and P.F. Tilley, Trans. Farad. Soc., 49, 195 (1953).

58. R.A. Beebe and E.L. Wildner, J. Am. Chem. Soc., 56, 642 (1934).

59. G.E. Parris and K. Kleir, J. Catal., 97, 374 (1986).

60. D. Jackson, Private communication.

61. G.A. Vedage, R. Pitchai, R.G. Herman and K. Kleir, Proc. 8th Int. Congr. Catal., Berlin 1984 (Verlag Chemie, Weinheim, 1985).

62. C.T. Au and M.W. Roberts, Chem. Phys. Letts., 74, 472 (1980).

63. M. Bertholet, Ann. Chim. Phys., 22, 303 (1901).

64. M. Barber, J.C. Vickerman and J. Wolstenholme, J. Chem. Soc. Farad. Trans (1), 72, 40 (1976).

65. D.L. Roberts and G.L. Griffin, Appl. Surf. Sci., 19, 298 (1984).

66. J.R. Monnier, M.J. Hanrahan and G. Apai, J. Catal., 92, 119 (1985).

67. C.T. Au, J. Breza and M.W. Roberts, Chem. Phys. Letts., 66, 340 (1979).

68. C.T. Campbell, Preprint J. Vac. Sci. Technol.

69. K. Bange, D. Grider and J.K. Sass, Surface Sci., 126, 437 (1983).

70. A. Spitzer and H. Luth, Surface Sci., 120, 376 (1982).

71. J.M. Heras, Proc. IVC-IX, ICSS-V Madrid (1983) p.52.

72. D.J.M. Fassaert, H. Verbeek and A. van der Avoird, Surface Sci., 29, 501 (1972).

73. H.S. Taylor and R.M. Burns, J. Am. Chem. Soc., 43, 1273 (1921).

74. W.A. Dew and H.S. Taylor, J. Phys. Chem., 31, 277 (1927).

75. J.H. Sinfelt, J.L. Carter and D.J.C. Yates, J. Catal., 24, 283 (1972).

76. D. Duprez, J. Barbier, Z. Ferhat-Hamida and M. Bettahar, Appl. Catal., 12, 219 (1984).

77. D.A. Cadenhead and N.J. Wagner, J. Catal., 21, 312 (1971).

78. J.A. Allen and J.W. Mitchell, Diss. Farad. Soc., 8, 357 (1950).

79. R.N. Lee and H.E. Farnsworth, Surface Sci., 3, 461 (1965).

80. R.A. Beebe and H.S. Taylor, J. Am. Chem. Soc., 46, 51 (1924).

81. J. Pritchard, T. Catterick and R.K. Gupta, Surface Sci., 53, 1 (1975).

82. M. Balooch, M.J. Cardillo, D.R. Mille and R.E. Stickney, Surface Sci., 46, 358 (1974).

83. J. Garcia-Prieto, M.E. Ruiz and O. Novero, J. Am. Chem. Soc., 107, 5635 (1985).

84. H.J. Freund and R.P. Messmer, Surface Sci., 172, 1 (1986).

85. F.H.P.M. Habraken, E. Kieffer and G.A. Bootsma, Surface Sci., 83, 45 (1979).

86. A.C. Collins and B.M.W. Trapnell, Trans. Farad. Soc., 53, 1476 (1957).

87. F.S. Stone and P.F. Tilley, Diss. Farad. Soc., 8, 246 (1950).

88. L. Pfaundler, Chem. Ztg., 16, 145 (1892).

89. V.H.J. Grabke, Ber. Bunsenges Phys. Chem., 71, 1067 (1967).

90. K. Kleir, Adv. Catal., 31, 243 (1982).

91. O. Ruggeri, F. Trifiro and A. Vaccari, J. Solid State Chem., 42, 20 (1982).

92. F. Solymosi and A. Berko, J. Catal., 101, 458 (1986).

93. T.N. Rhodin, Adv. Catal., 5, 39 (1953).

94. F.H.P.M. Habraken and G.A. Bootsma, Surface Sci., 87, 333 (1979).

95. F.H.P.M. Habraken, G.A. Bootsma, P. Hofmann, S. Hachicha and A.M. Bradshaw, Surface Sci., 88, 285 (1979).

96. F.H.P.M. Habraken, C.M.A.M. Mesters and G.A. Bootsma, Surface Sci., 97, 264 (1980).

97. S. Evans, J. Chem. Soc. Farad. Trans (10, 71, 1044 (1975).

98. C. Benndorf, B. Egert, G. Keller and F. Thieme, Surface Sci., 74, 216 (1978).

99. U. Dobler, K. Baberschke, D.D. Vvedensky and J.B. Pendry, Surface Sci., 178, 679 (1986).

100. T.A. Delchar, Surface Sci., 27, 11 (1971).

101. T.J. Osinga, B.G. Linsen and W. Pvan, J. Catal., 7, 277 (1967).

102. J.J.F. Scholten and J.A. Konvalinka, Trans. Farad. Soc., 65, 2465 (1969).

103. B. Pvorak and J. Pasek, J. Catal., 18, 108 (1970).

104. G.C. Chinchen, C.M. Hay, H.D. Vandervell and K.C. Waugh, J. Catal., 103, 79 (1987).

105. J.W. Evans, M.S. Wainwright, A.J. Bridgewater and D.J. Young, Appl. Catal., 7, 75 (1983).

106. K. Narita, N. Takezawa, H. Kobayashi and I. Toyoshima, React. Kinet. Catal. Lett., 19, 91 (1982).

107. S.J. Thomson and G. Webb, J. Chem. Soc. Chem. Commun., (1976) 526.

108. A. Lawson and S.J. Thomson, J. Chem. Soc., 365, 1861 (1964).

109. J.N. Russell, S.M. Gates and J.Y. Yates, Surface Sci., 163, 516 (1985).

110. G. Ertl, Surface Sci., 7, 309 (1967).

111. J.W. London and A.T. Bell, J. Catal., 31, 32 (1973).

112. V. Ponec, Z. Knor and S. Cerny, Diss. Farad. Soc., 41, 149 (1966).

113. M.W. Roberts and R. Ryder, ICI Methanol Conference, Billingham, 1986.

114. C.M.A.M. Mesters, T.J. Vink, O.L.J. Gijzeman and J.W. Geus, Surface Sci., 135, 428 (1983).

115. G.C. Chinchen, M.S. Spencer, K.C. Waugh and D.A. Whan, J. Chem. Soc. Farad. Trans. (1), 87, 280 (1987).

116. E.R.S. Winter, Adv. Catal., 10, 196 (1958).

117. G. Apai, J.R. Monnier and D.R. Preuss, J. Catal., 98, 563 (1986).

118. G. Sanker, S. Vasuderan and C.N.R. Rao, Chem. Phys. Letts., 127, 620 (1986).

119. G. Vlaic, J.C.J. Bart, W. Cavigiolo, B. Pianzola and S. Mobilio, J. Catal., 96, 314 (1986).

120. J.F. Edwards and G.L. Schrader, J. Catal., 94, 175 (1985).

121. K. Kleir, J. Nunan, C. Young, P.B. Himelfarb and R.G. Herman, J. Chem. Soc. Chem. Commun., (1986) 193.

122. G.A. Vedage, R.G. Herman and K. Kleir, J. Catal., 95, 423 (1985).

123. Y.B. Kagan, A.Y. Rozovskii, G.I. Liu, E.V. Slivinsky, S.M. Loktev, L.G. Liberov and A.N. Bashkirov, Kinet. Catal., 16, 809 (1975).

124. R. Bardet, J. Thioville-Cuzat and Y. Trambouze, 188th ACS meeting, Phil., PA, 1984.

125. O. Cherifi, S. Monteverdi, M.M. Bettahar, M. Forissier and V. Perrichon, Bul. Soc. Chem. France, 3, 405 (1985).

126. J.B. Friedrich, M.S. Wainwright and D.J. Young, J. Catal., 80, 1 (1983).

127. G.C. Chinchen, K.C. Waugh and D.A. Whan, Appl. Catal., 25, 101 (1986).

128. T. Tagawa, G. Pleizer and Y. Amenomiya, Appl. Catal., 18, 285 (1985).

129. Y. Okamoto, K. Fukino, T. Imanaka and S. Teranishi, J. Phys. Chem., 87, 3747 (1983).

130. S. Gusi, F. Trifiro, A. Vaccari and G. Del Piero, J. Catal., 94, 120 (1985).

131. R.H. Hoppener, E.B.M. Deesburg and J.J.F. Scholten, Appl. Catal., 25, 109 (1986).

132. E.H. Boomer and H.E. Morris, J. Am. Chem. Soc., 54, 407 (1932).

133. Y. Amenomiya and T. Tagawa, Proc. 8th Int. Congr. Catal., Berlin 1984 (Verlag Chemie, Weinheim, 1985).

134. E. Rameroson, R. Kieffer and A. Kiennemann, Appl. Catal., 4, 281 (1982).

135. G. Liu, D. Willcox, M. Garland and H. Kung, J. Catal., 96, 251 (1985).

136. H. Uchida, N. Isogai, M. Oba and T. Hasegawa, Bull. Chem. Soc., Japan, 40, 1981 (1967).

137. E.G.M. Kuijpers, R.B. Tjepkema and W.J.J. van der Wal, Appl. Catal., 25, 139 (1986).

138. D.C. Grenoble, M.M. Estadt and D.F. Ollis, J. Catal., 67, 90 (1981).

139. T. van Herwijnen and W.A. de Jong, J. Catal., 63, 83 and 94 (1980).

140. H. Uchida, M. Oba, N. Isogai and T. Hasegawa, Bull. Chem. Soc. Japan, 41, 479 (1968).

141. S.J. Thomson and J.L. Wishlade, Trans. Farad. Soc., 58, 1170 (1962).

142. D. Cormack, S.J. Thomson and G. Webb, J. Catal., 5, 224 (1966).

143. F. Schmidt-Bleek and F.S. Rowland, Anal. Chem., 36, 1695 (1964).

144. P.A. Redhead, Trans. Farad. Soc., 57, 641 (1961).

145. G.C. Bond, 'Catalysis by Metals', Academic Press, 1962, p.115.

146. S. Brunauer, P.H. Emmett and E. Teller, J. Am. Chem. Soc., 60, 309 (1938).

147. E.A. Arafa, M.Sc. Thesis, University of Glasgow, 1985.

148. S. Kinnaird, G. Webb and G.C. Chinchen, to be published.

149. M. Bowker, H. Houghton and K.C. Waugh, J. Chem. Soc. Farad. Trans.(1), 77, 3023 (1981).

150. E. Giamello, B. Fubini, P. Lauro and A. Bosso, J. Catal., 87, 443 (1984).

151. G.C. Chinchen, C. Plant, M.S. Spencer and D.A. Whan, Surface Sci., 184, L370 (1987).

152. R.P.H. Gasser, 'An Introduction to Chemisorption and Catalysis by Metals', Oxford University Press, 1985, p.69.

153. S. Evitt, Ph.D. Thesis, University of Glasgow, 1986.

154. M. Bowker, I.B. Parker and K.C. Waugh, Appl. Catal., 14, 101 (1985).

155. K.H. Reider and W. Stocker, Phys. Rev. Lett., 57, 2548 (1986).

156. M. Bowker, R.A.Hadden, H. Houghton, J.N.K. Hyland and K.C. Waugh, J. Catal., in press.

157. D.H.S. Ying and R.J. Madix, J. Catal., 61, 48 (1980).

158. M. Boudart and E. Iglesia, J. Phys. Chem., 90, 5272 (1986).

159. J.A. Rodriguez and C.T. Campbell, Surface Sci., 183, 449 (1987).